**Max Planck-Institut für Molekulare Pflanzenbiologie
und Universität Potsdam
Arbeitsgruppe Prof. Dr. Bernd Mueller-Roeber**

Unraveling the ORE1 Regulon in *Arabidopsis thaliana*: Molecular and Functional Characterization of Up- and Down-stream Components

**Dissertation
zur Erlangung des akademischen Grades
"doctor rerum naturalium"
(Dr. rer. nat.)
in der Wissenschaftsdisziplin "Molekularbiologie"**

**eingereicht an der
Mathematisch-Naturwissenschaftlichen Fakultät
der Universität Potsdam**

von Lilian Paola Matallana-Ramírez

Potsdam, den 11.04.2012

Dedicated

to my beloved deceased grandma Graciela

"-Try not to become a man of success but rather to become a man of value".
A. Einstein

Summary

Leaf senescence is an active process required for plant survival, and it is flexibly controlled, allowing plant adaptation to environmental conditions. Although senescence is largely an age-dependent process, it can be triggered by environmental signals and stresses. Leaf senescence coordinates the breakdown and turnover of many cellular components, allowing a massive remobilization and recycling of nutrients from senescing tissues to other organs (e.g., young leaves, roots, and seeds), thus enhancing the fitness of the plant. Such metabolic coordination requires a tight regulation of gene expression. One important mechanism for the regulation of gene expression is at the transcriptional level via transcription factors (TFs). The NAC TF family (*NAM, ATAF, CUC*) includes various members that show elevated expression during senescence, including *ORE1* (*ANAC092/AtNAC2*) among others. *ORE1* was first reported in a screen for mutants with delayed senescence (*oresara1, 2, 3,* and *11*). It was named after the Korean word "oresara," meaning "long-living," and abbreviated to *ORE1, 2, 3,* and *11*, respectively. Although the pivotal role of ORE1 in controlling leaf senescence has recently been demonstrated, the underlying molecular mechanisms and the pathways it regulates are still poorly understood.

To unravel the signaling cascade through which ORE1 exerts its function, we analyzed particular features of regulatory pathways up-stream and down-stream of ORE1. We identified characteristic spatial and temporal expression patterns of ORE1 that are conserved in *Arabidopsis thaliana* and *Nicotiana tabacum* and that link *ORE1* expression to senescence as well as to salt stress. We proved that ORE1 positively regulates natural and dark-induced senescence. Molecular characterization of the *ORE1* promoter *in silico* and experimentally suggested a role of the 5'UTR in mediating ORE1 expression. ORE1 is a putative substrate of a calcium-dependent protein kinase named CKOR (unpublished data). Promising data revealed a positive regulation of putative ORE1 targets by CKOR, suggesting the phosphorylation of ORE1 as a requirement for its regulation. Additionally, as part of the *ORE1* up-stream regulatory pathway, we identified the NAC TF ATAF1 which was able to transactivate the *ORE1* promoter *in vivo*. Expression studies using chemically inducible *ORE1* overexpression lines and transactivation assays employing leaf mesophyll cell protoplasts provided information on target genes whose expression was rapidly induced upon *ORE1* induction. First, a set of target genes was established and referred to as early

responding in the ORE1 regulatory network. The consensus binding site (BS) of ORE1 was characterized. Analysis of some putative targets revealed the presence of *ORE1* BSs in their promoters and the *in vitro* and *in vivo* binding of ORE1 to their promoters. Among these putative target genes, *BIFUNCTIONAL NUCLEASE I* (*BFN1*) and *VND-Interacting2* (*VNI2*) were further characterized. The expression of *BFN1* was found to be dependent on the presence of *ORE1*. Our results provide convincing data which support a role for *BFN1* as a direct target of *ORE1*. Characterization of *VNI2* in age-dependent and stress-induced senescence revealed ORE1 as a key up-stream regulator since it can bind and activate *VNI2* expression *in vivo* and *in vitro*. Furthermore, *VNI2* was able to promote or delay senescence depending on the presence of an activation domain located in its C-terminal region. The plasticity of this gene might include alternative splicing (AS) to regulate its function in different organs and at different developmental stages, particularly during senescence. A model is proposed on the molecular mechanism governing the dual role of VNI2 during senescence.

Acknowledgments

During these past few years I have one of the most enriching times of my entire life. I growth as a science person, I proved my capacities, my patient, my limits and my self-confidence. I learned the real value of my friends, my family and the simple things of life that I left in my country Colombia. The most valuable knowledge is not only the one that I learn as a molecular biologist is the one that help me to improve my life to become a better person and reinforces my moral and my ethics. Nevertheless, none of this valuable life lessons would have been possible without the friendship and encourage of all my friends, family and supervisors.

I would like to acknowledge my Ph.D supervisors, Prof Dr. Bernd Mueller-Roeber and Dr. Salma Balazadeh for giving me the opportunity to make my Ph.D thesis in the group and introduce me in the fascinating world of plant molecular biology, let me grow as a scientist. I want to thank the DAAD (Akademischer Austausch Dienst) for the financial support, the opportunity to learn another language and the facilities to integrate me into the German culture. I am heartily thankful to the DAAD representative for Latin America, Arpe Caspary for his friendship, for believing in me and my capacities. I wish also to thank the former Colombia referat Mrs. Silke Hamacher for her efficient work and nice attitude.

I want to thank exclusively Dr. Judith Lucia Gómez-Porras. She careful read and editorial assisted my thesis. She established with me nutritive scientific discussions and her criticisms, support and humor were the most powerful inputs to complete successfully the final level of my Ph.D. I want to thanks Dr. Alex Ivakov and Matt Neville to point key aspects to improve the document. I want to thanks Dr. Francesco Licausi for stimulating discussions of the experiments, improvements on the document and his unconditional friendship. I received thoughtful suggestions, discussions and warm spiritual support from my Ph.D committee members Prof. Dr. Ingo Dreyer and Dr. Dirk Hincha. All of them directed me become a good scientist.

I would specifically like to thank Dr. Eugenia Maximova who always takes the time to help me in microscopy, Dr. Karin Köhl and her Greenteam especially Linda Bartetzko, Katrin Seehaus, Sven Roigk, Helga Kulka, Britta Hausmann and Katrin Lepa for taking excellent care of plants and transformations and giving me always a smile and good advices; Josef

Contents

List of figures

List of tables

Chapter 1

Introduction

1.1. General concepts of plant senescence and its regulation

The process of aging and senescence in humans and plants has been the focus of major studies for a long time (Breeze *et al*., 2011; Howard *et al*., 2009; Kirkwood and Austad, 2000; Lim *et al*., 2007; Thomas 2002). A primary motivation for this is to understand what controls the decline of tissue and organ functionality and reproduction ability when higher organisms age, and which factors determine the length of life. Certainly, both aspects have a broad spectrum of explanations ranging from an inherent genetic control present in each organism to external factors such as environmental conditions and natural selection. In the following, I will give an overview of current knowledge with respect to the physiological process of senescence in plants.

Two major theories of senescence are currently acknowledged and have been developed mainly in the animal field: the antagonistic pleiotropic theory and the mutation accumulation theory. Both theories suggest that two classes of mutations are responsible for senescence: those with beneficial early-life, but deleterious late-life effects; and late-acting mutations with purely deleterious effects (Jing *et al*., 2007; Kirkwood and Austad, 2000). In animals and yeast, those theories have been well demonstrated based on physiological and molecular studies on individuals at the population and species levels (Kirkwood and Cremer, 1982; Williams, 1957). Plants exhibit modular growth, exposes a propensity for vegetative reproduction, and can begin senescence in one or more organs at different times throughout the life-span of the plant. Without doubt, senescence in plants exposes particular features that do not fit well into these theories (Bleecker, 1998). In an effort to reconcile the theories about animals with plants, some authors have proposed to scale them down and treat an individual leaf as an autonomous entity (Thomas, 2002). I agree with the concept that has already been exposed by different authors in which leaf senescence is conceived as a detrimental consequence of an indirect selection for traits that favor nutrient salvage, remobilization, and reassimilation to optimize the plant genome for reproduction (Bleecker, 1998; Jing *et al*., 2007). This highly regulated and orderly process controls an efficient redistribution of

valuable resources (especially nitrogen and carbon) to other developing organs (Bleecker, 1998; Breeze *et al*., 2011; Buchanan-Wollaston 1997; Gan and Amasino, 1997).

The concepts described above are complemented by the fact that leaf senescence can be influenced by hormonal and developmental processes and is fuelled by experimental and modeling assays in which a differential expression of genes is evident among the whole process (Buchanan-Wollaston, 1997; Pontier *et al*., 1999). Despite the fact that plants suffer drastic ultrastructural changes during the breakdown of chloroplasts, a decrease of cytoplasmic volume and ribosomes, and the dismantling of various organelles, other cellular entities remain largely intact initially to guarantee effective gene expression and energy production during the senescence process. Thus, the plasma membrane, mitochondria, and the nucleus remain intact until the latest senescence stages (Gan and Amasino, 1997). Apart from environmental nutrition deficiency and other stresses, plants ultimately initiate and progress leaf senescence in an independent manner. *Arabidopsis thaliana* is a monocarpic model plant, in which senescence is controlled by the reproductive structures. The seeds are being produced while the plant starts to senescence, reusing the storage nutrients from photosynthetic tissues (Gan and Amasino, 1997).

During the reassimilation and dismantling process, plants exhibit a strong biochemical activity to degrade most of the macromolecules such as chlorophyll, proteins, and lipids. Later, different strategies are used to modulate the progression of senescence, like hormonal changes and redistribution of the metabolic flux, particularly with respect to nitrogen and sugars (Lim *et al*., 2003; Liu *et al*., 2008; Noodén and Guiamet 1996; Otegui *et al*., 2005; Quirino *et al*., 2000).

Following this line of argument, the functional characterization of senescence-regulatory networks and their underlying genes represents an appropriate way to further discern the ongoing processes during senescence. In addition, such an approach will allow studying senescence from a cross-kingdom phylogenetic view and will likely add to our understanding of the evolutionary paths through which senescence developed.

1.2. Dismantling of chloroplasts

Chloroplasts break down early during the senescence process, prior to the loss of mitochondria and nuclei (Lim *et al*., 2007), and concomitantly undergo a progressive decrease in photosynthetic rate. The major fraction of nitrogen (70-90%) exported from senescent leaves comes from the degradation of Rubisco, light-harvesting chlorophyll a/b-binding proteins, and proteins from Photosystem II (PSII) and Photosystem I (PSI) which are located in the stroma and thylakoid membranes (Morita, 1980). During chloroplast formation in young, growing leaves, pigments and proteins are assembled as active and interacting complexes; therefore, the dismantling of these complexes during senescence

is a prerequisite for the enzymatic degradation of the individual components. A series of characteristic events can be observed during senescence using electron microscopy, x-ray diffraction, and immunological and fluorescence techniques (Barton, 1966; Biswal *et al.*, 2003; Freeman *et al.*, 1978; Hurkman, 1979; Sundqvist and Dahlin, 1997; Suzuki *et al.*, 1997). One of the earliest changes is the disappearance of stacked grana regions followed by the elongation of lamellae. This distension is followed by massive degradation with a concomitant increase in the number and size of lipid droplets called plastoglobules and a swelling of the intrathylakoid space (Baker, 1992; Biswal, 1995; Biswal and Biswal, 1984; Matile *et al.*, 1999; Roberts *et al.*, 2003).

Recently, it was shown that chloroplasts remain outside of the vacuole, even at late stages of senescence, while the thylakoid membranes are internally dismantled. As thylakoids were dismantled, Rubisco large subunit protein (Lhcb1) and chloroplast DNA levels declined, but variable levels of mRNA persisted. This observation demonstrates that even though certain plastid components are degraded in the vacuole, the whole chloroplast was not transported into the vacuole for degradation, as suggested in previous studies (Evans *et al.*, 2009; Minamikawa *et al.*, 2001; Wittenbach *et al.*, 1982).

1.2.1. Control of chlorophyll catabolism

During autumn, it is common to see beautifully colored leaves. This is a result of the action of the catabolic pathway of chlorophyll (Chl), combined with the partial retention of carotenoids, and the accumulation and unmasking of colorless breakdown products with newly synthesized red anthocyanins and dark-colored oxidation products of phenolic compounds. Nevertheless, some authors propose that the removal of greenness in leaves has been underestimated, even though it is catalogued as the simplest and most easily measured index of leaf senescence syndrome (Thomas, 1997). Evidence indicates that the physiological pathway of yellowing is a robust and consistent component of the senescence syndrome and justifies its study in isolated organs and tissues in the plant (Ougham *et al.*, 2008). Chlorophyll degradation is a symptom of the transition of chloroplasts to gerontoplasts. A gerontoplast is defined as a distinctive senescence-specific form of plastids and is entirely catabolic. Developing gerontoplasts persist and remain intact throughout leaf senescence (Baker, 1992; Parthier, 1988). As leaf senescence proceeds, chlorophyll (Chl) levels decrease and photochemical efficiency of photosystem II and Rubisco protein levels decline (Evans *et al.*, 2009). Pathogen attack, as well as other biotic or abiotic stresses, can also accelerate premature leaf senescence and color change. Nevertheless, this pathological degreening has only a superficial resemblance to true senescence, proposed by some authors as "pseudo-senescence". According to these authors, pseudo-senescence differs from the senescence in its genetic and biochemical components. Furthermore, it seems that senescence maintains viability in tissues that would otherwise rapidly divert into the pseudosenescence pathway and, therfore, avoid premature cell death (Ougham *et al.*, 2008).

The catabolic pathway of chlorophyll (Chl) during senescence and fruit ripening leads to the accumulation of colorless breakdown products so called non-fluorescent chlorophyll catabolites (NCCs) (Hörtensteiner, 2006). During catabolism, chlorophyll follows a route that initiates when chlorophyll is separated from the binding proteins within the thylakoid membranes (Ougham *et al*., 2008). In the first proposed pathway, the chlorophyllase enzyme (Chlase) hydrolyses the ester linkage of the phytol chain to the porphyrin macrocycle of chlorophyll (Jacob-Wilk *et al*., 1999; Matile *et al*., 1999; Tsuchiya *et al*., 1999), releasing phytol and chlorophyllide. In a second step, magnesium dechelatase removes the Mg^{2+} ion from the tetrapyrrole, converting chlorophyllide to the chlorin molecule pheophorbide (Pheide a) (Shioi *et al*., 1996). Chlorophyll and its immediate catabolites are colored and strongly excited by ambient light. Thus, the catabolic route is organized in a way to avoid photodynamic damage by free pigments. The opening of the tetrapyrrole ring is a two-stage reaction which is catalyzed by PaO (Phaephorbide a oxygenase) and adds oxygen across the methine bridge between rings A and B (Hörtensteiner, 2006). A metal chelating substance (MCS) has been shown to be required for the activity of magnesium dechelatase (Tadashi, 2005). This pathway avoids the risk of photodamage, and the green color disappears when PaO opens the macrocycle of Pheide a (Rodoni *et al*., 1997) and the red chlorophyll catabolite (RCC), a photoactive red pigment, appears (Ougham *et al*., 2008). Immediately after this reaction, the RCC reductase abolished the photodynamic properties of RCC, resulting in the production of the colorless fluorescent Chl catabolite (pFCC) (Ougham *et al*., 2008; Schenk *et al*., 2007). The colorless linear product is exported from the plastid and in different ways depending on the plant species, may conjugate in the cytosol before being transported into the cell vacuole where the final chemical modification may take place (Hörtensteiner, 2006; Kräutler and Hörtensteiner, 2006; Tanaka and Tanaka, 2006). However, evidence inconsistent with this model has been presented by other authors. *AtCLH1* and *AtCLH2* are the only two Chlase genes reported in *Arabidopsis*, and it has been shown that (i) neither of these isoforms is localized to plastids, (ii) double knockout mutant plants are still able to degrade chlorophyll during leaf senescence (Schenk *et al*., 2007), (iii) their activity could be detected prior to the onset of senescence (Benedetti and Arruda, 2002), and (iv) increases in Chl synthesis are also accompanied by increases in Chlase activity (Roca and Mínguez-Mosquera, 2003). This inconsistence generated an alternative description of the pathway during senescence. This model postulates that the removal of Mg^{2+} to form pheophytin occurs first and is followed by the removal of the phytol tail, catalyzed by pheophytinase (PPH) without a direct interaction with chlorophyll. This perspective generated the idea that chlorophyll synthesis and breakdown are metabolically separated during leaf senescence, and a careful revision of proposed pathway, as well as new experiments, are suggested to clarify the pathway of chlorophyll degradation during leaf senescence (Eckardt, 2009).

As a final step, the nonfluorescent chlorophyll catabolites (NCCs) produced during the opening of Chl macrocycles are deposited into the vacuole with any recycling of the nitrogen contained within them (Hinder *et al*., 1996; Tommasini *et al*., 1998). This presupposes that

degradation is required in principle to facilitate access to more valuable materials present in thylakoid proteins and lipids and to detoxify the cell of these highly reactive compounds, maintaining the viability of the cell during the process and not a nutrient salvage (Buchanan-Wollaston *et al*., 2003; Matile *et al.,* 1999).

1.2.2. Chloroplast protein loss

Protein metabolism guarantees normal development and homeostasis in a plant cell. This complex process involves a broad spectrum of enzymes and manifold proteolytic pathways localized in different subcellular compartments (Grudkowska and Zagdanska, 2004; Vierstra 1996). Nitrogen exists mainly in chlorophyll and proteins. More than 75% of leaf protein is located within the chloroplast (Feller *et al*., 2008a). Rubisco is the most abundant protein on earth and contributes up to 50% of the soluble proteins and up to 30% of total leaf nitrogen in leaves of C3 plants (Ellis, 1979; Feller *et al*., 2008b). Some plant species are able to complete a life-cycle based on the initial supply of nitrogen during young developmental stages and eventually achieve good seed production. The most fundamental process in N-reabsorption is degradation of proteins, and its efficiency is close to 90%, thus being one of the most efficient of all metabolic pathways (Himelblau and Amasino, 2001; Mei and Thimann, 1984).

Many genes involved in protein turnover, such as proteases (e.g. cysteine and aspartic proteases) (Woo *et al*., 2004) and protein kinases, are significantly upregulated during senescence (Buchanan-Wollaston *et al*., 2005). All of the amino acids derived from protein catabolism during senescence may be redistributed within the plant via the phloem and serve as basis/raw materials for protein synthesis in other organs of the plant. During senescence, a preferential expression of a specific set of ''senescence-associated genes'' (SAGs) has been reported, and based on the functional classes involved, there are three principal pathways that might regulate protein degradation: the ubiquitin/proteasome system; the chloroplast degradation pathway; and the vacuolar and autophagic (APG) pathway (Liu *et al.,* 2008).

In the ubiquitin/proteasome pathway, the covalent attachment of the 76-amino acid protein ubiquitin is used as a signal to target specific proteins for degradation by the 26S proteasome (Smalle and Vierstra, 2004). The principal enzymes involved are an ubiquitin-activating enzyme (El), ubiquitin-conjugating enzyme (E2), and ubiquitin protein ligase (E3). Expression profile analysis during leaf senescence in *Arabidopsis* revealed a large number of genes of the ubiquitin-26S proteasome pathway, suggesting that ubiquitin-dependent proteolysis might be an important step in protein degradation outside the chloroplast (Park *et al*., 1998). It has been shown that *UBQ3* and *UBQ4* are the predominant polyubiquitin genes up regulated, while other ubiquitin-related protein genes are also highly represented (Lin and Wu, 2004).

Proteolysis of chloroplast proteins (Chlp) takes place during the transition from proplastid to plastid, or during senescence (Adam, 1996). Proteases localized to the stroma, the

thylakoid membrane, and the thylakoid lumen have been described (Adam *et al*., 2001). The *Arabidopsis* genome contains at least 23 genes predicted to encode Chlp proteases located in the stroma, and most of them have been described during leaf senescence (Adam *et al.,* 2001; Adam and Clarke, 2002; Gottesman, 1996; Liu *et al.,* 2008; Sakamoto, 2006). Nevertheless, degradation of the light-harvesting complex of Photosystem II (LHCII) is still poorly characterized, and the protease/proteases involved, as well as their exact role, remain to be uncovered (Liu *et al.,* 2008).

The autophagy (APG) pathway is a catabolic process that allows recycling of cytoplasmic components (including organelles) into monomers and is the last proposed pathway of protein degradation. Through this pathway, protein degradation occurs via micro or macroautophagy. In microautophagy, targeted cytosolic components are enclosed in lysosomal or vacuolar membranes via invagination (Klionsky and Ohsumi, 1999; Mukaiyama *et al*., 2002). By contrast, macroautophagy takes place in the cytoplasm and is initiated with the generation of membranes that can eventually fuse and form autophagosomes in which enclosed material can be transported into the vacuoles and degraded by vacuolar exo- and endoproteases, such as cysteine proteinase (*SAG12*), aspartic proteinase, serine proteinase, and other peptidases which are well documented during leaf senescence (Buchanan-Wollaston, *et al.,* 2003; Buchanan-Wollaston, *et al.,* 2005; Klionsky and Ohsumi, 1999; Lin and Wu, 2004). Recently, it has been reported that autophagosome formation requires essentially two ubiquitin-like proteins, ATG8 and ATG12, which conjugate with phosphatidylethanolamine (PE) and ATG5, respectively, forming ATG8-PE and ATG12-ATG5 complexes in higher eukaryotes (Geng and Klionsky, 2008). Other studies in wheat, soybean, tobacco, and *Arabidopsis* revealed the presences of vesicles in the cytoplasm that include Rubisco and/or Rubisco degradation products and other stromal proteins, and also small senescence-associated vacuoles involved in the degradation of chloroplast proteins (Chiba *et al*., 2003; Martínez *et al*., 2008).

1.2.3. Degradation of membrane components and lipid breakdown

In plants, like in other eukaryotes, lipids are used for membrane biogenesis, in molecular signaling, as a source of energy, and as a protective layer that does not permit desiccation and infection. The chloroplast and other organelles present in plant cells have the capacity to synthetize fatty acids and confer to plants not only a different lipid composition, but also a different metabolic pathway when compared to animal cells. Contrary to animal lipid bilayers, chloroplast and other plastids are largely composed of galactolipids, rather than phospholipids, as the predominant lipids in green tissues. The thylakoid membrane system is mainly composed of phosphatidylglycerols, whereas most of the limited phosphatidylcholine in chloroplasts is associated with their outer membrane (Cullis *et al*., 1996). These fatty acids cannot be transported for long distances in the plant; due to this, the only way to use them as a practical carbon reserve for growing tissues is through the conversion of acetyl-CoA to sucrose by beta-oxidation. The content of fatty acids in green leaves represents

around 5% of their dry weight and 10% of the total energy (Nishimura *et al*., 1993; Schmid and Ohlrogge, 2002).

It has been reported that the levels of monogalactosyl diglyceride, digalactosyl diglyceride, and phospholipid phosphatidylglycerol decline at the onset of leaf senescence accompanied by a progressive decrease as senescence advances. In contrast, waxes present in *Arabidopsis* leaves exhibited only a minor reduction during senescence (Ferguson and Simon, 1973; Fong and Heath, 1977; Harwood *et al*., 1982; Koiwai *et al*., 1981; Wanner *et al*., 1991; Yamauchi *et al*., 1986). Active metabolism of fatty acids is a typical feature of seed germination and seedling growth. In addition, the process is also necessary during senescence to guarantee the flux of stored carbon from leaves to other developing organs like seeds, and to eliminate negative effects of free fatty acids after the hydrolysis of lipids (Graham, 2008). Membrane disruption has been proposed to be a key event in plant senescence. One of the most characteristic features in membrane deterioration is a progressive decline of phospholipid levels with a relative enrichment of free fatty acids and sterols in the membranes, accompanied by an increase in the level of different enzymes (McKersie and Thompson, 1978; Thompson *et al*., 1982).

It is well documented that leaf peroxisomes are transformed directly to glyoxysomes during senescence (Nishimura *et al.,* 1993). The peroxisome of senescent leaves metabolize the fatty acids after hydrolysis by the β-oxidation pathway (Gerhardt, 1992). Lipid-degrading enzymes, such as phospholipase D (PLD), phosphatidic acid phosphatase, lipolytic acyl hydrolase, and lipoxygenase, constitute the first degradation machinery of membrane phospholipids (Thompson *et al*., 1998). Some of the products from lipid catabolism may serve as substrates for other reactions; this is the case for free linoleic acid that is released during membrane lipid degradation and later used for jasmonic acid biosynthesis (Creelman and Mullet, 1997).

When lipid-degrading enzymes degrade membrane phospholipids and release free fatty acids, the bilayer structure of the membrane is perturbed. This facilitates the action of other lipid-degrading enzymes like SAG101 acyl hydrolase, which was proposed to be one of the key enzymes during the onset of leaf senescence (Thompson *et al.,* 1998; Yang and Ohlrogge, 2009). In addition, some authors have suggested an additional nonenzymatic oxidation pathway that includes an autoxidation due to reactive oxygen species, such as superoxide anion, hydrogen peroxide, and hydroxyl radical (Fong and Heath, 1977; Paliyath and Droillard, 1992; Thompson *et al.,* 1998). Finally, plants can use the fatty acids from this step of lipid degradation to obtain energy by oxidation of the fatty acids. The glyoxylate cycle produces succinate and malate. These are converted to oxaloacetate, which then enters into the gluconeogenesis pathway to produce sugars and, ultimately, sucrose. This final product can then be transported by the phloem to other plant organs (Buchanan-Wollaston, 1997; Smart, 1994).

7

1.3. Integration of hormonal changes during leaf senescence

Senescence of different organs in the plant can be regulated by external and internal factors. Internal factors influencing senescence include the developmental stage as well as endogenous levels of phytohormones and other growth substances. These factors may act individually or in concert (He *et al*., 2001). In general phytohormones are able to promote or repress the senescence process. Cytokinin, auxin, gibberellic acid (GA), and polyamines are considered to delay senescence, whereas ethylene, abscisic acid (ABA), jasmonic acid (JA) and its derivative methyl jasmonate (MeJA), salicylic acid (SA), and brassinosteroids (BRs) are thought to be involved in its induction. Published data show an overlap between different hormone signaling pathways during normal plant development and in response to different abiotic and biotic stresses, making the study a real complex task (Lim *et al.,* 2001). Research on phytohormones and their influence on plant senescence is normally based on the external application of the hormone, the measurement of endogenous levels before and after the onset of senescence, and finally, molecular analysis in which modification of the phytohormone levels in specific organs is measured in mutants or transgenic lines. A vast amount of documentation is available on the effects of plant hormones during senescence. In the following, I present a brief overview of the documentation and try to highlight important findings regarding hormonal effects on senescence.

1.3.1. Hormones promoting senescence

A correlation between ethylene production and leaf senescence has been reported in several plant species. An increase in the level of ethylene promotes senescence and some of its specific components, such as the degradation of chlorophyll, proteins, and other macromolecules, a rise in the expression of different senescence associated genes (SAGs), and the enhancement of catabolic enzyme activities (Mattoo and Aharoni, 1988). Molecular analysis of the ethylene perception and signal transduction mutants *etr1* and *ein2* revealed an increase of the lifespan as a consequence of a delay in the onset of senescence (Aeong Oh *et al*., 1997; Grbic and Bleecker, 1995). Nevertheless, some authors have pointed out that ethylene, itself, is neither necessary nor sufficient for promoting leaf senescence in some species such as *Arabidopsis*. Furthermore, this hormone may promote senescence only in mature or old leaves, and in comparison to floral organs or fruits, its effect on leaves is considerably less pronounced (Grbic and Bleecker, 1995).

The second plant hormone responsible for the promotion of senescence is JA. Some studies of wild type *Arabidopsis* plants revealed that the exogenous application of this phytohormone might induce premature senescence in attached and detached leaves, but its exogenous application to mutant coi1 plants could not induce premature senescence, suggesting the importance of the complete signaling pathway to promote leaf senescence (He *et al*., 2002). Transcriptional analysis revealed an upregulation of genes involved in JA biosynthesis during

leaf senescence; but even when plants underproduce JA (in the case of JA mutants), there is no significant retardation in leaf senescence, and this hormone pathway probably plays just a secondary role or complements other signaling pathways during senescence (Gan and Amasino, 1997; Harms *et al.*, 1995).

SA is another hormone involved in plant senescence. Its role in the process has recently been documented. SA plays a role in the initiation of senescence and may share the same pathway as stress responsive genes. The endogenous levels of SA increase in parallel with the progression of senescence, and *Arabidopsis* plants with a deficiency of SA exhibit a retardation of senescence and changes in SAG expression (Abreu and Munné-Bosch, 2008; Morris *et al.*, 2000).

The last two plant hormones involved in the promotion of senescence are brassinosteorids (BRs) and abscisic acid (ABA). Despite evidence for a positive influence on the progression of senescence, their specific roles are still unclear. In the case of BRs, there is evidence for the induction of senescence by external application of 24-epibrassinolide (eBR). Furthermore, *Arabidopsis* mutants which lack BR, such as *det2* or *bri1*, show a leaf senescence phenotype (Bishop and Koncz, 2002; Clouse, 1997; Clouse *et al.*, 1996). In addition, reactive oxygen species (ROS) signaling may have links with the BR signaling pathway, and through this, may mediate BR-induced senescence.

1.3.2. Hormones delaying senescence

Cytokinins have the strongest effect on the longevity of plant organs, and their impact in delaying senescence is one of the most documented topics in plant physiology (McCabe *et al.*, 2001; Richmond and Lang, 1957). Modifications in cytokinin biosynthesis allowed detection of a delay of senescence in different plant organs and a significant increase in plant productivity (Gan and Amasino, 1995; Nelson, 1988), whereas reduction of the endogenous levels resulted in an acceleration of the process (Masferrer *et al.*, 2002). There is an inverse correlation between the endogenous cytokinin levels and senescence progression. Mutants carrying defects in the cytokinin biosynthesis pathway gave strong evidence of its effect in the retardation of senescence (Gan and Amasino, 1996). Due to the fact that cytokinins are implicated in a wide range of physiological processes in plants and are often influenced by developmental processes of other organs/tissues, the effect of this phytohormone depends on several external and internal factors and varies under different experimental conditions (Gan and Amasino, 1995; Gan and Amasino, 1996).

Auxins are the second group of plant hormones involved in the retardation of senescence; external application of the hormone delays senescence, and a negative correlation exists between the endogenous auxin levels and the degree of leaf senescence. Some of the

senescence features, like chlorophyll loss and protein degradation, were established by the application of either synthetic or natural auxins (Noodén and Leopold, 1988). A more recent study finds that overexpression of the *Arabidopsis thaliana YUCCA6* gene, which encodes a member of the flavin monooxygenase protein family that limits de novo auxin biosynthesis, exhibits the classic delayed, dark-induced and hormone-induced senescence in detached rosette leaves, as showed the mutant (Kim *et al.*, 2011).

The effects of gibberellins on natural senescence, and their relationship with senescence, are not fully understood. Experimental data suggested that GAs are able to inhibit mitotic and postmitotic senescence in pea apical buds (Zhu and Davies, 1997), and postmitotic leaf senescence in many other plant species. The mitotic, or proliferative senescence is defined when germline-like meristem cells lose their ability to undergo mitotic cell division. In contrast, the postmitotic senescence refers to an active degenerative process that occurs in organs such as leaves and floral petals (Gan, 2003).The increase in GAs by external application inhibits the degradation of chlorophyll, proteins, and/or nucleic acids in leaves (Noodén and Leopold, 1988). Among different kinds of gibberellins, GA4 has a strong effect in delaying leaf senescence in different species (Gan, 2010; Kappers *et al.*, 1998; Ranwala and Miller, 2000). Like other groups of hormones, the effect of GAs is highly dependant on many internal and external factors as well as the species being used for the study.

1.4. Abiotic and biotic stresses

Leaf longevity and abiotic stress are closely related terms, and strong evidence supports the model that both physiological plant traits are regulated by a partially overlapping set of complex molecular networks (Buchanan-Wollaston *et al.*, 2005; Breeze *et al.*, 2011). Stress is generally understood as the reaction of a biological system to extreme environmental factors that, depending on intensity and duration, may cause significant changes in the system (Godbold, 1998; Orcutt and Hale, 2000). Favorable or disadvantageous factors press the plants throughout their entire life. Plants are sessile organisms and cannot move away from adverse environmental conditions or perturbations. To compensate for this deficiency, plants have developed a variety of molecular strategies against biotic and abiotic stresses. According to this idea, each organism displays a specific genetic tolerance to a specific stress. The definition of stress is present in the cases where external changes exceed this tolerance, and plants must not only change their metabolism but also lose the equilibrium. Thus, the normal energy consumption, growth, development, and productivity are affected and finally cause bodily injury, disease, or aberrant physiology (Gaspar *et al.*, 2002; Mandre, 2002). Those biotic stressors are concerned with the mechanism of interaction between different species like in the case of diseases and herbivores; these are of particular interest to forest and agricultural systems (Orcutt and Hale, 2000). Abiotic stressors may be of physical or chemical character and include stresses associated with temperature, salinity, and drought, and they may act alone or in combination. (Mandre, 2002; Orcutt and Hale, 2000).

Various gene expression-profiling studies revealed that many genes encoding NAC transcription factors are induced during both natural and abiotic stress-induced senescence (Buchanan-Wollaston, 1997; Olsen *et al*., 2005; Uauy *et al*., 2006; Yang *et al*., 2001, 2003; Balazadeh *et al*., 2008b). Therefore, the functional characterization of senescence-associated NAC transcription factors may provide important information with respect to understanding senescence-regulatory pathways and their overlap with stress-response signaling pathways.

1.5. Regulation of gene expression: the role of transcription factors

The development of any organism depends on proper coordination of gene expression. The genetic information encoded in the DNA must first be converted into mRNA through the action of RNA polymerase II in a process called transcription; subsequently, the produced transcript serves as a template for the generation of a specific protein through translation. RNA polymerase II cannot bind directly to promoters and initiate transcription itself. Therefore, one of the most important points in this mechanism is the regulation of gene transcription via transcription factors (TFs). TFs are a very broad category of DNA binding proteins with a positive (activation) or negative (repression) effect on transcription. The central role of transcription in the process of gene expression is exemplified by general transcription factors (GTFs), such as TFIIA, TFIIB, TFIID, TFIIE, TFIIF, and TFIIH, present in eukaryotes. These are necessary not only for control in a large-scale regulation of different genes, but also for the initiation of transcription itself (Facciotti *et al*., 2007). A key challenge in genetic research is to understand how TFs bind the correct DNA sequence to control gene expression. Transcription establishes a control point for regulating gene expression and gives the ability to perform different functions by generating alternative splicing of the same transcript. Several factors are required to locate and orient the RNA polymerase correctly, and each is given by different time-specific molecular events at the end the expression of a gene. In addition to the GTFs, recognition and response to regulatory signals requires promoter-regulatory sequences (*cis*-regulatory elements). The specific recognition of a *cis*-element is given by the conformation and three-dimensional structure of the TF, allowing its DNA to bind. A multiprotein complex called transcriptional mediator, or mediator complex, is required to transmit signals from transcription factors to the RNA polymerase II initiation complex (**Fig. 1**) (Latchman, 2008).
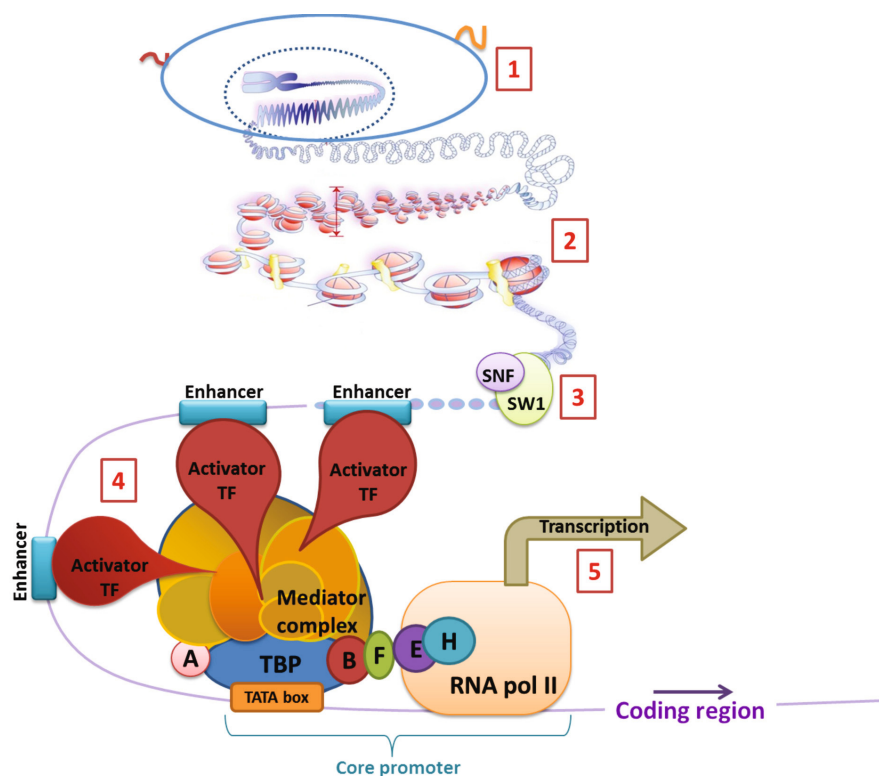
Figure 1. Schematic view of the molecular events in the expression of a gene. (1) Transduction of signals from the cell surface to the nucleus. **(2)** Beads on a string form of chromatin. **(3)** Nucleosome disassembly by SWI/SNF complexes and histone chaperones. **(4)** In combination with general transcription factors, RNA polymerase II forms the preinitiation complex (PIC). This complex is assembled at the core promoter region and is able to initiate transcription. The core promoter is the minimal promoter (approximately 34 bp up-stream of the start codon) which is required for transcription initiation. It is form by TBP (TATA binding protein), some activators (as TF), and some coactivators. Those factors are required to transmit regulatory signals from transcription factors to the RNA pol II. In addition to promoters, other regulatory regions, such as enhancers, may be required for full expression. **(5)** Gene transcription by RNA polymerase II.

TF families are classified based on structural similarities. The PlnTFDB (Plant Transcription Factor Database) reports 2657 protein models and 2451 distinct protein sequences of *Arabidopsis thaliana* arranged in 81 gene families (Pérez-Rodríguez *et al.*, 2010). Classification of those TFs is given on the basis of sequence similarities, most often in the DNA-binding domain (DBD) (Guo *et al.*, 2005). Within families, the members are similar to each other only in their DNA-binding. The names of the DBDs (e.g., AP2/ERF or EREBP, WRKY, NAC) are also used as the names of the transcription factor families. Frequently, the same family binds DNA in a sequence-specific manner, and this region is highly conserved. In contrast, the transcription regulatory domain (TRD) has been classified according to its amino acid profile, i.e., as acidic, glutamine-, proline- or serine/threonine-rich, and exhibits protein segments that determine the three-dimensional structure of the TF with a relative flexibility (Luscombe and Thornton, 2002; Skriver *et al.*, 2010; Tompa, 2005). The NAC transcription factors, along with the MYB, AP2/EREBP,

and bHLH proteins, are the largest families of transcription factors in the plant kingdom (Riechmann *et al*., 2000). The specificity of the DNA-binding activity could be modulated by the presence of more than one domain in a single TF as well as homodimerization or heterodimerization. Modifications like phosphorylation, glycosylation, nuclear transport, and oligomerization are important post-translation modifications that can control TF activity (Meshi and Iwabuchi, 1995).

1.5.1. Molecular regulation of senescence

Breakdown of different macromolecules, and their massive remobilization from senescent to young tissues, requires that cells retain their nuclear integrity to allow for effective transcription and further translation of proteins; thus nuclei remain intact until the very late stages of senescence. In the particular case of senescence, regulation of the process is reported to be strictly controlled by the molecular interaction of genes known as senescence associated genes (SAGs) and modulated by internal and environmental signals (Buchanan-Wollaston, 1997; Gan and Amasino, 1997). It is well known that its progression can be inhibited by enucleation and inhibitors of RNA and protein biosynthesis, and it is highly controlled by gene expression (Noodén and Leopold, 1988). There are more than 100 genes differentially up regulated during the process. Among them, NAC and WRKY TFs constitute a large proportion of the senescence-regulated genes already assigned to play an important role in *Arabidopsis* senescence (Balazadeh *et al*., 2008a,b; Breeze *et al.,* 2011). Despite the importance of senescence, few SAGs have been completely characterized; some of them, like *SAG12* (encoding a cystein protease), *SAG13* (oxidoreductase), *SAG101* (acyl hydrolase) from *Arabidopsis* (He and Gan, 2002), and *LSC54* (a gene encoding methallothionein) from *Brassica napus* (Buchanan-Wollaston, 1994) are highly upregulated during the onset and progression of senescence. Nevertheless, their expression is not exclusive to the senescence process, and expression of *SAG12* and *SAG13* was also reported in floral organs. Other genes involved in the genetic control of senescence, like the *senescence-associated gene 1* (*SEN1*), are detectable during all stages of leaf development but show a significant increase in expression during senescence (Gan and Amasino, 1997).

1.5.2. The NAC transcription factor family

The NAC transcription factor family was first reported as the *RESPONSIVE TO DEHYDRATION 26* (*RD26*) gene in *Arabidopsis*. The name "NAC" has been derived from the first letters of the first three genes described as containing the NAC domain: (i) the petunia gene *NAM* (no apical meristem); (ii) *ATAF1/2*; and (iii) *CUC2* (cup-shaped cotyledon) from *Arabidopsis* (Miyoshi *et al*., 2002; Nakashima *et al*., 2007; Yamaguchi-Shinozaki *et al*., 1992). NAC proteins appear to be widespread in plants. For example, the genome of *Arabidopsis thaliana* contains around 100 NAC-encoding genes, whereas NAC

13

genes appear to be absent from algae and other eukaryotes, indicating that the family has emerged from an event likely related to the water-to-land transition in plants along with the challenges that this transition may have imposed (*Arabidopsis*, 2000; Lang *et al*., 2010; Ooka *et al*., 2003; Riechemann *et al*., 2000). NAC transcription factors are related to a variety of plant-specific processes, such as development of plant-specific organs (Aida *et al*., 1997; Souer *et al*., 1996), responses to plant hormones (Greve *et al*., 2003; Xie *et al*., 2000; Yang *et al*., 2011), and responses to drought and high salinity stresses (Balazadeh *et al*., 2008b; Balazadeh *et al*., 2010a,b; Seki *et al*., 2002; Yamasaki *et al*., 2008). Analysis of conserved amino acid residues and construction of a phylogeny with the conserved NAC domain in *Arabidopsis*, rice, lycophyte (*Selaginella moellendorffii*), and moss (*Physcomitrella patens*) gave strong support for an early appearance of NACs in an ancient plant lineage, which probably emerged after the separation of lycophytes and other vascular plants prior to the separation of monocots from dicots (Nakashima *et al*., 2011). Crystallography and global transcriptional analysis not only revealed a structural similarity, but also demonstrated that the NAC domain lacks a classical helix–turn–helix motif, and it possesses a new type of TF-fold consisting of a twisted beta-sheet that is surrounded by a few helical elements (Olsen *et al*., 2005b).

The typical NAC domain (DNA-binding domain) is located in the N-terminal region and is divided into five conserved regions, or subdomains (A to E), containing around 150 amino acids (Ooka *et al*., 2003; Yamasaki *et al*., 2008). This domain also contains a nuclear localization signal. In contrast, the variable C-terminal region contains a transactivation domain and exhibits protein-binding activity (Seo *et al*., 2008; Tran *et al*., 2010; Yamasaki *et al*., 2008) (**Fig. 2.A**). Additionally, some NACs from *Arabidopsis* and rice have been shown to contain α-helical transmembrane motifs in the terminal part of the C-terminal region. These motifs help the proteins anchor to intracellular membranes, and at the same time, make them inactive; only through controlled proteolytic cleavage from this anchor can the proteins recover their activity and exert their functions (Kim *et al*., 2007). Even though NAC proteins share a common structure, recent studies revealed few atypical NAC genes that show variations from the usual structure. Some encoded only the NAC domains, while others exhibit a C-terminal NAC domain with variable regions in the terminal part of the N-terminal region (Christiansen *et al*., 2011; Ooka *et al*., 2003) (**Fig. 2.B**).
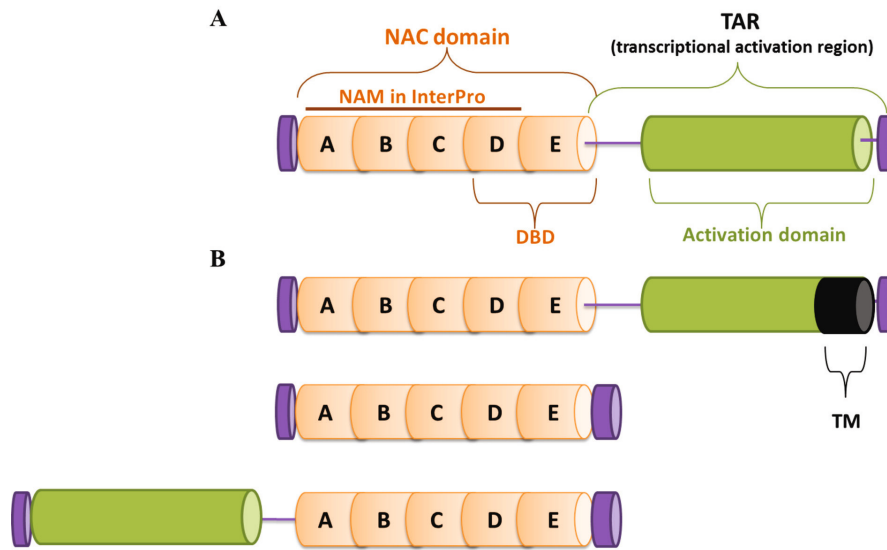
Figure 2. Structural characteristic of NAC proteins. (A) The highly conserved NAC domain is located at the N-terminal region and consists of five sub domains (A to E). The C-terminal region includes a highly divergent transcriptional activation region. **(B)** Structural modifications of the typical NAC protein. Some NAC proteins exhibit transmembrane domains (TM) in the C-terminal region. Other NACs encode only the NAC domain or have the NAC domain in the C-terminal region. Modified from (Christiansen *et al*., 2011; Ooka *et al*., 2003).

The molecular characterization of NAC proteins began with the report of two NAC proteins that were able to activate the Cauliflower Mosaic Virus (CaMV) 35S promoter in yeast (Souer *et al.,* 1996), and it was followed by the characterization of *NAC1*, *AtNAM* and *ANAC019* in *Arabidopsis*, and others in *Brassica napus* (Duval *et al*., 2002; Ernst *et al*., 2004; Hegedus *et al*., 2003; Xie *et al*., 2000). Later, the core sequence (CACG) was identified as the DNA motif recognized by the ANAC proteins *ANAC019*, *ANAC055*, and *ANAC072* that allows their binding to a fragment of the *ERD1* (*EARLY RESPONSE TO DEHYDRATION STRESS 1*) promoter (Tran *et al*., 2004). One year later, the consensus binding sequences of three members of the NAC family were determined by two different methods. The DNA protein binding (DPB)-CelD-fusion method was used to identify the consensus sequence of the wheat TF *TaNAC69*, a homologue of *AtNAP* from *Arabidopsis* (Xue, 2005), and the CASTing (cyclic amplification and selection of targets) method allowed the identification of the core binding sequence (CGT(G/A)) of *ANAC019* and *ANAC092* (Olsen *et al*., 2005a). After determinating the core sequence, electrophoretic mobility gel shift assays (EMSAs) confirmed that NAC domains are able to bind to a sequence containing one identified binding site (CGTG) and a sequence containing two identified binding sites in a palindromic orientation (TTGCGTGTTNNCACGCAA) (Olsen *et al*., 2005a). One of the most recently characterized NAC genes is *ORS1*, a paralog of *ANAC092* that positively regulates senescence through a regulatory network that might be involved in the cross-talk between salt and H_2O_2-dependent signaling pathways. Determination of its consensus binding sequence was reported and analyzed among *ORS1* down-stream genes (Balazadeh *et al*., 2011).

The large number of biological processes regulated by NAC TFs in plants not only highlights their general importance in plant biology, but also indicates that its functional characterization will provide valuable information about the initial inputs and final outputs through which plants regulate the senescence syndrome.

1.6. Aim of the thesis

Leaf senescence is a complex developmental process that delimits the lifespan of one of the most important organs responsible for photosynthesis in plants. During senescence, leaves undergo a massive degradation process that affects all of their physiological traits including their photosynthetic capability. Leaf senescence requires a tight control that ensures the synchronous dismantling of the cellular components, relocation of the degraded products, and maintenance of the nucleus integrity in the leaf until the very end. Primarily, senescence regulatory genes and their signaling networks must be fully characterized to understand senescence as an integrative process. The progress in the plant senescence field must later be extended to practical approaches to improve food longevity and decrease food losses in all stages of the crop postharvest system, as well as to understand the environmental factors that cause precocious senescence, which makes plants more susceptible to diseases and plagues.

My contribution to this ambitious idea is contained in the main objective of my thesis: unravel the signaling cascade through which ORE1, a key regulator of leaf senescence, exerts its function. To this end, I analyzed particular features of *ORE1* up-stream and down-stream regulatory pathways.

Chapter 2

Unraveling the up-stream regulatory pathway of *ORE1*

"A gene regulatory network controlled by the NAC transcription factor
ANAC092/AtNAC2/ORE1 during salt-promoted senescence"

Balazadeh, S., Siddiqui, H., Allu, A.D., **Matallana-Ramirez, L.P.,** Caldana, C., Mehrnia,
M., Zanor, M.I., Köhler, B. and Mueller-Roeber, B.

[1] University of Potsdam, Institute of Biochemistry and Biology, Karl-Liebknecht-Straße 24-25, Haus 20, 14476 Potsdam-Golm, Germany, and [2] Max-Planck Institute of Molecular Plant Physiology, Am Mühlenberg 1, 14476 Potsdam-Golm, Germany

2.1. Introduction

The plant transcription factor *ORE1* (At5g39610) has been reported to play a key role in natural and induced senescence in *Arabidopsis* (Kim *et al*., 2009; Balazadeh *et al*., 2010a,b; Breeze *et al*., 2011). A general approach to unravel transcriptional regulatory pathways includes the analysis of the up-stream signaling pathways that control the expression of the respective gene. Besides others, this involves the identification of *cis*-regulatory elements (CREs) present in the promoters of the genes under analysis and, subsequently, the search for TFs that bind to them. Currently, CREs of the *ORE1* promoters are poorly characterized. There are only one up-stream regulator of *ORE1* described thus far: *miR164*. This regulation corresponds to a trifurcate feed-forward regulation that involves *EIN2, miR164*, and *ORE1* (Kim *et al*., 2009). EIN2 is a membrane-spanning protein whose biochemical functions are still unknown, but genetic studies indicate that it is absolutely required for ethylene signaling (Alonso *et al*., 1999; Kim *et al*., 2009). It has been shown that ORE1 expression increases in an age-dependent manner, apparently through induction by *EIN2. miR164*

targets *ORE1* and down-regulates its expression. However, expression of *miR164* decreases with age through an unknown mechanism. This complex regulatory mechanism suggests that *ORE1* expression is tightly regulated to avoid up-regulation in young leaves that lead to premature senescence and cell-death (Kim *et al.*, 2009). The MADS-box transcription factor *SEPALLATA3* (*SEP3*) was characterized based on a genome-wide DNA-binding profile and targets ORE1. Chromatin immunoprecipitation (ChIP), followed by ultrahigh-throughput Solexa sequencing (ChIP-seq), were used to obtain direct target genes of *SEP3* and construct a framework for a hierarchical transcriptional network underlying the formation of floral organs. Interestingly, the study determined that *SEP3* binds *in vivo* to the *ORE1* promoter. Nevertheless, the biological relevance of this interaction remains unknown (Kaufmann *et al.*, 2009). Understanding how the expression of *ORE1* is modulated is essential to reconstruct its regulatory network and provide information on the molecular mechanisms that control senescence in *Arabidopsis*.

2.2. Results

2.2.1. Tissue-specific expression of *ORE1* is conserved in *Arabidopsis thaliana* and *Nicotiana tabacum*

Reporter genes were used to investigate the tissue-specific expression of *ORE1* transgenic lines harboring a 1.5 kb sequence up-stream of the start codon ATG fused to the *Staphylococcus β-glucuronidase* (*GUS*). *Prom1-ORE1:GUS* constructs were transformed into *A. thaliana* ecotype Col-0 and *N. tabacum* L. cv. Samsun plants. Independent transgenic lines of the T4 and T5 generations were used to assess the GUS activity mediated by the *ORE1* promoter. We identified conserved expression patterns in both species among different organs and tissues. Representative expression patterns are shown in **Figure 3**. In both species, the expression of GUS was observed in most tissues from early stages right after germination to the end of the plant´s life cycle. Strong and rapidly appearing GUS activity was observed in mature embryos extracted from seeds (detected already after 30 minutes of staining) and in cotyledons (**Fig. 3. Panel A.a-f**). Embryos were extracted after imbibition in water for 10 hours to avoid damage of the tissues while removing the testa. The expression of the *ORE1* promoter in cotyledons and in the tip and margin regions of the leaves in young seedlings (15-day-old) was in accordance with reported progression of aging from the tip to the base of the leaves (**Fig. 3. Panel B.a-b**) (Hill, 1980). In primary roots, we observed *ORE1* promoter-driven GUS staining particularly in the columella root cap (**Fig. 3. Panel B.c-d**). GUS activity was absent in young leaves (data not shown). In contrast, older leaf parts exhibited the same expression patterns detected on seedling leaves (tip and margin regions) when senescence became apparent. *GUS* staining was evident in response to mechanical damage in mature leaves in both species (**Fig. 3. Panel C and D.c-d**). Expression was also detected in floral organs, especially in sepal and petal tips and mature anthers in *Arabidopsis* and tobacco. Strong GUS activity was detected in
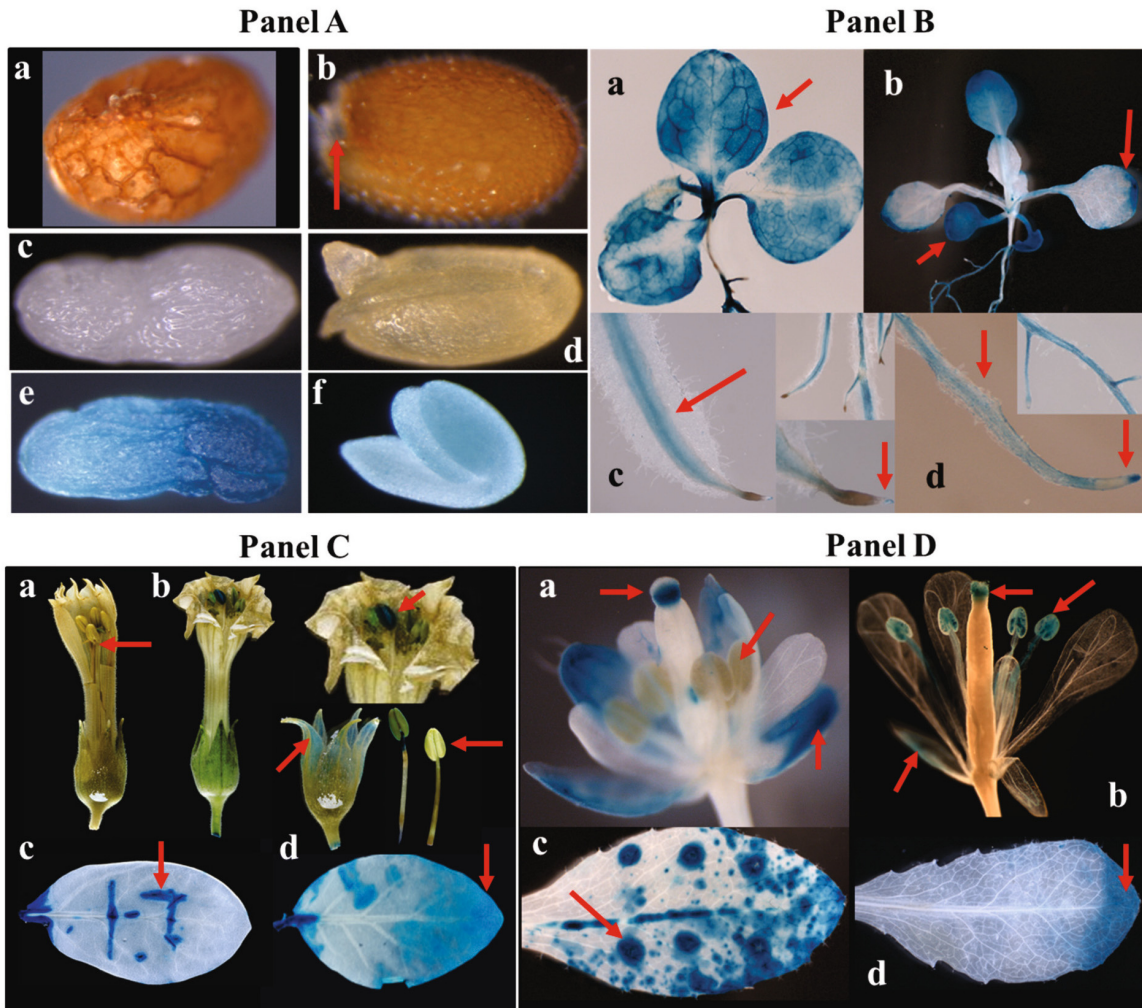
Figure 3. ORE1 driven GUS expression in tobacco and *Arabidopsis*. Panel A. (**a**) Tobacco and (**b**) *Arabidopsis* seeds with testa. Faint GUS staining was detected near to the testa rupture site in *Arabidopsis* (indicated by arrow). (**c-d**) Tobacco and *Arabidopsis* mature embryos without testa before *GUS* staining, respectively. (**e-f**) The same embryos after GUS staining (30 minutes). **Panel B**. (Upper corner right). (**a**) Tobacco seedling (15-day-old) after 12 hours GUS staining. (**b**) *Arabidopsis* seedling (15-day-old) after one hour GUS staining. Strong GUS activity was detected in both species in cotyledons and the tip regions of leaves in *Arabidopsis* (indicated by arrows). (**c**) Tobacco and (**d**) *Arabidopsis* main roots from seedlings (15-day-old). Strong GUS staining in the columella root cap and among the roots covering the elongation zone (indicated by arrows). **Panel C**. (Lower corner left) (**a**) Young tobacco flower. Promoter GUS expression was absent in immature anthers and was weak in the stigma papillae and tip region of the sepals (indicated by arrows). (**b**) Mature tobacco flower exhibited strong promoter GUS activity in mature anthers and faint activity in sepal tips (indicated by arrows). (**c-d**) Mature leaves from tobacco showed strong GUS activity in the tip of the leaves and also in response to mechanical damage. **Panel D**. (Lower corner right) (**a**) *Arabidopsis* unfertilized flower at stage 12 of development into mature plant (28-day-old) showing strong GUS activity in tips of sepals and in upper part of stigma corresponding to the stigmatic papillae. GUS activity was absent in immature anthers (indicated by arrow, flower was opened for picture). (**b**) Open flower from mature *Arabidopsis* at stage 15 of development exhibiting strong GUS activity in mature anthers and faint activity in tip region of sepals. (**c-d**) *Arabidopsis* leaves from mature plant (40-day-old). GUS promoter activity detected in response to mechanical damage (left) and in tip region of the leaves corresponding to oldest tissue (right).

the stigma at the stigmatic papillae in unfertilized *Arabidopsis* young flowers at stage 12 of floral development. This was when the stigmatic papillae was visible, the petals reach the height of the medial stamens, and anthesis had not yet taken place (Smyth *et al*., 1990). In a mature plant at stage 15 (28 days old), strong GUS activity was also detected in the stigmatic papillae of mature stigma in the opened mature flowers when stigma extended above the long anthers (Ferrándiz *et al*., 1999) Immature anthers and petals did not show any GUS activity in *Arabidopsis* or tobacco (**Fig. 3. Panel C-D.a**). Expression was also detected in floral organs, especially in sepal tips and mature anthers in *Arabidopsis* and tobacco.

2.2.2. *ORE1* controls dark-induced senescence in *Arabidopsis*

It is well established that senescence can be triggered and enhanced by endogenous and exogenous factors (Bleecker, 1998; Buchanan-Wollaston *et al*., 2005; Gan and Amasino, 1997; Gepstein *et al*., 2003; Howard *et al*., 2009; Weaver and Amasino, 2001). Despite the relevance of light as an exogenous factor involved in both senescence inhibition and promotion, the regulatory pathways involved in those processes are not well understood (Biswal and Biswal, 1984; Noodén and Guiamet, 1996; Weaver and Amasino, 2001). Based on published studies, the absence of light is more commonly considered an inducer of senescence. The artificial induction of senescence has been reported in detached leaves placed for several days in the dark (Weaver and Amasino, 2001). Several genes associated with dark-induced senescence have been identified in *Arabidopsis* (Blank and McKeon 1991; Kleber-Janke and Krupinska 1997; Buchanan-Wollaston *et al*., 2005; Van Der Graaff *et al*., 2006). To test whether *ORE1* plays a role in dark-induced senescence, *Arabidopsis* wild type plants, as well as *35S:ORE1* overexpressor line and the *anac092-1* T-DNA insertion mutant (Balazadeh *et al*., 2010a), were assayed. As an additional control, plants transformed with an empty vector (E.V.) were included.

Senescence was artificially induced in *Arabidopsis* leaves by darkness. Detached leaves from 27-day-old plants corresponding to the lines described above were incubated for four days. Leaves were placed on moist filter paper and incubated at room temperature. As a control, detached leaves from the same lines were placed on moist filter paper under long-day photoperiod (16 hours of light; 8 hours of darkness). As seen in **Figure 4**, wild type *anac092-1* T-DNA insertion mutant and empty vector (E.V.) control leaves that were kept in a long-day photo period showed only slight yellowing in some leaves. Moreover, the tissue became dry in comparison to leaves placed in darkness. When compared to control detached leaves (E.V.), senescence was notably pronounced in leaves from the *35S:ORE1* overexpressor line that had been placed in darkness. Senescence was inhibited in leaves from the *anac092-1* T-DNA insertion mutant when compared to wild type leaves that had been placed in darkness. Thus, we suggest that *ORE1* constitutes a key transcriptional regulator of the dark-induce senescence network.
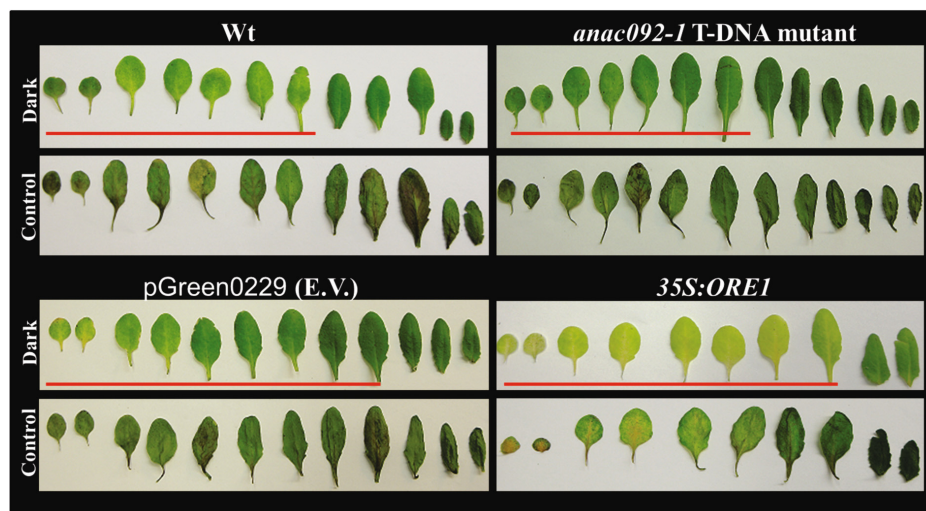
Figure 4. *ORE1* overexpression enhances the effect of dark-induced senescence in *Arabidopsis* leaves. Detached leaves from 27-day-old plants from wild type (Wt), *anac092-1* T-DNA insertion mutant, *35S:ORE1* overexpressor line, and Empty Vector (E.V.) control were placed in the dark. Leaves from E.V. and Wt served to compare the effect on *anac092-1* T-DNA insertion mutant and *35S:ORE1* overexpressor line, respectively. Control detached leaves from each tested line were placed in moist filter paper in open boxes. Overexpression of *ORE1* enhanced dark-induced senescence, whereas senescence was delayed in the *anac092-1* T-DNA insertion mutant. Underlined detached leaves exhibited the clearest comparative patterns.

2.2.3. Salt stress enhances *ORE1* expression

Screening of microarrays from public repositories revealed that *ORE1* was induced by salt stress in roots and shoots of *Arabidopsis* (Hruz *et al*., 2008; Winter *et al*., 2007). Furthermore, He *et al*. (2005) reported that intact ethylene and auxin signaling pathways are required for salt stress responsiveness in seedlings. To test if the response of *ORE1* to salt stress is regulated at the transcriptional level, *Arabidopsis Prom-ORE1:GUS* lines were grown on Murashige-Skoog (MS) (Murashige and Skoog, 1962) agar plates without salt. After 15 days, seedlings were transferred for 40 hours to a liquid MS medium containing 150 mM NaCl. GUS activity was enhanced in salt-treated seedlings compared to untreated controls (**Fig. 5.g-h**). We also analyzed *ORE1* promoter activity in transgenic tobacco plants (*Nicotiana tabacum*). Elevated GUS activity was observed in salt-treated (150 mM NaCl) leaves and other tissues including anthers, sepals, and petals (**Fig. 5.a-f**). The elevated expression of *ORE1* detected by histochemical analysis was confirmed by fluorometric measurements using 4-methylumbelliferyl-beta-D-glucuronide (4-MUG) and qRT-PCR (detailed information about these experiments has been published in Balazadeh *et al*., (2010)).
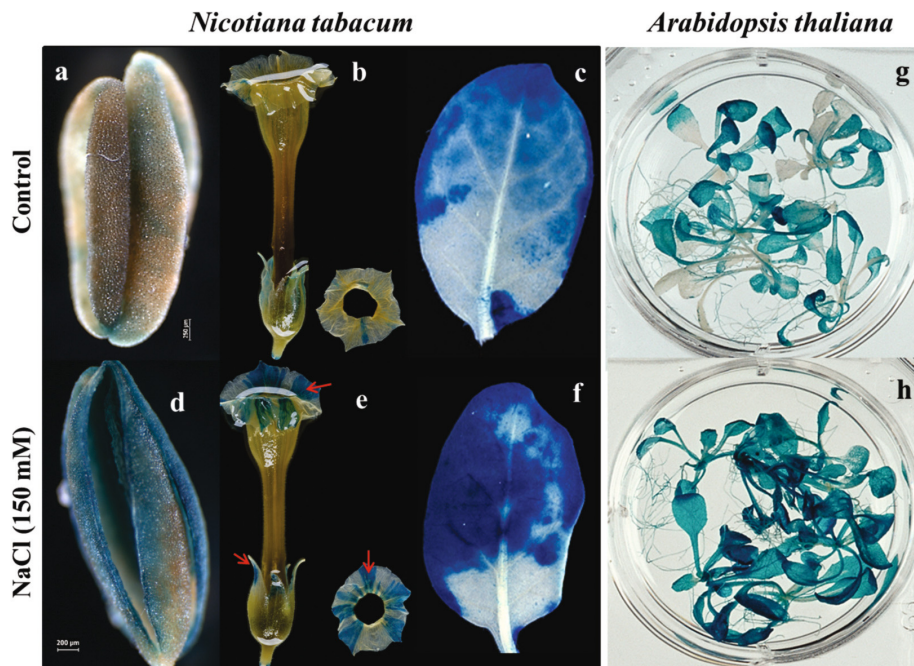
Figure 5. Salt stress activates transcription of the *ORE1* promoter. Left panel. GUS expression in different tobacco organs. (**a**) Anther, (**b**) flower, and (**c**) leaves were placed in water for 40 hours as controls. (**d-f**) Enhanced GUS activity in leaves and floral organs after 40 hours of salt treatment (150 mM NaCl). **Right panel**. Two-week-old *Arabidopsis* seedlings were treated for 40 hours with (g) 0 mM NaCl (Control) or (h) 150 mM NaCl.

2.2.4. *ORE1* senescence-specific expression is regulated by *cis*-elements in the 5'UTR

The specific relationship among gene regulatory networks is dependent on direct interactions between transcription factors and *cis*-regulatory elements (CREs) in promoter regions. One major area of study focuses on the understanding of the interaction between transcription factors and different CREs. Some well characterized CREs include the abscisic acid-responsive element (ABRE) (Marcotte Jr *et al*., 1989; Mundy *et al*., 1990), the dehydration-responsive element (DRE) (Yamaguchi-Shinozaki and Shinozaki, 1994), the C-repeat motif (Baker *et al*., 1994), and the W-box (Rushton *et al*., 1996), among others. Therefore, the elucidation of CREs that confers specificity in the expression of a given TF is crucial to understanding its regulatory pathway.

To gain further insights into the regulation of *ORE1* expression, promoter deletions were made to narrow down regions that confer the specific expression patterns observed (see patterns in **Fig. 3**). Results obtained with the long version of the *ORE1* promoter (1.5 kb) were described above (**section 2.2.1**). Two principle criteria were used to select the positions for the promoter deletions: (i) the presence of conserved sequences within the *ORE1* promoter, taking into consideration sequences that are present in orthologous promoters

22

from other plant species (**Fig. 6.A**); and (ii) the locations of CREs predicted to be present in the promoter (**Table 1**).

We produced two deletions that encompassed 230 bp (*Prom2-ORE1:GUS*) and 120 bp (*Prom3-ORE1:GUS*), respectively, up-stream of the start codon ATG, and transformed *Arabidopsis* plants. GUS staining patterns were determined in transgenic plants and compared with those obtained in plants harboring the 1.5 kb long up-stream region fused to the *GUS* reporter gene. The expression patterns were conserved in at least 70% of the evaluated plants (*Prom2-ORE1:GUS*; data not shown). The only visible difference between lines was a slight reduction in GUS activity in some senescent tissues, like leaves and cotyledons, of plants carrying the shortest version of the *ORE1* promoter (*Prom3-ORE1:GUS*) (see **Fig. 6**). Balazadeh *et al*., (2011) analyzed conserved regions of *ORE1* up-stream of the ATG (1 kb up-stream of the ATG). This region included the 5'UTR regarded as a specific, highly conserved marker segment. Nevertheless, the analysis of the two truncated promoters described above suggested that a region proximal to the ATG is important to confer *ORE1* senescence-specific expression observed in leaves. Thus, we performed a comparative promoter analysis. First, we searched for clade orthologs of *ORE1* that exhibited high amino acid similarity using the Phytozome webpage (Goodstein *et al*., 2012). The program performed a sequence alignment of all proteins in the platform against the sequence of *ORE1*. Any peptide similar to *ORE1* was listed with its percentage of similarity in parenthesis. *Arabidopsis lyrata* (97.2%), *Capsella rubella* (81.8%), *Brassica rapa* (89.8%), *Manihot esculenta* (69.5%), *Populus trichocarpa* (67.7%), and *Vitis vinifera* (67.7%) proteins were selected based on the highest similarity to *ORE1* from the species listed. The up-stream sequences of these genes, corresponding to the peptides, were retrieved and compared to the *ORE1* promoter (120 bp up-stream of the ATG). The MEME Suite web server (Bailey *et al*., 2009) searched for conserved motifs to predict conserved putative regulatory elements (Bailey*et al*., 2009). As shown in **Figure 6.A**, the selected up-stream sequences share conserved motifs among different plant species and may be taken as putative CREs important for *ORE1* tissue-specific expression. The program allowed us to define three different conserved motifs, although only the first and second motifs were present in *Arabidopsis thaliana*. Notably, the first motif identified in *Arabidopsis* is similar to the LE~5UTR-Py-rich stretch motif. This motif has been described as a CRE that confers a high transcription level without the need for further up-stream CREs except for a TATA-box (Daraselia *et al*., 1996; Lescot *et al*., 2002). Furthermore, this motif consists of highly conserved *ORE1* putative orthologs. The second motif is similar to a described light responsive AAAC-motif, and is placed around 50 bp up-stream of the ATG; it is only conserved between *Arabidopsis thaliana* and *Capsella rubella*. We performed a CRE analysis to identify previously described CREs present in the *ORE1* promoter (1.2 kb) (**Table 1**). This analysis led us to identify two LE~5UTR-Py-rich stretch motifs in the 5'UTR of *ORE1*. Despite the high similarity between the promoters of *ORE1* and *ORS1* (70%) (Balazadeh *et al*., 2011), *ORS1* does not have a LE~5UTR-Py-rich stretch motif in the proximity of the ATG (data not shown). The motifs obtained by MEME

are similar to some CREs that have already been described. As shown in **Figure 6.A**, the region 100 bp up-stream of the ATG showed the presence of a motif highly similar to the LE~5UTR-Py-rich stretch motif (exact location -111 bp) and a second motif similarity to the AAAC-motif that corresponds to a light responsive motif (exact location 50 bp up-stream of the ATG).

To test if the CREs identified in silico may have relevance *in vivo*, we designed new deletions. The final constructs were designated *Prom4-ORE1:GUS*, *Prom5-ORE1:GUS*, and *Prom6-ORE1:GUS*. The regions covered by these constructs are schematically shown in **Fig. 6.B**. Three independent lines per construct were selected for further analysis. *Prom6-ORE1:GUS* lines that lacked the entire 5'UTR showed highly reduced GUS activity that was in some cases almost undetectable (see **Fig. 6.B**). In contrast, *Prom3-ORE1:GUS* lines, carrying a small fragment of the 5'UTR (120 bp) where one LE~5UTR-Py-rich stretch motifs lay, showed *GUS* activity in the tip and margin regions of senescent leaves (**Fig. 6.B**) and in cotyledons of seedlings (data not shown). Both expression patterns are characteristic features of the senescence syndrome. In **Figure 6.B**, it is shown that *Prom5-ORE1:GUS* lines carrying the same up-stream region as *Prom6-ORE1:GUS* lines, plus a short region of the 5'UTR, have the characteristic *ORE1* expression pattern in senescence leaves. The part of the 5'UTR present in *Prom5-ORE1:GUS* contains the other LE~5UTR-Py-rich stretch motif. Our data clearly show that *ORE1* promoter activity was highly dependent on the presence of the 5'UTR. In particular, the two LE~5UTR-Py-rich stretch motifs appeared to be necessary for the tissue-specific expression of *ORE1* during senescence. Nevertheless, a visible reduction of GUS activity in *Prom5-ORE1:GUS* and *Prom3-ORE1:GUS* lines suggests that other CREs outside the 5'UTR are needed to reach the high expression levels during senescence. Interestingly, the *ORE1* promoter contains more than 13 motifs described as light responsive elements and circadian regulatory elements within the first 1.0 kb up-stream of the ATG. One heat stress responsive element (HSE), a drought regulator element (MBS), and three TC-rich repeat elements involved in defense and stress responses are also predicted in the up-stream region (**Table 1**). These data are in good agreement with our findings regarding dark-induced senescence (see **section 2.2.2**) and *ORE1* activity in wounded leaves (see **section 2.2.2**) and in response to salt stress (see **section 2.2.3**). Further experiments are required to confirm which of these predicted CREs are, in fact, involved in dark-induced, salt stress, and wounded responsiveness of *ORE1*.
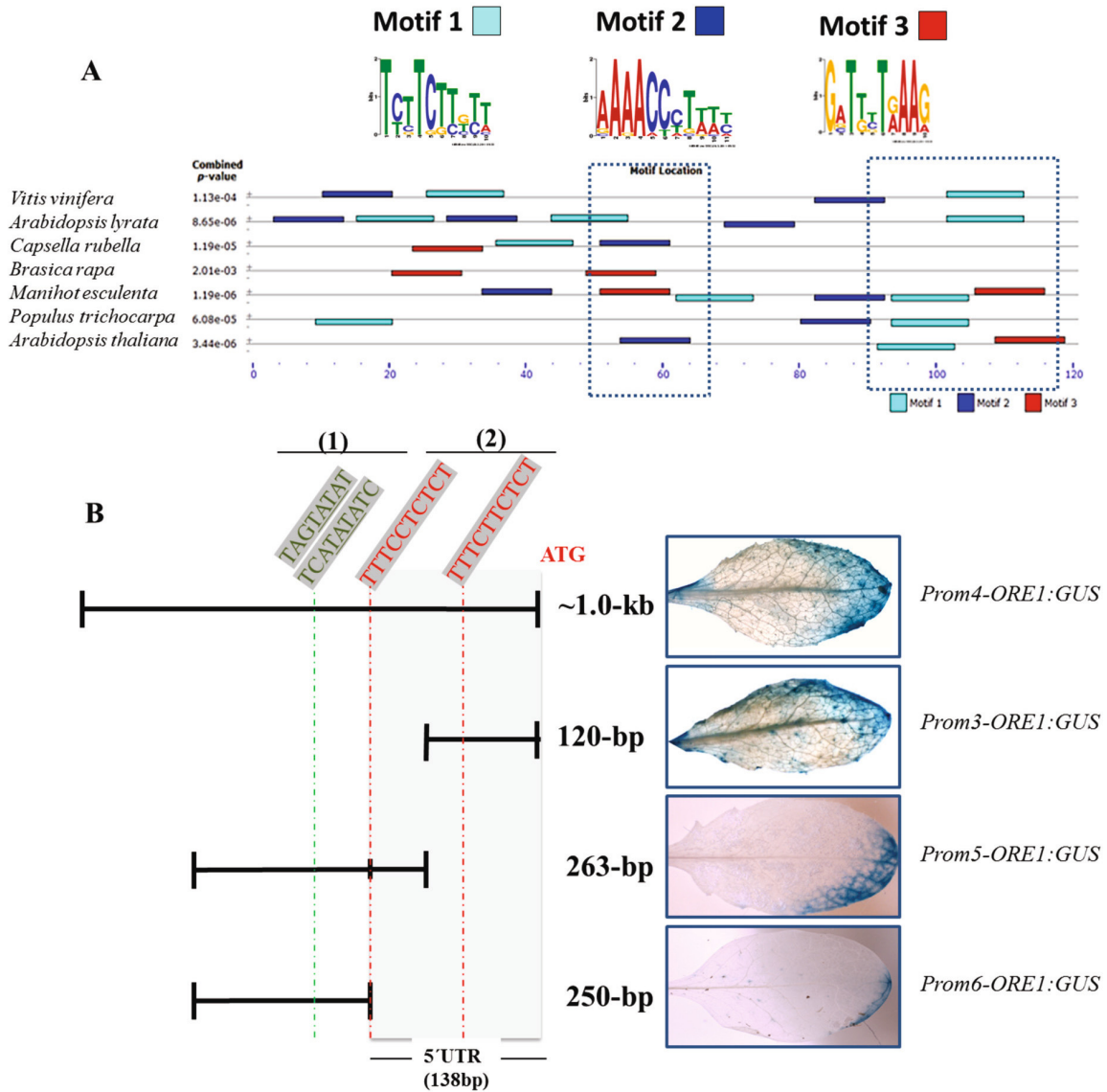
Figure 6. Deletion analysis of the *ORE1* up-stream region. (**A**) Non-coding sequences conserved in the *ORE1* promoter and six *ORE1* orthologs (120 bp up-stream of the ATG). The first motif is highly similar to the LE~5UTR-Py-rich stretch motif and is highly conserved in the promoters of *ORE1* orthologs (**B**) Four different deletions in the *ORE1* promoter showed that the decrease of *ORE1* expression is dependent on the presence of the 5'UTR. Boxes shown in colors indicate CREs predicted by the PlantCARE database (Lescot*et al*., 2002). (**1**) Represents the sites of two predicted TATA-boxes. (**2**) Represents two predicted LE~5UTR-Py-rich stretch motifs (positions -111 and -136 from the ATG) that may confer high transcription levels (Daraselia *et al*., 1996).

Table 1. Putative CREs found in the *ORE1* promoter (1.2 kb up-stream of the ATG).

MOTIF	SEQUENCE	MATRIX SCORE	STRAND	POSITION[a]	FUNCTION
LE~5UTR-Py-rich stretch	TTTCTTCTCT	9/10	(+)	-136*	Element conferring high transcription levels
		10/10	(+)	-111*	
AAAC-motif	CAACAAAAACCT	11/12	(+)	-50*	Light responsive element
ATCT-motif	AATCTAATCC	7/7	(-)	-390	
ACE	CTAACGTATT	9/10	(+)	-802	
Box 4	ATTAAT	6/6	(+)	-1150	
G-box	CACATGG	7/7	(+)	-1241	
		7/7	(-)	-990	
TCT-motif	TCTTAC	6/6	(-)	-924	
		6/6	(+)	-41*	
		6/6	(-)	-334	
I-box	GATAAGATT	9/9	(-)	-627	
Gap-Box	CAAATGAA(A/G)A	9.5/10	(+)	-181	
ARE	TGGTTT	6/6	(-)	-852	Anaerobic induction
Box III	CATTTACACT	9/10	(+)	-848	Protein binding site
Box-W1	TTGACC	6/6	(-)	-573	Fungal elicitor responsive element
		6/6	(-)	-227	
		6/6	(+)	-240	
HD-Zip 1	CAAT(A/T)ATTG	8.5/9	(+)	-235	Differentiation of the palisade mesophyll cells
HSE	AAAAAATTTC	9/10	(-)	-984	Heat stress responsiveness
MBS	CAACTG	6/6	(-)	-1098	Drought-inducibility
RY-element	CATGCATG	8/8	(+)	-1059	Seed-specific regulation
Skn-1_motif	GTCAT	5/5	(+)	-900	Endosperm expression
		5/5	(+)	-864	
TC-rich repeats	ATTTTCTTCA	9/10	(+)	-861	Defense and stress responsiveness
	GTTTTCTTAC	9/10	(-)	-334	
	GTTTTCTTAC	9/10	(-)	-441	
Circadian	CAAAAACATC	6/10	(+)	-658	Circadian control
	ATCTTATCAC	6/10	(+)	-628	
	CAAGAAGATC	6/10	(+)	-36*	

a   Numbers represent the locations of the regulatory elements relative to the ATG. Distal CREs correspond to position -1281. Proximal CREs correspond to position -1.

*   Motifs present in the 5'UTR

2.2.5. ATAF1 positively regulates *ORE1* expression

The identification of the crosstalk between different signal transduction pathways, especially in relation to senescence, abiotic stress tolerance, and leaf growth in general, is a major task in our research group. Based on transcriptional profiling of lines overexpressing the NAC TF *ATAF1* under the control of an estradiol-inducible promoter (after 10 hours and 24 hours of estradiol induction), *ATAF1* was identified as a potential up-stream activator of *ORE1* (**Fig. 7**). Like *ORE1* (At5g39610), *ATAF1* (At1g01720) also encodes a NAC TF; both have

been reported as senescence associated genes (SAGs) (Buchanan-Wollaston *et al.*, 2005; Balazadeh *et al.*, 2008b). Additionally, both genes are regulators of common signaling pathways related to drought and wounding responses, salt stress response, (Balazadeh *et al.*, 2010a,b; Buchanan-Wollaston *et al.*, 2005; Mauch-Mani and Flors 2009; Wu *et al.*, 2009), and defense response (Al-Daoud and Cameron 2011; Collinge *et al.*, 2008; Wang *et al.*, 2009).
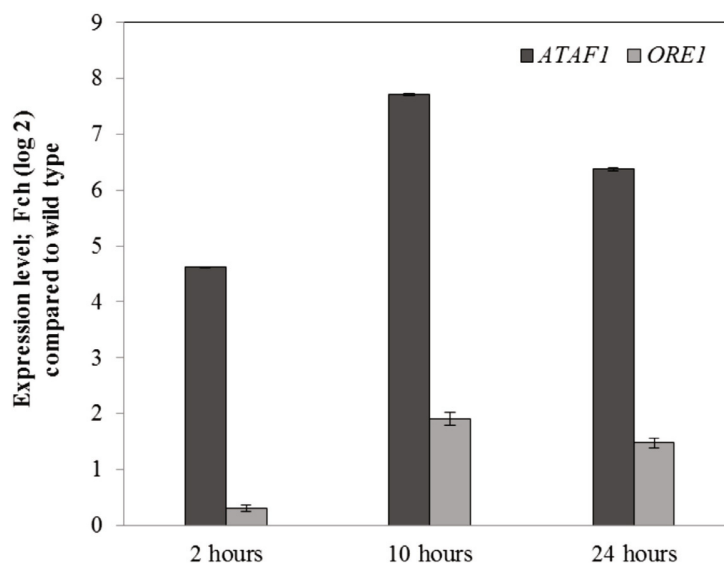
Figure 7. Transcription levels of *ORE1* and *ATAF1* in *ATAF1* inducible overexpressor (*ATAF1-IOE*) lines upon estradiol (EST) induction. *ORE1* transcript abundance increased concomitantly with *ATAF1*. Maximal level of *ORE1* transcript abundance was reached after 10 hours of EST induction.

The induction of *ORE1* upon inducible overexpression of *ATAF1* suggests a possible direct control of *ATAF1* over *ORE1* and, by this, the regulation of natural and stress-induced senescence. In order to test a direct interaction *in vivo* between *ATAF1* and *ORE1*, I used protoplast transactivation assays. The *ORE1* promoter (1.0 kb up-stream of the ATG) was amplified by PCR from *Arabidopsis* genomic DNA (ecotype Col-0), cloned into the pENTR/D-topo vector (Invitrogen), and then recombined into the Gateway-compatible destination vector *p2GWL7.0* (Karimi *et al.*, 2002) to obtain the final reporter vector *ORE1-LUC*. The effector plasmid was the *35S:ATAF1* construct. For detailed descriptions, see **sections 2.4.3 and 2.4.7**. Briefly, a dual-reporter system determines the transcriptional activation of the *ORE1-LUC* promoter. Activation is detected by the relative light emitted from firefly luciferase (LUC) enzymatic activity. The internal control reporter, *Renilla* luciferase (*35S:RLuc*) (Licausi *et al.*, 2011) provides the parameter to normalize the data and calculate *ORE1-LUC* promoter activity (**Fig. 8.A**). *Arabidopsis* mesophyll cell protoplasts co-transfected with the *ORE1-LUC* and *35S:ATAF1* constructs showed high luciferase activity indicating an activation of the *ORE1* promoter by the *ATAF1* TF (**Fig. 8.B**).

27
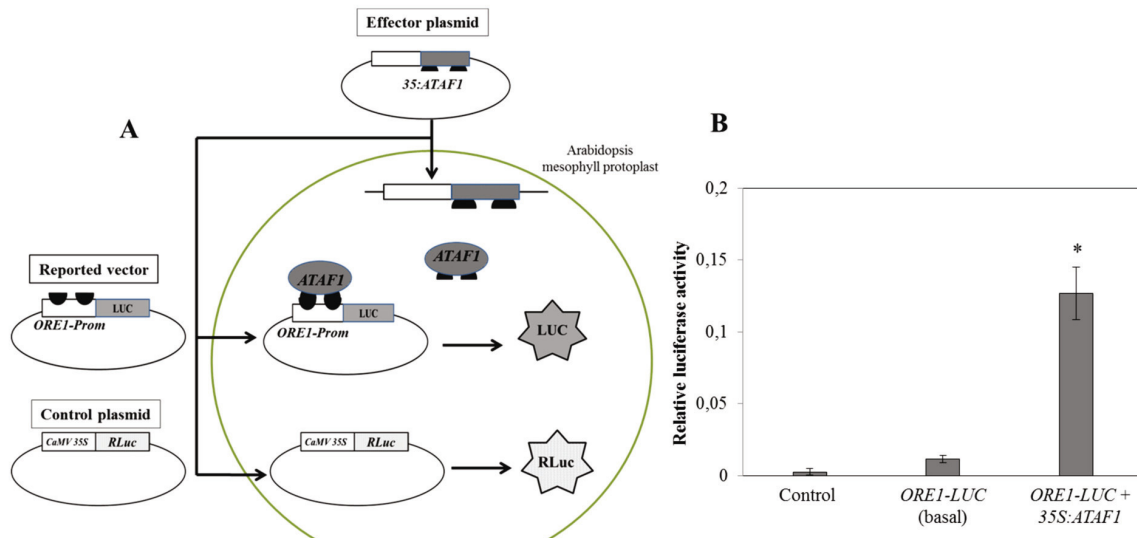
Figure 8. Protoplast transactivation assay of ATAF1 and *ORE1* promoter. A. Schematic representation of the transactivation assay. Effector and reporter/control vectors are shown. **B.** Relative luciferase activity detected in mesophyll cell protoplasts co-transfected with *ORE1-LUC* and *35S:ATAF1*. Results are the mean of two biological replicates with three technical replicates per probe. Data were normalized to the corresponding *Renilla* luciferase activity. *$P<0.05$.

2.3.   Conclusions

In this study we confirmed the evolutionary conservation of *ORE1* expression in two different plant species (*Arabidopsis thaliana* and *Nicotiana tabacum*). The conservation of *ORE1* expression is extended from early mature embryos and primary roots until advanced stages of aging. Also the responsiveness to salt stress of *ORE1* is conserved in both species. We found that *ORE1* positively regulates dark-induced senescence. The characterization of the *ORE1* promoter led us to suggest that the 5'UTR plays an important role in mediating the characteristic expression pattern observed during natural senescence. *ORE1* is transcriptionally activated by another NAC transcription factor, *ATAF1*. Considering that *ATAF1* has been reported as a senescence associated gene (SAG) (Buchanan-Wollaston *et al*., 2005; Balazadeh *et al*., 2008b) and that ATAF1 activates the expression of *ORE1*, we propose ATAF1 as a positive regulator of *ORE1* in the regulatory pathway that mediates age-dependent senescence. Further analyses are required to confirm direct regulation of *ORE1* by *ATAF1*.

2.4. Experimental procedures

2.4.1. General

Standard molecular techniques were performed as described (Sambrook and Russell, 2001). Oligonucleotides were obtained from MWG (Ebersberg, Germany). DNA sequencing was performed by MWG. Unless otherwise indicated, other chemicals were purchased from Roche

(Mannheim, Germany), Merck (Darmstadt, Germany), or Sigma (Deisenhofen, Germany). The *Arabidopsis* Information Resource (TAIR; http://www.Arabidopsis.org/) and the Plant Transcription Factor Database (http://plntfdb.bio.uni-potsdam.de/v2.0/) were used to obtain CDS and promoter sequences. The tools used for sequence analyses were provided by the National Center for Biotechnology Information (http://www.ncbi.nlm.nih.gov/) and NCBI's BLAST database/genebank (http://blast.ncbi.nlm.nih.gov/Blast.cgi) (Altschul *et al.*, 1997). qRT-PC reactions were conducted using an ABI PRISM 7900HT sequence detection system (Applied Biosystems Applera). Except for those already published, primers used during this study are described and codified by an internal labor code (**Annex 1**).

2.4.2. Plants and growth conditions

All *Arabidopsis thaliana* lines used were in the wild type (Col-0 ecotype) background. Seeds from *Arabidopsis* and tobacco were surface sterilized with 70% ethanol (1 minute), 20% sodium hypochlorite (30 minutes) and rinsed with sterile water (six times). *Arabidopsis* seeds were immediately germinated on Murashige–Skoog (MS) half-strength medium (Murashige and Skoog, 1962) supplemented with 7% agar and 1% sucrose. Seeds were stratified for 48 hours in the dark at 4°C and then transferred into a climate chamber with 16 hours of day light provided by fluorescent light at 100 µE m^{-2} sec^{-2} intensity and a day/night temperature of 20/16°C and relative humidity (RH) of 60/75%. In the case of tobacco, plants were grown with 16 hours of day light at 25°C and 8 hours of darkness (20°C). The homozygous T-DNA insertion line (*anac092-1* T-DNA insertion mutant) originated from the SALK collection (ID 090154) described in Balazadeh *et al*. (2010a). In cases were plants were grown directly on soil, seeds were stratified for one week at 4°C, then transfer to long-day photoperiod in phytotron and after two weeks transferred into a climate chamber with 16 hours of day light provided by fluorescent light at 100 µE m^{-2} sec^{-2} intensity and a day/night temperature of 20/16°C and relative humidity (RH) of 60/75%.

2.4.3. Constructs

Description of the ***Prom-ORE1:GUS*** and the ***35S:ORE1*** overexpressor line were given in Balazadeh *et al*., (2010a).

Prom3-ORE1:GUS. A 120 bp genomic fragment up-stream of the start codon (ATG) of *ORE1* (At5g39610) was amplified by a polymerase chain reaction (PCR) using forward (110) and reverse (111) primers. The isolated fragments were inserted first into plasmid pCR2.1-TOPO (Invitrogen), and after sequencing were fused via *BamHI* and *NcoI* sites to the GUS reporter gene into *pCAMBIA1305*. 1-hygromycin (CAMBIA).

ORE1:GUS promoters. The promoter regions corresponding to 1.0 kb, 263 bp, and 250 bp up-stream of the ATG, respectively, were amplified from genomic DNA by PCR using an Advantage HF 2 PCR Kit (Clontech) with gene-specific forward and reverse primer sets for

each promoter region (**Annex 1**). The fragments were subcloned into a pENTR-D-TOPO vector (Invitrogen) to generate the entry vectors *pProm4-*, *pProm5-*, and *pProm6- ORE1-ENTRY*. Entry vectors were recombined into Gateway destination vector *pKGWSF7,0* using the LR reaction mix II (Invitrogen) to obtain the final reporter vectors *Prom4-*, *Prom5-*, and *Prom6- ORE1:GUS*.

ORE1-LUC. This vector was used as a reporter vector in the transactivation assays (**section 2.2.5**). The *pProm4-ORE1-ENTRY* entry vector was recombined into Gateway destination vector *p2GWL7.0*, which is a recombination of the gateway vectors *pBGWL7.0* (transcription reporter vector) and *p2GW7.0* (overexpression vector) (Licausi *et al.*, 2011) using the LR reaction mix II (Invitrogen) to obtain the final reporter vector *ORE1-LUC.*

ATAF1-IOE. PCR was used to amplify the *ATAF1* (At1g01720) coding region using *Arabidopsis* Col-0 leaf cDNA as a template and by using forward (204) and reverse (205) primers (**Annex 1**). The *ATAF1* cDNA was inserted into the pCR2.1-TOPO vector and, after sequence confirmation, cloned via *XhoI* and *SpeI* sites into the pER-8 vector (Zuo *et al.*, 2000).

35S:ATAF1. The vector was used as effector plasmid in transactactivation assays (**section 2.2.5**). The *ATAF1* (At1g01720) coding region was amplified by PCR using a combination of forward (206) and reverse (207) primers (**Annex 1**) and by using *Arabidopsis* Col-0 leaf cDNA as a template, and then it was inserted into pUni/V5-His-TOPO (Invitrogen). After sequence confirmation, the cDNAs were cloned via added *PmeI/PacI* sites into a modified pGreen0229 plant transformation vector (www.pgreen.ac.uk) containing the Cauliflower Mosaic Virus (*CaMV*) *35S* promoter located in the *PmeI/PacI* restriction sites (Skirycz *et al.*, 2006).

2.4.4. Plant transformation

Agrobacterium tumefaciens strain GV2260 and GV3101 (pMP90) containing specific *ORE1* promoter deletions fused to the *GUS* reporter gene were used to transform tobacco and *Arabidopsis*, respectively. In all cases, positive clones were confirmed by PCR and sequencing. *Agrobacterium* cultures were grown overnight (O.N) in constant agitation (200 rpm) at 28°C in liquid Yeast –Extract –Broth (YEB)/ rifampicin (50 mg/ml)/gentamicin (20 mg/ml) and the bacterial resistance marker antibiotic hygromycin (10 mg/ml). In the case of *Arabidopsis*, wild type (Col-0) flower buds were immersed in the suspension of *A. tumefaciens* and transformed by dipping method (Bechtold and Pelletier, 1998; Clough and Bent, 1998). In the case of tobacco plants, a transformed *Agrobacterium* pellet was collected by centrifugation (4000 rpm) for 10 minutes at room temperature (RT). The pellet was resuspended in 10 mL (10 mM) $MgSO_4$. Leaf squares of tobacco plants grown *in vitro* (max. 4-week old) were placed in resuspended bacteria for 3-4 minutes. Leaf squares were transferred to MS media for two days and placed in the dark and RT. The callus formation

initiated in only putative transformed leaf squares; untransformed leaf squares yellowed after 3-5 days. The transformed leaflets developed into bright white-green calluses and were transferred to shoot induction tobacco media containing gentamicin (20 mg/mL) and carbenicillin (500 mg/L).

2.4.5. Histochemical GUS assay

Histochemical *in situ* staining was used to determine the expression pattern in different tissues of transformed-GUS plants. Plant tissues at different developmental stages were submerged in a staining solution of 50 mM sodium phosphate pH 7.0, 0.1% (v/v) Triton X-100, 0.1 mM potassium ferricyanide, 0.1 mM potassium ferrocyanide, 1 mM Na_2 EDTA pH 8.0, 20% (v/v) methanol, and 0.5 mg/mL 5-bromo-4-chloro-3-indolyl-b-D-glucuronid acid (X-gluc; Duchefa). Samples were incubated at 37°C for a period of several hours to overnight depending on the tissue type, construct, and color rate. Chlorophyll was removed by submerging the samples in ethanol 70% (v/v). GUS staining was visualized using a stereomicroscope Leica MZ 12,5 with software LAS (Leica).

2.4.6. Dark-induced senescence

Experiments for artificial induction of senescence were performed with all rosettes leaves of 27-day-old plants from wild type (Wt), *anac092-1* T-DNA insertion mutant, *35S:ORE1* overexpressor line and Empty Vector (E.V.). Detached leaves were incubated in the dark into boxes on moist filter paper during four days at RT (room temperature). As control detaches leaves from the same lines were placed on moist filter paper under long-day photoperiod (16 hours light; 8 hours darkness) on moist filter paper. In both cases filter papers were maintained always humid.

2.4.7. Salt treatment for *Arabidopsis* and tobacco plants

Arabidopsis seedlings were grown in long-day conditions (**section 2.4.2**) and after two weeks were transfer to liquid media and treated for 40 hours with 0 mM NaCl (Control) or 150 mM NaCl. In the case of tobacco, detached leaves and flowers from different developmental stages were isolated from mature tobacco plants (five months after sowing) and treated for 40 hours with 0 mM NaCl (Control) or 150 mM NaCl. Immediately after treatment, tobacco and *Arabidopsis* seedlings were stained with GUS buffer as described in **section 2.4.5**.

2.4.8. Dual-luciferase assay

This experimental procedure was used in different assays, and for this reason, the description will be given as a general protocol. Promoter regions of *ORE1* putative target genes were used as reporter plasmids: a 1.0 kb up-stream of the translation start site were amplified

from genomic *Arabidopsis* ecotype Col-0 DNA to generate reporter final constructs. A detailed description of each *prom-LUC* construct is described in the experimental procedure section of each chapter. In this case, we used *ORE1-LUC* construct as the reporter (**section 2.4.3**). Renilla luciferase CDS was amplified using pRL-null (Promega) as a template. The resulting amplicon was ligated into the pENTR/D-topo vector (Invitrogen) and subsequently recombined in *p2GW7* (Karimi *et al*., 2002) using the LR clonase enzyme (Invitrogen) to generate the *35S:RLuc* normalization vector (Licausi *et al*., 2011). A *35S:ATAF1* construct was used as effector plasmid (described in **section 2.4.3**). The effector, reporter, and reference plasmids were co-transfected into mesophyll cell protoplasts that were prepared from rosette leaves of 4-week-old *Arabidopsis* plants, as reported by Sheen (Sheen, 2002). The protoplasts had a maximum reaction volume of 10 ul and contained 6.0 ug DNA of each construct. Luciferase activity was assayed with the Dual Luciferase Reporter Assay System (Promega), and the luminescence was read in a GloMax 20∕20 Luminometer (Promega). All tests were performed in 3-4 independent biological replications with three technical replications per assay. Assays by t-test using the SigmaPlot software (http://www.sigmaplot.com) were statistically significant.

2.4.9. cDNA synthesis and quantitative real-time PCR (qRT-PCR)

Total RNA extraction, cDNA synthesis, and qRT-PCR were done as previously described (Balazadeh *et al*., 2008b; Caldana *et al*., 2007). Primer sequences used for qRT-PCR analysis to quantify transcript levels of *ORE1* (At5g39610) and *ATAF1* (At1g01720) are given in **Annex 1**. The PCR reactions were run on an ABI PRISM 7900HT sequence detection system (Applied Biosystems Applera). At least five measurements were carried out to determine the mRNA abundance of each gene in each sample. The absence of genomic DNA was verified by PCR using forward (202) and reverse (203) primers designed to amplify an intergenic region in a control gene (At5g65080). cDNA was produced from 2.0 μg total RNA using SuperScriptT III Reverse Transcriptase (Invitrogen). cDNA synthesis efficiency was controlled by qRT-PCR amplification of a housekeeping gene *ACTIN2* (At3g18780) using specific forward (204) and reverse (205) primers (**Annex 1**). Data analysis was performed using SDS 2.2.1 software (Applied Biosystems Applera). Amplification curves were analyzed with a normalized reporter (R_n: the ratio of the fluorescence emission intensity of SYBR Green to the fluorescence signal of the passive reference dye) threshold of 0.2 to obtain C_T values (threshold cycle). Dates were normalized to *ACTIN2* as follows $\Delta C_T = C_T$ (gene) $- C_T$ (*ACTIN2*). The expression was measured with three replicates in each PCR run, and the average C_T was used for relative expression analyses. Relative transcript abundance was determined using the comparative $\Delta\Delta C_T$ method ($\Delta\Delta C_T = \Delta C_T$ (condition of interest) $- \Delta C_T$ (control condition)), and the Fold Change (Fch) was calculated using the expression $2^{-\Delta\Delta CT}$, where the obtained results were Log_2 transformed. In some cases, the expression was expressed as $40 - \Delta\Delta C_T$ to improve visualization.

Contributions

The *Prom1-ORE1:GUS*, *ORE1-IOE*, *35S:ORE1* lines and *anac092-1 T-DNA* insertion mutant screening were performed by Dr. Hamad Sidiqui (Molecular Biology, Potsdam University). *ATAF1-IOE* constructs were provided by Dr. Dagmar Kupper (Molecular Biology, Potsdam University). *35S:ATAF1* construct and *ATAF1* transcriptome data were provided by Prashant Garapati, Ph.D student of Prof. Dr. Mueller-Roeber's Group.

Chapter 3

A calcium-dependent protein kinase CKOR positively regulates the expression of three ORE1 putative target genes

This work has been developed through a collaboration with Prof. Tina Romeis's Group (Biochemistry of Plants Group. Institute of Biology. Freie Universität Berlin)

3.1. Introduction

Cells are exposed to a broad spectrum of internal and external stimuli. The cell-to-cell interactions during development, as well as the environmental fluctuations and stresses, constitute messages that need a correct integration into the molecular signaling pathways to generate specific and appropriate responses (Krebs, 1993). Signal transduction frames include post-transcriptional modification of sundry proteins by kinases. During protein phosphorylation, protein kinases covalently link phosphate groups to the target proteins (Feilner *et al*., 2005). Calcium-dependent protein kinases (CDPKs) are a group of serine/threonine kinases that are regulated by a Ca^{+2}/ calmodulin complex. Therefore, calcium-stimulated kinase activities could be activated by direct calcium biding (Cheng *et al*., 2002). Because osmotic stress elicits calcium signaling (Knight *et al*., 1997), calcium-dependent protein kinases are prime candidates that link the calcium signal to down-stream responses (Zhu, 2002).

In order to interact with their target DNA sequences, transcription factors (TFs) need to be located in the cell nucleus. Several TFs are constitutively nuclear, and phosphorylation and dephosphorylation by protein kinases and protein phosphatases take place within the nucleus. However, TFs can be mobilized between cytoplasm and the nucleus, and in many cases this mobilization is regulated by phosphorylation/dephosphorylation (Whitmarsh and Davis, 2000). DNA binding activity of TFs may also be regulated indirectly by phosphorylation at residues that are remote from the DNA binding domain. The deletion of genes that encode protein kinases and protein phosphatases that target particular transcription factors, as well

as targeted mutations of the codons that encode the phosphoacceptor sites on TFs, provide genetic evidence for the importance of these signaling molecules in regulating particular functions of a transcription factor (Whitmarsh and Davis, 2000). For instance, the NAC transcription factor *ORE1* has been reported as a putative substrate of the mitogen-activated protein kinases (MPKs) MPK2, MPK5, MPK8, and MPK10 *in vitro* (Popescu *et al*., 2009). However, the implications in planta of this modification remain unknown.

A phosphoproteomic approach using transgenic lines that were overexpressing a CDPK named CKOR (for calcium-dependent kinase regulating ORE1) revealed ORE1 is one of the few proteins differentially phosphorylated (unpublished data, Biochemistry of Plants Group, Prof. Tina Romeis, Freie Universität Berlin). We determined that the overexpression of ORE1 led to a significant increase in the transcriptional activation of three putative target genes of ORE1 (*BFN1*, *VNI2* and *RNS3*) *in vivo*, and that ORE1 binds directly to the promoters of their putative targets (see Chapter 4). Furthermore, *BFN1*, *VNI2*, and *ORE1* are senescence associated genes (SAGs) (Balazadeh *et al*., 2008a; Breeze *et al*., 2011; Buchanan-Wollaston *et al*., 2005; Guo *et al*., 2004), and *RNS3* is involved in inorganic phosphate (Pi) remobilization during Pi starvation and senescence. The molecular mechanisms initiated by nutrient remobilization during senescence are poorly characterized, but in the case of Pi starvation, ribonucleases are considered to play important roles in the remobilization process (Bariola *et al*., 1994). Here, we show that the transcriptional activation of *BFN1* (At1g11190), *VNI2* (At5g13180), and *RNS3* (At1g26820) is strongly influenced by the co-expression of CKOR. Mesophyll protoplasts co-transfected with CKOR showed an increase in transcriptional activity, while protoplasts co-trasfected with a mutated version of CKOR (that renders an inactive kinase) showed a marked decrease in the transcriptional activity of *BFN1*, and they left the activity of *VNI2* and *RNS3* undistinguishable from the basal activity.

3.2. Results

3.2.1. CKOR influences the transcriptional activation of ORE1 direct targets

ORE1 is a key regulator of natural and induced senescence, and evidences suggest that interaction to *BFN1*, *VNI2* and *RNS3* could play an important role in senescence regulation. In an effort to identify the effect of *ORE1* phosphorylation by CKOR, we tested the expression of ORE1 targets in cells co-transformed with two different versions of CKOR. The promoter regions (1.0 kb up-stream of the start codon (ATG)) of *BFN1*, *RNS3*, and *VNI2* were cloned into the Gateway destination vector *p2GWL7.0* (Licausi *et al*., 2011) that contains the firefly luciferase reporter gene (*LUC*). Thus, the expression of *LUC* is under the transcriptional control of each promoter. The final vectors *BFN1-LUC*, *RNS3-LUC*, and *VNI2-LUC* (**Chapter 4, section 4.4.4**) were used as reporters. Two different versions of CKOR were used as effector vectors: either the wild type version of the protein (CKORac), or a mutated version (CKORm) where one aspartic acid is replaced by alanine in the catalytic domain (rendering

the kinase inactive) (see **section 3.4.3**). As an internal control, we used reporter *Renilla* luciferase (*35S:RLuc*) (Licausi *et al*., 2011) to normalize the data and calculate the activity of each tested promoter. We co-transfected *Arabidopsis* wild type mesophyll cell protoplasts in a series of protoplast transactivation assays using the PEG method (Sheen, 2002). Each *promoter-LUC* construct and *35S:RLuc* were co-transfected with/without CKORac (active form) or with/without CKORm (inactive form). In each case, we evaluated the promoter activation upon overexpression of CKOR (active or mutated) as well as the basal promoter expression.

All promoters showed a basal activity (*BFN1*, *VNI2*, and *RNS3*), likely due to the TFs present in the protoplasts (including *ORE1*) that can activate these promoters. *BFN1* exhibited the stronger basal activity (10-fold) compared to *VNI2* or *RNS3*. Thus, we inferred that protoplasts from five-week-old plants have a stronger *BFN1* expression than *VNI2* or *RNS3* (**Fig. 9.A**). Co-transfection with a catalytically active CKOR protein (CKORac) increased the expression of all promoters tested in comparison to the basal expression (**Fig. 9.A-C**). In contrast, co-transfection with the catalytically inactive CKOR (CKORm) resulted in a transcriptional activity undistinguishable from the basal activity for VNI2 and RNS3, and a significant decrease of transcriptional activity in the case of BFN1 (**Fig. 9.D-F**).

To explain the increase in transcriptional activation observed in *BFN1*, *VNI2*, and *RNS3* upon co-transfecting with CKORac (**Fig. 9.A-C**), we hypothesized that CKORac overexpression may have resulted in increased ORE1 phosphorylation that, in turn, increased the activation level of its direct targets. These results provide some insights into the role of CKOR as a positive regulator of *BFN1*, *VNI2*, and *RNS3* perhaps through the phosphorylation of the transcription factor *ORE1* (**Fig. 9.A-C**).

On the contrary, the overexpression of CKORm, which is unable to phosphorylate its targets, led to a decreased level of *BFN1* promoter activity and a decrease in activities that are undistinguishable from the basal activity for the promoters of *VNI2* and *RNS3*. This result may indicate that the overexpression of CKORm, which is unable to phosphorylate ORE1 (although is able to bind the protein), hinders the normal activity of ORE1. Thus, an excess of CKORm leads to an even lower *BFN1* promoter activity. The basal activity of the other tested promoters (*VNI2* and *RNS3*) is already so low at the starting conditions that overexpression of CKORm has just a minor effect on these promoters. Currently, our collaborating partner (Biochemistry of Plants Group, Prof. Dr. Tina Romeis, Freie Universität Berlin) is carrying out further experiments to unravel detailed interactions between CKOR and ORE1.

3.3. Conclusions

We suggest that ORE1 is post-transcriptionally regulated by CKOR. The phosphorylation of ORE1 plays a crucial role in its activity and favors the transcriptional activation of its targets

BFN1, *VNI2*, and *RNS3*. Nevertheless, phosphorylation seems to affect the activation of *BFN1* more severely than the other promoters. These results provide important information related to additional mechanisms influencing the activity of ORE1.
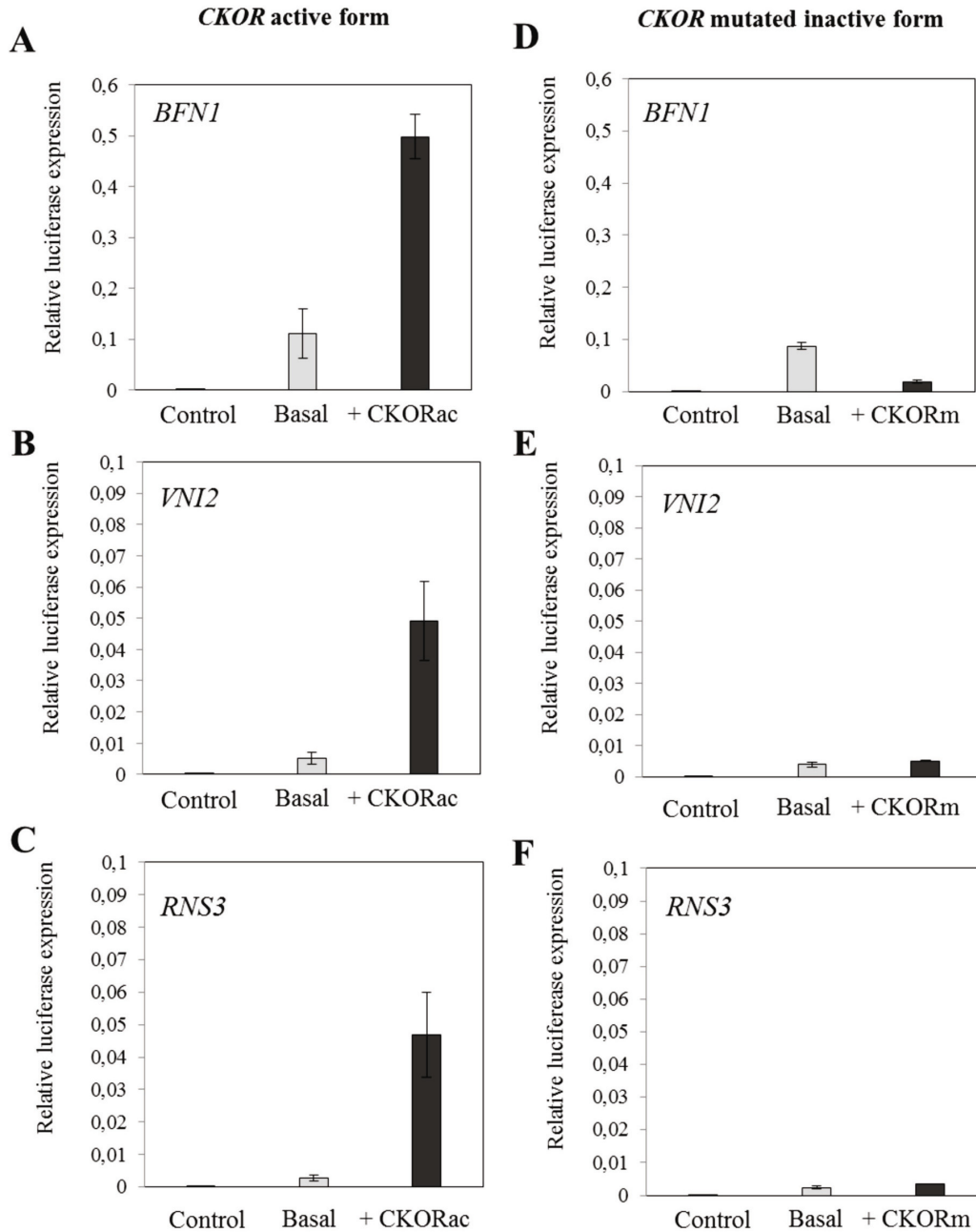
Figure 9. Activation of ORE1 direct targets by CKOR. (A-C) Co-transfection of *BFN1:LUC, VNI2:LUC*, and *RNS3:LUC* with *35S:RLuc* and with or without (basal) CKORac (active form). **(D-E)** Co-transfection of *BFN1:LUC*, *VNI2:LUC* and *RNS3:LUC* with *35S:RLuc* and with or without (basal) CKORm (inactive form). Data represent mean values ± standard deviation (SD) (n=2) 3 technical replicates. Luciferase values are normalized to the corresponding Renilla expression level.

3.4. Experimental procedures

3.4.1. General

Standard molecular techniques were performed as described in **Chapter 2, section 2.4.1.**

3.4.2. Plant material

Plant material and growth conditions were similar to those described in **Chapter 2, section 2.4.2.**

3.4.3. Constructs

Promoter-LUC **constructs:** promoter regions spanning 1.5 kb up-stream of the ATG of *VNI2, BFN1*, and *RNS3* were amplified from genomic DNA by PCR using an Advantage HF 2 PCR Kit (Clontech) with gene-specific forward and reverse primers (**Annex 1**). Promoter fragments were subcloned into pENTR-D-TOPO vectors (Invitrogen), to generate individual entry vectors. The entry vectors were then recombined into a *p2GWL7.0* Gateway destination vector which is a recombination of the *pBGWL7.0* gateway vector (transcription reporter vector) (Karimi *et al*., 2002) and *p2GW7.0* vector (overexpression vector) (Licausi *et al*., 2011)) using the LR reaction mix II (Invitrogen) to obtain the final *BFN1-LUC, VNI2-LUC, RNS3-LUC* reporter vectors.

CKORac and CKORm: Plasmids containing the constitutively active and mutated versions of CKOR in the pXCS-G-StrepII binary vector were kindly provided by G. Durian (Freie Universität Berlin). This vector uses the pamPATMCS backbone (accession number AY436765) and allows convenient and rapid expression of proteins *in planta* (Witte *et al*., 2004). The effectors vectors are named *CKORac* and *CKORm* for normal (active) and mutated (inactive) versions, respectively.

3.4.4. Dual-luciferase assay (Transactivation assay)

A detailed description of the procedure was given in **Chapter 2, section 2.4.7.** Based on previous data (data not shown) for this particular assay, the time of protoplast co-transfection was decreased from 24 hours to 14 hours to avoid tissue damage and cell death.

Chapter 4

Inferring putative targets of ORE1 through transcriptome-based expression analysis

Part of this work will be submitted to *The Plant Journal* with the tittle:

"Expression of *BIFUNCTIONAL NUCLEASE1* (*BFN1*) during senescence in *Arabidopsis* is regulated by the NAC transcription factor ORE1/ANAC092/AtNAC2"

Lilian P. Matallana-Ramirez,[1,2] Mamoona Rauf,[1] Hakan Dortay,[1] Liliane Sorego,[3] Amnon Lers,[3] Gang-Ping Xue,[4] Wolfgang Dröge-Laser,[5] Salma Balazadeh,[1,2,] and Bernd Mueller-Roeber[1,2,]

[1]University of Potsdam, Institute of Biochemistry and Biology, Karl-Liebknecht-Straße 24-25, 14476 Potsdam-Golm, Germany; [2]Max-Planck Institute of Molecular Plant Physiology, 14476 Potsdam-Golm, Germany, [3]Department of Postharvest Science of Fresh Produce. Volcani Center, Agricultural Research Organization, Bet Dagan, 50250 - Israel; [4]CSIRO Plant Industry, 306 Carmody Road, St Lucia, Qld 4067, Australia; [5]Julius-Maximilians-Universität Würzburg, Julius-von-Sachs-Platz 2, 97082 Würzburg, Germany.

4.1. Introduction

Plant senescence is a highly regulated process that involves many regulatory proteins, including transcription factors (TFs), which control the expression of target genes and constitute up-stream control elements of gene regulatory networks (GRNs). ORE1, a NAC TF, has recently been shown to be a central regulator of senescence in *Arabidopsis thaliana* (Balazadeh *et al*., 2008; Balazadeh *et al*., 2010a; Kim *et al*., 2009). In our previous work, we identified ORE1 responsive genes using estradiol-inducible overexpressor lines (*ORE1-IOE*) (Balazadeh *et al*., 2010a). Many of the up-regulated genes encode proteins known to function in the degradation of different macromolecules as part of the mechanism of

nutrient salvage that occurs in plants during senescence (Bleecker, 1998). The ORE1 regulon includes proteins involved in further signal transduction pathways such as other TFs (NAC TF among them). In this study, in order to identify direct target genes of ORE1, additional global transcriptome analyses were carried out. Inducible ORE1 overexpressing plants (*ORE1-IOE*) were incubated for two hours in estradiol (EST). To account for artifacts cuased by the use of EST, further global expression profiling experiments were made using *Arabidopsis* mesophyll cell protoplasts transformed with a *35S:ORE1* construct and harvested six hours after transfection. We determined the ORE1 binding site (BS) and its frequency within the promoter regions of putative target genes. Additionally, our results showed that ORE1 is able to bind to the promoters of *BFN1, VNI2*, and *RNS3 in vitro* and to transactivate them *in vivo*. Our data strongly suggests that *BFN1, VNI2*, and *RNS3* are putative direct targets of ORE1.

4.2. Results

4.2.1. Transcriptome profiling reveals a core set of putative ORE1 direct targets

In our previous study, we observed that after five hours of estradiol induction, 218 genes were differentially expressed. From these, 170 were significantly up-regulated and 48 were significantly down-regulated (Balazadeh *et al*., 2010a). In this study, in order to identify direct targets of ORE1, additional expression profiling experiments were carried out using cells/plants that were overexpressing *ORE1* constitutively (using the strong constitutive promoter 35S (CaMV) Cauliflower mosaic virus) or inducibly (using an estradiol-inducible promoter). Log2 intensity values were converted to Log2 fold change ratios by comparing the intensity of induced/transformed and uninduced/untransformed plants/cells. Differentially expressed genes were determined by setting a twofold cut-off (Log2 ± 1). Our data revealed that 78 genes were differentially expressed after two hours EST induction in *ORE1-IOE* plants. From these genes, 54 were up- and 24 were down-regulated (**Annex 3**). After five hours of EST induction in our new profiling experiments, 269 genes were differentially expressed. From these, 195 genes were up- and 74 were down-regulated (**Annex 4**). Six transcription factors were identified after five hours ORE1 induction including one zinc-ion binding factor (At2g28200), one signal transduction response regulator (At2g40670), one *MYB TF* (At3g10590), and three members of the NAC TF family (*ANAC010, ANAC041*, and *VNI2*). In our datasets, we observed that the number of up-regulated genes after EST induction increased around fourfold (from 54 after two hours to 195 after five hours). Among them, only less than 1.0% overlapped (two genes). The number of down-regulated genes increased threefold (from 24 after two hours to 74 after five hours), and none overlapped between datasets. Upon transient overexpression of ORE1 in mesophyll protoplasts, 831 genes were found differentially expressed, of which 643 were up- and 188 were down-regulated (**Annex 5 only in the electronic version**). Venn diagrams show overlapping up- (**Fig. 10.A**) or down-regulated genes among datasets (**Fig. 10.B**). Taking together all datasets, 731 genes were significantly up-regulated while 273 were significantly down-regulated upon ORE1

overexpression. There is a larger overlap between genes up- or down-regulated from five to six hours overexpression (144 up- and 10 down-regulated) than from two to five hours overexpression (**Fig. 10.A-B**). Interestingly, there were no common down-regulated genes among the three datasets (**Fig. 10.B**). We were able to identify a set of 17 commonly up-regulated genes among the three datasets (**Fig. 10.A**).
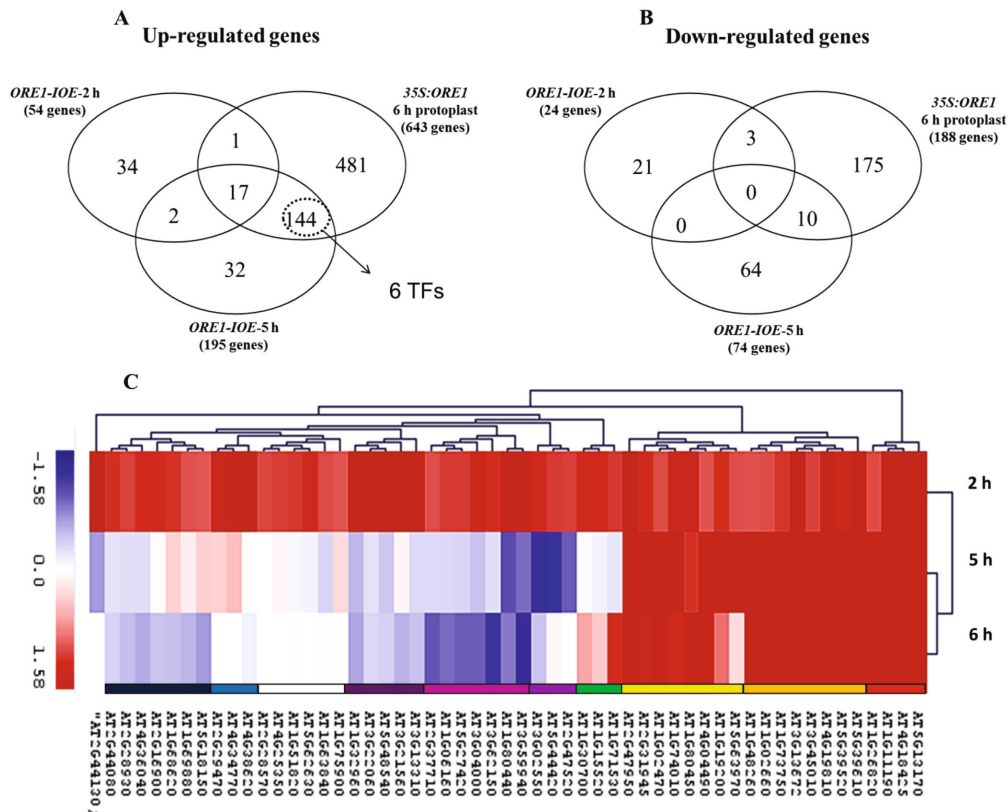
Figure 10. Differentially expressed genes in plants/cells overexpressing ORE1. (A-B) Venn diagrams to compare up/down-regulated genes in *ORE1-IOE-2* hours plants, *ORE1-IOE-5* hours plants, and *35S:ORE1-6* hours protoplasts. (**C**) Hierarchical clustering based on 54 up-regulated genes after two hours of EST induction (*ORE1-IOE* plants). Ten clusters were identified and color coded from right to left.

The cluster analysis, based on genes significantly up-regulated in *ORE1-IOE* plants induced for two hours with EST (54 genes), revealed ten different patterns of expression when compared to datasets two (*ORE1-IOE* induced five hours with EST) and three (constitutive overexpression for six hours in protoplasts). In **Figure 1.C,** cluster 1 (in red) includes highly up-regulated genes in all data-sets. Clusters 2 and 3 (in light and dark yellow, respectively) include highly up-regulated genes in at least two datasets and less induced in the other. Cluster 4 (in green) encompasses up-regulated genes in data set one and three, but not differentially expressed or slightly down-regulated genes in data set two. Clusters 5, 6, and 7 (in different shades of magenta) group up-regulated genes in data set one and not differentially expressed or slightly down-regulated genes in datasets two and three. Cluster 8 (in white) groups up-

regulated genes in data set one, slightly up/down-regulated genes in data set two, and not differentially expressed genes in data set three. Clusters 9 and 10 (in light and dark blue) group up-regulated genes in data set one, slightly up- or down-regulated genes in data set two, and not differentially expressed or down-regulated genes in data set three. The common set of up-regulated genes (17) comprises clusters 1, 2, and 3. These 17 genes (**Table 2**) are good candidates to be direct targets of *ORE1* as they are rapidly induced after *ORE1* overexpression (two hours) and are expressed in elevated levels at later time points (five hours) and in mesophyll cell protoplasts transiently overexpressing ORE1 for six hours. From 17 up-regulated genes, 14 are senescence associated genes (SAGs) (Buchanan-Wollaston *et al.*, 2005; Parlitz *et al.*, 2011; Van Der Graaff *et al.*, 2006; Balazadeh *et al.*, 2008a; Breeze *et al.*, 2011). We aimed to determine the role of other NACs within the ORE1 regulon and included *VNI2* (*ANAC083*) and *ORE1* (*ANAC092*) to complete our set of putative ORE1 direct targets. *VNI2* is one of the six TFs that were up-regulated at later time points (after five hours EST induction) as we described before, and based on published data (Breeze *et al.*, 2011), we decided to test a possible auto-regulation of ORE1; therefore, we also include ORE1 itself in our analyses (**Table 2**).

Table 2. Common set of up-regulated genes upon ORE1 overexpression. Expression is given as Log2 Fch (fold change). Data represent the mean of three biological replicates for *ORE1-IOE-5* hours and two biological replicates for the *ORE1-IOE-2* hours datasets and transfected protoplast (six hours). Bold letters indicate the subset of selected putative genes to prove direct interaction with ORE1.

AGI	Description	IOE-2 h	IOE-5 h	Protoplast-6 h
AT5G39610*	**ORE1/ANAC092/ATNAC2/ATNAC6 (*Arabidopsis*)**	3,646	3,454	3,259
AT1G02470*	similar to unknown protein	1,065	2,955	1,736
AT1G02660*	lipase class 3 family protein	1,052	2,397	3,677
AT1G11190*	**BFN1 (BIFUNCTIONAL NUCLEASE I);**	2,029	5,291	10,026
AT1G26820	**RNS3 (RIBONUCLEASE 3); endoribonuclease**	1,060	4,634	10,553
AT1G48260*	CIPK17 (CIPK17); kinase	1,027	2,454	4,437
AT1G73750	similar to unknown protein similar to unknown protein	1,178	2,616	2,928
AT1G74010*	strictosidine synthase family protein	1,404	2,782	1,303
AT1G80450*	VQ motif-containing protein	1,445	1,191	1,642
AT2G31945*	similar to unknown protein	1,253	2,230	1,469
AT2G47950	similar to unknown protein	2,757	1,863	1,803
AT3G13672*	**seven in absentia (SINA1) family protein**	1,806	4,338	4,002
AT3G45010*	SCPL48 (serine carboxypeptidase-like 48)	1,109	3,689	4,292
AT4G04490*	protein kinase family protein	1,017	1,605	1,509
AT4G18425*	similar to unknown protein	1,542	4,984	10,013
AT4G19810*	glycosyl hydrolase family 18 protein	1,620	3,973	2,712
AT5G13170*	**nodulin MtN3 family protein (SAG29)**	2,083	4,549	9,151
AT5G39520*	similar to unknown protein	1,373	4,205	3,047
AT5G13180*	**VNI2/ANAC083 (*Arabidopsis*)**	0,615	2,119	1,035

* Senescence up-regulated genes (Buchanan-Wollaston *et al.*, 2005; Parlitz *et al.*, 2011, Van Der Graaff *et al.*, 2006; Balazadeh *et al.*, 2008a; Breeze *et al.*, 2011).

In an attempt to characterize particular pathways that are over-represented in the set of differentially expressed genes, we classified the genes into functional categories using PageMan (Usadel *et al*., 2006). Over-representation was assessed using the Wilcoxon rank sum test. We selected the set of commonly up-regulated genes (17 genes, presented in **Table 2**). Due to the fact that we could not identify a set of commonly down-regulated genes, we assayed the over-represented functional categories in down-regulated genes of each dataset and produced a consolidated table of over-represented functional categories in all three data sets. Over-representation is assayed by comparing the categories in the set under analysis with the represented functional categories of the whole Affymetrix ATH1 array.

Significantly over-represented categories in the set of commonly up-regulated genes involved "lipid metabolism and degradation," "secondary metabolism," "stress" (particularly "abiotic stress"), "RNA processing" (particularly "ribonucleases"), "DNA synthesis and chromatin structure," "protein, posttranscriptional modification, and degradation," and "signaling" (particularly "receptor kinases") (**Table 3a**). Significantly over-represented functional categories in the set of down-regulated genes included "RNA regulation of transcription," "lipid metabolism and degradation," "stress" including both, abiotic and biotic, "secondary metabolism" (particularly "phenylpropanoids"), "hormone metabolism," "redox," and "transport." In the case of over-represented categories in down-regulated genes, the *P*-values are not given since for each dataset we obtained a *p*-value. Nonetheless, in all cases, the differences observed are statistically significant (**Table 3b**).

Table 3. Significantly over-represented functional categories in up- or down-regulated genes after six hours constitutive overexpression of ORE1 (*35S:ORE1/*6 hours cotransfected protoplasts) relative to the categories represented by the ATH1 array. (**a**) Up- and (**b**) down-regulated categories found using the Wilcoxon statistical test.

Functional Category	P-value
a) Up-regulated classes	
Lipid metabolism, degradation	7, 92E-04
Secondary metabolism	7, 92E-04
Stress.abiotic	7, 92E-04
RNA.processing, ribonucleases	7, 92E-04
DNA Synthesis, Chromatin structure	7,92E-04
Protein. postranslational modification, degradation	7,92E-04
Signaling.receptor kinases	7,92E-04
Development unspecified	4,15E-10
b) Down-regulated classes	
RNA regulation of transcription	
Lipid metabolism, degradation	
Stress, biotic, abiotic	
Protein	
Development unspecified	
Secondary metabolism, phenylpropanoids	
Hormone metabolism	
Redox	
Misc	
Transport	

4.2.2. Characterization of the ORE1 binding site and its occurrence in putative target genes

The group of genes that are direct targets of a transcription factor can be identified among early responsive genes by screening for the presence of its binding site (BS). Therefore, the characterization of the sequences bound by a transcription factor is an essential step in the identification of true targets. Olsen *et al*. (2005) reported the binding site of ORE1 as TTAGGACGTGATCATAG. The binding site of other NAC TFs has been characterized by the DNA-binding-protein-CELD method (DBP-CELD). Xue *et al*. (2005) reported that sequences bound by NAC TFs are rather long, including two consensus motifs separated by a spacer that is a few bp long (Balazadeh *et al*., 2011; Wu *et al*., 2012; Xue 2005). To deduce the BS of ORE1, our collaboration partner, Dr. Gang-Ping Xue, performed a binding site selection assay using a fusion protein consisting of a translational fusion of the ORE1 cDNA to a 6-His-tagged cellulase D (CELD), which serves for the affinity purification of the ORE1-DNA complex (Xue, 2005) (**Fig. 11.A, C-D**). As shown in **Figure 11.B,** positive clones carrying the *ORE1-CELD* construct were identified by a light red halo around the clones growing on a medium containing CMC (carboxymethyl cellulose). The halo is produced by the hydrolysis of cellulose and is visible after staining with a Congo-Red solution. A detailed description of the assay is given in experimental procedures **section 4.4.4.**
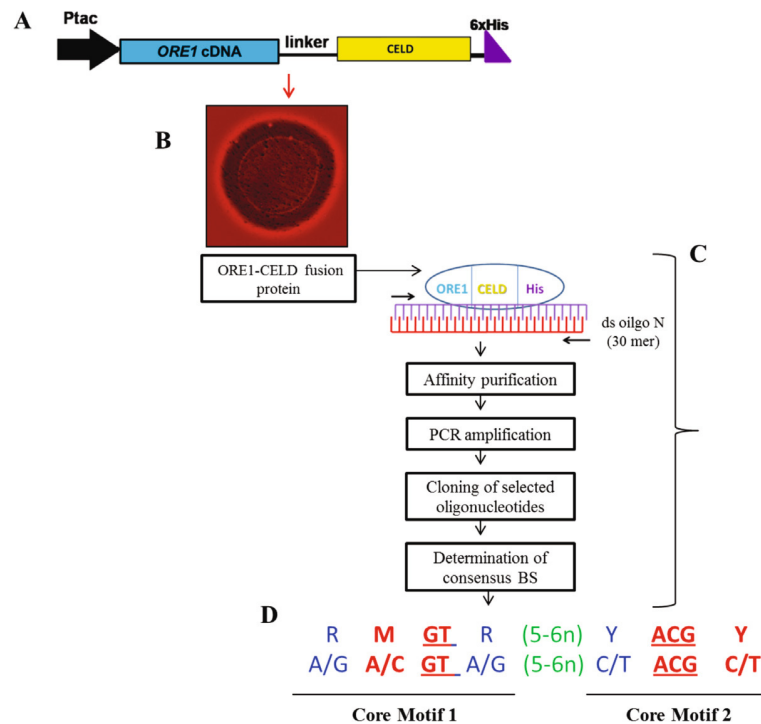
Figure 11.ORE1-BS selection assay. (A) Schematic representation of the *ORE1-CELD* construct. **(B)** *E. coli* colony expressing ORE1-CELD; bacteria were plated in sterile LB medium supplemented with Carboxymethyl-Cellulose (CMC, sodium salt). Positive colonies are detected after staining with a clear halo due to the positive cellulase activity. **(C)** Schematic representation of the CELD method. **(D)** ORE1 has high affinity to a target DNA where two core motifs, (RMGTR) and (YACGY), are spaced by 5-6 bp.

It has been shown that NAC TFs require more stringent binding sequences, not just the conserved core motif. Previously, we had reported R**CGT**R(4-5n)RY**ACG**CAA as the consensus sequence recognized by ORS1/ANAC059 (Balazadeh *et al.*, 2011). According to Ooka *et al.* (2003), *ORS1* and *ORE1* are closely related proteins and represent paralogous in *Arabidopsis*. Within their NAM domains, they share an overall amino acid identity of 94% and a sequence identity of around 41% at the C-terminal region. Considering such high similarity between the NAM domains, we hypothesized that ORE1 binding specificity may be similar to that of ORS1. We tested the binding affinity of ORE1 with the ORS1-BS and with different oligonucleotides with small variations (substitutions or deletions/additions). As shown in **Table 4,** ORE1 binding specificity to ORS1-BSs (ORS1) is very high (1.00). Nevertheless, a transversion in the first motif (ORS1m2) from C to A causes only a slight reduction in binding from 1.00 to 0.93, while a transition in the second binding motif (ORS1m1) from G to A results in a greater reduction in binding affinity from 1.00 to 0.63. To test the influence of the spacer between the first and second motifs, deletions and additions analyses were carried out (motifs ORE1m5 to ORE1m7). It can be seen that a spacer of either 4 bp or 7 bp causes a drastic reduction in binding affinity (from 1.00 to 0.17 and 0.33, respectively). These data allowed us to conclude that ORE1 preferentially binds to the consensus sequence R**MGT**R(5-6n)Y**ACGY** (**Fig. 11.D**).

Table 4. ORE1 binding sequence determined by comparison with the ORS1-BS. Tested oligonucleotides are in the first column. Grey shadowing indicates the first core motif of ORE-BS, and red coloring indicates the spacer. Blue indicates the second core motif of ORE1-BS. Transitions are underlined in each case.

Selected oligonucleotides		
Synthetic oligos	**Sequence**	**ORE1**
ORS1	CGGGGTT A**CGTA** CGGCA **CACGC**AACCGTGC	**1.00 ± 0.09**
Mutated oligos (substitutions)		
ORS1m1	CGGGGTT A**CGTA** CGGCA **CAC**A**C**AACCGTGC	**0.63 ± 0.01**
ORS1m2	CGGGGTT A**A**G**TA** CGGCA **CACGC**AACCGTGC	**0.93 ± 0.11**
ORS1m3	CGGGGTT **G**C**GTA** CGGCA **CACGC**AACCGTGC	**1.13 ± 0.02**
ORS1m4	CGGGGTT A**CGTA** CGGCA **CACG**T**AACCGTGC**	**1.20 ± 0.20**
Mutated oligos (deletions and additions)		
ORS1m5	CGGGGTT A**CGTA** GGCA **CACGC**AACCGTGC	**0.17 ± 0.01**
ORS1m6	CGGGGTT A**CGTA** CCGGCA **CACGC**AACCGTGC	**1.07 ± 0.06**
ORS1m7	CGGGGTT A**CGTA** CTCGGCA **CA**C**GC**AACCGTGC	**0.33 ± 0.01**

Values are means ± SD of three assays.

4.2.3. ORE1 activates its putative target genes *in vivo*

We performed a series of *in vivo* and *in vitro* analyses to test whether ORE1 can directly bind and activate the promoters of its putative target genes. First, we searched *in silico* for the

presence of the ORE1 binding site as determined by the DBP-CELD method (**section 4.2.2**) in the promoter regions of *BFN1* (1084 bp), *VNI2* (1571 bp), *RNS3* (1062 bp), *ORE1* (1281 bp), *SINA1* (1018 bp), and *SAG29* (831 bp) (sequences refer to up-stream of the start codon ATG). The program fuzznuc from EMBOSS was used to search for the presence of the complete or partial ORE1-BS that covers at least the first core motif (http://helixweb.nih.gov/emboss/html/fuzznuc.html) (Rice *et al.*, 2000). We identified 11 putative binding sites in *BFN1*, 19 in *VNI2*, nine in *RNS3*, eight in *ORE1*, 16 in *SINA1*, and 13 in *SAG29*. Notably, exclusively up-stream sequence of *VNI2* exhibited a putative ORE1-BS spanning the whole ORE1-BS RMGTR(5n)YACGC. This binding site corresponds to the sequence GAGTATGGTTTACGC and is located 164 bp up-stream of the ATG. *BFN1* contains the second longest version of the ORE1-BS with a transversion in the second motif (T instead of A in the twelve position) the sequence is ACGTATGAGACTCGC and is located 196 bp up-stream of the ATG (**Annex 2**).

To test whether ORE1 activates the promoter regions of its putative target genes *in vivo*, we performed a series of transactivation assays. The promoter regions of the putative target genes linked to the firefly luciferase reporter (*BFN1-LUC, VNI2-LUC, RNS3-LUC, SAG29-LUC, SINA1-LUC,* and *ORE1-LUC*) were co-transfected into *Arabidopsis* mesophyll protoplasts in the presence or absence of ORE1 fused to the Cauliflower Mosaic Virus (CaMV) 35S promoter (*35S:ORE1*) (Balazadeh *et al.*, 2010a) by PEG-mediated transformation (see Experimental Procedures, **section 4.4.8**). As shown in **Figure 12,** luciferase activity was significantly higher if the promoters of *BFN1*, *VNI2*, and *RNS3* were co-transfected with *35S:ORE1*, indicating that ORE1 transactivates the expression of these targets in mesophyll cell protoplasts. Promoter activity of *SAG29*, *SINA1*, and *ORE1* was not significantly different from basal expression; therefore, we concluded that these genes might not be direct targets of ORE1 (**Fig. 12**).
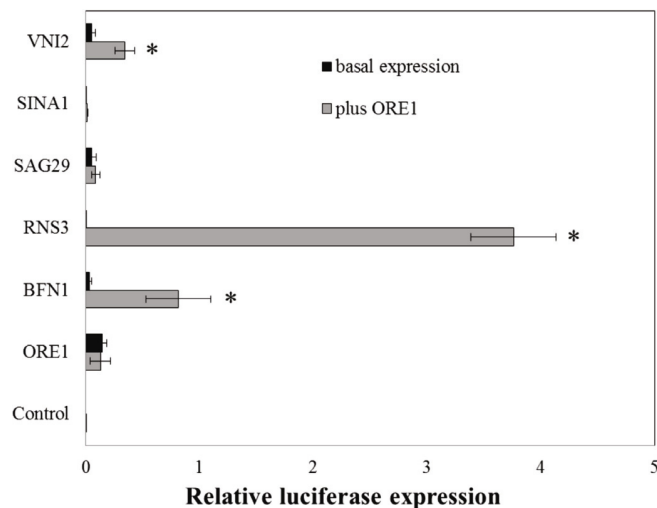
Figure 12. Protoplast transactivation of ORE1 and promoter regions of its targets. *Promoter-LUC* constructs were co-transfected into mesophyll protoplast with *35:RLuc* and with/without *35S:ORE1*. Luciferase activities were determined with the Dual Luciferase Reporter Assay System (Promega) 24 hours after transfection. Transfections were conducted in triplicate, and repeated once with a separate set of plants. Luciferase activities were normalized to corresponding Renilla luciferase activities (*P value<0,05).

46

4.2.4. ORE1 binds to its putative target genes *in vitro*

Regulation of gene expression is in part mediated through the direct interaction of transcription factors with their consensus motifs located in the promoter of targets. In order to investigate the physical interaction of ORE1 with promoter regions of its putative target genes, we performed electrophoretic mobility shift assays (EMSAs). We designed primers by (**Annex 1**) flaking one of the ORE1-BS identified by the program fuzznuc (except for the gene *SAG29*) (**Fig. 13.A**). In our analysis, we included a primer designed for *SINA1*, although we found that *in vivo* this promoter is not significantly transactivated by ORE1 overexpression (**section 4.2.3**). We selected the longest and perfect biding site of *VNI2* and *BFN1* genes, and we selected *RNS3* and *SINA1* oligos by searching for a sequence containing the invariable core for ORE1 (ACGTA) and tested in CELD method (**section 4.2.2**). As a positive control, we used the sequence that showed the highest binding affinity in the CELD experiment: ORS1 synthetic oligo 5´-CGGGGTTACGTACGGCACACGCAACCGTGC-´3 (**Table 4**). Recombinant ORE1 protein fused to glutathione S-transferase (GST-ORE1) was incubated with 5´-DY682-labeled 40-bp double-stranded DNA fragments containing the different ORE1-BSs. GST-ORE1 was able to bind to all tested promoter fragments, including promoters that were not effective in the transactivation assays. All probes contained the same concentration of ORE1 protein and oligonucleotides. Thus, we assume that differences in band intensity are related to differences in binding affinity that may reflect the effect of the presence of the two core motifs of ORE1-BS. As shown in **Figure 13.B**, GST-ORE1 protein complexes migrate slower than the free DNA due to the interaction of ORE1 with its targets. ORE1 exhibited the strongest affinity to the *VNI2* promoter fragment in comparison to all other promoter-fragments tested. We attribute this strong affinity to the presence of a complete and perfect version (15 nucleotides) of the ORE1-BS in the *VNI2* promoter fragment. In the cases where the fragments span only the first core motif, like for *RNS3*, or only up to the first nucleotide of the second core motif, like in *SINA1*, the biding affinity was strongly reduced. Nevertheless, in the case of *BFN1*, the promoter fragment contained 15 nucleotides of the ORE1-BS and exhibited a low binding affinity. The *BFN1* promoter fragment contained a transversion in the second core motif of ORE1-BS (see above **section 4.2.3**). Therefore, we concluded that conservation of the first and second motif is essential to preserve ORE1 binding affinity. Binding affinity was significantly reduced if unlabeled promoter fragments were added in excess (competitor). The competition was dose-dependent, and no mobility shift was detected if the competitor was added in excess, indicating specific binding of ORE1 (**Fig. 13.B**).
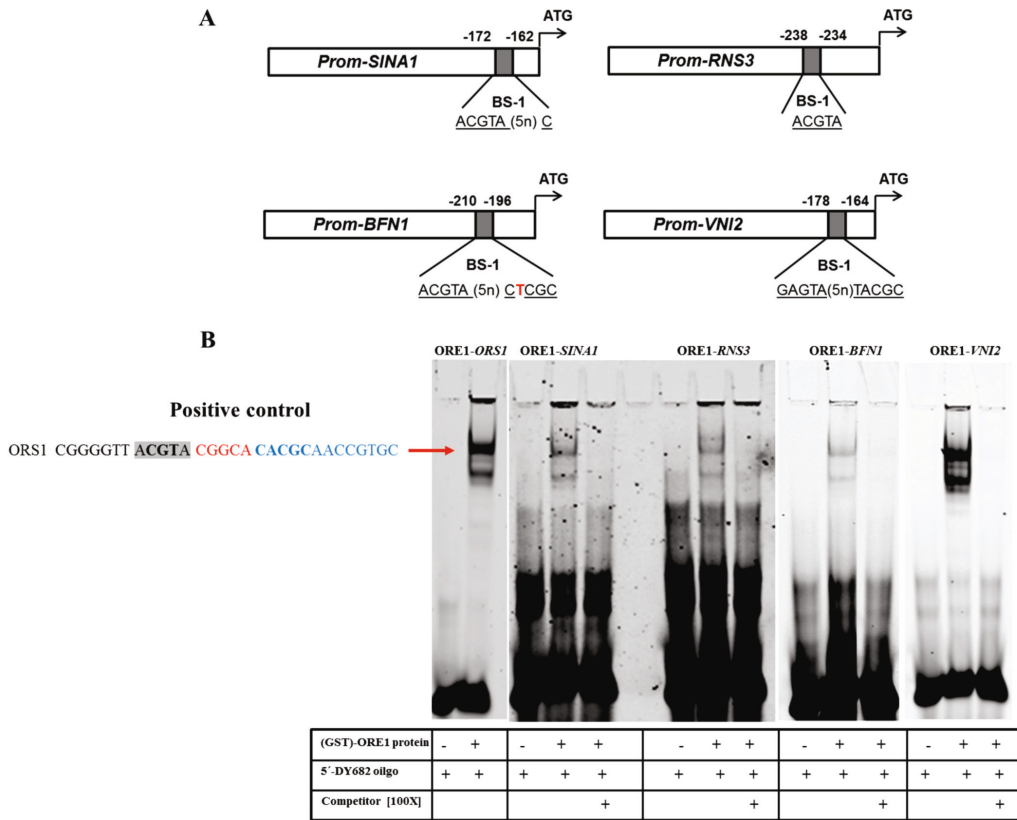
Figure 13. ORE1 binding activity *in vitro* by EMSA. (A) Schematic representation of 5′-DY682-labeled 40-bp DNA fragments **(B)** Electrophoretic mobility shift assays (EMSAs). Positive shift for all tested ORE1-putative-target genes in the presence of GST-ORE1 protein is indicated by a red arrow. Free DNA-oligos are seen at the bottom of the gel.

4.3. Conclusions

The transcriptome analyses provided important information about early regulated genes upon overexpression of ORE1. We identified a set of 17 commonly up-regulated genes that are highly and rapidly induced upon ORE1 overexpression. In contrast, we did not identify commonly down-regulated genes, and therefore, propose that ORE1 functions as a transcriptional activator like many other NAC TFs. The analysis for over-represented functional categories among the genes up- or down-regulated revealed that up-regulated genes are associated primarily with the degradation of macromolecules and signaling. We designed a list of six up-regulated genes to test if they are direct targets (*BFN1*, *VNI2*, *RNS3*, *ORE1*, *SINA1*, and *SAG29*). All the genes selected are known senescence-associated genes (SAGs), and two of them encode NAC TFs (Buchanan-Wollaston *et al*., 2005; Balazadeh *et al*., 2008a,b; Breeze *et al*.,2011). We have characterized ORE1-BS as RMGTR(5-6n) YACGY and found that all selected targets contained different versions of ORE1-BSs in their promoters. ORE1 was able to bind to all of them *in vitro* (except for *SAG29* that was not tested). Additionally, *BFN1*, *VNI2*, and *RNS3* were significantly transactivated by ORE1 in

mesophyll cell protoplasts from *Arabidopsis*. Our results provide convincing evidence that supports *BFN1*, *VNI2* and *RNS3* as direct targets down-stream of ORE1. Further analyses are required to elucidate the biological relevance of these targets in the context of natural and induced-senescence.

4.4. Experimental procedures

4.4.1. General

Standard molecular techniques were performed as described in **Chapter 2, section 2.4.1.**

4.4.2. Plant material

The plant material and growth conditions used were similar to those described in **Chapter 2, section 2.4.2.**

4.4.3. Plant transformation

Arabidopsis transformation was performed as described in **Chapter 2, section 2.4.4.**

4.4.4. Constructs

Description of the overexpressor construct (**35S:ORE1**) was given in Balazadeh *et al*. (2010a).

***Promoter-LUC* constructs:** promoter regions spanning 1.5 kb up-stream of the translation start codon ATG of *VNI2, BFN1*, *RNS3*, *ORE1*, *SINA1* and *RNS3* were amplified from genomic DNA by PCR using an Advantage HF 2 PCR Kit (Clontech) with gene-specific forward and reverse primers (**Annex 1**). Promoter fragments were subcloned into a pENTR-D-TOPO vector (Invitrogen, www.invitrogen.com) to generate individual entry vectors. The entry vectors were then recombined into the Gateway destination vector *p2GWL7.0* which is a recombination of the gateway vectors *pBGWL7.0* (transcription reporter vector) (Karimi *et al*., 2002) and *p2GW7.0* (overexpression vector) (Licausi *et al*., 2011) using the LR reaction mix II (Invitrogen) to obtain the final *BFN1-LUC, VNI2-LUC, RNS3-LUC, ORE1-LUC, SINA1-LUC*, and *SAG29-LUC* reporter vectors.

ORE1–CELD: *ORE1* cDNA was amplified by PCR from leaf cDNA with forward (116) and reverse (117) primers (**Annex 1**). The amplified fragment was inserted into pCR2.1–TOPO and then cloned via *NheI and BamHI* sites into plasmid pTacLCELD6XHis (Xue, 2005) to create an *ORE1–CELD* in-frame fusion construct (pTacORE1LCELD6XHis).

4.4.5. Transient expression of *ORE1* in protoplasts for transcriptome profiling

The protoplast preparation protocol was adapted from Sheen (2002). *Arabidopsis* mesophyll cell protoplasts were isolated from leaves (the second and/or third/fourth pair) of 5-week-old Col-0 (CS60000) plants grown on soil under long-day (16 hours light/8 hours dark) conditions. Leaves were placed in enzyme solution (1% cellulase R10, 0.3% macerozyme R10 (Yakult Honsha, Tokyo, Japan), 0.4 M mannitol, 20 mM KCl, 10 mM $CaCl_2$, 20 mM MES, 0.1% BSA (Sigma A-6793), pH 5.7) for 8.5 hours. Protoplasts were collected and kept on ice in W5 medium (154 mM NaCl, 125 mM $CaCl_2$, 5 mM KCl, 2 mM MES, pH 5.7) for 13 hours in the growth cabinet. Protoplasts were transferred to MMG solution (0.4 M mannitol, 15 mM $MgCl_2$, 4 mM MES pH 5.7), and subjected to PEG transfection. To 2.12×10^6 protoplasts, a total of 250 µg plasmid DNA was added followed by 30 minutes of incubation in 1 vol. of PEG solution (40% PEG 3500, 3 mL H_2O, 0.2 M mannitol, 0.1 M $CaCl_2$). After transfection, the samples were diluted with 2 vol. of W5 solution and collected by centrifugation at 100 g for two minutes. Protoplasts were then resuspended in 4 mL WI medium (0.5 M mannitol, 20 mM KCl, 4 mM MES, pH 5.7), transferred to 5 cm Petri dishes pre-coated with 5% calf serum, and incubated for 6 hours in the growth cabinet. After the incubation, protoplasts were collected, and 100 - 200 mg aliquots were flash-frozen in liquid nitrogen for subsequent RNA isolation and expression profiling.

4.4.6. Gene expression analysis by microarray

Three micrograms of quality-checked total RNA obtained from leaves of two and three biological replicates of *IOE-ORE1* and wild type lines, respectively (two hours and five hours after 10 µM estradiol treatment), and two biological replicates of the mesophyll cell protoplasts transiently overexpressing *35S:ORE1*, were processed for use in Affymetrix GeneChip hybridisations (GeneChip® *Arabidopsis* ATH1 array) as described (Redman *et al*., 2004). RNA was obtained from *IOE-ORE1* and wild type 15-day-old seedlings grown in half MS (Murashige and Skoog, 1962) media with the selective antibiotic hygromycin (as described in **Chapter 2**). Seedlings were transferred from solid to liquid MS media one day before treatment to minimize secondary effects by stress. Seedlings of *ORE1-IOE* and wild type were treated/non treated with EST and, immediately after, whole seedlings were frozen in liquid nitrogen (N) for RNA extraction. ATH1 arrays allow the analysis of around 24.000 *Arabidopsis* genes. Labeling, hybridization, washing, staining, and scanning procedures were performed by Affymetrix Authorized Service Provider (ATLAS Biolabs, Berlin, Germany) as described in the Affymetrix technical manual. Raw data (CEL files) obtained from RNA hybridization experiments were normalized with the affyPLM package from the Bioconductor software project (Gentleman *et al*., 2004) using the GCRMA that uses GC content of probes in normalization with RMA (Robust Multiple array Average) and gives one value for each probe set instead of keeping probe level information (Wu and Irizarry, 2004).The heat map was produced using the software gplots from R. The Log2FC

results for the 54 probe sets up-regulated in the ATH1 Affymetrix after two hours inducible overexpression of ORE1 were clustered together with the corresponding results after five hours inducible overexpression and 6 hours constitutive overexpression. The hierarchal clustering was performed using Euclidian-distance as the method of pairwise distance calculation. The dendrograms group treatments (columns) and probe sets (rows) according to their similarity (Warnes *et al.*, 2009)

4.4.7. ORE1 binding affinity to ORS1 perfect and mutated binding sites

This work was performed in collaboration with Dr. Gang-Ping Xue, CSIRO Plant Industry, St. Lucia, Australia. The DNA-binding activity of ORE1-CELD protein was measured using methylumbelliferyl β-D-cellobioside (MUC) as substrate as described in Xue (2002). DNA-binding assays with a biotin-labeled single-stranded oligonucleotide, or a biotin-labeled double-stranded oligonucleotide without a target binding site, were used as controls.

4.4.8. Dual-luciferase assay

Dual-luciferase assay was performed as described in **Chapter 2, section 2.4.7.** Promoter regions of ORE1 putative genes were used as reporter plasmids: a 1.0 kb up-stream of the ATG was amplified from genomic *Arabidopsis* ecotype Col-0 DNA to generate reporter final constructs: *BFN1-LUC*, *VNI2-LUC*, *RNS3-LUC*, *SAG29-LUC*, *SINA1-LUC*, and *ORE1-LUC* (described in **section 4.4.4**). As an effector plasmid, a *35S:ORE1* construct was used. Normalization of data was performed based on relative luciferase of the *35S:RLuc* normalization vector (Licausi *et al.*, 2011).

4.4.9. EMSA

For protein expression and purification, the *ORE1* cDNA was recombined in vitro into the Gateway vector pDEST24 (Invitrogen) encoding a C-terminal GST-tag, and transformed into the E. coli expression strain BL21 (DE3) pLysS (Agilent Technologies). The pDEST15 vector (Invitrogen) was used for expression and purification of GST alone. Expression of GST and ORE1-GST fusion proteins was carried out in 400-smL cultures and induced at 30°C by 1 mM isopropyl thio-β-D-galactoside for 3 hours. Harvested cells were lysed in 20 mL GST lysis buffer (20 mM sodium phosphate buffer, pH7.3, 150 mM NaCl, 1 mM EDTA, 0.2% Triton X-100, 1 mM dithiotreitol, 1 mM phenylmethanesulfonyl fluoride, 10 µg/mL aprotonin, 10 µg/mL leupeptin, 2 mM benzamidin) and ultrasound treatment. According to the instructions of the manufacturer, the supernatant of ultracentrifuged samples was used for affinity purification with 70 mg of pre-equilibrated glutathione-agarose beads (Sigma-Aldrich). Aliquots of the elution fractions were analyzed by SDS-PAGE and Coomassie staining. One-mL fractions containing the purified proteins were pooled and dialyzed against PBS buffer (20 mM sodium phosphate buffer, pH7.4 and 150 mM NaCl). Concentrations

of purified proteins were determined by SDS-PAGE and Coomassie staining using BSA standards. 5-DY682-labeled DNA fragments were obtained from MWG (Ebersberg, Germany). Sequences of labeled DNA fragments, unlabeled competitors, and mutated fragments are given in **Annex 1**. Annealing was performed by heating the primers to 100°C followed by slow cooling to room temperature (RT). Binding reaction was performed at RT for 20 minutes as described in the Odyssey Infrared EMSA kit instruction manual. DNA-protein complexes were separated on 6% retardation gel while DY682 signal was detected using the Odyssey Infrared Imaging System for LI-COR Biosciences.

Contributions

Dr. Gang Ping Xue performed the CELD experiment. Dr. Wolfgan Dröge Laser performed transient overexpression of *ORE1* in *Arabidopsis* protoplasts (*35S:ORE1/*6 hours). Dr. Hakan Dortay and Katharina Schulz produced recombinant ORE1-GST protein.

Chapter 5

Expression of *BIFUNCTIONAL NUCLEASE1* (*BFN1*) during senescence in *Arabidopsis* is regulated by the NAC transcription factor ORE1/ANAC092/AtNAC2

A version of this work will be submitted to *The Plant Journal*

Lilian P. Matallana-Ramirez,[1,2] Mamoona Rauf,[1] Hakan Dortay,[1] Liliane Sorego,[3] Amnon Lers,[3] Gang-Ping Xue,[4] Wolfgang Dröge-Laser,[5] Salma Balazadeh,[1,2,] and Bernd Mueller-Roeber[1,2,]

[1]University of Potsdam, Institute of Biochemistry and Biology, Karl-Liebknecht-Straße 24-25, 14476 Potsdam-Golm, Germany; [2]Max-Planck Institute of Molecular Plant Physiology, 14476 Potsdam-Golm, Germany, [3]Department of Postharvest Science of Fresh Produce. Volcani Center, Agricultural Research Organization, Bet Dagan, 50250 - Israel; [4]CSIRO Plant Industry, 306 Carmody Road, St Lucia, Qld 4067, Australia; [5]Julius-Maximilians-Universität Würzburg, Julius-von-Sachs-Platz 2, 97082 Würzburg, Germany.

5.1. Introduction

Senescence is a regulated process associated with the final developmental stages in plants. It can also be triggered by abiotic and biotic stresses. Several of the more than 20 senescence up-regulated NAC TFs in *Arabidopsis thaliana* have been shown to regulate senescence, including (among others) *AtNAP/ANAC029* (Guo and Gan, 2006), *ORE1/ANAC092/ AtNAC2* (Balazadeh *et al*., 2010a,b; Kim *et al*., 2009), and *ORESARA1 SISTER1/ORS1/ ANAC059* (Balazadeh *et al*., 2011) which all promote senescence, and recently, the NAC factor *VASCULAR-RELATED NAC-DOMAIN (VND) INTERACTING2* (*VNI2, ANAC083*) has been reported to integrate ABA signaling and leaf senescence (Yang *et al*., 2011). *ORE1* has been shown to be a central regulator of senescence in *Arabidopsis thaliana* (Balazadeh *et al*., 2010a,b; Breeze *et al*.,2011). Despite the amount of available data, the exact mechanisms

that govern the onset and progression of senescence remain unknown at present, but direct interactions between this NAC TF (ORE1) and their target genes are clearly needed for this process. ORE1 has recently been shown to play a role in developmental and induced senescence as well as programmed cell death (PC) (Balazadeh *et al.*, 2010a,b; Kim *et al.*, 2009).

It was establish that the *ore1-1* allele isolated from an EMS-mutagenized pool, and the *ore1-2* allele isolated from a population of fast neutron-mutagenized Col-0 seeds, conferring the delayed leaf senescence phenotype (Aeong Oh *et al.*, 1997; Kim *et al.*, 2009) as well as the *anac092-1* T-DNA insertion mutant. In contrast, *ORE1* overexpression strongly enhances senescence (Balazadeh *et al.*, 2010a). Kim *et al.* (2009) proposed a trifurcate feed-forward pathway involving *ORE1*, *microRNA164* (*miR164*), and *EIN2* (*ethylene insensitive 2*) ensuring highly robust regulation of leaf senescence and aging induced cell death. *ORE1* expression is positively regulated by *EIN2* but negatively by *miR164* with leaf age. *EIN2* functions as a negative regulator of *miR164* expression in an age-dependent manner. Age-dependent down-regulation of *miR164* leads to accumulation of ORE1 expression. Despite clear evidence of ORE1 as a key role in the regulation of leaf senescence, knowledge about the molecular mechanism(s) and gene network(s) through which ORE1 exert its senescence regulatory function is still limited. We have previously described genes whose mRNA expression is rapidly induced upon ORE1 induction (ORE1 regulon), and are, therefore, candidates for being direct targets of ORE1 (**Chapter 4**). Bioinformatics analysis and network modeling, based on high-resolution time-course profiles of gene expression during leaf development, predict genes whose expression is positively influenced by ORE1 (Breeze *et al.*, 2011). *BFN1*, which is among the genes that are rapidly and positively regulated by ORE1, encodes a type I nuclease; it shares high amino acid sequence similarity to DSA6 nuclease, which is associated with petal senescence in daylilies (Panavas, 1999), and to ZEN1 nuclease, which is associated with PCD in *Zinnia elegans* (Ito and Fukuda, 2002). *BFN1* expression was already enhanced by around fourfold two hours after EST treatment in *ORE1-IOE* lines. Its expression further increased to fortyfold within five hours of EST treatment. An extreme activation of *BFN1* expression (a thousandfold) was observed in the *35S:ORE1* six hours after protoplast transfection (**section 4.2.1**). *BFN1* expression has been shown to be specifically enhanced during leaf and stem senescence, as well as in the floral abscission zone and during developmental PCD (Breeze *et al.*, 2011; Buchanan-Wollaston *et al.*, 2005; Farage-Barhom *et al.*, 2011; Pérez-Amador *et al.*, 2000; Wagstaff *et al.*, 2009). Intracellular localization studies revealed that at later stages of senescence, BFN1-GFP is localized with fragmented nuclei in membrane coated vesicles, suggesting the role for BFN1 in regulated nucleic acid degradation occurs during senescence and developmental PCD (Farage-Barhom *et al.*, 2011). In **Chapter 4** we obtained strong evidence that support a possible direct interaction of *BFN1* by ORE1. Here, we demonstrated that ORE1 specifically activates the *BFN1* promoter. *BFN1* and *ORE1* tissue-specific expression show largely over-lapping patterns, reaffirming the idea of co-expression. We proved that binding of ORE1

to *BNF1* promoter is highly specific, and single mutations in ORE-BS that are present in the *BFN1* promoter hardly affect binding activity *in vivo*. Moreover, we revealed that senescence-enhanced expression of *BFN1* is abolished in the *anac092-1* T-DNA insertion mutant, indicating ORE1 as a major regulator of *BFN1* expression during senescence. Our results give convincing data that supports *BFN1* as a direct target down-stream of ORE1.

5.2. Results

5.2.1. Overlapping patterns of transcriptional activities of *BFN1* and *ORE1* promoters

The elevated expression of *BFN1* in the cells and transgenic plants overexpressing ORE1 indicated that the NAC TF acts as an up-stream positive regulator of *BFN1*. We, therefore, analyzed the extent of co-expression of both genes in *Arabidopsis* plants. Gene expression profiling data revealed induction of both *BFN1* and *ORE1* during leaf and pistil developmental senescence (Breeze *et al*., 2011; Buchanan-Wollaston *et al*., 2005; Farage-Barhom *et al*., 2011; Pérez-Amador *et al*., 2000; Wagstaff *et al*., 2009) and during dark- and salt-induced senescence (Balazadeh *et al*., 2010b; Buchanan-Wollaston *et al*., 2005). Moreover, expression of both genes was highly induced upon 180 minutes ABA treatment in 7-day-old seedlings (*Arabidopsis* Hormone Database) (Jiang *et al*., 2011) and significantly reduced in the ein2 mutant that lacks a major component of the ethylene signaling pathway (Buchanan-Wollaston *et al*., 2005). To investigate the extent of overlapping promoter activities during senescence, we looked at *ORE1* and *BFN1* promoter activities using promoter-β-glucuronidase (GUS) reporter lines. Transgenic *Arabidopsis* lines expressing the *GUS* reporter gene, driven by the 2.3 kb *BFN1* up-stream region (Farage-Barhom *et al*., 2008) or the 1.5 kb *ORE1* up-stream region (Balazadeh *et al*., 2010a), were analyzed side by side to identify unique and overlapping expression patterns of both genes. In general, expression patterns of both promoter fusions were highly similar in leaves and floral organs at different developmental stages, while expression was largely absent in young tissues, consistent with the function of both genes during senescence (**Fig. 14**). Examination of GUS expression in 15-day-old seedlings revealed high *BFN1* and *ORE1* expression in cotyledons as well as in the tip regions of leaves. *BFN1* expression was faint in roots (**Fig. 14.a**) compared to *ORE1* expression in the same tissues (**Fig. 14.f**). In both *BFN1* and *ORE1* plants 40 days after sowing (DAS), GUS activity was specifically detected in tip and margin regions of senescence leaves (**Fig. 14.b,g**). GUS activity was prominent in the stigma, mature anthers, and sepals of mature/fully opened flowers (flower stage 13/14 as classified by Ferrandiz *et al*. (1999) (**Fig. 14.d,i and c,h**). Expression in mature siliques was detectable in abscission zones (AZ) at the bottom and upper parts of the valve margins for both *Prom-ORE1:GUS* and *Prom-BFN1:GUS* (**Fig. 14.e,j**). We also observed GUS expression in *Prom-ORE1:GUS* lines in the replum of mature fruits and faintly in *Prom-BFN1:GUS* (**Fig. 14.j**). Thus, our data largely demonstrated overlapping expression patterns for the NAC transcription factor *ORE1* and its direct down-stream target *BFN1*.
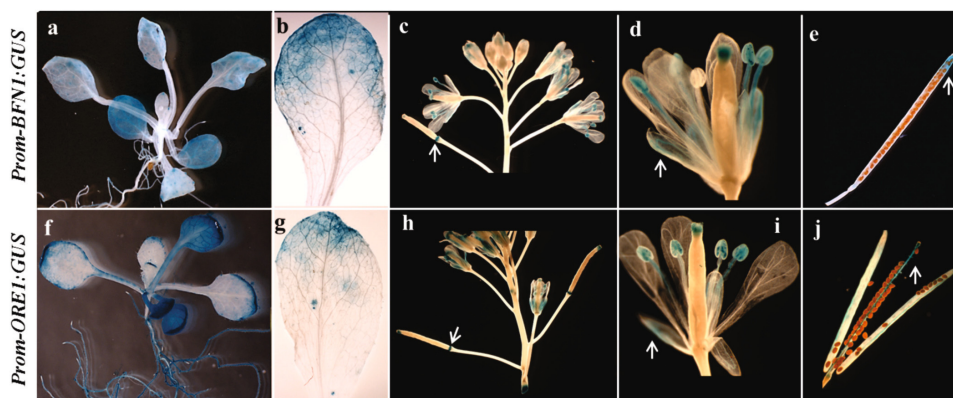
Figure 14. Histochemical GUS staining of *Prom-BFN1:GUS* and *Prom-ORE1:GUS* in *Arabidopsis*. Plants were transformed with *Prom-BFN1:GUS* (top) and *Prom-ORE1:GUS* (bottom): (**a, f**) *Arabidopsis* seedlings (15-day-old) exhibited strong GUS activity in cotyledons and tip regions of leaves. (**b, g**) *Arabidopsis* leaves (40 DAS) showed strong GUS activity in the tip and margin regions of leaves corresponding to the oldest tissues. (**c, h**) Bolting branch with young and old flowers. GUS was observed in mature/opened flowers. GUS activity was observed in the flower abscission zone (indicated by arrows). (**d,i**) close-up of mature/opened flowers (flower stage 13/14 as classified by Ferrandiz *et al*. (1999). Strong GUS activity on stigma and mature anthers was detected. GUS activity was faint in sepals (indicated by arrows). (**e,j**) close-up of mature siliques. GUS activity was detected in abscission zones (AZ) at the bottom and upper part of the siliques. In the case of *Prom-ORE1:GUS*, promoter activity was also detected in the replum (indicate by arrows) and along the aperture site of the valves.

5.2.2. Altered level of BFN1 protein in ORE1 transgenic plants

Nuclease I enzymes are involved in the degradation of RNA and single-stranded DNA during several plant growth and developmental processes, including senescence. BFN1 RNase and DNase nuclease activities were detected in activity gels at about 38 kDa using leaves from transgenic *Arabidopsis* plants overexpressing *BFN1*. Nuclease activity was almost undetectable when using roots and non-senescent leaves and stems. Furthermore, senescent flowers also exhibited enhanced nuclease activity. These results demonstrated that *BFN1* encodes a bifunctional nuclease capable of degrading RNA and DNA (Pérez-Amador *et al*., 2000). To further confirm that *BFN1* expression is ORE1-dependent, we measured changes in BFN1 nuclease protein levels in plants overexpressing or lacking ORE1 protein. All protein was extracted from (i) estradiol (EST) treated and (ii) non-treated (15-day-old) *ORE1-IOE* seedlings after 24 hours of induction. In order to avoid artifacts due to the EST treatment, we analyzed BFN1 activity in *ORE1* overexpressor lines (*35S:ORE1*, lines 23 and 24) using protein extracts from leaves in which senescence was artificially induced. All leaves were at full senescence, as judged by complete yellowing of the tissue, and empty vector lines (E.V.) were used as controls. Additionally, BFN1 nuclease protein level was measured in the *anac092-1* T-DNA insertion mutant and wild type plants (30-DAS). Same position leaves (6 and 7) were detached and incubated in the dark until full senescence was obtained (after seven days in the wild type and nine days in the mutant). Proteins were extracted from the plant material described above and used for Western blot analysis using BFN1 antiserum.

The position of the senescence-induced BFN1 protein was clearly visible in the analysis, indicated by black arrows on the gels. The expression level of BFN1 nuclease protein was detected in *ORE1-IOE* seedlings upon treatment with EST (**Fig. 15.D**), whereas it was undetectable in untreated *ORE1-IOE* seedlings (**Fig. 15.C**). This result strongly supports that at earlier developmental stages, BFN1 expression is absent. Nevertheless, an increase in the ORE1 protein level after EST treatment is able to trigger the expression of BFN1, even in young plants like seedlings (**Fig. 15.D**). Interestingly, proteins extracted from inducible *ORE1* lines and constitutive *ORE1* overexpressors (**Fig. 15.D, G-H**) exhibited a substantial reduction in the amount of proteins compared to non-treated *ORE1-IOE* seedlings and wild type protein extracts; in particular, degradation of Rubisco LSU (ribulose bisphosphate carboxylase/oxygenase large subunit) was evident, which is in accordance with the fact that overexpression of ORE1 triggers senescence and accelerates protein degradation. Rubisco protein is indicated by red arrows on the gel images. As expected, BFN1 nuclease protein was almost absent in senescent leaves of the *anac092-1* T-DNA insertion mutant compared to senescing leaf protein extract from wild type plants. As expected, the *anac092-1* T-DNA insertion mutant plants showed bands of Rubisco signal which is in accordance with the delay of senescence in these lines and the retardation of protein degradation (**Fig. 15.A-B**). Overall, our results confirm that *BFN1* expression is ORE1-dependent.
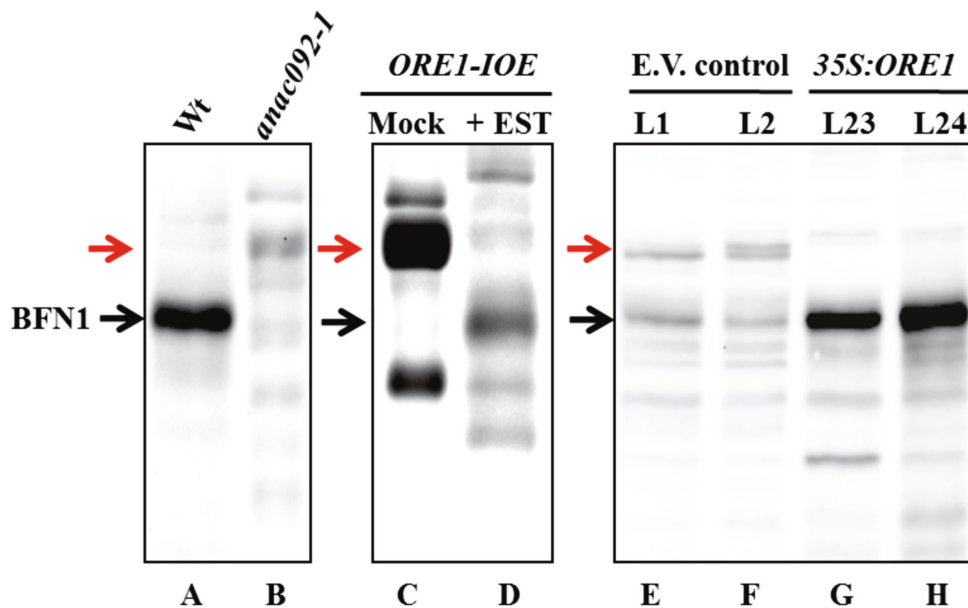
Figure 15. Altered level of BFN1 protein in *ORE1* transgenic plants detected by Western blot. In all blots, red arrows corresponds to Rubisco LSU (ribulose bisphosphate carboxylase/oxygenase large subunit) and black arrows correspond to BFN1 protein. (**A**) Enhanced BFN1 protein level in wild type protein extract. (**B**) BFN1 protein is almost absent in anac092-1 T-DNA insertion mutant. *anac092-1* T-DNA insertion mutant shows a considerable concentration of Rubisco LSU, indicating that protein degradation is almost absent. BFN1 protein level was absent in untreated inducible *ORE1* overexpression seedlings (**C**) compared to treated seedlings after 24 hours EST treatment (**D**). Lower levels of BFN1 protein were detected in pGreen empty vector lines (E.V.) control plants (**E-F**) compared to a markedly BFN1 protein level in *35S:ORE1* overexpressor lines (L24 and L25) (**G-H**).

5.2.3. Senescence-specific expression of BFN1 is ORE1-dependent

In order to test whether the senescence-induced expression of *BFN1* is dependent on the presence of functional ORE1, we tested *BFN1* expression in the *ore1-1* EMS mutant using plants from different developmental stages; plants were grown in soil and leaves were harvested from plants 12, 16, 20, 24, 28, 32, and 36 days after sowing. As shown in **Figure 16,** *BFN1* expression strongly increased with age in wild type plants; expression was sixtyfold higher in leaves of 28-day-old plants compared to leaves of 24-day-old plants. Expression of *BFN1* remained high and increased further at later time points (in 32- and 36-day-old plants), consistent with previous observations that *BFN1* is a senescence-associated gene (Farage-Barhom *et al.*, 2011; Pérez-Amador *et al.*, 2000; Wagstaff *et al.*, 2009). In contrast, the age-dependent increase of *BFN1* transcript abundance was completely abolished in leaves of the *ore1-1* EMS mutant. These data indicate that senescence-associated expression of *BFN1* is mainly, if not exclusively, regulated by ORE1. Considering the negative regulation of *ORE1* by *mir164abc* during leaf aging, we next tested *BFN1* transcript level in the *mir164abc* triple mutant at different leaf developmental stages (as described above). The difference in *BFN1* transcript between younger and older leaves was greater in *mir164abc* mutants than wild type plants (**Fig. 16.A**).

To further confirm that expression of *BFN1* is ORE1-dependent, we tested the expression of an exclusively senescence marker. *SAG12* mRNA expression was measured in the same plant material. As expected, *SAG12* expression increased with age in wild type plants with a maximum value at the later time point (36-day-old plant). In contrast to *BFN1* mRNA expression in *ore1-1* EMS mutant, *SAG12* increased with age following the same pattern as in wild type and *mir164abc* mutants. *SAG12* expression increased at a lower rate in the *ore1-1* EMS mutant than in wild type and *mi164abc* mutants, confirming that the absence of ORE1 delays senescence. In the end, expression of *SAG12* was the same in all tested plants. These results confirm that all tested plants reach senescence in the latest time point (after 36 days after germination), and the absence of functional ORE1 not only delays senescence but directly controls the expression of *BFN1* (**Fig. 16.B**).
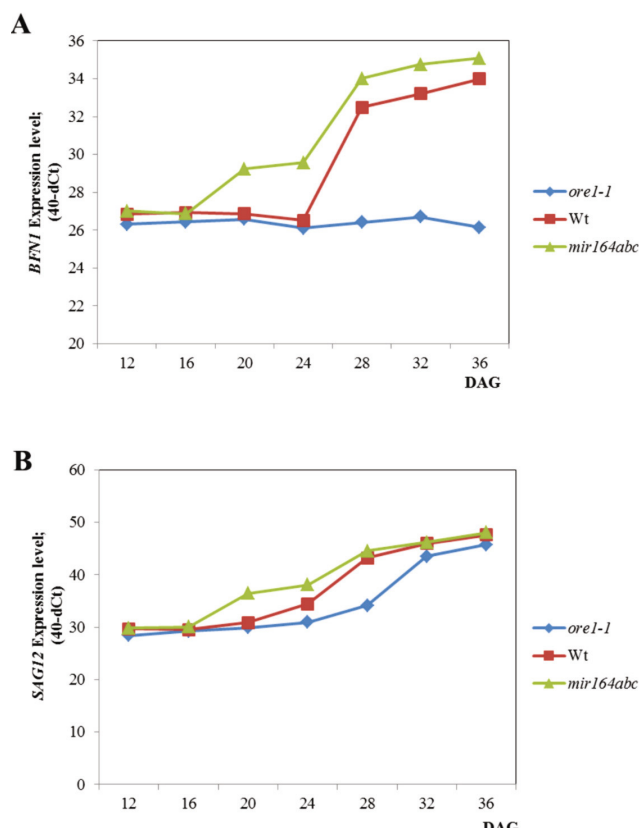
Figure 16. *BFN1* and *SAG12* expression in *ore1-1* EMS mutant, *mir164abc*, and wild type plants. (**A**) *BFN1* and (**B**) *SAG12* transcript levels in leaves of *ore1-1* EMS mutant, *mi164abc* mutant, and wild type *Arabidopsis* plants at different ages (12, 16, 20, 24, 28, 32, and 36 days after germination). Expression level was determined by qRT-PCR, and data are means of two biological replicates.

To further confirm ORE1-dependent expression of *BFN1* during senescence, we transformed the *anac092-1* T-DNA insertion mutant with the *Prom-BFN1:GUS* construct (Farage-Barhom *et al.*, 2008) and compared it to the expression patterns and GUS activity in wild type plants that were transformed using the same construct. To minimize the potential effect of the integration point, we analyzed more than 50 independent lines transformed with *Prom-BFN1:GUS*. The presence of the *GUS* gene in all lines was confirmed by PCR on genomic DNA (**Fig. 17.E**). Histochemical staining revealed strong reduction, and in most cases, absence of detectable *BFN1* promoter activity in the *anac092-1* T-DNA insertion mutant background compared to wild type (**Fig. 17.A-B**). Additionally, we quantitatively determined GUS activity using 4-methylumbelliferyl-ß-D-glucoronide (4-MUG) as substrate in an assay and taking fully expanded juvenile leaves (from 20-day-old plants) and senescent leaves showing less than 50% yellowing (from 40-day-old plants) of *Prom-BFN1:GUS* transgenic lines. As shown in **Figure 17.F,** reporter gene activity was significantly reduced in *Prom-BFN1:GUS/anac092-1* T-DNA insertion mutant lines compared to *Prom-BFN11:GUS/*wild type plants. Reduced GUS activity was particularly pronounced in senescent leaves compared to young leaves.

These data confirm that ORE1 plays a central role as an up-stream transcriptional regulator of *BFN1*.
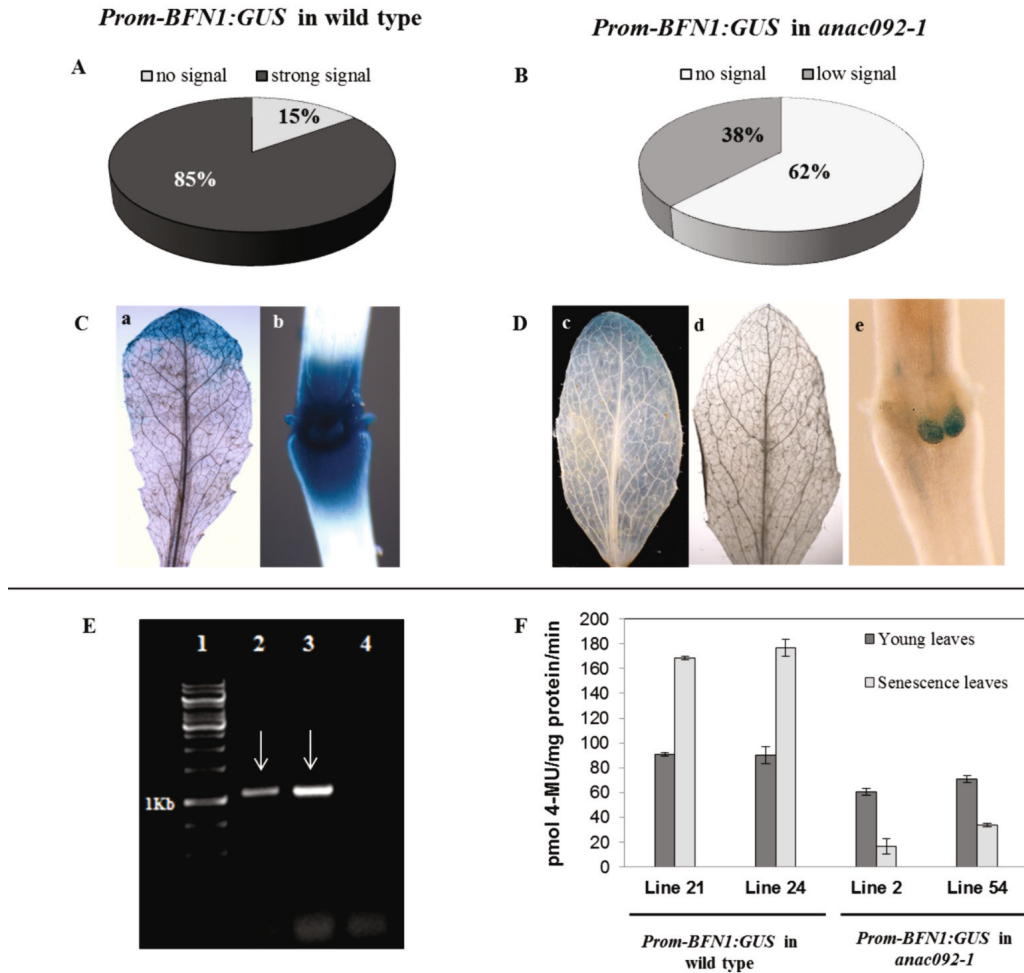
Figure 17. Expression patterns of *Prom-BFN1:GUS* in wild type (Col-0) (upper left panel) and *anac092-1* T-DNA insertion mutant (upper right panel) backgrounds. (A) Percentage of transgenic lines (*Prom-BFN1:GUS* in wild type background) with strong GUS activity (strong signal) compared to percentage of plants without GUS activity (no signal). **(B)** Percentage of transgenic lines (*Prom-BFN1:GUS* in *anac092-1* T-DNA insertion mutant background) that exhibited reduction (low signal) or absence of GUS activity (no signal). **(C.a)** Strong GUS activity in the tip region of an old leaf (line 24). **(D.c)** Faith GUS activity in the tip region of an old leaf (line 54). **(D.d)** Absence of GUS activity in tip region of an old leaf (line 2). **(C.b–D.e)** GUS activity within floral abscission zone (AZs) in the remaining cells for protective scar tissue and the region surrounded. The images displayed are representative of at least 30 plants examined for each line per experiment. **Bottom right panel: (F)** Quantitative GUS activity of *Prom-BFN1:GUS* measured by a MUG assay in fully expanded transgenic lines from young leaves (from 20-day-old plants) and senescent leaves (from 40-day-old plants); *Prom-BFN1:GUS* in wild type background (lines 21 and 24) and *Prom-BFN1:GUS* in *anac092-1* T-DNA insertion mutant background (lines 2 and 24). Data are the means of two biological and three technical replicates. **Bottom left panel: (E)** PCR analysis of 40-day-old *Prom-BFN1:GUS* transgenic plants. DNA was isolated and used as templates for GUS specific amplification. Lane 1 is DNA size marker. Lane 2 is PCR product of *Prom-BFN1:GUS* in wild type background (line 21). Lane 3 is PCR product of *Prom-BFN1:GUS* in *anac092-1* T-DNA insertion mutant line background (line 2; plants showed no GUS staining). Lane 4 is the negative control. White arrows indicate GUS-specific amplification, fragment size 1139 bp. The sequence of GUS-specific primers is given in **Annex 1**.

5.2.4. ORE1 binding activity to BFN1 promoter is highly regulated by ORE1-binding site (BS)

Transient transactivation assays have been widely used as a powerful and rapid method to predict transcription factor direct target genes and elucidate functional *cis*-regulatory motifs within promoters of target genes (Licausi *et al*., 2011; Park *et al*., 2010; Yang *et al*.,2011; Zhong *et al*., 2010, Zhou *et al*., 2009). In **section 4.2.3,** we established that ORE1 transactivates *BFN1*-promoter in mesophyll protoplast. Additionally, we determined that the *BFN1* promoter contains 11 different versions of the ORE1 binding site (BS), but only one corresponds to the longest version (ACGTATGAGACTCGC) that is 15 nucleotides long and contains one transition ("T" instead of "A"). This ORE1-BS is located 196 bp up-stream of the ATG and was named BS-1 for further analysis. We aimed to test if BS-1 is crucial for ORE1-mediated transactivation of the *BFN1* promoter. We compared the effect in the transcriptional activation of *BFN1* using three different *BFN1* promoters fused to luciferase (reporter gene): (i) 1084 bp up-stream of the start codon ATG and contained the original BS-1 (*BFN1-LUC*); (ii) a second version *BFN1-M-LUC* covered the same region but carried a substitution in the first core motif of BS-1 (``CGT`` was substituted with ``AAA``); and (iii) *BFN1-S-LUC* comprised truncated promoter (192 bp) that lacked all ORE1-BSs (binding sites) (**Fig. 18.A**). Our luciferase-based assay data demonstrate that the introduction of these substitutions in BS-1 significantly reduced the ORE1 mediated transactivation (**Fig. 18.B**). This data made us conclude that BS-1 regulated the direct interaction of ORE1 to *BFN1* promoter. However, the change in BS-1 did not lead to a complete abolishment of *BFN1* transactivation, indicating that other active binding sites in *BFN1* promoter mediated its transactivation. Analyses *in silico* indicated that *BFN1* promoter contains 11 ORE1-BS in the promoter which covers at least the complete first core motif (**Annex 2**). Thus, it is plausible to think that those ORE1-BS are active and able to transactivate *BFN1*. Indeed, the deletion of *BFN1* promoter to a 192 bp fragment resulted in further reduction of *BFN1* transactivation. Interestingly, *BFN1-S-LUC* transcriptional activity was still detectable at a higher level than basal activity. Therefore, we conclude that ORE1 is a major regulator of *BFN1* but might possess other active BSs that are able to lead transactivation of its promoter.
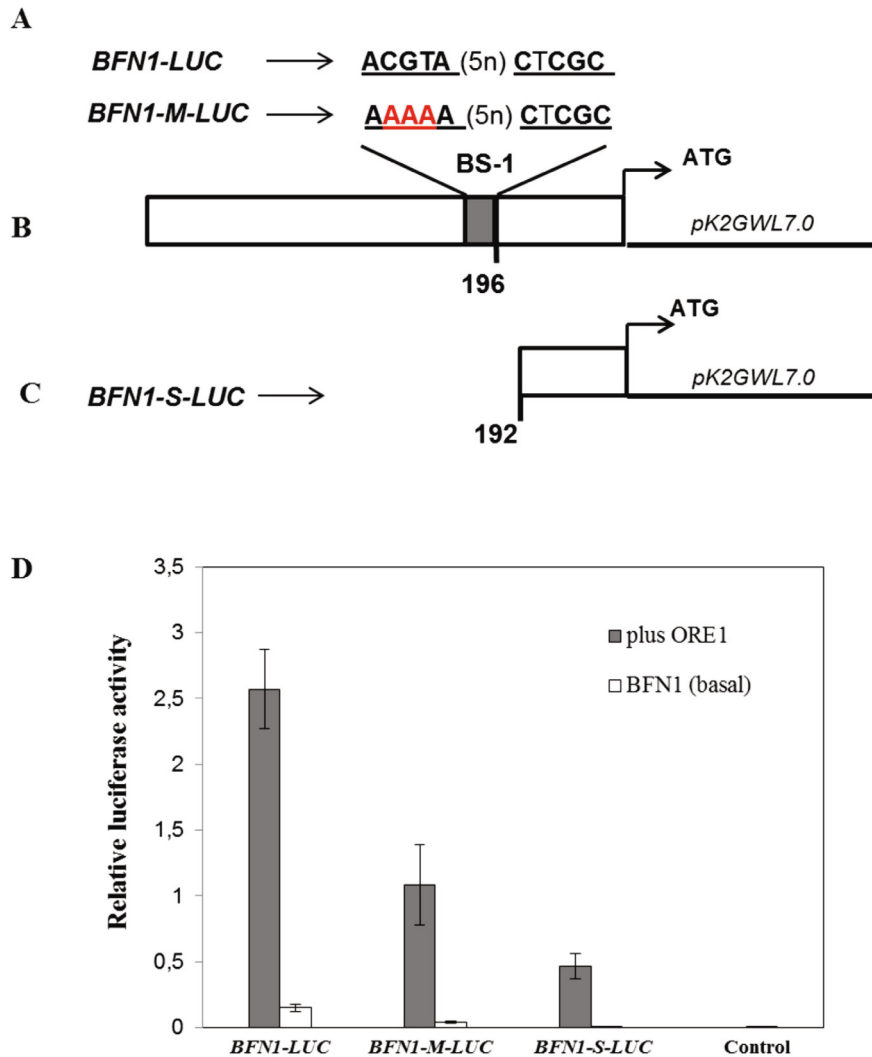
Figure 18. Transactivation of *BFN1* expression by ORE1 in *Arabidopsis* mesophyll protoplasts. Schematic representation of the constructs co-transfected in *Arabidopsis* mesophyll protoplast. (**A**) 1.0 kb promoter fused to luciferase (*BFN1-LUC*), (**B**) 1.0 kb promoter carrying substitutions (*BFN1-M-LUC*), and (**C**) 192 bp (*BFN1-S-LUC*) lack all ORE1-BSs. (**D**) Luciferase activity of each version of *BFN1* promoter in presence (plus ORE1) or absence (BFN1-basal) of *35S:ORE1*. Luciferase activity was determined using the Dual Luciferase Reporter Assay System (Promega) 24 hours after transfection. In all cases, normalization of data was performed using the CaMV *35S:Rluc* plasmid. Bars indicate the standard errors of three biological replicates.

5.3. Conclusions

We determined that ORE1 binds to the *BFN1* promoter *in vitro* and is able to transactivate the *BFN1* promoter in vivo. In this study, we show that *BFN1* and *ORE1* tissue-specific expression show largely over-lapping patterns, and *BFN1* expression is highly dependent on the presence of ORE1. We confirmed that ORE1 and BFN1 are highly expressive during senescence. Our results demonstrate that senescence-induced *BFN1* expression is

regulated by ORE1. Previous studies have demonstrated the central importance of ORE1 for the control of leaf senescence and developmental PCD. Considering the possible role of *BFN1* in degradation of nucleic acids during senescence, it is assumed that ORE1 exerts its senescence promoting function partly through BFN1.

5.4. Experimental procedures

5.4.1. General

Standard molecular techniques were performed as described in **Chapter 2, section 2.4.1.**

5.4.2. Plant material

The plant material and growth conditions were as described in **Chapter 2, section 2.4.2.**

5.4.3. Plant transformation

Wild type *Arabidopsis* transformation and supertransformation of the *anac092-1* T-DNA insertion mutant with the *Prom-BFN1:GUS* was performed as described in **Chapter 2**, **section 2.4.4.** T0 seedlings were selected on kanamycin (50 mg/L). Kanamycin-resistant lines were analyzed by PCR for GUS reporter gene-specific amplification.

5.4.4. Constructs

Description of **BFN1-LUC** construct was given in **section 4.4.4.** Descriptions of overexpressor construct (**35S:ORE1**) and **Prom-BFN1:GUS** were given in Balazadeh *et al*. (2010a) and Farage-Barhom *et al*. (2008), respectively.

***Promoter-LUC* construct:** The 1.0 kb *BFN1* promoter and a 0.2 kb long truncated versions (counted from the translation initiation codon) were amplified from genomic *Arabidopsis* (Col-0) DNA by PCR using an Advantage HF 2 PCR Kit (Clontech) and specific primer pairs listed for each construct (**Annex 1**). A mutated version of *BFN1* promoter (*BFN1-M-LUC*) was generated by site-directed-mutagenesis. Briefly, two short complementary promoter fragments were amplified by PCR and introduced into the final vector. Primers were used in two independent PCR reactions combining (i) forward primer (139) with reverse mutated primer (148), and (ii) forward mutated primers (147) with reverse primer (140) (**Annex 1**). The final products were isolated and purified using a QUIAGEN-PCR cleanup kit (QUIAGEN)) and used as a template for a final PCR to amplify the long version (1084 bp) of the promoter using forward (139) and reverse (140) primers (**Annex 1**). The amplified DNA fragments were cloned into the pENTR/D-topo vector (Invitrogen) to generate entry vectors. The entry vectors were then recombined into the Gateway destination vector *p2GWL7.0* (Karimi *et*

al., 2002) which is a recombination of the gateway *pBGWL7.0* (transcription reporter and *p2GW7.0* (overexpression vector) vectors (Licausi *et al*.,2011) using the LR reaction mix II (Invitrogen) to obtain the final reporter *BFN1-M-LUC* (full-length mutated promoter) and *BFN1-S-LUC* (short promoter).

5.4.5. Histochemical and quantitative GUS assay

Histochemical GUS assay was performed as described in **Chapter 2, section 2.3.4.** Quantitative measurements of GUS activity were made by fluorometric GUS assays using 4-methylumbelliferyl glucuronide (MUG) as substrate for the GUS enzymatic reaction, in which the fluorescent product 4-methyl umbelliferone (4-MU) can be detected (Jefferson *et al*. 1987). Tissue samples were ground in GUS extraction buffer 50 mM NaH_2PO_4, 1 mM EDTA, 0.1% Triton X-100, 0.1% (w/v) sarcosine, and 10 mM dithiothreitol (DTT), and following removal of tissue debris by centrifugation at 10 000 g for 10 minutes at 4°C, the crude total protein extract was used to measure GUS activity with a Fluorescence microplate reader (FLUOstar Omega). A standard curve was prepared with 4-MU, and GUS activity was expressed as pmol 4-MU mg/ul (Jefferson *et al*., 1987). Protein content was determined in the same sample used for the GUS assay by Bradford (Bio-Rad Protein assay) (Bradford, 1976). Tissue-specific expression was analyzed using plants of the T3 generation.

5.4.6. Dark-induced senescence

Experiments for artificial induction of senescence were performed with leaves in position 6th or 7th of the *Arabidopsis* plant rossete. The leaves were detached and incubated in the dark in containers fitted with inlet and outlet ports, and they were stored for 6-9 days in the dark at 25°C. The containers were sealed and connected to a flow-through air supply that was bubbled through sterile water to maintain humidity.

5.4.7. BFN1 protein extraction and Western Blots

Proteins for immunoblot analysis were extracted from leaf tissues. The tissue was homogenized in the presence of 150 µL extraction buffer (50 mM Tris-HCl, pH 7.5, 0.1% w/v SDS, 10% w/v polyvinylpyrrolidone, and 1 mM phenylmethylsulfonyl fluoride) in a microtube by means of a fitted pestle and a motorized drill. Following 15 minutes of centrifugation at 4°C, the soluble protein extract was assayed for protein content by Bradford assay (Bio-Rad, Hercules, CA, USA) and stored at -80°C. Protein extracts of 10-20 µg were mixed with sample buffer and boiled for five minutes before separation on a 15% SDS-polyacrylamide gel (Laemmli, 1970). Separated proteins were blotted onto nitrocellulose membranes with a gel blotter (Bio-Rad). Membranes were blocked with a solution containing 5% (v/v) nonfat milk and 0.1% Tween 20 in Tris-buffered saline for 60 minutes. The anti-BFN1 serum (Farage-Barhom *et al*., 2008) was diluted 1:2.000 in the blocking solution and incubated with the

membrane for 12 to 16 hours at 4°C. The membrane was washed for 30 minutes in several changes of Tris-buffered saline containing 0.1% Tween 20. The secondary antibody was goat anti-rabbit IgG:horseradish peroxidase conjugate (Bio-Rad), which was diluted 1:50.000 in blocking solution and incubated with the membrane for 1 hour at room temperature. For signal detection, EZ-ECL Chemiluminescent (Biological Industries Ltd., Beit Haemek, Israel) or WesternBright ECL (Advansta Ltd, CA, USA) kits were used.

5.4.8. Dual-luciferase assay

The truncated *BFN1* promoters (*BFN1-LUC, BFN1-M-LUC*, and *BFN1-S-LUC*) were used as reporter plasmids. Renilla luciferase was used as an internal control and *35S:ORE1* construct was used as effector plasmid. Detailed description of the procedure is described in **Chapter 2, section 2.4.7.**

Contributions

The *ore 1-1* EMS mutant plant material was provided by Dr. Hong Gil Nam (Department of Agronomy, Korea University). Mamoona Rauf tested expression of *ORE1* and *SAG12* in *ore1-1* EMS mutant and *mir164abc* triple mutant. Dr. Amnon Lers provided seeds of the *Prom-$_{BFN1}$:GUS* lines; Dr. Amnon Lers and Liliane Sorego carried out immunoblotting experiments.

Chapter 6

VND-Interacting2 (*VNI2*) is a potential down-stream target of ORE1

6.1. Introduction

The *Arabidopsis thaliana* NAC transcription factor *VND-Interacting2* (*VNI2*) has been recently identified as a key regulator of xylem vessel differentiation acting as a repressor of gene expression (Yamaguchi *et al*., 2010). Furthermore, VNI2 also works as a mediator of signaling crosstalk between salt stress-response and leaf aging in an ABA-dependent manner (Yang *et al*., 2011). VNI2 has a complex structure. As a NAC transcription factor (TF), it has a characteristic DNA-binding domain (DBD) at the N-terminal region. Within the DBD a potential repression-related sequence has been identified. The C-terminal region includes a putative PEST proteolysis target motif and a transcriptional activation domain (TAD) (Yang *et al*., 2011). We have provided evidence that *VNI2* might be a direct target of ORE1 (**Chapter 4, section 4.2.1**). In fact, overexpression of ORE1 transactivates the *VNI2* promoter in *Arabidopsis* mesophyll cell protoplasts (**Chapter 4, section 4.2.3**) and ORE1 binds directly to the *VNI2* promoter *in vitro* (**Chapter 4, section 4.2.4**). Here we aimed to elucidate the signal transduction cascade that links ORE1 and *VNI2* during leaf senescence in *Arabidopsis*.

6.2. Results

6.2.1. *VNI2* Encodes a NAC TF regulated by ORE1

In **Chapter 4** we described experiments carried out to identify genes up- or down regulated by ORE1. According to our data *VNI2* is one direct target down-stream of ORE1 (tested *in vivo* and *in vitro*) (**see Chapter 4, section 4.2.1**). *VNI2* was highly up-regulated after five hours of estradiol induction in estradiol-inducible *ORE1* overexpressing lines and after six hours of constitutive overexpression in protoplasts (**Fig. 19.A**). Considering that VNI2 is another NAC transcription factor down-stream of ORE1, it motivated our interest to analyse *VNI2* expression in plants with altered levels of ORE1. We measured the expression of *VNI2* in constitute overexpressing

plants (*35S:ORE1*) and in plants loss-of-function mutants (*anac092-1* T-DNA insertion mutant); as controls we used plants transformed with the pGreen0229 empty vector (E.V.) (Skirycz *et al*., 2006). As expected, *VNI2* was significantly up-regulated in plants overexpressing ORE1 and showed a decreased expression in the *anac092-1* mutant (**Fig. 19.B**).
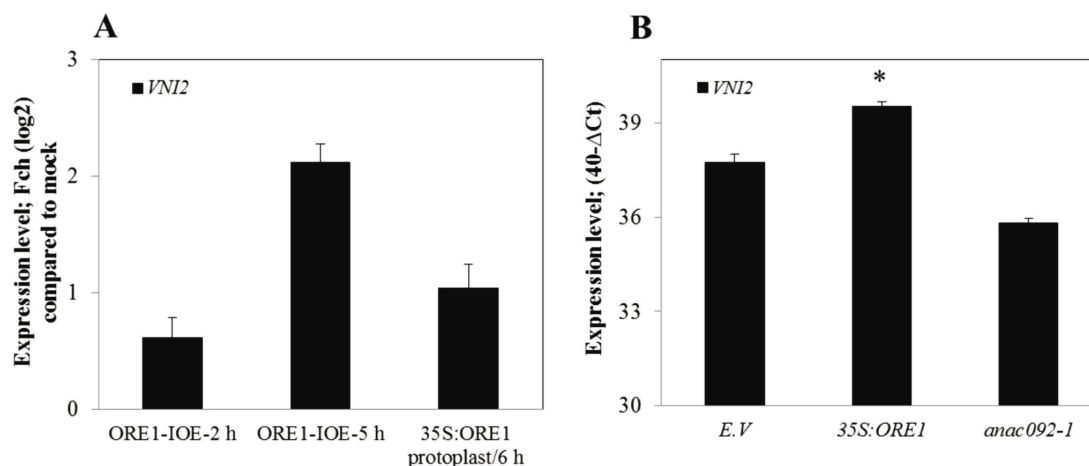
Figure 19. *VNI2* expression in *ORE1* gain- and loss-of-function mutant plants. (**A**) *VNI2* expression determined by microarrays (Affymetrix ATH1 array, Probe Id 245987_at) using plants and protoplasts overexpressing ORE1. (**B**) *VNI2* expression determined by qRT-PCR. Levels measured in estradiol-inducible overexpressing lines (*ORE-IOE*), *anac092-1* T-DNA insertion mutant and empty vector (E.V.) control plants. Statistical significance was assessed using Student´s *t*-test implemented in the SigmaPlot Software. *P<0.05.

6.2.2. *VNI2* expression *in planta* associates with senescence

To investigate the tissue-specific expression of *VNI2* and whether it correlates with the expression of *ORE1* (**Chapter 2, section 2.2.1**) we created *VNI2* promoter fusion lines using the *Staphylococcus* ß-glucuronidase (*GUS*) as a reporter gene. We generated two promoter versions, a long version (*VNI2$_{LVProm}$:GUS*) spanning ~1.5 kb up-stream (LV) of the translation start site (SST), and a short version (*VNI2$_{SVProm}$:GUS*) comprising ~0.5 kb (SV) up-stream of the SST. The most representative expression patterns are shown in **Figure 20.** GUS expression driven by the *VNI2* promoters (*VNI2$_{LVProm}$:GUS* and *VNI2$_{SVProm}$:GUS*) was tested in eight independent transgenic lines per construct (T2 and T3 generations). GUS activity was mainly but not exclusively associated whit senescent tissues throughout the plant (**Fig. 20**). Our observations confirmed published data (Yang *et al*., 2011) and expression patterns reported in GENEVESTIGATOR (Hruz *et al*., 2008). In the early stages of development (15-day-old seedlings), strong GUS activity was detected in cotyledons, margins and tips of leaves as well as roots (**Fig. 20.f**). Bolts (stems with inflorescences) exhibited faint GUS activity in flower buds particularly in flowers of stage 12 of development before the bud opens (**Fig. 20.c**) and in 1.0 cm primary bolts in the axis of the secondary inflorescence stem as indicated by arrows (**Fig. 20.d**). A strong and characteristic pattern was found among the axillary inflorescence axes and pedicels (**Fig. 20.c**). A closer look into opened mature flowers of stage 15 where the stigma

extends above the anthers (Smyth *et al.*, 1990) revealed strong GUS activity in the upper part of the stigma, in anthers and filaments as well as in the abscission zone (AZ), in older petals and sepals (**Fig. 20.a**). Mature opened flowers of stage 14 when long anthers extend above the stigma (Smyth *et al.*, 1990) exhibited strong *VNI2* promoter-driven GUS activity specifically in the upper part of the stigma, anthers, filaments and among the vascular tissues of sepals. Abscission zones lack GUS expression at this developmental stage (indicated by arrow) (**Fig. 20.b**). *VNI2* expression in senescent siliques was detected in the upper and bottom part of the valves near the abscission zone (AZ) (**Fig. 20.e**). These observations are in good agreement with the reported *VNI2* expression patterns derived from transcriptome analyses of senescing siliques, leaves and petals (Wagstaff *et al.*, 2009). Like other senescence-associated genes (SAGs) (e.g., *ORE1* (Balazadeh *et al.*, 2010), *ORS1* (Balazadeh *et al.*, 2011) and *BFN1* (Farage-Barhom *et al.*, 2008)), *VNI2* shares a common expression pattern in the tips and margins of senescence leaves which corresponds to the older regions of the leaves (**Fig. 20.g**). We could not identify substantial differences between the expression patterns determined by the long or short versions of the *VNI2* promoter at any of the developmental stages tested (comparison of both constructs not shown). This suggests that the region ~500 bp up-stream of the initiation codon is sufficient to drive *VNI2* promoter tissue-specific expression and that cis-regulatory elements (CREs) that confer the specific pattern observed during senescence may be within this region.
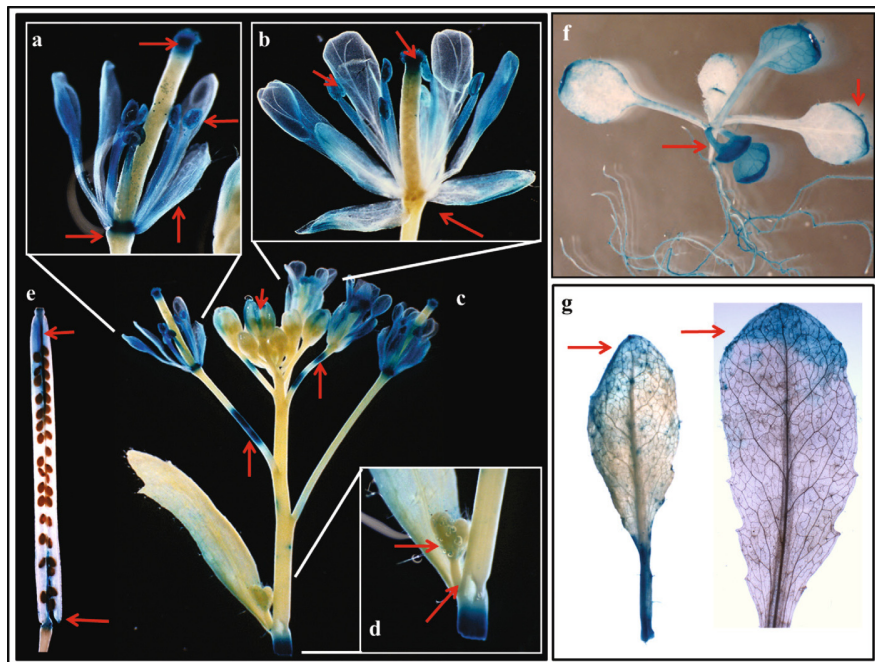
Figure 20. Tissue-specific expression of *VNI2* in *Arabidopsis*. (**a-d**) *VNI2* promoter-driven GUS expression in bolts of mature plants (25 days after sowing, DAS). Close-ups of (**a**) opened mature flower in stage 15 of development in which the stigma extends above long anthers (Smyth *et al.*, 1990). (**b**) Mature opened flower in stage 14 of development in which long anthers extend above the stigma (Smyth *et al.*, 1990). (**c**) Strong and characteristic pattern among the axillary inflorescence and pedicels (indicated by arrows). (**d**) One-cm bolt of primary inflorescence. (**e**) Mature silique (three weeks after sowing). (**f**) *VNI2* promoter activity in 15-day-old seedlings. (**g**) Enhanced *VNI2* promoter activity in the tip and margin regions of leaves from a rosette three weeks after sowing on soil (percentage of yellowing in leaves ~20%). All pictures correspond to *VNI2$_{LVProm}$:GUS* lines.

6.2.3. *VNI2* expression is strongly regulated by salt

A considerable number of SAGs are regulated by abiotic-stresses. In our published data we determined that *VNI2* is regulated by salt, like *ORE1*. Wild type plants were grew in a hydroponic culture system and subjected them to salt stress at two developmental stages. Stage 1: 28-day-old plants and (ii) Stage 2: 34-day-old plants. Plants were subjected to short- (six hours) or long-term (4, 9 and 12 days) salt stress (150 mM NaCl). Similarly to *ORE1*, *VNI2* expression was highly up-regulated by long-term stress. In young plants that still have expanding leaves (Stage 1), *VNI2* transcript level increased around 4-fold after four days of salt stress compared to non-treated plants (**Fig. 21**). In mature plants which were still in the vegetative stage (Stage 2, 34 days old), *VNI2* levels were up-regulated ~4-fold and ~2-fold, respectively, after nine and 12 days of salt stress (**Fig. 21**).
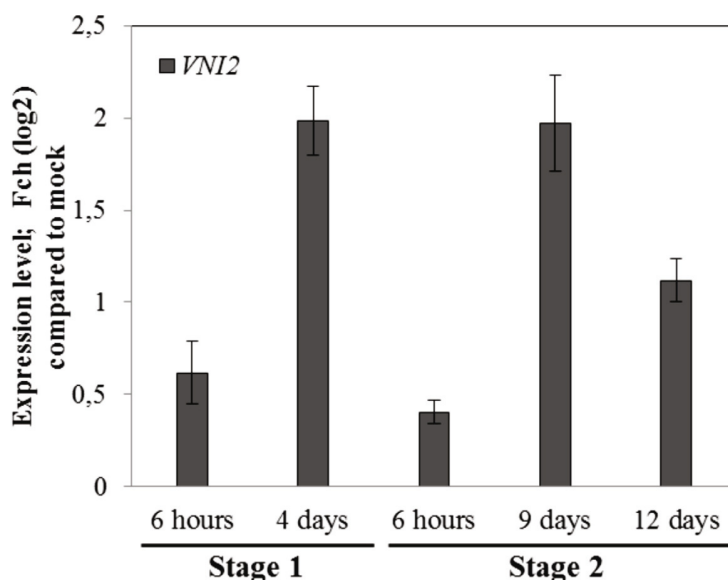
Figure 21. *VNI2* levels in response to salt stress. Expression of *VNI2* determined by quantitative real-time PCR (qRT-PCR) in plants subjected to salt stress at two plant developmental stages. Values expressed as expression ratios (salt-treated compared to control). Data are means of two independent experiments ± Standard deviation (SD) according to published data (Balazadeh *et al*., 2010).

6.2.4. Identification of *vni2-2* a T-DNA insertion mutant

To investigate the role of *VNI2* in leaf aging and longevity we obtained a *VNI2* T-DNA insertion line (GABI-KAT 799-H09) in the Col-0 background from the GABI-Kat consortium (Li *et al*. 2003). Homozygous *VNI2* knockout mutants (*vni2-2*) were isolated (**section 6.4.5**). The T-DNA insertion was confirmed via PCR using primers annealing between the start and stop codon of the *VNI2* open reading frame. A second combination of primers consisting of the previous forward primer and the T-DNA left border primer (LB) was used to confirm the T-DNA insertion (**Fig. 22.B**). Two homozygous plants (P1, P2) were selected based

on selection in sulfadiazine (**section 6.4.6**) and on-gel results using wild type as a positive control (**Fig. 22.C**). The band amplified from the line P1 using forward and LB primer was used to determine the exact position of the T-DNA insertion by sequencing (http://www. eurofinsdna.com/). In **Figure 22.A** a schematic representation of the protein is shown. The sequence allowed us to locate the T-DNA insertion to the third exon. It is placed within the PEST proteolysis target motif (TTDLNLLPSSPSSD; PEST score of +4.94; threshold +5.0) (Gasteiger *et al.*, 2003). This motif covers the region between nucleotides 640 - 681 that corresponds to amino acids 214-227 in the protein (**Fig. 23**). The T-DNA insertion lies in the middle of the PEST motif. The second half of the motif is enriched in proline and serine residues and is required to maximize the proteolytic activity of the PEST motif (**Fig. 23**). We could not detect a full version of the *VNI2* transcript in the homozygous vni2-2 mutant (**Fig. 22.D**).
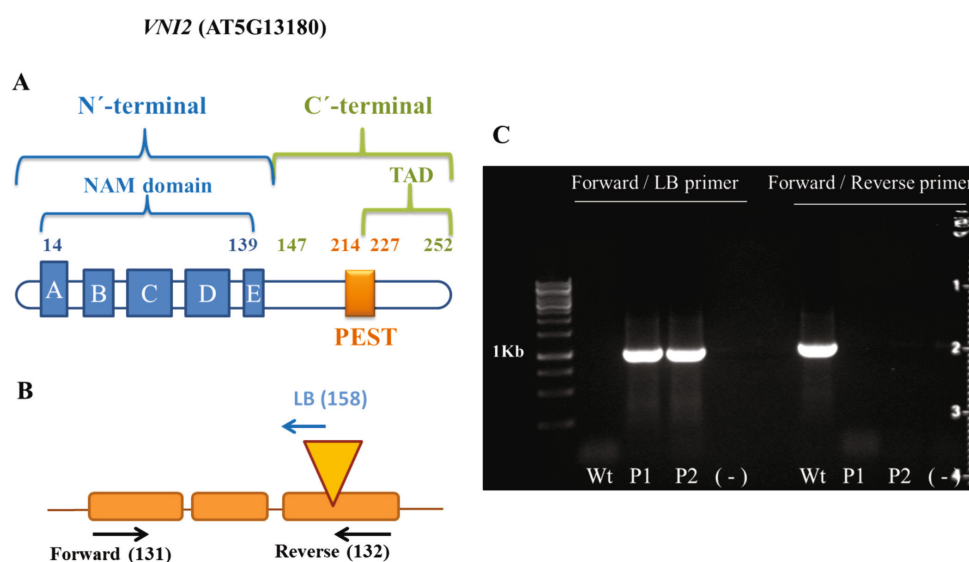
Figure 22. *vni2-2* T-DNA insertion line. (A) Schematic representation of the VNI2 protein. The N-terminal domain covers the conserved NAM domain, which contains five subdomains (A-E). The C-terminal region contains a predicted PEST domain and the transactivation domain (TAD) (protein length 252 amino acids, aa) **(B)** Schematic representation of the primers used to identify homozygous mutant lines. The yellow triangle indicates the T-DNA insertion point (*vni2-2*). **(C)** Identification of homozygous lines by PCR. Genomic DNA was used for amplification. Two homozygous plants were selected (P1 and P2). The *VNI2* transcript was amplified only in the wild type, while the *vni2-2* mutant was positive for amplification using of T-DNA left border primer.

Considering the location of the T-DNA insertion in the third exon (**Fig. 23**), we designed specific primers that cover the three exons (I -III) of the *VNI2* gene in gene to test transcript abundance of each exon in *vni2-2*. RNA isolated from leaves of 30 DAS plants was used to determined transcript abundance by qRT-PCR. The combination of primers used to analyze the transcript level of the third exon covered the whole PEST motif. No product was amplified using this combination of primers, while products corresponding to the first and second exon were amplified. These data suggest that *vni2-2* might be able to produce a

truncated *VNI2* transcript that may potentially lead to the generating of a truncated protein (**Fig. 23**). Further analyses are required to clarify whether this mRNA indeed produces a (partially functional) protein.
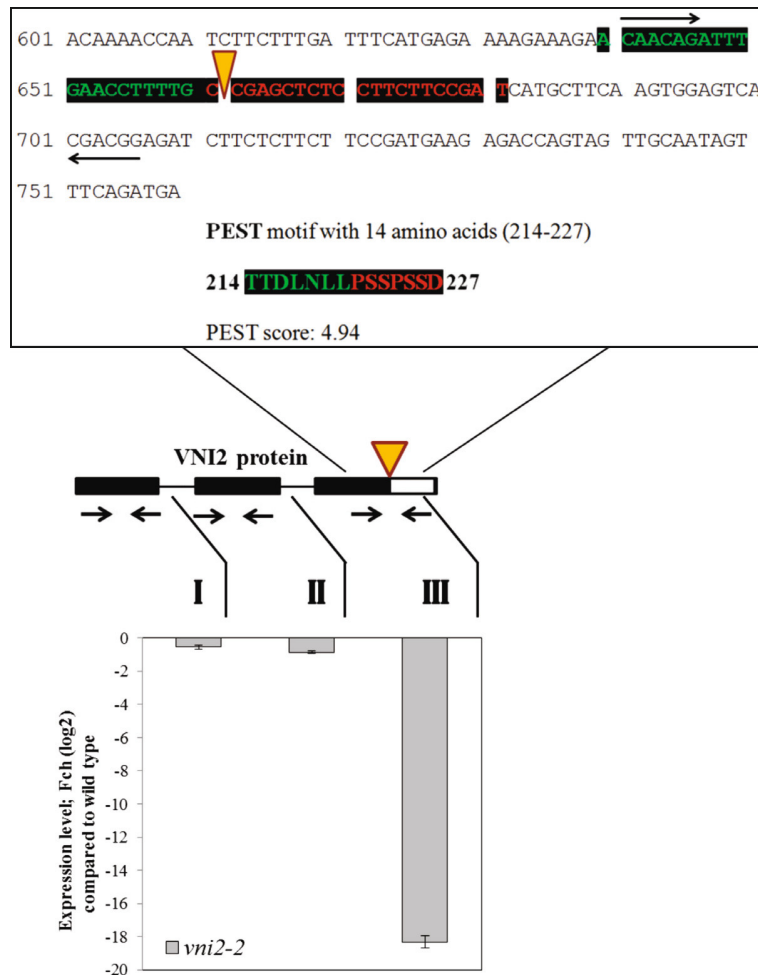
Figure 23. Amplification of *VNI2* exons by qRT-PCR in *vni2-2*. Upper part: The combination of primers used to analyze the transcript level of the third exon (indicated by arrows), covered the whole PEST motif region (PEST motif is indicated by colored letters). The T-DNA insertion is marked with a triangle. Red letters indicate the half of the PEST motif that confers a higher proteolytic activity of the PEST region. **Bottom part:** *VNI2* transcript abundance was analyzed using primers annealing to each exon (I - III) of the gene.

6.2.5. Bolting and leaf aging are delayed in *vni2-2*

Phenotypic analysis of *vni2-2* showed a delay in bolting in comparison to wild type (**Fig. 24.A**). We counted the number of bolted plants (80 different plants) 32 DAS as well as the number of cauline and rosette leaves at the time of flowering. Mutant plants flowered later than wild type plants under long photoperiod (16 hours light /8 hours dark) (**Fig. 24.B**). At 26 DAS only around 20% *vni2-2* plants have bolted compared to 80% in the wild type plants.

The number of leaves at bolting was significantly less in *vni2-2* (around 10 leaves) than in wild type plants (around 18) (**Fig. 24.B-C**). Nevertheless, at the end of our observations (at 32 DAS) the difference in the numbers of leaves between wild type and *vni2-2* mutants was not statistically significant. Besides a delayed bolting in *vni2-2*, we observed two remarkable other features (i) a prolonged life-span with green rosette leaves even at advanced flowering stages and (ii) an increased biomass represented by bigger leaves (**25. A-B**).
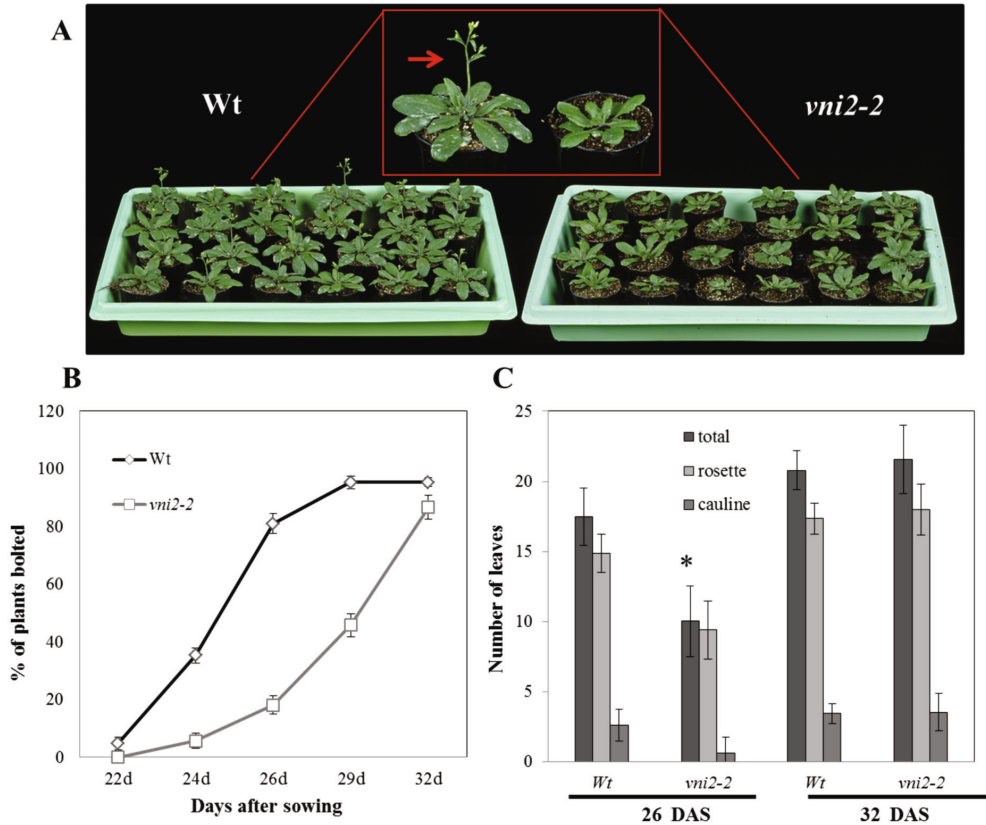
Figure 24. Delayed bolting in *vni2-2*. (A) Onset of bolting in wild type and *vni2-2* plants of the same age (26 DAS). *vni2-2* showed delayed bolting compared to wild type (bolting indicated by an arrow). **(B)** Percentage of bolted plants 22 to 32 DAS **(C)** Total number of leaves (cauline and rosette leaves) were counted at 26 DAS (beginning of counting) and 32-DAS (last day of counting). *$P<0.05$.

To confirm our observations regarding a prolonged life span in *vni2-2* we examined the expression of four senescence associated genes (SAGs) (Buchanan-Wollaston *et al*. 2005; Balazadeh *et al*., 2008b; Breeze *et al*., 2011). We extracted total RNA from three independent biological replicates 29 DAS, synthesized cDNA and tested the expression of *SAG12* (At5g45890), *ORE1* (At5g39610), *BFN1* (At1g11190) and *RNS3* (At1g26820) by qRT-PCR (**Fig. 25.C**). The expression of three out of four SAGs (*SAG12*, *ORE1* and *BFN1*) was significantly reduced in *vni2-2* compared to wild type. This result is in accordance with the delay senescence observed in *vni2-2*.
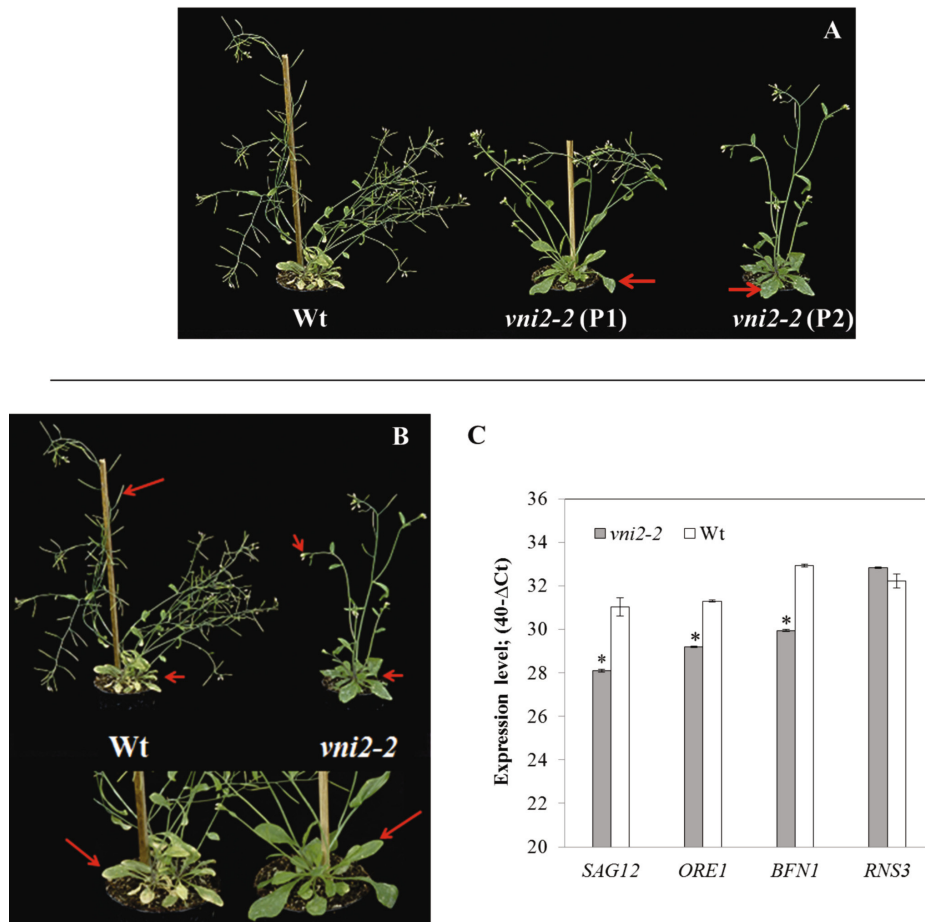
Figure 25. Prolonged life span in the *vni2-2* mutant. Upper panel: (**A**) Developmental delay in *vni2-2* (two different plants) compared to wild type plants at the same time after sowing. **Bottom panel**: Close up shows extended longevity of *vni2-2* and increased biomass represented as bigger leaves (plant age: 32 DAS). (**B**) Transcriptional level of *SAGs* in *vni2-2* (29 DAS) compared to wild type. *SAG12*, *ORE1*, *BFN1* transcript abundance was significantly reduced in *vni2-2*. SD±3. (*$*P<0.05$).

6.2.6. Salt stress tolerance is enhanced in *vni2-2*

It is known that seed germination can be delayed under unfavorable environmental conditions such as high salinity (Kim and Park, 2008). Salt stress also retards plant growth and accelerates senescence (Lee and Zhu, 2010). Considering that *ORE1* and *VNI2* expression is enhanced under long-term salt stress and that *VNI2* is regulated by ORE1, we tested whether the response of *vni2-2* to salt stress is impaired. We assayed seed germination rate under high salinity conditions. *vni2-2* and wild type plants were grown on sterile plates with or without sodium chloride (100 mM, 150 mM and 200 mM NaCl). Germination rate was scored 15 days after sowing. Seeds were considered germinated if the radicles had penetrated the seed coats (Lee and Zhu, 2010). The assay was performed in three independent biological replicates for each salt concentration including controls. As can be seen in **Figure 26.B,** around 80% of the seeds germinated in the

absence of salt stress (Mock). As expected, the germination rate decreased concomitantly with increasing salt concentration in the medium. Nevertheless, *vni2-2* germinated better in saline conditions than the wild type (**Fig. 26.A**). There was no difference in germination rate among wild type and mutants in control conditions. At 100 mM NaCl this difference was around 2-fold. At 150 mM NaCl the difference increased to 5-fold, and at 200 mM NaCl *vni2-2* was around 7-fold more tolerant to salt stress than the wild type (**Fig. 26.B**). The negative effect of salt was already evident at the lowest concentration (100 mM). Roughly all germinated seeds in both lines developed with a notable decrease in size and exhibited yellowish color. At 150 and 200 mM NaCl only the radicles of *vni2-2* could penetrate the seed coat and generated very small leaves (**Fig. 26.A**). In contrast, nearly all wild type seeds died at 200 mM NaCl and the small percentage of seeds that germinated did not survive.
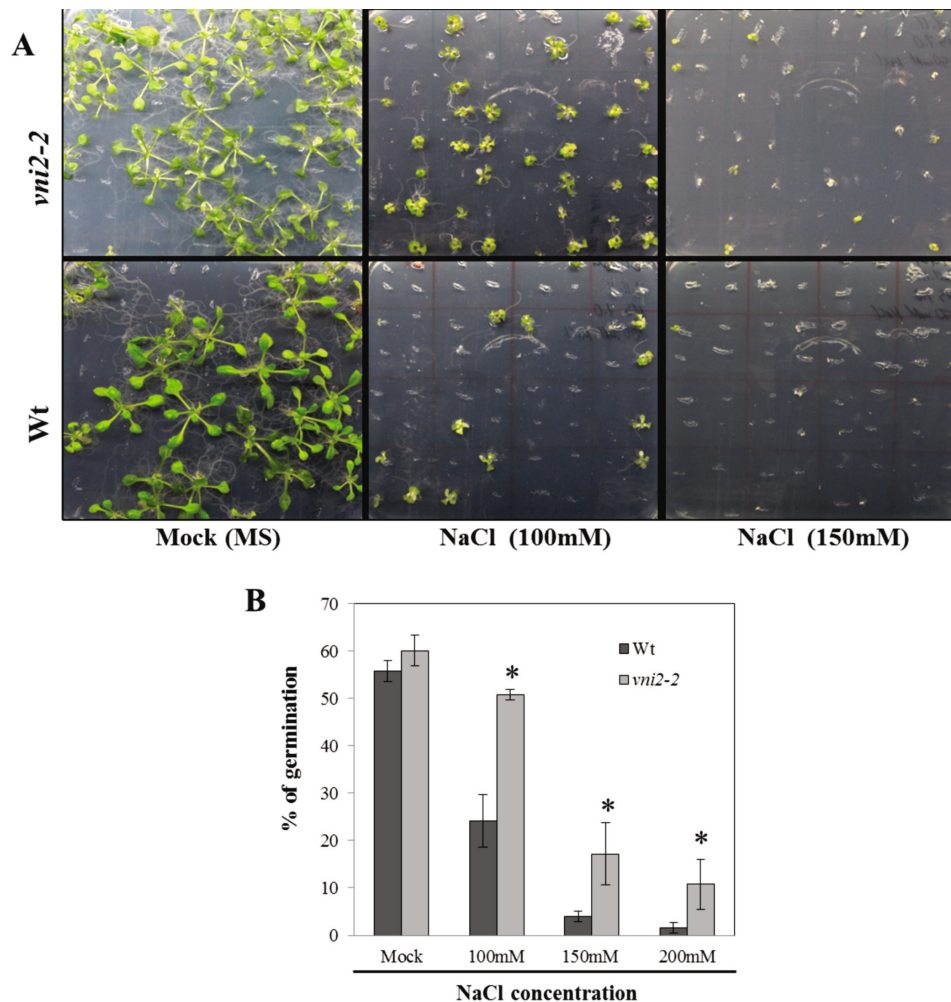
Figure 26. Salt stress tolerance is enhanced in *vni2-2*. (**A**) 15-DAS seedling growth under two different concentration of salt (100 and 150 mM NaCl). The *vni2-2* mutant showed enhanced salt-stress tolerance compared to wild type. (**B**) Germination rate of *vni2-2* mutants and wild type plants at three different salt concentrations. SD±2 biological replicas and two technical replicas. *$P<0.05$.

6.2.7. The activation domain of VNI2 exerts a marked influence on development and senescence regulation

Recently, Yamaguchi *et al*. (2010) established that the protein stability of VNI2 is regulated by the PEST motif located at the C-terminal. A truncated version which lacks the PEST motif was more stable, and the full version was more stable if proteasome inhibitors were applied. Transgenic seedlings expressing the truncated version under the control of the endogenous *VNI2* promoter showed impaired xylem vessel differentiation. Moreover, constitutive overexpression of *VNI2* resulted in the formation of discontinuous vessels and slow plant growth. To examine if the role of VNI2 in senescence requires the PEST motif and the activation domain, we generated two inducible overexpression lines using a chimeric transcription activator system (XVE) (Zuo *et al*., 2000). We designed two versions of *VNI2* (**Fig. 27.A**). One version, designated *VNI2-IOE*, refers to the full protein (252 aa). The other version, *VNI2-IOE-ΔC* refers to a truncated protein lacking the C-terminal region corresponding to half of the PEST motif (221 aa) and the whole transcriptional activator. For both constructs we generated transgenic lines in the *Arabidopsis* wild type (Col-0) background. Transformed plants were selected on hygromycin and subsequently transferred to soil. Induction of *VNI2* was tested in the T1 generation; detached leaves were subjected to estradiol induction for five hours. Based on the induction level, two independent lines for each construct were selected for further experiments.

Transcript levels were determined by qRT-PCR using cDNA from seedlings of both constructs lines grown in media supplemented with estradiol (EST). Wild type seedlings in media with/ without EST were used as controls. Two combinations of primers annealing to the first two exons (I, II) were used for expression analyses. *VNI2* expression was significantly higher in transgenic seedlings overexpressing the truncated version of the protein (*VNI2-IOE-ΔC*) than in plants overexpressing the full-length version (*VNI2-IOE*) compared to wild type (**Fig. 27. B**).
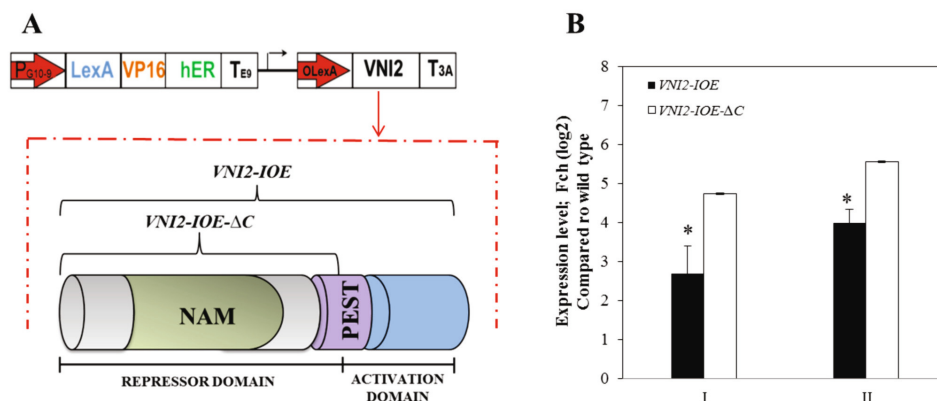
Figure 27. Differences in *VNI2* transcript level with/without the activation domain. (A) Upper: Schematic representation of the *VNI2* coding sequence used to produce estradiol-inducible *VNI2* expression lines (Zuo *et al*., 2000a). **Bottom:** Schematic representation of the constructs used. The *VNI2-IOE-ΔC* construct lacks the whole transcriptional activation domain and almost half the PEST motif. (**B**) Transcript abundance of *VNI2* in seedlings (15 DAS) carrying the complete and the truncated version of *VNI2*. I and II correspond to primers annealing to the first and second exon of *VNI2*. SD±2 biological replicas and three technical replicates.

We detected phenotypic differences between seedlings expressing either the full or the truncated version of the protein even without estradiol induction. These differences were determined also at transcript level. Seedlings expressing the truncated version of the protein were smaller than wild type and *VNI2-IOE*, and exhibited signs of yellowing (**Fig. 28.B**). The effect was more pronounced in media supplemented with estradiol. The *VNI2-IOE-ΔC* seedlings were markedly smaller and showed increased premature yellowing, indicating an accelerated senescence. To test if these plants showed indeed accelerated senescence the expression of the senescence associated gene (SAG) *SAG12* was tested. We extracted total RNA from 15-day-old seedlings and synthetized cDNA from two independent biological replicates. It was previously shown that *SAG12* expression is exclusively detected during senescence (V., 2003). Therefore, we used its expression as a molecular marker of senescence. *SAG12* expression was significantly increased in plants over-expressing both versions of VNI2 (*VNI2-IOE* and *VNI2-IOE-ΔC*) compared to wild type. *SAG12* was markedly up-regulated in *VNI2-IOE* seedlings expressing the full version of the protein (~6-fold) and only ~3-fold up-regulated in *VNI2-IOE-ΔC* seedlings that showed more extensive yellowing. These results suggest (i) the presence of the VNI2 full-length protein positively regulates senescence and (ii) overexpression of a truncated version lacking the transcriptional activation domain and the PEST motif results in plants with considerable developmental disruptions unrelated to senescence albeit the seedlings show precocious yellowing (**Fig. 28.B**).
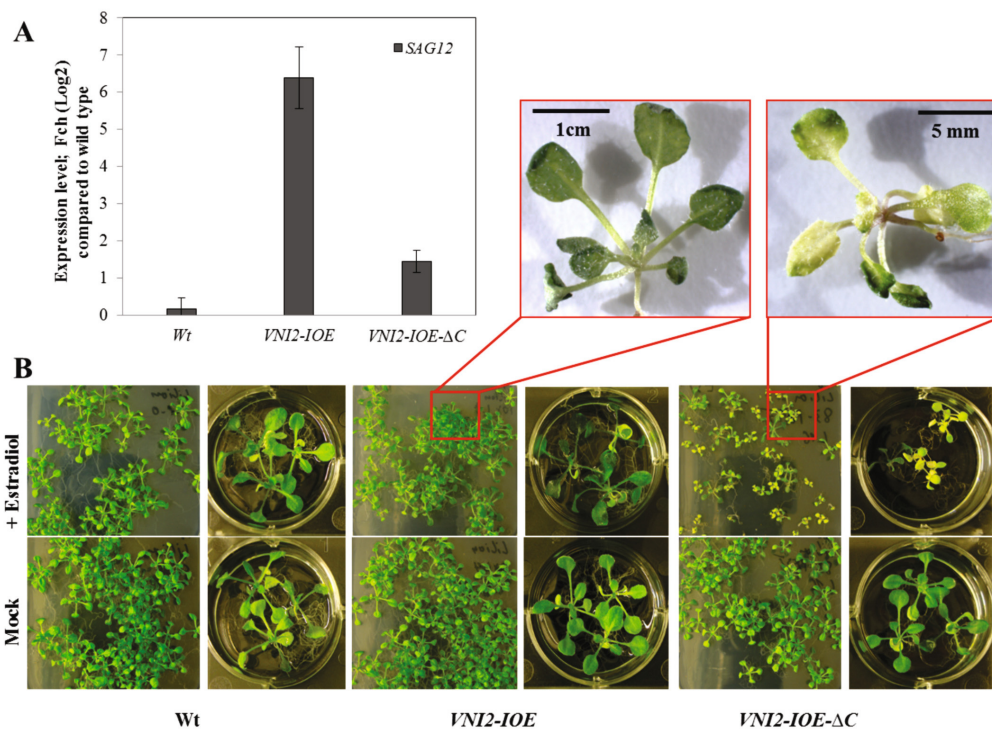
Figure 28. *VNI2-IOE* and *VNI2-IOE-ΔC* plants under estradiol induction. (**A**) Enhanced expression of *SAG12* in *VNI2-IOE* and *VNI2-IOE-ΔC* plants grown under estradiol induction. (**B**) Phenotypic analysis of *VNI2-IOE* and *VNI2-IOE-ΔC* seedlings (15 days old). Close-ups of *VNI2-IOE* and *VNI2-IOE-ΔC* plants show that plants overexpressing a truncated version of VNI2 were considerably smaller than plants overexpressing the full version of the protein.

6.2.8. ATAF1 positively regulates *VNI2* expression

We determined that *ORE1* is positively and significantly up-regulated by ATAF1. We probed that *ORE1* promoter is transactivated by ATAF1 in protoplast, suggesting that ATAF1 is a direct regulator of *ORE1* (**Chapter 2**). We determined that overexpression of a CDPK named CKOR (for calcium-dependent kinase regulating ORE1) *in vivo* leads to an increase in transcriptional activity of *VNI2* (**Chapter 3**). Additionally, based on our observations that ORE1 binds *in vitro* to a *VNI2* promoter fragment containing an ORE1-BS and transactivated *in vivo VNI2* promoter (**Chapter 4**) we propose that *VNI2* is a putative direct target gene of ORE1. In order to unravel the transcriptional network and possible regulatory loops among these NAC TFs involved in senescence and salt-stress responses we performed a series of assays. Using whole genome transcriptomics assays we uncover that along *ORE1 VNI2* expression is significantly up-regulated by ATAF1. Expression profiles are based in lines overexpressing *ATAF1* under the control of an estradiol-inducible promoter (**Fig. 29**).
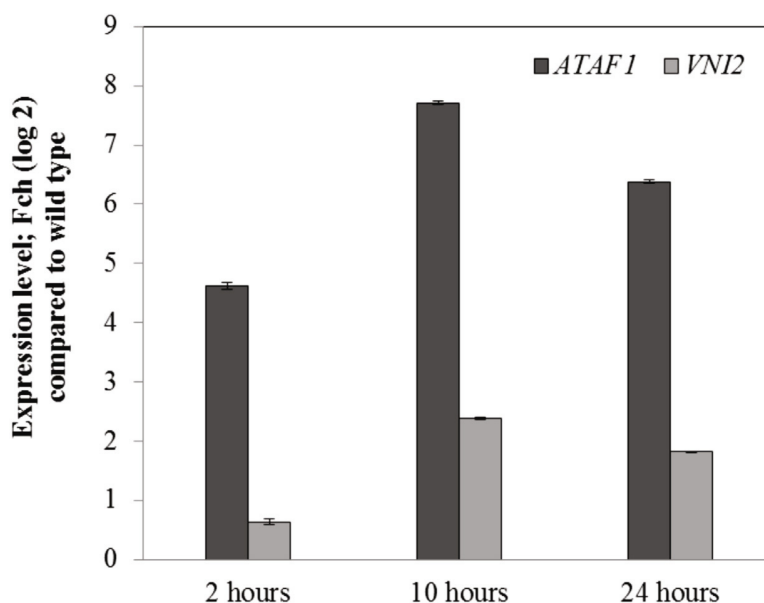
Figure 29. *VNI2* and *ATAF1* expression in ATAF1 inducible overexpressing lines (*ATAF1-IOE*) upon estradiol (EST) induction. *VNI2* expression determined by microarrays (Affymetrix ATH array, probe Id 245987_at). Significant up-regulation (two cut-off) after 10 hours upon *ATAF1* induction. Maximal level of *VNI2* was reached after 10 hours EST induction.

The rapid induction of *VNI2* upon inducible over-expression of *ATAF1* after two hours EST induction suggests a positive control of ATAF1 over *VNI2*. Interestingly, the expression pattern of *VNI2* highly resembles the expression pattern of *ORE1* under the same conditions (**Chapter 2, section 2.2.5**). Two hours after EST induction VNI2 expression is less than 2-fold up related. Nevertheless, ten hours after EST induction VNI2 expression if more than 4-fold up-regulated (**Fig. 29**). These observations suggest two hypotheses: either *VNI2* is

activated through a signal cascade in which ATAF1 activates *ORE1* and then ORE1 directly activates *VNI2*; or ATAF1 can directly activate *VNI2* as well as *ORE1* meaning that VNI2 activation occurs independently of ORE1. In order to test if VNI2 up-regulations occurs independently or depends on *ORE1* activation by ATAF1 we used transactivation assays in mesophyll protoplasts. A *VNI2* region spanning ~1.5 kb up-stream of the translation start site was amplified by PCR from *Arabidopsis* genomic DNA (Col-0), and then cloned into pENTR/D-topo vector (Invitrogen) and recombined into the Gateway destination vector *p2GWL7.0* (Karimi *et al*., 2002) to obtain the final reporter vector *VNI2-LUC*. The effector plasmid was the *35S:ATAF1* construct. For detail description see **Experimental procedures** in **Chapters 2 and 4**. A dual-reporter system determines the transcriptional activation of the *VNI2-LUC* promoter when ATAF1 is overexpressed. The internal control reporter, *Renilla* luciferase (*35S:RLuc*) (Licausi *et al*., 2011) provides the parameter to normalize the measured luciferase activity. *Arabidopsis* mesophyll cell protoplasts from wild-type and *anac092-1* lines were co-transfected with the *VNI2-LUC* and *35S:ATAF1* constructs. No statistical differences in luciferase activity were detected when using either wild type or *anac092-1* mesophyll protoplasts; evidencing that *VNI2* transactivation does not requires ORE1 and can be achieved directly by ATAF1 overexpression (**Fig. 30**).
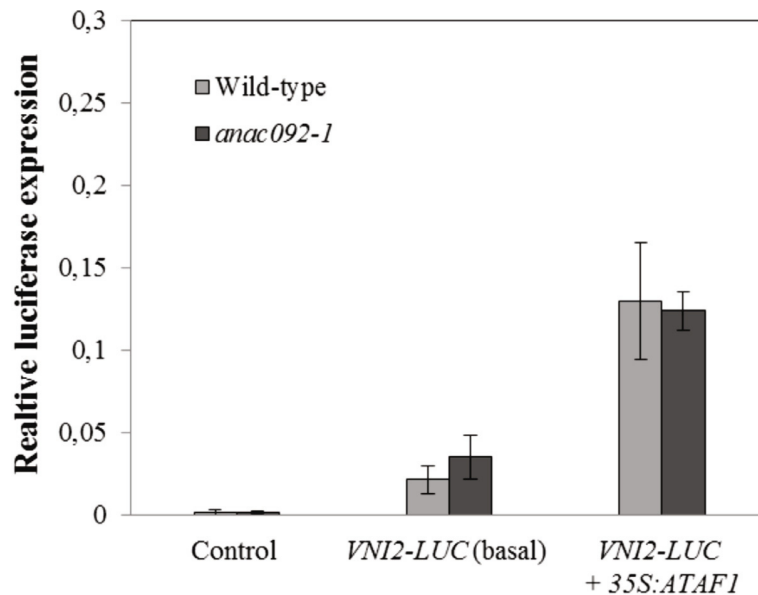
Figure 30. Protoplast transactivation assay of ATAF1 and *VNI2* promoter. *Arabidopsis* wild type or *anac092-1* T-DNA insertion mutant mesophyll protoplasts were co-transfected with *VNI2-LUC* and *35S:ATAF1*. Results are the mean of two biological replicates with three technical replicates per probe. Data were normalized to the corresponding *Renilla* luciferase activity.

6.3. Conclusions

Transcriptome analyses revealed *VNI2* as a highly up-regulated gene downstream of the key senescence regulator ORE1 (a NAC TF). *VNI2* was preferentially expressed in senescence

tissues at different developmental stages. The CREs required for senescence-dependent expression are located within ~500 bp up-stream of the transcription start site. We confirmed that *ORE1* is a transcriptional activator of *VNI2*. Moreover, ORE1 binding to the *VNI2*-promoter was confirmed *in vitro* and *in vivo* (**Chapter 4, section 4.2.3 and 4.2.4**). Our data support the conclusion that *VNI2* is a direct target of *ORE1*.

We show that salt stress tolerance is enhanced in *vni2-2* mutants. *vni2-2* mutants also exhibited a prolonged life-span, delayed onset of bolting, higher salt stress tolerance and apparently increased in biomass demonstrating a role of VNI2 not only in the regulation of natural- and stress-induced senescence in *Arabidopsis*. The delayed senescence phenotype observed in *vni2-2* may be due to the absence of the transcriptional activation domain and the PEST motif although a truncated VNI2 protein may still be produced.

6.4. Experimental procedures

6.4.1. General

Standard molecular techniques were performed as described in **Chapter 2, section 2.4.1.**

6.4.2. Plant material

The plant material and growth conditions used were similar as described in **Chapter 2, section 2.4.2.**

6.4.3. Plant transformation

Arabidopsis transformation was performed as described in **Chapter 2, section 2.4.4.**

6.4.4. Constructs

Description of the *35S:ORE1* overexpressor line was given in Balazadeh *et al*., (2010a). Description of the *ATAF1-IOE* and *35S:ATAF1* constructs were given in **section 2.4.3.**

***VNI2-GUS* constructs:** approximately ~1.5 kb (long version) and ~0.5 kb (short version) fragments up-stream of the *VNI2* ATG were amplified from genomic *Arabidopsis* Col-0 DNA by PCR using primers forward (133) and reverse (134) for the long version, and forward (135) and reverse (134) primers for amplification of the short version (**Annex 1**). Isolated fragments were inserted first into plasmid pCR2.1-TOPO (Invitrogen), and after sequencing fused via *Bam*HI and *Nco*I sites to the GUS reporter gene into pCAMBIA1305. 1-hygromycin (CAMBIA). The final constructs were designated as *VNI2$_{LVProm}$:GUS* and *VNI2$_{SVProm}$:GUS*.

Estradiol-inducible overexpression (IOE) constructs. The complete *VNI2* coding sequence (CDS) was amplified by PCR using leaf cDNA from *Arabidopsis* plants. We used primers forward (142) and reverse (201) (**Annex 1**). To generate a version without the transcriptional activation domain, we used forward (142) and reverse (141) primers (**Annex 1**). Both fragments were inserted into pBluescript SK and then cloned via *Xho*I and SpeI sites into the pER8 vector (Zuo *et al*., 2000b). The resultant plasmids were electroporated into *Agrobacterium tumefaciens* strain GV3101/pMP90, which was used to transform *Arabidopsis* ecotype Col-0. The final vectors were named *VNI2-IOE* (complete CDS) and *VNI2-IOE-ΔC* (CDS without transcriptional activation domain). The T1 generation of transgenic seedlings was selected on MS medium supplemented with (10 mg/L) spectinomycin for 15 days.

6.4.5. Histochemical GUS assay

Histochemical GUS assay was performed as described in **Chapter 2, section 2.4.5.**

6.4.6. Identification of homozygous T-DNA insertion line

The *vni2-2* homozygous mutant was isolated from a T-DNA line (GABI-KAT 799-H09) (Li *et al*., 2003). Firstly, lines were selected based on resistance to sulfadiazine (7.5 mg/mL). Seeds were sown on MS medium (Murashige and Skoog, 1962) supplemented with sulfadiazine (7.5 mg/mL) for 15 days. Surviving green seedlings were transferred to soil and two weeks later genomic DNA was extracted. Homozygous line was identified via PCR screening on genomic DNA using gene-specific primers forward (131) and reverse (132) together with T-DNA-specific primer LB (158) (**Annex 1**). Additionally, we determined the transcript abundance of *VNI2* by qRT-PCR using specific sets of primers covering the first exon (149-150), second exon (70-71) or the third exon (160-161) (**Annex 1**).

6.4.7. cDNA synthesis and quantitative real-time PCR (qRT-PCR)

Total RNA extraction, cDNA synthesis and qRT-PCR were done similarly as described (Balazadeh *et al*., 2008; Caldana *et al*., 2007). Primer sequences used for qRT-PCR analysis to quantify transcript levels of *SAG12* (At5g45890), *ORE1* (At5g39610), *BFN1* (At1g11190) and *RNS3* (At1g26820) are given in **Annex 1**. The PCR reactions were run on an ABI PRISM 7900HT sequence detection system (Applied Biosystems Applera, http://www.appliedbiosystems.com/). At least triplicate measurements were carried out to determine the mRNA abundance of each gene in each sample. The absence of genomic DNA was verified by PCR using primers forward (202) and reverse (203) designed to amplify an intergenic region of a control gene (At5g65080). cDNA was produced from 2 μg total RNA using SuperScriptT III Reverse Transcriptase (Invitrogen). cDNA synthesis efficiency was controlled by qRT-PCR amplification of transcripts from a housekeeping gene *ACTIN2* (At3g18780) using specific forward (204) and reverse (205) primers (**Annex 1**). Data analysis was performed using SDS

2.2.1 software (Applied Biosystems Applera). Amplification curves were analyzed with a normalized reporter (R_n: the ratio of the fluorescence emission intensity of SYBR Green to the fluorescence signal of the passive reference dye) threshold of 0.2 to obtain the C_T values (threshold cycle). Date were normalized to the *ACTIN2* transcript as follows $\Delta C_T = C_T$ (gene) $- C_T$ (*ACTIN*). The expression was measured with three replicates in each PCR run, and the average C_T was used for relative expression analyses. Relative transcript abundance was determined using the comparative $\Delta\Delta C_T$ method ($\Delta\Delta C_T = \Delta C_T$ (condition of interest) $- \Delta C_T$ (control condition) and the Fold Change (Fch) was calculated using the expression $2^{-\Delta\Delta CT}$, where the obtained results were transformed to Log2 scale. In some cases the expression was expressed as $40 - \Delta\Delta C_T$ to improve the visualization of results.

Contributions

The *ORE1-IOE*, *35S:ORE1* lines and *anac092-1* T-DNA insertion mutant screening were performed by Dr. Hamad Sidiqui (Molecular Biology, Potsdam University). *ATAF1-IOE* constructs was provided by Dr. Dagmar Kupper (Molecular Biology, Potsdam University). *35S:ATAF1* construct and ATAF1 transcriptome data were provided by Prashant Garapati, Ph.D student of Prof. Dr. Mueller-Roeber's Group.

Discussion

The recent years have seen considerable progress with respect to the dissection of the molecular pathways controlling the induction and progression of senescence in plants, mainly in the model plant *Arabidopsis thaliana*. Leaf senescence determines the end of leaf development and constitutes an efficient recycling process that involves the breakdown of cellular organelles, the hydrolysis of different macromolecules, and the mobilization of nutrients from senescent tissues to young and reproductive organs. An example of the important role that recycling processes play in plants is the increase in nitrogen-use efficiency by resorption of foliar nitrogen (N) (Himelblau and Amasino, 2001). N is stored in younger and reproductive tissues and can be used for early growth in the subsequent progeny to supply the demands of developing foliage (Kang *et al*., 1982). Therefore, senescence favors the fitness of plants and is thought to be an evolutionary acquired process (Nam, 1997; Noodén and Leopold, 1988). Leaf senescence must be synchronized and tightly controlled to ensure not only the disassembling of cellular components like photosynthetic apparatus in early senescence, but also the conservation of cellular compartmentalization (Hörtensteiner and Feller, 2002), as well as nucleus and mitochondria integrity, until advanced senescence stages (Noodén and Guiamet, 1996; Noodén and Leopold, 1988). Transcriptome analysis of senescence leaves in *Arabidopsis thaliana* revealed a complex network of genes involved in the process, including many transcription factors (TFs) (Buchanan-Wollaston *et al*., 2005; Gepstein *et al*., 2003; Balazadeh *et al*., 2008; Breeze *et al*., 2011) . TFs recognize specific regions on the promoter region of targets regulating their activation or repression. NAC (*NAM*, *ATAF*, and *CUC*) TFs represent a large fraction of the genes regulated during developmental and induced senescence in many plant species, including monocots and dicots, some of which are of particular agronomic importance (Balazadeh *et al*., 2008; Buchanan-Wollaston *et al*., 2005; Christiansen *et al*., 2011; Guo *et al*., 2004). The importance of the NAC TF ORE1 (also called *ANAC092*, *AtNAC2*, or At5g39610) is well documented as a senescence regulatory protein (Balazadeh *et al*., 2010a; He *et al*., 2005; Kim *et al*., 2009; Ooka *et al*., 2003). Its role in senescence was first described by Kim *et al*., (2009) who observed that the *oresara1* (*ore1*) EMS mutant displayed a delayed senescence phenotype. Despite the importance of ORE1 as a positive regulator of senescence, mechanisms and elements of its regulatory pathway are still poorly understood. In this study, we describe two previously unknown regulatory pathways up-stream of ORE1, and we addressed the challenging task of identifying potential direct targets of ORE1.

Up-stream regulation of *ORE1*

As we described in **Chapter 2,** *miR164* is the only regulator up-stream of ORE1 described so far. *miR164* together with *EIN2* and *ORE1* form a trifurcate feed-forward loop. EIN2 is a membrane-spanning protein whose biochemical function is still unknown, but genetic studies indicate that it is absolutely required for ethylene signaling (Alonso *et al.*, 1999; Kim *et al.*, 2009). It has been shown that ORE1 expression increases in a leaf age-dependent manner, apparently through induction by *EIN2*. *miR164* targets *ORE1* mRNA and down-regulates its expression. Nevertheless, the mechanism that governs an age-dependent decrease in *miR164* expression remains unknown. All that can be speculated is that *miR164* functions in younger leaves as a "guard" against premature overexpression of *ORE1*. Kim *et al.* (2009) proposed that this feed-forward loop exists to guarantee that senescence and the accompanying programmed cell death occurs when leaves are aged (Kim *et al.*, 2009). Notably, a screening for down-stream targets of the MADS-box transcription factor *SEPALLATA3* (*SEP3*) revealed that SEP3 binds to the *ORE1* promoter. Chromatin immunoprecipitation (ChIP), followed by next-generation sequencing (ChIP-Seq) or hybridization to whole-genome tiling arrays, revealed four aspects of particular interest: (i) SEP3 binds to the *ORE1* promoter *in vivo*; (ii) *ORE1* is SEP3 target-specific during stamen and carpel development; (iii) DNA-binding sites of SEP3 are predominantly located a few hundred base pairs directly up-stream of the ATG of its targets; and finally, (iv) ChIP-Seq data revealed a dependency between the presence of perfectly matching CArG boxes and the binding of SEP3 *in vivo*.

In this study, we report for the first time two mechanisms that positively influence *ORE1* expression. First, using transcriptional profiling, we identified that *ORE1* expression is up-regulated by the NAC transcription factor ATAF1. Moreover, co-transfection of the *ORE1* promoter (*ORE1-LUC*) together with *35S:ATAF1* leads to transactivation of the promoter in mesophyll protoplasts, suggesting a direct interaction between *ORE1* promoter and ATAF1 (**section 2.2.5**). Interestingly, ATAF1 also transactivates *VND interacting factor 2* (*VNI2*), another NAC TF that we characterized in this study as a putative direct target of ORE1. The possible interaction between *ATAF1* and *VNI2* mediated by ORE1 will be further described in this discussion.

The second mechanism we described in this work was discovered in collaboration with the group of Prof. Dr. Tina Romeis from the Freie Universität in Berlin. They performed a phosphoproteomic approach that revealed that CKOR, a calcium-dependent protein kinase (CDPK), is able to phosphorylate ORE1. We found that overexpression of CKOR in wild type mesophyll protoplasts led to a marked increase in the transcriptional activation of the ORE1 direct target BFN1 and the putative targets *VNI2* and *RNS3* (**Section 3.2.1**). On the contrary, the overexpression of CKORm, which is unable to phosphorylate its targets, led to a decreased *BFN1* promoter activation but did not affect the activation of *VNI2* and *RNS3*. It is widely acknowledged that phosphorylation and dephosphorylation of transcription factors

can directly regulate distinct aspects of their function (Whitmarsh and Davis, 2000). *ORE1*, *BFN1*, and *VNI2* are senescence associated genes (SAGs) (Balazadeh *et al*., 2008; Breeze *et al*., 2011; Buchanan-Wollaston *et al*., 2005) and the S-like RNase *RNS3* gene is induced during phosphate (Pi) starvation and has been associated with the nutrient remobilization process (Bariola *et al*., 1994; Taylor *et al*., 1993). If we assume that phosphorylation of ORE1 by CKOR enhances its transcriptional activity, we would expect that an increase in phosphorylated ORE1 level would, in turn, result in a higher transcriptional activity. We observed that *BFN1*, whose expression is strongly up-regulated by ORE1, shows a significant increase in transcriptional activation when the amount of phosphorylated ORE1 increases (achieved by the overexpression of CKOR in mesophyll protoplasts). This tight transcriptional dependency is further supported by the significant reduction in *BFN1* activation if a mutated version of CKOR is overexpressed in mesophyll protoplasts. In the case of *VNI2* and *RNS3*, the overexpression of a mutated version of CKOR did not lead to a reduction in transcriptional activity, unlike *BFN1*. It can be assumed that both genes are strongly up-regulated by ORE1 phosphorylation. Nevertheless, it is plausible that *VNI2* and *RNS3* require a higher accumulation of ORE1 to be activated, and the ORE1 concentration in wild type protoplast, concurrently with the overexpression of a mutated version of CKOR that binds but is unable to phosphorylate ORE1, contributes to make any changes in transcriptional activity indistinguishable from the basal expression. In the Outlook section at the end of the discussion, a set of experiments is proposed to shed light on the role of ORE1 phosphorylation in regulating its activity.

ORE1, as well as most of its putative targets, have been characterized in ABA-dependent responses to stresses such as salt stress (**section 2.2.3 and 6.2.3**) (Balazadeh *et al*., 2010b; Jiang *et al*., 2011; Yang *et al*., 2011). The role of phosphorylation in ABA-dependent regulation of transcriptional expression has been well documented (Furihata *et al*., 2006; Lopez-Molina *et al*., 2001; Zhu 2002). Thus, it may be suggested that phosphorylation of ORE1 by CKOR integrates a regulatory pathway involved in both developmental and stress-induced leaf senescence. Further analyses are required to elucidate the exact role of this novel ORE1 regulatory pathway.

Tissue-specific expression of *ORE1* gives direct insights linking ORE1 with germination, floral development, and senescence

We have shown that tissue-specific promoter activity of *ORE1* is not restricted to senescent tissues in *Arabidopsis* or tobacco (*Nicotiana tabacum*) transformed with the same chimeric gene. In both plant species, *ORE1* promoter expression shared the same tissue-specific patterns in almost all the evaluated tissues and organs. During early developmental stages, *ORE1* promoter activity was detected in roots and was particularly enhanced in embryos from mature seeds and cotyledons of 15-day-old seedlings in both species (**section 2.2.1**). These observations are in agreement with previous studies that reported *ORE1* promoter

expression during lateral root development (He *et al.*, 2005), and in embryos under different stress conditions (Penfield *et al.*, 2006). Cotyledons are embryonic leaves that undergo a fast tissue differentiation (Fridlender *et al.*, 1996) and serve as storage to supply nutrient demand. We know that many *ORE1* up-regulated genes that are related to senescence share common patterns during the last stages of seed development (Balazadeh *et al.*, 2010a). Nevertheless, the biological relevance of this common pattern has not yet been studied. Seed germination shares some clear similarities with leaf senescence; both involve the degradation and transport of macromolecules, and the organs involved (leaves and cotyledons) keep structural similarities. Nevertheless, this does not account for the particular expression in mature embryos of *Arabidopsis* and tobacco. Interestingly, we have found a recent discovery that describes *ORE1* expression during seed germination. It has been shown that in *Arabidopsis* seeds, glutamate decarboxylase (GAD) catalyze the unidirectional decarboxylation of glutamate to form γ-aminobutyric acid (GABA) (Fait *et al.*, 2011). Fait *et al.* (2011) described that GABA is strongly associated with early seed germination. In plants, glutamate (Glu) metabolism is pivotal for efficient N incorporation, and its levels are maintained under tight regulation (Forde and Lea, 2007; Stitt and Fernie, 2003). Furthermore, accumulation of GABA is associated with enhanced amino acid contents and associates with an up-regulation of genes involved in the degradation of proteins and cellular components (Fait *et al.*, 2011). Hyperaccumulation of GABA enhanced the expression of two senescence associated genes (SAGs), i.e. *ORE1* and *SAG21* (*SENESCENCE-ASSOCIATED GENE 21*), as well as *DOG1* (*DELAY-OF-GERMINATION1*), which is one of the major regulators of seed dormancy (Bentsink *et al.*, 2010). Their results highlight a link between seed maturation and the expression of *ORE1*. However, our promoter expression analyses are based on wild type seeds carrying an *ORE1* promoter fusion (*ORE1:GUS*) that should not hyperaccumulate GABA. Moreover, according to our published germination assays, we suggested that ORE1 might contribute to seed dormancy, which may be partly lost or enhanced, at least under salt stress , in *anac092-1* T-DNA insertion mutants and *35S:ORE1* overexpressors, respectively (Balazadeh *et al.*, 2010a). The enhanced *ORE1* promoter activity observed in embryos (imbibed in water for 12 hours before testa removal) suggests that ORE1 is more deeply implicated in seed germination than has been considered so far. Additional studies are required to elucidate the signaling pathways governed by ORE1 during seed germination.

The promoter expression of *ORE1*, as identified by GUS staining, is in accordance with the role of ORE1 during senescence. The expression along the leaf blade is consistent with the reported progression of aging from the tip to the base of leaves due to remobilization of nutrients out of the leaf and in the direction of the rest of the plant organs (Hill, 1980). *ORE1* promoter activity was also detected in floral organs of mature opened flowers in the carpel/pistil, especially in the upper region of the stigma. This observation is in agreement with the recent discovery that *Arabidopsis* unfertilized/fertilized carpels exhibit senescence first in the stigma, and then it progresses from basal to apical ovules (Carbonell-Bejerano *et al.*, 2010). Furthermore, *ORE1* has been reported as up-regulated during carpel senescence

(Carbonell-Bejerano *et al.*, 2010). ORE1 expression was strongly evident in mature anthers, whereas it was absent in immature anthers (**section 2.2.1**). Notably, GUS staining, driven by the *ORE1* promoter, was also detected in the tip region of the stigma in *Arabidopsis* unfertilized flowers (**section 2.2.1**), suggesting that ORE1 is not exclusively involved in floral senescence, but also during early developmental stages.

Recently, two works linked ORE1 with flower development. First, whole transcriptome analyses and chromatin immunoprecipitation assays, combined with massive parallel DNA sequencing (ChIP-Seq), were used to characterize the down-stream regulatory pathway of SEPALLATA3 (SEP3). SEP3 is a MADS-box TF that plays a crucial role in the transition from vegetative to reproductive growth and finally to floral meristems (Kaufmann *et al.*, 2009). It was found that SEP3 binds to the *ORE1* promoter *in vivo* and that *ORE1* is a SEP3 target specifically during stamen and carpel development. The *ORE1* promoter displays two perfect CArG boxes, one C[AAAAAAA]GG located at position -601 bp (from the ATG) and the other C[AATTATT]GG located at position -225 bp (from the ATG); a third box located within the 5'UTR differs only one nucleotide from the perfect CArG matching C[CTATTA] GG (position -5 bp). Moreover, Al-Daoud *et al.*, (2011) have found that ORE1 promotes floral transition under short-day photoperiods. Results from other research groups, taken together with our results (**section 2.2.1**), suggest it is feasible that ORE1 may play a role during early flower development that has not yet been explored, and it offers a new facet of ORE1 that is complementary to its role as a master regulator of leaf senescence.

ORE1 5'UTR contains important regulatory elements required for senescence-specific expression

In an attempt to characterize the promoter region essential for the characteristic senescence associated pattern of *ORE1* expression, we performed promoter deletion analyses. Our results give insights into the pivotal role of the 5'UTR in maintaining the characteristic expression of *ORE1* during senescence. Nevertheless, a visible reduction in the strength of the signal indicates that other elements outside the 5'UTR are needed to reach the high expression levels observed during senescence (**section 2.2.4**). It has been demonstrated that in some particular cases, the region that is up-stream of the TATA box is not essential to reach high levels of expression, and that this particular feature associates with the presence of pyrimidine-rich sequences (5UTR-Py-rich stretch) in the 5'UTR. The Py-rich stretches seem to have a positive effect on the overall expression level of a gene, as seen in tomatos (Daraselia *et al.*, 1996) spinach (Bolle *et al.*, 1994), Chinese wild *Vitis pseudoreticulata* (Xu *et al.*, 2011), rice, and *Arabidopsis* (Xue *et al.*, 2008). Recently, it has been demonstrated that actin genes, from bryophytes to angiosperms, include a 5UTR-Py-rich stretch that confers high levels of transcription (Vitale *et al.*, 2003; Weise *et al.*, 2006). Interestingly, we found that the *ORE1* promoter contains two Py-rich stretch motifs in its 5'UTR. On the one hand, we have shown that plants transformed with the *Prom6-ORE1:GUS* construct that contains two predicted TATA boxes but lacks both

5UTR-Py-rich stretch motifs, lose the senescence-specific pattern from the tip to the base of the leaves (**Section 2.2.4**). On the other hand, plants overexpressing a short fragment of the 5'UTR (*Prom3-ORE1:GUS*) that contains one 5UTR-Py-rich stretch maintain the leaf senescence specific expression pattern, albeit at a much lower level. Our results suggest a pivotal role of the 5UTR-Py-rich stretch motifs. The fact that plants transformed with the *Prom3-ORE1:GUS* construct display GUS activity suggests the presence of an alternative start codon ATG since the predicted TATA boxes lie up-stream of this fragment. Interestingly, despite the high homology between *ORE1* and *ORS1* (*ORESARA1 SISTER1*), an evolutionary closer NAC TF (Balazadeh *et al.*, 2011; Ooka *et al.*, 2003), *ORS1* does not contain any 5UTR-Py-rich stretch within its promoter (data not shown), confirming that ORE1 5'UTR conserves typical features and plays an important role in *ORE1* up-stream regulation. To conclusively probe the contribution of the 5'UTR to the *ORE1* expression pattern in senescent tissues, two approaches may be taken. The first is to replace the *ORE1* 5'UTR with a standard 5'UTR such as the GSTF8 minimal promoter (Thatcher *et al.*, 2007). We would expect a minimal promoter to completely abolish the senescence-specific pattern of expression. The second approach is to mutate both 5UTR-Py-rich motifs present in the 5'UTR, which should also lead to abolishment of the senescence-specific pattern of expression.

Defining the ORE1 regulon based on a genome-wide analysis

The rate at which individual genes are transcribed is controlled by the binding of transcription factors (TFs) to their up-stream promoter regions. Over 2,000 TFs are encoded by *Arabidopsis* (Pérez-Rodríguez *et al.*, 2010). Nevertheless, so far only a minority (around one-third) of all TFs have been functionally characterized in *Arabidopsis*. The determination of the regulatory circuits controlled by each TF, and the identification of the cis-regulatory elements (CREs) for all genes, have been identified as two of the goals of the Multinational Coordinated *Arabidopsis thaliana* Functional Genomic Project by the Multinational *Arabidopsis* Steering Committee (June, 2002) (Davuluri *et al.*, 2003).

Recently, high-resolution temporal profiling of transcripts during *Arabidopsis* leaf senescence revealed a distinct chronology of the process and its regulation (Breeze *et al.*, 2011). Surprisingly, , this model of the senescence regulatory network identified *ORE1* as a master regulatory element that controls several genes implicated in leaf senescence. Therefore, we combined three different approaches to unravel key elements in the architecture of the ORE1 regulatory network. First, a transcriptome analysis included short- and long-term induction of ORE1 in order to identify putative direct target genes (**section 4.2.1**). Next, we characterized the ORE1 consensus binding site (BS) to identify ORE1-BSs in the promoter region of putative ORE1 targets (**section 4.2.2**), and we selected a group of genes for further confirmation of the direct interaction with ORE1 (**section 4.2.3 and 4.2.4**). Finally, we characterized the genes at the molecular and physiological level to be able to categorize them as direct targets. (**Chapters 5** and **6**).

Based on our previous work (Balazadeh *et al*., 2010a), we have identified a set of differentially expressed genes after inducible over-expression of ORE1, and we confirmed some by qRT-PCR. Additional global transcriptome analyses were carried out. We incubated *ORE1-IOE* seedlings for two hours and five hours in estradiol (EST), and we constitutively overexpressed ORE1 for six hours in *Arabidopsis* mesophyll protoplasts. In total, we found 711 genes up- and 273 genes down-regulated in the three experiments. As expected, upon *ORE1* overexpression, we observed a significant over-representation of genes involved in metabolism and degradation among the up-regulated genes. The significant over-representation of genes from these functional categories may be due to the prevalent role of degradation of different macromolecules as part of the mechanism of nutrient salvage that occurs in the plant during senescence (Bleecker, 1998). Considering we found more genes up- than down-regulated, and we were able to identify 17 genes commonly up-regulated but none commonly down-regulated in all three data sets, we propose that ORE1, like most NAC TFs, functions as a transcriptional activator. Among these 17 putative targets are genes encoding proteins for degradation and dismantling processes such as lipases, kinases, synthases, hydrolases, and nucleases (Balazadeh *et al*., 2003). We found six TFs that were up-regulated after five hours of ORE1 induction. All of them were commonly up-regulated after five hours inducible overexpression or six hours constitutive overexpression. The TFs include one zinc-ion binding factor (At2g28200), one signal transduction response regulator (At2g40670), one *MYB TF* (At3g10590), and three members of the NAC TF (*ANAC010*, *ANAC041*, *VNI2*). Thus, most of the up-regulated TFs belong to the NAC TF family, highlighting the predominant role of this family in leaf senescence (Buchanan-Wollaston *et al*., 2005; Guo and Gan, 2004; Guo and Gan, 2012). The fact that overexpression of ORE1 leads to the up-regulation of 711 genes, most of which are SAGs, and to the up-regulation of six TFs, highlights the importance of *ORE1* as a key regulator of leaf senescence. Considering that six TFs are significantly up-regulated also underlines the apparent fact that not many transcriptional networks are activated down-stream of ORE1, and it is tempting to speculate that *ORE1* expression plays a pivotal role in the progression rather than the onset of senescence. Our results strongly support the importance of the molecular characterization of regulatory pathways governed by NAC TFs, especially ORE1, not only during senescence but also in *Arabidopsis* development.

Validation of putative direct targets of ORE1 and their functional characterization

Several members of the NAC TF family, including *ORE1/ANAC092/AtNAC2* (Guo and Gan, 2006) and ORS1/ANAC059, have been shown to positively regulate leaf senescence in *Arabidopsis* (Balazadeh *et al*., 2011). Knocking out the function of each of those genes generates a delay-of-senescence phenotype. In contrast, other members of the NAC TF family, like VNI2/ANAC083 (Yang *et al*., 2011) and JUB1/ANAC042 (Wu *et al*., 2012), have recently been shown to negatively regulate leaf senescence and enhance plant longevity in *Arabidopsis*. Despite the fact that *ORE1* and *ORS1* are paralogues that exhibit evolutionary

conservation (Balazadeh *et al.*, 2011) and share a common function as positive regulators of leaf senescence, only eight genes are commonly up-regulated by both TFs upon inducible overexpression (At3g01830, At3g61190, At2g32680, At5g38710, At5g39520, At3g29250, At4g27280 andAt3g61930) (Balazadeh *et al.*, 2011). All overlapping genes are SAGs, but only At5g39520 that encodes an unknown protein is among the 17 genes commonly up-regulated by *ORE1* overexpression. Thus, overexpression of a single senNAC TF (senescence-associated NAC transcription factor) affects specific down-stream genes, suggesting that functional redundancy between NAC genes controlling senescence is limited. This can be explained if each of those senNACs controls a specific or partially specific subset of down-stream target genes, which is essential for the correct timing of the onset and progression of senescence. Therefore, unraveling the gene regulatory network administrated by senNAC TFs and discovering the specificity of those regulations is of particular importance. Nevertheless, direct or indirect regulation between senNACs and their putative targets can only be determined experimentally. It is well known that characterization of the sequences bound by a transcription factor is an essential step in the identification of its true targets. The ORE1 binding site was originally reported by Olsen *et al.* (2005). However, recent studies demonstrated that sequences bound by NAC TFs are rather long and include two consensus motifs separated by a spacer of few bp (base pairs) (Balazadeh *et al.*, 2011; Xue, 2005; Wu *et al.*, 2012). The binding affinity of ORE1 to certain oligonucleotides in vitro was evaluated by the DNA-binding-protein-CELD method (DBP-CELD). The binding sequence of ORE1 was characterized as containing the two core motifs (RMGTR) and (YACGY) spaced apart by 5-6 bp. Thus, the ORE1 binding site (ORE1-BS) was determined to be RMGTR(5-6n) YACGY (**section 4.2.2**).

We focused our efforts to elucidate ORE1 directly from indirect interactions within a subset of six highly up-regulated genes. We selected *BFN1* (At1g11190), *RNS3* (At1g26820), *SINA1* (At3g13672), and *SAG29* (At5g13170) from the 17 commonly up-regulated genes, and we selected *ORE1* and *VNI2* based on (i) the novel hypothetical model proposed by Breeze *et al.* (2011) that predicts an autoregulatory feedback loop for *ORE1* and shows *VNI2* as a possible ORE1 direct target and (ii) the strong up-regulation of *VNI2* in our long-term transcriptome analyses (**section 4.2.1**). We tested whether ORE1 was able to transactivate the promoter regions of those six putative targets *in vivo*. Our results show that overexpression of ORE1 transactivates the expression of *BFN1*, *VNI2*, and *RNS3* (**section 4.2.3**). In the case of *ORE1*, we were unable to identify the proposed autoregulatory feedback loop . Based on our results, we decided to test the ability of ORE1 to bind *in vitro* by EMSA to ORE1 binding sites (ORE1-BSs) identified *in silico* in the promoters of *BFN1*, *VNI2*, and *RNS3*. Additionally, we included *SINA1* to test whether non-significant transactivation *in vivo* correlates with no binding *in vitro* (**section 4.2.4**). The selected genes contained more than ten different versions of ORE1-BSs taken as ORE1-BS sequences containing at least the first core motif. Nevertheless, in general, only the longest ORE1-BS found in each promoter was considered for the EMSAs. We found that ORE1 is able to bind to all tested promoters *in vitro*, but

the binding affinity was different among them. Based on the intensity of the band in the retardation gels, we were able to determine that ORE1 exhibits the highest affinity to the BS in *VNI2*. The oligonucleotides tested for *RNS3* and *SINA1* contained 5 bp and 11 bp long ORE1-BSs, respectively, and for the most part lacked the second core of the ORE1-BS. In this study, we characterized for the first time the longest consensus sequence that corresponds to the ORE1-BS and is probed by two different methods (DBP-CELD and EMSA). ORE1 binding affinity is highly dependent on the presence of both core motifs. We found that ORE1 overexpression results in a strong transactivation of *RNS3 in vivo*, and only a slight binding affinity *in vitro*. Additional EMSAs are required to pin-point the ORE1-BSs that causes the strong *RNS3* transactivation *in vivo*. Currently, we have better candidates that may fit as ORE1-BS in *RNS3*.

Based on these observations, we aimed to prove that ORE1 binds directly to these putative target genes *in vivo* by Chromatin Inmunoprecipitation (CHiP) using two different tags linked to ORE1. In both cases, we used transgenic plants expressing ORE1 tagged with the green fluorescence protein (GFP) or a newly developed HaloTag (Urh *et al*., 2008). This was the first attempt focused on the implementation of HaloTags in plants, and it represented a challenge to implementing new methods for the characterization of down-stream regulatory pathways in TFs in plants. In the case of ORE1-GFP, the cassette contains the constitutive *35S* promoter, whereas ORE1-HaloTag is under the control of an estradiol-inducible promoter. Striking results were obtained in both cases. As expected, we were able to obtain high expression of ORE1, and we were able to determine the subcellular location of ORE1 in the nucleus of guard cells in *Arabidopsis* leaves (**Annex 6**). Nevertheless, none of the selected putative targets that are highly regulated by ORE1 were induced in those plants. In both cases, constructs were confirmed by sequencing for the presence of the HaloTag and GFP on transformed plants and by ORE1 expression. One possible explanation for these results is that the linked tag placed at the end of the C-terminal region of ORE1 blocked or restricted the interaction with target promoters and, therefore, expression of ORE1 putative targets was notdetectable. In order to probe this hypothesis, we suggest transforming *Arabidopsis* with a different cassette in which the Tag is fused to the N-terminal region. Although we were unable to check the binding of ORE1 to the target promoters by CHiP, different assays in planta strongly support the hypothesis that *BFN1*, *VNI2*, and *RNS3* are direct targets of ORE1.

We selected *BFN1*, *RNS3*, *SINA1*, *SAG29*, and *VNI2* to test if they are direct targets of ORE1. Remarkably, *VNI2*, *RNS3*, and *BFN1* have been described as prominent players in another process quite unrelated to leaf senescence: xylem vessel differentiation (Pesquet *et al*., 2010; Yamaguchi *et al*., 2010). The most interesting thing about the unexplored connection between both processes comes from the programmed cell death. Nonetheless, Zhong *et al*. (2010) showed that NAC transcription factors involved in secondary wall biosynthesis (SWNs) do not include ORE1 as a key player. The conclusion that can be drawn from our study and Zhong's analyses is that different processes, such as senescence and xylem vessel differentiation that

results in the up-regulation of a core set of genes, are transduced by separated pathways involving different transcription factors from the same family (the NAC family).

For the targets *BFN1* and *VNI2*, we addressed two tasks: (i) prove that *BFN1* is a direct *ORE1* target during senescence; and (ii) characterize the molecular pathway through which ORE1 regulates *VNI2* by proposing a model of this control mechanism during senescence and of their direct interaction.

ORE1 and *BFN1* constitute a non-described senescence regulatory pathway in *Arabidopsis*

Leaf senescence undergoes three general phases: (i) the initiation phase in which chlorophyll is affected, leading to a decrease in photosynthetic activity and the transition in leaves from a nutrient sink to a nutrient source; (ii) a degenerative phase, mainly characterized by the dismantling of cellular components and their degradation; and (iii) a terminal phase, where cell integrity is lost prior to cell death and death of the whole organ (Lim *et al*., 2003; Yoshida, 2003). During the degenerative and terminal phase, a marked decrease in total RNA levels is evident, whereas nuclear DNA is maintained to allow gene expression to continue until late in the process. The up-regulation of genes that are encoding for several nucleases has been reported, and they presumably act to degrade nucleic acids during senescence (Blank and McKeon, 1989; Buchanan-Wollaston *et al*., 2003; Buchanan-Wollaston *et al*., 2005; Lers *et al*., 2001; Wood *et al*., 1998). As we described before in the discussion, we were able to determine more than 700 up-regulated genes upon ORE1 induction (**section 4.2.1**). The *BFN1* transcript level rapidly increased upon induction of *ORE1*, both in intact *Arabidopsis* plants and in isolated mesophyll protoplasts. In order to integrate our results, we described a hypothetical model that combines our findings with published data in which ORE1 directly regulates BFN1 and favors senescence and programmed cell death (PCD) in *Arabidopsis*.

Aging and a variety of environmental inputs can induce senescence. These external and internal stimuli must be integrated into the senescence signal transduction to initiate senescence syndrome. ORE1 function as a positive regulator of leaf senescence in *Arabidopsis*, limiting the longevity of the leaf. Breeze *et al*. (2011) determined that a wide number of SAGs are under the control of ORE1. Thus, ORE1 may function as an up-stream regulator in the regulatory cascade of the senescence pathway. *BFN1* was the first senescence-associated gene encoding a nuclease I enzyme as described in *Arabidopsis* (Pérez-Amador *et al*., 2000). Despite the relevance of chlorophyll degradation as the first visible symptom during senescence, by the time yellowing of the leaf has become apparent, the majority of the senescence process has already occurred (Buchanan-Wollaston *et al*., 2003). We determined a marked overlap in the expression patterns of *ORE1* and *BFN1-GUS* lines in advanced senescence stages (**section 5.2.1**), and we were able to identify enhanced DNase and RNase activity in protein extract from ORE1 overexpressor lines as well as from advanced dark-induced senescence leaves

(**section 5.2.2**). Thus, we suggest that ORE1 and *BFN1* interact and exert their functions during the late degenerative and terminal phases of senescence.

Analysis of the *BFN1* promoter revealed the presence of several partial ORE1 binding sites (ORE1-BS), all of which contained the first core motif, but lacked the second core motif. Interestingly, *BFN1* promoter contains one complete ORE1-BS that differs by just one nucleotide in the second core motif to the consensus motif defined by us (**section 4.2.2**). Although punctual transversion severely affects ORE1 binding *in vitro* and *in vivo*, transcriptional activation was still observed, indicating that these partial binding sites are functional. Apparently all or at least many of the BSs present in the BFN1 promoter are functional since the deletion promoter (190 bp) that removed all sites strongly reduced *BFN1* transactivation (**section 5.2.4**). It is plausible to think that up-regulation of BFN1 is fundamental in the senescence progression and, therefore, must be guaranteed by having several ORE1-BSs that favor an activation, even if one of the binding sites is absent. Remarkably, the absence of ORE1-BS does not completely abolish BFN1 expression. Nonetheless, our data strongly support that ORE1 is the most prominent direct regulator of *BFN1*, and it is likely that other TFs may bind and be co-regulators of *BFN1*. Overall, our observations confirm that, on the one hand, BFN1 plays a pivotal role during senescence, and on the other hand, if ORE1 activation is not possible (as is the case in one promoter deletion), other TFs can activate *BFN1*, but ORE1 is the *BFN1* master regulator.

In this study, we found extended overlapping expression of *BFN1* and *ORE1* in *Arabidopsis* (**section 5.2.1**). *BFN1* is completely lost in the *anac092-1* T-DNA insertion mutant background, as shown by PCR and *BFN1* promoter-GUS reporter studies (**section 5.2.3**). The strong decrease of *BFN1* promoter expression in the *anac092-1* insertion mutant is consistent with the model that ORE1 is the master regulator of *BFN1*. Prominent expression of *BFN1* in senescence leaves, mature flowers, stigma, anthers, and the abscission zone in mature siliques agrees with the common knowledge that during senescence of floral parts, the degradation of DNA and RNA is the most common feature (Thomas *et al*., 2003). Senescence petals of Petunia were found to be associated with DNA laddering and increased nuclease activity (Xu and Hanson, 2000); in senescence petals of Ipomea, enhanced DNA degradation, chromatin condensation, and nuclear fragmentation during PCD have been reported (Taylor *et al*., 1993). Recently, senescence-associated RNases have also been characterized from petals of *Arabidopsis* (Taylor *et al*., 1993) and tomato (Farage-Barhom *et al*., 2008; Lers *et al*., 2001).

As we described above, the up-stream regulatory pathway of *ORE1* has not been characterized extensively. *ORE1* transcript is targeted by *micro-RNA164* (*miR164*), triggering its degradation. Kim *et al*. (2009) suggested a trifurcate feed-forward regulatory pathway involving *ORE1*, *miR164*, and *EIN2* (*ethylene insensitive 2*) that ensures a robust regulation of leaf senescence and age-induced cell death. *EIN2* negatively affects *miR164* expression in an age-dependent manner, and through this allows *ORE1* mRNA to accumulate, thus acting

as a positive control element. *ORE1* and *BFN1* are highly induced during leaf senescence in the wild type mutant, but not in the *ein2* (Buchanan-Wollaston *et al.*, 2005), and it is up-regulated during pistil senescence (Carbonell-Bejerano *et al.*, 2010). We determined that the difference in *BFN1* transcript abundance between younger and older leaves was greater in *mir164abc* mutants than wild type plants (**section 5.2.3**). From published work, we know that *miR164* functions as a guard against premature overexpression of *ORE1*, fine-tuning senescence timing (Kim *et al.*, 2009). We identified that *BFN1* expression in the *mir164abc* triple mutant resembles exactly the age-dependent expression of *ORE1* in *mir164abc* (Kim *et al.*, 2009). Thus, we propose that the regulatory pathway that involves *ORE1*, *mir164*, and *EIN2*, and favors senescence and programmed cell death, includes the up-regulation of *BFN1* by the direct biding of ORE1 to the *BFN1* promoter (**Fig. 31**).
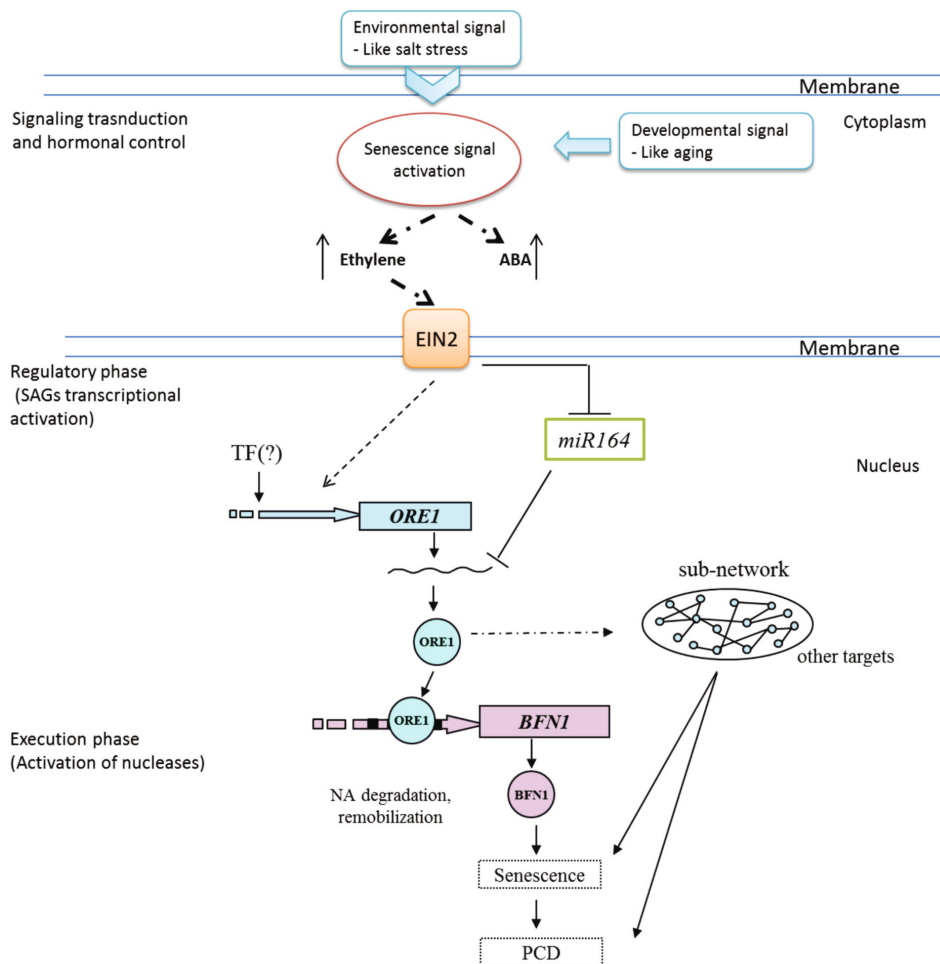
Figure 31. Hypothetical model of ORE1 as a direct regulator of *BFN1*. Environmental and developmental signals trigger senescence syndrome, increasing ethylene and ABA levels. *ORE1* transcript is targeted by *micro-RNA164* (*miR164*), triggering its degradation and suggesting a trifurcate feed-forward regulatory pathway involving *ORE1*, *miR164*, and EIN2 (*ethylene insensitive 2*) that ensures a robust regulation of leaf senescence and aged-induced cell death partially by the direct regulation of *BFN1*.

Abscission is an active process that occurs in different organs and regulates the detachment of organs from the main body of the plant. This process is triggered during developmental senescence and in response to environmental cues such as disease or pathogen attack (Patterson and Bleecker, 2004). The fact that *ORE1* and *BFN1* were co-expressed during flower senescence, especially in abscission zones (AZ), is a fascinating finding in our study. Taking leaf and silique senescence as an entire process, we suggest that both ORE1 and BFN1 may be involved not only during the progression of senescence, but as modulators in the detachment of non-functional organs in the plant. So far it is known that most genes expressed in the abscission zone do not directly affect abscission, but rather represent general housekeeping genes or genes involved in basic plant processes (Patterson and Bleecker, 2004). It is tempting to suggest that ORE1 and BFN1 expression are specific for the abscission process through EIN2. Therefore, unraveling the molecular mechanism involved represents a promising challenge.

In conclusion, our results demonstrate that senescence-induced BFN1 expression is regulated by ORE1. Previous studies have demonstrated the central importance of ORE1 for the control of leaf senescence and developmental PCD. Considering the role of BFN1 in degradation of nucleic acids during senescence, it is reasonable to assume that ORE1 exerts its senescence promoting function partly through BFN1.

Dual function of *VND Interacting2-VNI2* in developmental and induced leaf senescence in *Arabidopsis*

In **section 4.2.1**, the up-regulation of *VNI2* as a result of ORE1 overexpression was described. Presumably, this up-regulation is at the transcriptional level and mediated by the direct interaction of ORE1 with the VNI2 promoter (**section 4.2. 3 and 4.2.4**). The role of VNI2 in relation to senescence has been published by Yang *et al*. (2011). In this study, controversial evidences came to light regarding the role of VNI2 in senescence and seed germination under salt stress. Previously, it has been published that *vni2-1* shows accelerated senescence, while constitutive expression of VNI2 leads to delayed senescence. The overall morphology and size of the full-grown transgenic plants overexpressing *VNI2* was similar to wild type plants. Moreover, bolting time was similar in wild type, *VNI2* overexpressor, and *vni2-1* mutant plants. The expression of the stress-responsive genes *COR15A*, *COR15B*, *RD29A*, and *RD29B* was up-regulated in overexpressing lines and unchanged in the *vni2-1* mutant under normal growth condition. Likewise, effects of ABA and high salinity on gene expression were significantly reduced in the vni2-1 mutant (Yang *et al*., 2011). The T-DNA insertion line used in this study, *vni2-2*, displays delayed senescence, delayed onset of bolting, longer and wider leaves (**section 6.2.5**), and increased salt tolerance (**section 6.2.6**). Yang *et al*. (2011) used the T-DNA insertion mutant SALK_143793, while I used GABI-KAT 799-H09. In *vni2-2*, the T-DNA insertion mutant was identified in the third exon (**section 6.2.4**), and the production of a truncated protein lacking the activation domain and the PEST motif

cannot be discarded. On the contrary, *vni2-1* insertion lies either immediately up-stream of the coding region (Yamaguchi *et al.*, 2010) or in the first intron (Yang *et al.*, 2011).

To explain the dual role of *VNI2* during leaf senescence and salt stress, the following molecular model is proposed: expression of ORE1 that is triggered during the onset and progression of leaf senescence leads to an increase in *VNI2* transcript and favors senescence. Inducible overexpression of VNI2 (full transcript) confirms an accelerated senescence in seedlings underlined by the dramatic up-regulation of the senescence marker *SAG12* (**section 6.2.7**). Nonetheless, constitutive overexpression of VNI2 (*35S:VNI2*) leads to delayed senescence (Yang *et al.*, 2011), more likely due to an unknown transcriptional regulatory loop that may lead to an increased mRNA turnover (Hypothesis 1) (**Fig. 32**). Seedling inducible overexpressing VNI2 (*VNI2-IOE*-lines) exhibited a slight reduction in size, whereas seedling inducible overexpressing truncated VNI2 (*VNI2-ΔC-IOE*-lines) was severely affected and exhibited a dwarfed, yellowish phenotype (**section 6.2.7**).

According to Yamaguchi *et al.* (2010), a C-terminal truncated VNI2 is more stable than the full-length protein, and the overexpression of a truncated VNI2 protein effectively causes a vessel defect. Thus, it is plausible to think that the marked reduction in size observed in the *VNI2-ΔC-IOE* seedlings is caused by severe defects in root vessel formation. Microscopic analyses of these lines are required to confirm this assertion. The inducible overexpression of *VNI2-ΔC-IOE* results in higher levels of mRNA (tested by qRT-PCR) than the inducible over-expression of the full transcript (*VNI2-IOE*) (**section 6.2.7**). Moreover, seedlings that were overexpressing a truncated version of *VNI2* exhibited higher levels of *SAG12* compared to wild type, but a marked decrease compared to seedlings that were overexpressing a full *VNI2* transcript, suggesting a delay in senescence. Strikingly, *vni2-2* also displays a delayed senescence phenotype, along with a delayed onset of bolting and an apparent increase in biomass, represented by bigger leaves (**section 6.2.7**). Likely, vni2-2 is able to produce a truncated protein that comprises only the NAC domain which has been characterized to be a transcriptional repressor under normal growth condition and a transcriptional activator under salt stress (Yamaguchi *et al.*, 2010; Yang *et al.*, 2011). It is feasible to think that this protein is, in fact, produced *in planta* since a screening of databases revealed that an alternative splicing (AS) form of *VNI2* has been reported (Iida *et al.*, 2009) (Hyphothesis 2) (**Fig. 32**). Ostensibly, an uncharacterized switch is activated during salt stress and also if VNI2 is constitutively overexpressed which, in turn, promotes the expression of stress responsive genes, such as *COR15A/B* and *RD29A/B*, and represses the expression of genes involved in senescence progression (such as *SAG12*), thus enhancing salt and cold resistance (Yang *et al.*, 2011). The delayed senescence phenotype observed in seedling inducible overexpressing truncated VNI2 and in the *vni2-2* mutant, as well as the enhanced salt resistance displayed by the *vni2-2* mutants, might be associated with the same mechanism. It is feasible to assume that the switch is transcriptional and post-transcriptional, and it may likely influence both mRNA and protein stability (Hypothesis 3) (**Fig. 32**).
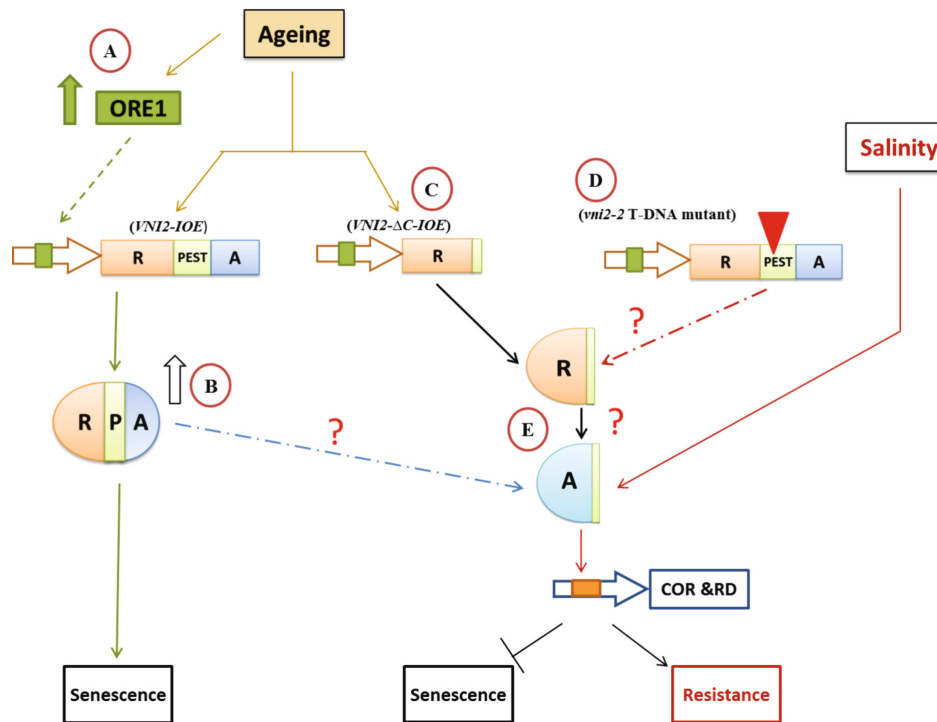
Figure 32. Molecular model of VNI2 dualole during developmental and salt-induced leaf senescence. Hypothesis 1. (**A**). Overexpression of ORE1 leads to an increase of *VNI2*, probably by direct binding of ORE1 to the *VNI2* promoter. (**B**). *VNI2* protein has a conserved NAC domain in the N-terminal region described as a repressor (R). The C-terminal region has a characterized activator domain (A) and a PEST motif (P) that regulates protein stability. Inducible overexpression of *VNI2* (*VNI2-IOE*) leads to up-regulation of *SAG12*, suggesting that ORE1 and VNI2 integrate a regulatory pathway that positively controls developmental senescence. **Hypothesis 2.** (**C**). Overexpressing of a truncated *VNI2* protein *VNI2-DC-IOE* (lacking half P and A) leads to delayed senescence. **Hypothesis 3.** (**D**). *vni2-2* likely produces a truncated protein (lacking half P and A) and exhibits delayed senescence. (**E**). VNI2 acts as activator and repress senescence, and it induces resistance under salt stress by up-regulation of COR/RD genes. Presumably, this role is controlled by uncharacterized mechanisms involving post-transcriptional and/or post-translational changes.

The evidence obtained from this study, along with available public data, suggests a connection between *ATAF1*, *ORE1*, and *VNI2* during senescence. Therefore, the following model (**Fig. 33**) is proposed, and it integrates these senescence NAC TFs (senNAC TF) into the senescence regulatory pathway. The model considers the dual role of VNI2 during developmental and induced leaf senescence, and it describes two regulatory pathways that positively/negatively regulate senescence. *ORE1* and *VNI2* mRNA expression are positively and significantly regulated by ATAF1. Both promoters are transactivated by ATAF1 (**section 2.2.5** and **section 6.2.8**), but transactivation of the *VNI2* promoter occurs even in the absent of ORE1, suggesting that ATAF1 might exert its regulatory function directly on *VNI2* and/or ORE1 (**section 6.2.8**). We determined that overexpression of a CDPK named CKOR (calcium-dependent kinase regulating ORE1) *in vivo* leads to an increase in the transcriptional activity of *VNI2*, and apparently *VNI2* requires a considerable accumulation of phosphorylated ORE1 protein to be activated (**Chapter 3**). This is likely the phosphorylated ORE1 that binds to one (or more)

ORE1-BS (binding site) present in the *VNI2* promoter and then proceeds with senescence. Based on experimental data using knockout and *VNI2* overexpressor lines, it can be speculated that under the control of an uncharacterized post-transcriptional/post-translational mechanism, VNI2 can turn from a transcriptional repressor to an activator. This likely involves the production of two *VNI2* splicing forms; one that generates a full protein (showing an increased proteasome-mediated proteolysis), and a more stable truncated VNI2 mRNA whose protein lacks the PEST motif and the activator domain. During developmental leaf senescence, *VNI2* up-regulation may lead to the repression of a set of genes that prevent senescence, most likely *COR/RD* genes. As we described above, there is evidence that the constitutive overexpression of *VNI2* delays senescence and increases salt resistance (Yang *et al*., 2011), whereas inducible overexpression of *VNI2* has the opposite effect on seedlings growing in estradiol. Moreover, the *vni2-2* T-DNA insertion mutant (T-DNA insertion in the third exon) and an inducible overexpressor line carrying a truncated version of *VNI2* (producing a protein lacking part of the third exon) exhibited a prolonged life span and enhanced salt tolerance, presumably due to the expression of a VNI2 that harbors the NAC domain and lacks the PEST motif as well as the activation domain located in the N-terminal region.

It is well establish that *ATAF1*, *ORE1*, and *VNI2* are highly induce by salt stress and ABA (Balazadeh *et al*., 2010a,b; He *et al*., 2005; Lu *et al*., 2007; Yang *et al*., 2011). According to published data, in the case of *ATAF1*, the induction in response to drought salinity is achieved in an ABA-independent manner, even though ABA alone is able to induce *ATAF1* expression (Wu *et al*., 2009). Under short-term salt stress (two hours of treatment), plants overexpressing ATAF1 showed down-regulation of three *COLD-REGULATED* (*COR*) and *RESPONSIVE TO DEHYDRATION* (*RD*) genes (*RD22, RD29A*, and *COR47*). Interestingly, these transcripts were slightly up-regulated in the same line of plants after long-term salt stress (10 hours). Authors suggested that there should be a feedback regulation of those genes affected by ATAF1 under salt stress (Wu *et al*., 2009). In addition, *VNI2* has been reported to integrate ABA-mediated abiotic stress signals into leaf aging by regulating a subset of *COR/RD* genes. Constitutive overexpression of *VNI2* leads to an up-regulation of *COR15A/B* and*RD29A/B*. The expression of these genes was unchanged in vni2-1 mutants under normal growth conditions and significantly reduced under ABA and high salinity. Notably, VNI2 behaves like a transcriptional activator under high salinity. To explain these observations, the authors suggest that high salinity may induce structural and/or activity changes of VNI2 (Yang *et al*., 2011). All observations strongly support the existence of an uncharacterized mechanism that regulates the transcriptional activity of VNI2. The novelty is that such a mechanism has not yet been elucidated for any senNAC TFs. The challenge is to determine if it is a structural change or a post-transcriptional/post-translational regulatory loop that results in turning VNI2 from a transcriptional repressor to a transcriptional activator. Nevertheless, salt stress and ABA seem to be master input signals for the regulatory pathway that integrates *ATAF1*, *ORE1*, and *VNI2* during developmental and induced leaf senescence (**Fig. 33**).
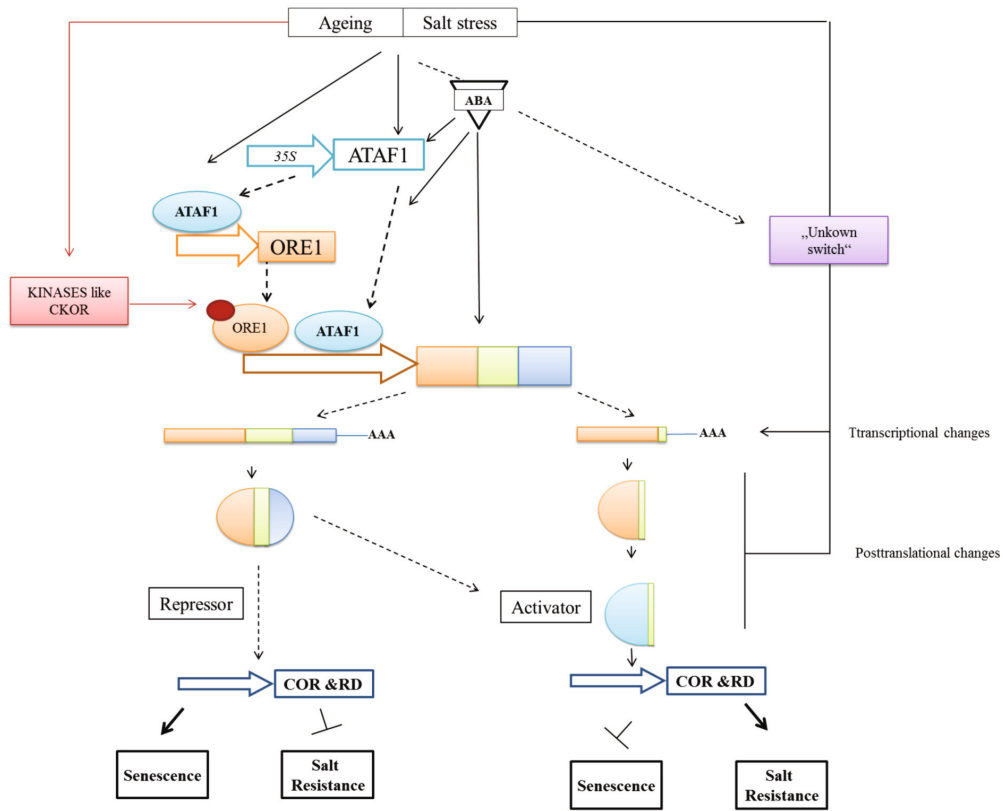
Figure 33. Model of *ATAF1*, *ORE1*, and *VNI2* in the regulation of developmental and induced leaf senescence. 1. ATAF1 is able to regulate expression of *ORE1* and *VNI2*. Aging activates the expression of CKOR that regulates ORE1 and favors the transcriptional activation of *VNI2*. An uncharacterized switch controls post-transcriptional and/or post-translational changes in VNI2. Progression of senescence might be regulated by a full version of VNI2 that represses the expression of *COR/RD* genes. It is likely another version of VNI2 is produced or activated under certain conditions and involves the activator domain and the PEST motif present in the C-terminal region of VNI2. Delayed senescence and enhanced salt resistance may be achieved through the production of VNI2 which lacks the activator domain and the PEST motif.

Future challenges and outlook

This PhD focused in unraveling the ORE1 regulon, elucidating up- and down-stream components. Substantial evidences were obtained that demonstrate the role of ORE1 as a TF that positively regulates the expression of more than 700 genes related to the senescence syndrome. A set of 17 genes were identified as putatively regulated by a direct interaction with ORE1. The interaction of ORE1 with the promoter region of some targets was tested *in vitro* and *in vivo*. Furthermore, the direct regulation of *BFN1* by *ORE1* during senescence was probed and important evidences that suggest *VNI2* and *RNS3* as putative direct targets of ORE1 were collected. Nevertheless, this knowledge is only the starting point to suggest conclusive models about the exact mode of interaction of ORE1 during developmental and induced leaf senescence with these targets. Therefore, here further experiments are proposed with the aim to elucidate the signal transduction cascades activated by ORE1. For a better view of the future challenges, the following work packages are suggested (WP):

WP1: Extension of the ORE1 up-stream regulatory pathway

As described in **Chapter 2** the up-stream regulatory pathway of *ORE1* still poorly characterized. Therefore, the novel discover of ATAF1 and CKOR as possible regulators of ORE1 provide a good starting point for further studies. It is necessary to confirm if the senNAC TF ATAF1 and the calcium-dependent protein kinase CKOR control ORE1 and favors senescence in *Arabidopsis*. Using chromatin immunoprecipitation (ChIP) coupled with deep-sequencing or tilling arrays (ChIP-CHIP) employing transgenic plants expressing ATAF1-GFP and/or ATAF1-Halotag fusion proteins, will help to confirm the direct binding of ATAF1 to *ORE1* promoter and maybe to the promoter regions of some ORE1 putative targets like *VNI2 in vivo*. These results will help to clarify not only if ATAF1 binds directly to *ORE1* promoter but also which ORE1 putative targets may also be regulated by ATAF1. This work will allow to define up to which point there is a redundancy between ATAF1 and ORE1 during senescence. It would be of great advantage implementing promoter arrays to identify sequences bound by all three senNAC TFs that are of primary interest after this study. Also, yeast one-hybrid experiments can be used to identify TFs that bind specifically to the *ORE1* promoter. Due to the important role of *ATAF1* and *ORE1* in salt stress responses and the dual role of *VNI2* upon salt stress, transactivation assays that includes a phase of salt

stress will give insights into a possible cross-talk between these three senNAC TFs during developmental and salt- induced leaf senescence.

Previous phosphoproteomic approach using a CKOR overexpressor lines revealed ORE1 as one of the few proteins differentially phosphorylated. We determine that *BFN1*, *VNI2* and *RNS3* promoter transactivation was enhanced in presence of overexpression of CKOR in wild type protoplast (**Chapter 3**). The extent and dynamic changes in ORE1 phosphorylation have not been studied. As a baseline for these future studies, firstly a series of transactivation assays using protoplasts that lack the expression of ORE1 compared to transactivation of promoter regions in protoplasts that overexpress ORE1 will be required. Secondly, affinity chromatography will be used to purify/enrich phosphorylated ORE1 to identify the sites phosphorylated using high-accuracy mass spectrometry. Thirdly, the physiological characterization of CKOR transgenic lines and the phenotypic characteristics of such lines will provide information if they exhibit a particular developmental senescence phenotype or particular resistance to abiotic stresses such as salt and cold stress.

ORE1 promoter deletion analysis gave the first insights to generate the hypothesis that the 5UTR-Py-rich motifs are related to ORE1 senescence-specific expression patterns. Additional experiments are required to confirm that the 5'UTR in general and both motifs in particular are the important motifs and if their absence causes a lost of promoter-driven GUS activity or if our observations are purely an artifact due to the shortening of the promoter that renders an unspecific weaken signal. Thus, mutations of this specific motifs as well as substitution of the ORE1 5'UTR for a conventional 5'UTR will clarify the role of this region in *ORE1* promoter activity related to the senescence syndrome.

WP2: Analysis of the role of ORE1 during germination and abscission

Two interesting findings of this work were related to the marked and rapid promoter expression of *ORE1* in mature embryos and abscission zones in mature siliques in *Arabidopsis* (**Chapter 2 and Chapter 4**). Some recent studies suggested the possible role of *ORE1* as a regulator during embryo and seed development (Fait *et al*., 2011) and *anac092-1 T-DNA* insertion mutant was reported to have a delayed flowering phenotype (AL-Daoud and Cameron, 2011). Nevertheless, these are unexplored facets of ORE1 and therefore there is not available data yet. The characterization of expression patterns during embryo development and seed maturation are required to shed light on the role of ORE1 in both processes. One significant contribution to understand the role of ORE1 during abscission will be gain by the identification and characterization of *anac092-1* T-DNA insertion mutant pattern during abscission. It is feasible that the *anac092-1* T-DNA insertion mutant reveals as a delayed abscission mutant.

WP3: Determination of the dual role of VNI2 during senescence

The novel finding of VNI2 as a possible NAC TF that has (i) a dual role as activator or repressor of senescence (**Chapter 6**) and (ii) a mutant that exhibits a prolonged life span, delayed onset of bolting, higher salt stress tolerance and a presumable increase on biomass open a complete new research on this NAC TF. Firstly, a confirmation of the production of a truncated VNI2 protein in *vni2-2* T-DNA insertion mutant is required using for instance Western blots. The complete characterization if the presumable increase on biomass really takes place is also required.

The role of the PEST-motif in regulating the stability of the protein has already been studied (Yamaguchi *et al*., 2010) using proteasome inhibitors. Nevertheless, we found that the inducible overexpression of a full or truncated version of *VNI2* (with or lacking the PEST motif) result also in differences at the transcriptional level (**section 6.2.7**). Clearly the transcript corresponding to the truncated protein was strongly overexpressed as the transcript corresponding to the full version. This unexpected and exciting discovery may indicate that VNI2 stability is regulated both at the transcriptional as well as at the post-transcriptional level. To really differentiate if the overexpression of a shorter transcript (lacking the PEST motif and the activation domain) leads to a higher production of mRNA or simply to a longer half-life of the mRNA, experiments using the widely known inhibitor of transcription Actinomycin D are required.

The base of our work to identify target genes regulated by ORE1 relies on the use of Affymetrix chip arrays. The prominent role of microRNAs in the regulation of ORE1 is known (Kim *et al*., 2009) and evidently at least ATH1 Affymetrix chips do not consider this level of regulation, since no microRNA is represented in this chip. In order to extend our knowledge and measure transcript levels using an unbiased method that allows us the identification of all kinds of RNAs present in a particular line/cell/condition including mRNAs, non-coding RNAs and small RNAs new technologies must be implemented for the analysis of TFs in our group. RNA-Seq a transcriptome profiling approach based on deep-sequencing technologies offers itself as the most promising tool to acquire more precise measurements of transcript levels and their isoforms. The implementation of this technology is of particular interest for the analysis of VNI2 to establish with certainty if indeed this senNAC TF may be regulated at the transcriptional level by alternative splicing.

And last but not least, the knowledge gain in our transcriptome profiling assays, functional and molecular characterization of transgenic lines and *in vivo*, *in vitro* and *in silico* analysis of promoters need to be integrated to allow the reconstruction of the gene regulatory networks (GRN) during developmental and salt induced senescence. The reconstruction of the GRN that joins ATAF1, ORE1 and VNI2 will serve not only to complete our knowledge on onset and progression of developmental and induced senescence, but also will allow us to predict new components and regulatory mechanisms that may remain unforeseen if the current knowledge is not combined to make use of the advantages of computer modeling.

Annex 1

List of oligonucleotides used in this study

VN12 Primers

Internal code	Direction	Sequences of the oligonucleotides (5´-3´)	Purpose
133	F	GGATCCAATTACTCAGAGTTCCATA	Amplification of *VNI2* (1570 bp) promoter. *BamHI* restriction site underlined
135	F	GGATCCCACATGAAAGCAAGCAAAT	Amplification of *VNI2* (571 bp) promoter. *BamHI* restriction site underlined
134	R	CCATGGGGTGGTTCCAAACAAAG	Amplification of *VNI2* (571 bp) promoter. *NcoI* restriction site underlined
142	F	CTCGAGATGGATAATGTCAAACTTGTTAAG	Amplification of *VNI2* CDS. *XhoI* restriction site underlined
201	R	ACTAGTTCATCTGAAACTATTGCAACTAC	Amplification of *VNI2* CDS. *SpeI* restriction site underlined
141	R	ACTAGTTCACGGCAAAAGGTTCAAATCTGTTG	Amplification of *VNI2* CDS. *SpeI* restriction site underlined
149	F	GGATTTACCTGGCAATTTGGAG	To determined transcript abundance (*VNI2* first exon)
150	R	AATAACCAGACCCAGTTGCCC	To determined transcript abundance (*VNI2* first exon)
70	F	CAAAGGCAAACCACCTCATGGC	To determined transcript abundance (*VNI2* second exon)
71	R	CTGAGTGGGACCCATAGAACTCG	To determined transcript abundance (*VNI2* second exon)
160	F	CAGATTT GAACCTTTTGCCGAG	To determined transcript abundance (*VNI2* third exon)
161	R	GTCGTGACTCCACTTGAAGCAT	To determined transcript abundance (*VNI2* third exon)
131	F	GAGATTGCCACCTGGATTCAG	Confirmation homozygocity T-DNA insertion line
132	R	GAAGAATTGAAATTCGCTAGAGAA	Confirmation homozygocity T-DNA insertion line
158	R	CCCATTTGGACGTGAATGTAGACAC	Confirmation homozygocity T-DNA insertion line

ORE1 Primers

Internal code	Direction	Sequences of the oligonucleotides (5´-3´)	Purpose
110	F	GGATCCAACCTCAACTTTCTTCTC	Amplification of *ORE1* (120 bp) promoter. *BamHI* restriction site underlined
111	R	CCATGGTTTATCCTAATAGGGTTTC	Amplification of *ORE1* (120 bp) promoter. *NcoI* restriction site underlined
151	F	CACCCATCATCAACATCCTCATCATTC	Amplification of *ORE1* (1281bp) promoter for cloning into pENTR-D-TOPO
152	R	TTTATCCTAATAGGGTTTCTAAAAATG	Amplification of *ORE1* (1281bp) promoter for cloning into pENTR-D-TOPO
153	F	CACCATTTAAACGCGAAACCTCATG	Amplification of *ORE1* (250bp) promoter for clonning into pENTR-D-TOPO

No.	F/R	Sequence	Description
154	R	AAAGTGTTTGAGCAACGAAGCTCC	Amplification of *ORE1* (250bp) promoter for clonning into pENTR-D-TOPO
155	R	TTTAAGAGAGGAAAGTGTTTGAGC	Amplification of *ORE1* (263bp) promoter for clonning into pENTR-D-TOPO
116	F	GCTAGCGATTACGAGGCATCAAG	Amplification of *ORE1* (CDS) to clone into CELD vector. *NheI* restriction site underlined
117	R	GGATCCGAAATTCCAAACGCAATCCAATTC	Amplification of *ORE1* (CDS) to clone into CELD vector. *BamHI* restriction site underlined
123	F	CACC ATGGATTACGAGGCATCAAG	Amplification of *ORE1* (CDS) to clone into pENTR-D-TOPO vector for GFP assay
124	R	GAAATTCCAAACGCAATCCAATTC	Amplification of *ORE1* (CDS) to clone into pENTR-D-TOPO vector for GFP assay

ATAF1 Primers

No.	F/R	Sequence	Description
204	F	CTCGAGATGTCAGAATTATTACAGTTGCCT	Amplification of *ATAF1* cDNA. *XhoI* restriction site underlined
205	R	ACTAGTCTAGTAAGGCTTCTGCATGTAC	Amplification of *ATAF1* cDNA. *SpeI* restriction site underlined
206	F	GTTTAAACAAGTTTCAAAAACGCCAAGTTTC	Amplification of *ATAF1* cDNA. *PmeI* restriction site underlined
207	R	TTAATTAAGAAAATATTAAATTGATTGCGGCAC	Amplification of *ATAF1* cDNA. *PacI* restriction site underlined

Primers for GUS amplification (pCAMBIA-1381Z)

No.	F/R	Sequence	Description
164		GGCCTGTGGGCATTCAGTCT	Amplification of *GUS* gene (pCAMBIA-1381Z)
165		CTGTACAGTTCTTTCGGCTTGT	Amplification of *GUS* gene (pCAMBIA-1381Z)

Primers for Transactivation assays

No.	F/R	Sequence	Description
280	F	CACCCCAATATAGATGAAACCAGT	Amplification of *SAG29* promoter (831 bp) upstream of ATG to clone into pENTR-D-TOPO
281	F	TTTCTATAGCAATTGAGAAAACTTT	Amplification of *SAG29* promoter (831 bp) upstream of ATG to clone into pENTR-D-TOPO
282	F	CACCACATAGGTGTATCAGCACACAAC	Amplification of *SINA1* promoter (1118 bp) upstream of ATG to clone into pENTR-D-TOPO
283	F	TTCGCAGGAATTAATGAATTCGA	Amplification of *SINA1* promoter (1118 bp) upstream of ATG to clone into pENTR-D-TOPO
284	F	CACCCTTGAAGCCATTTTCTGGAAAGC	Amplification of *RNS3* promoter (1062bp) upstream of ATG to clone into pENTR-D-TOPO
285	F	TTCCTCAAGATATCAAATAATTTGTGG	Amplification of *RNS3* promoter (1062bp) upstream of ATG to clone into pENTR-D-TOPO
151	F	CACCCATCATCAACATCCTCATCATTC	Amplification of *ORE1* promoter (1281bp) upstream of ATG to clone into pENTR-D-TOPO
152	R	TTTATCCTAATAGGGTTTCTAAAAATG	Amplification of *ORE1* promoter (1281bp) upstream of ATG to clone into pENTR-D-TOPO
142	F	CACCCAAATTACTCAGAGTTCCATA	Amplification of *VNI2* promoter (1571 bp) upstream of ATG to clone into pENTR-D-TOPO
143	R	GGTGGTTCCAAACAAAGAGAGAG	Amplification of *VNI2* promoter (1571 bp) upstream of ATG to clone into pENTR-D-TOPO

Number	F/R	Sequence	Description
139	F	CACCAGACTGAATAGAACTAAAA	Amplification of BFN1 (1084 bp) upstream of ATG to clone into pENTR-D-TOPO
140	R	ATCTTCAAAGTTTGAAACTTATATAA	Amplification of BFN1 (1084 bp) upstream of ATG to clone into pENTR-D-TOPO
147	F	GAGGAAAAATGAGACTCGCAATGTC	Amplification of BFN1 promoter fragment. point mutation underlined
148	R	GACATTGCGAGTCTCATTTTTCCTC	Amplification of BFN1 promoter fragment. point mutation underlined
145	F	CACCGTCTTGCTTGCACACAAA	Amplification of BFN1 (192 bp) upstream of ATG to clone into pENTR-D-TOPO
146	R	ATCTTCAAAGTTTGAAACTTATATAA	Amplification of BFN1 (192 bp) upstream of ATG to clone into pENTR-D-TOPO
Primers for qRT-PCR			
202	F	TTTTTTGCCCCCTTCGAATC	Intron specific primer (amplification intergenic region)
203	R	ATCTTCCGCCACCACATTGTAC	Intron specific primer (amplification intergenic region)
204	F	TCCCTCAGCACATTCCAGCAGAT	Control housekeeping gene ACTIN2 (At3g18780)
205	R	AACGATTCCTGGACCTGCCTCATC	Control housekeeping gene ACTIN2 (At3g18780)
28	F	TCGCTTGTCCACAAGTATGC	BFN1(At5g11190) for qRT-PCR
29	R	ACCAGACTTGACGCCTTTGTATCC	BFN1(At5g11190) for qRT-PCR
32	F	AAGCTGGTCTCAAGCTCAAACACG	RNS3(At1g26820) for qRT-PCR
33	R	TCCGGTTTGATCCCAGCATTGG	RNS3(At1g26820) for qRT-PCR
66	F	TCT TCC CCA AACAGC TAA GAA CGA	ORE1(At5g39610) for qRT-PCR
67	R	GGCTGGTTCCAT TCGGTTAAT GTG	ORE1(At5g39610) for qRT-PCR
278	F	ACAAAGGCGAAGACGCTACTTG	SAG12 (At5g45890) for qRT-PCR anaylsis
279	R	ACCGGGACATCCTCATAACCTG	SAG12 (At5g45890) for qRT-PCR anaylsis
Oligos used for EMSAs			
258	F	CGGGGTTACGTACGGCACACGCAACCGTGC	Label Fragment (LF) for EMSA-ORS1
259	R	GCACGGTTGCGTGTGCCGTACGTAACCCCG	Label Fragment (LF) for EMSA-ORS1
260	F	CGGGGTTACGTACGGCACACGCAACCGTGC	Unlabeled Fragment (ULF). Competitor for EMSA-ORS1
261	R	GCACGGTTGCGTGTGCCGTACGTAACCCCG	Unlabeled Fragment (ULF). Competitor for EMSA-ORS1
262	F	TTCCGGAGATTACGTACGTCAAAGAGCTTAATTGTAGGAG	Label Fragment (LF) for EMSA-SINA1

263	R	CTCCTACAATTAAGCTCTTTGACGTACGTAATCTCCGGAA	Label Fragment (LF) for EMSA-*SINA1*
264	F	TTCCGGAGATTACGTACGTCAAAGAGCTTAATTGTAGGAG	Unlabeled Fragment (ULF). Competitor for EMSA-*SINA1*
265	R	CTCCTACAATTAAGCTCTTTGACGTACGTAATCTCCGGAA	Unlabeled Fragment (ULF). Competitor for EMSA-*SINA1*
266	F	CTCCAATTAACGTAACGTAAGGCAAACTTTCCAGCTCCAA	Label Fragment (LF) for EMSA-*RNS3*
267	R	TTGGAGCTGGAAAGTTTGCCTTACGTTACGTTAATTGGAG	Label Fragment (LF) for EMSA-*RNS3*
268	F	CTCCAATTAACGTAACGTAAGGCAAACTTTCCAGCTCCAA	Unlabeled Fragment (ULF). Competitor for EMSA-*RNS3*
269	R	TTGGAGCTGGAAAGTTTGCCTTACGTTACGTTAATTGGAG	Unlabeled Fragment (ULF). Competitor for EMSA-*RNS3*
270	F	CAACTTTTATGAGGAACGTATGAGACTCGCAATGTCTTGC	Label Fragment (LF) for EMSA-*BFN1*
271	R	GCAAGACATTGCGAGTCTCATACGTTCCTCATAAAAGTTG	Label Fragment (LF) for EMSA-*BFN1*
272	F	CAACTTTTATGAGGAACGTATGAGACTCGCAATGTCTTGC	Unlabeled Fragment (ULF). Competitor for EMSA-BFN1
273	R	GCAAGACATTGCGAGTCTCATACGTTCCTCATAAAAGTTG	Unlabeled Fragment (ULF). Competitor for EMSA-BFN1
274	F	AGAGGAAGGAGATTGAGTATGGTTTACGCCAAACGAAATA	Label Fragment (LF) for EMSA-VNI2
275	R	TATTTCGTTTGGCGTAAACCATACTCAATCTCCTTCCTCT	Label Fragment (LF) for EMSA-VNI2
276	F	AGAGGAAGGAGATTGAGTATGGTTTACGCCAAACGAAATA	Unlabeled Fragment (ULF). Competitor for EMSA-VNI2
277	R	TATTTCGTTTGGCGTAAACCATACTACTCAATCTCCTTCCTCT	Unlabeled Fragment (ULF). Competitor for EMSA-VNI2

Annex 2

ORE1-BS (Binding Sites) present in the up-stream region of ORE1-putative target genes. Positions are on relation to the ATG (first nucleotide up-stream is -1). Size of the upstream regions *BFN1* 1084 bp, *VNI2* 1571 bp, *RNS3* 1062 bp, *ORE1* 1281 bp, *SINA1* 1018 bp, *SAG29* 831 bp. Bold letters indicate ORE1-BSs tested by EMSA. The program fuzznuc from EMBOSS was used to detect ORE1-BSs (Rice *et al*. 2000). Underlined letter in the *BFN1* promoter (position -196) indicates one nucleotide difference from the consensus ORE1-BS.

Gene	ORE1 BS-Binding Sequence	Strand	Start position	Final position	Sequence in promoter	Nucleotides
BFN1	RMGTR	+	-771	-775	AAGTA	5
(At5g11190)	RMGTR	+	-295	-299	GAGTA	5
	RMGTR	-	-987	-991	AAGTA	5
	RMGTR	-	-1017	-1021	AAGTA	5
	RMGTR(6n)Y	+	-864	-875	GAGTAACTATAC	12
	RMGTR(6n)Y	-	-846	-857	AAGTAATGGGTT	12
	RMGTR(6n)Y	-	-862	-873	GCGTATAGTTAC	12
	RMGTR(6n)Y	-	-958	-969	GAGTATAAGATC	12
	RMGTR(6n)Y	-	-997	-1008	AAGTAGTGAGGT	12
	RMGTR(6n)YA	-	-239	-251	GAGTATAAACATA	13
	RMGTR(5n)YACGY	**+**	**-196**	**-210**	**ACGTATGAGAC_T_CGC**	**15**
VNI2	RMGTR(6n)Y	+	-1430	-1441	AAGTAAAACTCT	12
(At5g13180)	RMGTR(5n)Y	+	-1130	-1140	GCGTGCCCATT	11
	RMGTR(6n)Y	+	-760	-771	GAGTGCAAGATC	12
	RMGTR(6n)Y	+	-396	-407	AAGTAGTCCTTT	12
	RMGTR(5n)Y	-	-1178	-1188	AAGTGCTTTCC	11
	RMGTR(6n)Y	-	-337	-348	AAGTGTAAACTC	12
	RMGTR(6n)Y	-	-672	-683	AAGTGAGAAGTT	12
	RMGTR(5n)Y	-	-1101	-1111	GAGTAACTAAT	11
	RMGTR(6n)Y	-	-1233	-1244	AAGTGACGCAAC	12
	RMGTR(6n)Y	-	-1368	-1379	GAGTGGGTGAGC	12
	RMGTR(5n)YA	+	-1338	-1349	AAGTGATTCATA	12
	RMGTR(6n)YA	+	-1065	-1077	ACGTATGTGTATA	13
	RMGTR(5n)YA	+	-1032	-1043	ACGTGTTGAACA	12
	RMGTR(6n)YA	+	-459	-471	GAGTGTATGATTA	13
	RMGTR(5n)YA	-	-57	-68	GAGTGCGGTGTA	12
	RMGTR(5n)YA	-	-164	-175	GCGTAAACCATA	12
	RMGTR(5n)YA	-	-483	-494	ACGTGGAGGTTA	12
	RMGTR(6n)YA	-	-1074	-1086	ACGTACAGTTTTA	13
	RMGTR(5n)YACGY	**+**	**-164**	**-178**	**GAGTATGGTTTACGC**	**15**
RNS3	RMGTR	+	-761	-765	AAGTA	5
(At1g26820)	RMGTR	+	-587	-591	AAGTA	5
	RMGTR	+	-422	-426	AAGTG	5
	RMGTR	-	-143	-147	ACGTG	5
	RMGTR	**-**	**-234**	**-238**	**ACGTA**	**5**
	RMGTR	-	-298	-302	ACGTA	5
	RMGTR	-	-303	-307	ACGTA	5
	RMGTR	-	-489	-493	AAGTG	5
	RMGTR	-	-541	-545	ACGTA	5
	RMGTR(6n)Y	+	-537	-548	ACGTACGTTTCC	12

Gene	ORE1 BS-Binding Sequence	Strand	Start position	Final position	Sequence in promoter	Nucleotides
RNS3	RMGTR(5n)Y	-	-104	-114	ACGTGAAGTGT	11
(At1g26820)	RMGTR(6n)Y	-	-109	-120	AAGTGTGATATT	12
	RMGTR(5n)Y	-	-138	-148	ACGTGACGTGT	11
	RMGTR(6n)Y	-	-378	-389	GAGTATTCGATT	12
	RMGTR(5n)YA	+	-570	-581	AAGTAGCCAACA	12
	RMGTR(5n)YA	+	-415	-426	AAGTGAATACTA	12
	RMGTR(6n)YA	-	-226	-238	AAGTAATAACGTA	13
	RMGTR(5n)YA	-	-276	-287	GAGTATTTTGTA	12
	RMGTR(6n)YA	-	-971	-983	AAGTAAGAAGATA	13
ORE1	RMGTR	+	-573	-577	AAGTG	5
(At5g39610)	RMGTR	-	-962	-972	AAGTA	5
	RMGTR(6n)Y	+	-788	-799	ACGTATTAGTAC	12
	RMGTR(6n)Y	-	-796	-807	ACGTAAGGTTAC	12
	RMGTR(6n)YA	+	-324	-336	AAGTAAGATAACA	13
	RMGTR(6n)YA	-	-135	-147	AAGTGTTTGAGCA	13
	RMGTR(6n)YA	-	-465	-477	GCGTAGATTGTTA	13
	RMGTR(6n)YA	-	-1069	-1081	AAGTATATTTTTA	13
SINA1	RMGTR	+	-413	-417	GAGTG	5
(At3g13672)	RMGTR	-	-23	-27	AAGTG	5
	RMGTR	-	-127	-131	ACGTG	5
	RMGTR	-	-169	-173	ACGTA	5
	RMGTR(5n)Y	+	-491	-501	GAGTAATCAAT	11
	RMGTR(6n)Y	+	-165	-176	ACGTACGTAATC	12
	RMGTR(5n)Y	**+**	**-162**	**-172**	**ACGTAATCTCC**	**11**
	RMGTR(6n)Y	+	-81	-92	ACGTAAACGTAT	12
	RMGTR(6n)Y	+	-75	-86	ACGTATCTATGT	12
	RMGTR(6n)Y	+	-38	-48	ACGTACACCTTT	12
	RMGTR(5n)Y	-	-132	-142	GAGTAAATGGT	11
	RMGTR(6n)Y	-	-307	-318	AAGTATCCAATT	12
	RMGTR(6n)Y	-	-356	-367	AAGTGGACAAAT	12
	RMGTR(5n)Y	-	-751	-760	AAGTAATGTGT	11
	RMGTR(6n)YA	+	-836	-848	AAGTATGTGATCA	13
	RMGTR(5n)YA	+	-274	-285	GAGTGTCGTGTA	12
SAG29	RMGTR	+	-476	-480	GAGTA	5
(At5g13170)	RMGTR	+	-423	-427	GCGTG	5
	RMGTR	+	-377	-381	GAGTA	5
	RMGTR	+	-361	-365	AAGTA	5
	RMGTR	-	-252	-256	AATAA	5
	RMGTR(6n)Y	+	-640	-651	ACGTGGGATATT	12
	RMGTR(5n)Y	+	-384	-394	GCGTACGAGAT	11
	RMGTR(5n)Y	-	-232	-242	GCGTGTAACGT	11
	RMGTR(6n)Y	-	-310	-322	AAGTGGAGATAT	12
	RMGTR(5n)YA	+	-344	-355	GAGTGAATGATA	12
	RMGTR(5n)YA	-	-239	-250	ACGTGTTGAGTA	12
	RMGTR(6n)YA	-	-648	-660	ACGTATCTATTCA	13
	RMGTR(6n)YA	-	-729	-741	AAGTATGATTACA	13

Annex 3

Expression of 54 up-regulated and 24 down-regulated genes (two-fold cut-off) in *ORE1-IOE* line two hours after estradiol induction (ATH1 Affymetrix Array). Data are means of two replicates.

AGI Identifier	Affymetrix ID	Description	1st replicate (Est/Mock) log2 FCh	2nd (Est/Mock) log2 FCh	Average (Est/Mock) (log2 FCh)
AT1G02470	260933_at	similar to unknown protein [*Arabidopsis* thaliana] (TAIR:AT1G02475.1)	0,97	1,16	1,06
AT1G02660	260915_at	lipase class 3 family protein	1,62	0,48	1,05
AT1G06160	260783_at	ethylene-responsive factor, putative	1,74	0,56	1,15
AT1G11190	262454_at	BFN1 (BIFUNCTIONAL NUCLEASE I)	2,04	2,02	2,03
AT1G15520	261763_at	ATPDR12/PDR12 (PLEIOTROPIC DRUG RESISTANCE 12)	1,32	1,33	1,33
AT1G19200	256014_at	senescence-associated protein-related	1,16	1,28	1,22
AT1G26820	263689_at	RNS3 (RIBONUCLEASE 3); endoribonuclease	0,79	1,33	1,06
AT1G30700	263228_at	FAD-binding domain-containing protein	1,51	1,08	1,29
AT1G32960	261242_at	subtilase family protein	1,67	1,41	1,54
AT1G48260	262244_at	CIPK17 (CIPK17); kinase	1,18	0,88	1,03
AT1G51820	256181_at	leucine-rich repeat protein kinase, putative	1,31	1,00	1,15
AT1G63840	260327_at	zinc finger (C3HC4-type RING finger) family protein	1,04	1,09	1,07
AT1G68620	262229_at	similar to unknown protein [*Arabidopsis* thaliana] (TAIR:AT5G16080.1)	0,92	1,44	1,18
AT1G69880	260408_at	ATH8 (thioredoxin H-type 8); thiol-disulfide exchange intermediate	0,87	1,18	1,02
AT1G71530	259947_at	protein kinase family protein	1,46	0,85	1,15
AT1G73750	260048_at	similar to unknown protein [*Arabidopsis* thaliana] (TAIR:AT1G15060.1)	1,02	1,34	1,18
AT1G74010	260386_at	strictosidine synthase family protein	1,68	1,12	1,40
AT1G75900	262682_at	family II extracellular lipase 3 (EXL3)	1,24	0,79	1,02
AT1G80440	260287_at	kelch repeat-containing F-box family protein	2,19	1,55	1,87
AT1G80450	260276_at	VQ motif-containing protein	1,89	1,00	1,44
AT2G16900	266536_at	similar to unknown protein [*Arabidopsis* thaliana] (TAIR:AT4G35110.3)	1,39	1,09	1,24
AT2G28570	264082_at	unknown protein	1,64	0,52	1,08
AT2G28930	266803_at	APK1B (*Arabidopsis* protein kinase 1B); kinase	1,49	0,72	1,11
AT2G29470	266270_at	ATGSTU3 (GLUTATHIONE S-TRANSFERASE 21); glutathione transferase	1,50	1,40	1,45
AT2G31945	263475_at	similar to unknown protein [*Arabidopsis* thaliana] (TAIR:AT1G05575.1)	1,38	1,12	1,25
AT2G37710	267165_at	RLK (RECEPTOR LECTIN KINASE); kinase	1,24	0,85	1,05

AGI Identifier	Affymetrix ID	Description	1st replicate (Est/Mock) log2 FCh	2nd (Est/Mock) log2 FCh	Average (Est/Mock) (log2 FCh)
AT2G44080	267230_at	ARL (ARGOS-LIKE)	1,75	0,67	1,21
AT2G44130	267238_at	[AT2G44130, kelch repeat-containing F-box family protein]	4,61	2,97	3,79
AT2G47520	245173_at	AP2 domain-containing transcription factor, putative	1,49	0,75	1,12
AT2G47950	266486_at	similar to unknown protein [Arabidopsis thaliana] (TAIR:AT3G62990.1)	3,12	2,40	2,76
AT3G02550	258487_at	LOB domain protein 41 / lateral organ boundaries domain protein 41 (LBD41)	2,31	0,26	1,29
AT3G04000	258815_at	short-chain dehydrogenase/reductase (SDR) family protein	1,30	1,39	1,35
AT3G13310	257654_at	DNAJ heat shock N-terminal domain-containing protein	2,36	2,49	2,42
AT3G13672	256789_at	seven in absentia (SINA) family protein	2,00	1,62	1,81
AT3G21560	258167_at	UGT84A2; UDP-glycosyltransferase/ sinapate 1-glucosyltransferase	1,98	1,73	1,85
AT3G22060	257264_at	receptor protein kinase-related	1,73	1,71	1,72
AT3G45010	252606_at	SCPL48 (serine carboxypeptidase-like 48); serine carboxypeptidase	1,34	0,88	1,11
AT3G59940	251443_at	kelch repeat-containing F-box family protein	1,93	1,11	1,52
AT3G62150	251248_at	PGP21 (P-GLYCOPROTEIN 21)	1,51	0,94	1,22
AT4G04490	255340_at	protein kinase family protein	0,43	1,61	1,02
AT4G18425	254629_at	similar to unknown protein [Arabidopsis thaliana] (TAIR:AT5G46090.1)	1,40	1,68	1,54
AT4G19810	254543_at	glycosyl hydrolase family 18 protein	1,74	1,50	1,62
AT4G25350	254060_at	SHB1 (SHORT HYPOCOTYL UNDER BLUE1)	1,58	0,68	1,13
AT4G34770	253207_at	auxin-responsive family protein	2,57	0,41	1,49
AT4G36040	253125_at	DNAJ heat shock N-terminal domain-containing protein (J11)	1,15	1,34	1,25
AT4G38620	252958_at	MYB4 (myb domain protein 4); transcription factor	1,57	1,45	1,51
AT5G13170	245982_at	nodulin MtN3 family protein (SAG29)	2,64	1,53	2,08
AT5G18150	250018_at	similar to unknown protein [Arabidopsis thaliana] (TAIR:AT5G58375.1)	1,29	0,72	1,00
AT5G27420	246777_at	zinc finger (C3HC4-type RING finger) family protein	1,17	1,13	1,15
AT5G39520	249454_at	similar to unknown protein [Arabidopsis thaliana] (TAIR:AT5G39530.1)	1,37	1,37	1,37
AT5G44420	249052_at	PDF1.2 (Low-molecular-weight cysteine-rich 77)	0,62	1,67	1,15
AT5G48540	248686_at	33 kDa secretory protein-related	1,85	1,75	1,80
AT5G62630	247444_at	HIPL2 (HIPL2 PROTEIN PRECURSOR)	1,70	0,86	1,28
AT5G63970	247312_at	copine-related	1,14	0,95	1,04
AT5G59510	247704_at	DVL18/RTFL5 (ROTUNDIFOLIA LIKE 5)	-2,51	-0,82	-1,66

AGI Identifier	Affymetrix ID	Description	1st replicate (Est/Mock) log2 FCh	2nd (Est/Mock) log2 FCh	Average (Est/Mock) (log2 FCh)
AT5G54300	248205_at	similar to unknown protein [Arabidopsis thaliana] (TAIR:AT1G61260.1); similar to Protein of unknown function DUF761, plant [Medicago truncatula] (GB:ABE84235.1); contains InterPro domain Protein of unknown function DUF761, plant; (InterPro:IPR008480)	-1,85	-0,97	-1,41
AT3G51590	252063_at	function DUF761, plant [Medicago truncatula] (GB:ABE84235.1); contains InterPro domain Protein	-2,13	-0,63	-1,38
AT4G21680	254396_at	of unknown function DUF761, plant; (InterPro:IPR008480)	-1,65	-1,05	-1,35
AT3G11170	256417_s_at	[AT3G11170, FAD7 (FATTY ACID DESATURASE 7); omega-3 fatty acid desaturase];[AT5G05580, FAD8 (FATTY ACID DESATURASE 8); omega-3 fatty acid desaturase]	-1,47	-1,21	-1,34
AT5G05410	250781_at	FAD8 (FATTY ACID DESATURASE 8); omega-3 fatty acid desaturase]	-1,80	-0,81	-1,31
AT1G05575	263182_at	similar to unknown protein [Arabidopsis thaliana] (TAIR:AT2G31945.1)(GB:NP_001057099.1); similar t	-2,03	-0,53	-1,28
AT5G61890	247492_at	AP2 domain-containing transcription factor family protein	-1,26	-1,25	-1,26
AT1G52000	265053_at	jacalin lectin family protein	-1,63	-0,81	-1,22
AT3G47340	252415_at	ASN1 (DARK INDUCIBLE 6)	-1,28	-1,13	-1,20
AT1G71000	262307_at	DNAJ heat shock N-terminal domain-containing protein	-1,87	-0,54	-1,20
AT1G28480	261443_at	glutaredoxin family protein	-1,98	-0,29	-1,14
AT2G46240	266590_at	ATBAG6/BAG6 (ARABIDOPSIS THALIANA BCL-2-ASSOCIATED ATHANOGENE 6); calmodulin binding / protein binding	-1,09	-1,19	-1,14
AT1G72920	262382_at	binding / protein binding	-1,66	-0,60	-1,13
AT5G22500	249895_at	acyl CoA reductase, putative / male-sterility protein, putative	-1,25	-1,00	-1,13
AT4G24960	254085_at	ATHVA22D (Arabidopsis thaliana HVA22 homologue D)	-1,32	-0,92	-1,12
AT2G26150	266841_at	ATHSFA2 (Arabidopsis thaliana heat shock transcription factor A2); DNA binding / transcription factor	-1,18	-1,00	-1,09
AT1G53885	262226_at	senescence-associated protein-related	-1,40	-0,77	-1,09
AT1G43160	264415_at	RAP2.6 (related to AP2 6); DNA binding / transcription factor	-1,25	-0,91	-1,08
AT3G21230	258037_at	4CL5 (4-COUMARATE:COA LIGASE 5); 4-coumarate-CoA ligase	-0,80	-1,34	-1,07
AT4G24380	254158_at	hydrolase, acting on ester bonds	-1,30	-0,77	-1,03
AT1G80840	261892_at	WRKY40 (WRKY DNA-binding protein 40); transcription factor	-1,37	-0,69	-1,03
AT2G40205	256438_s_at	[AT2G40205, 60S ribosomal protein L41 (RPL41C)];[AT3G08520, 60S ribosomal protein L41 (RPL41D)];[AT3G11120, 60S ribosomal protein L41 (RPL41E)];[AT3G56020, 60S ribosomal protein L41 (RPL41G)]	-1,08	-0,97	-1,02
AT3G23250	257919_at	AtMYB15/AtY19/MYB15 (myb domain protein 15); DNA binding / transcription factor	-1,43	-0,58	-1,01

Annex 4

Expression of 269 genes differentially expressed after five hours estradiol induction. 195 genes were found up- and 74 down-regulated up regulated (Affymetrix data). Data are means of three replicates. Bold letters indicate the selected putative ORE1 targets. (*) Transcription factors.

Affymetrix ID	AGI Identifier	Description	1st replicate (Est/Mock) log2 FCh	2nd (Est/Mock) log2 FCh	3rd (Est/Mock) log2 FCh	Average (log2 FCh) (Est/Mock)
260933_at	AT1G02470	similar to unknown protein [*Arabidopsis thaliana*]	2,622	3,103	3,140	2,955
260914_at	AT1G02640	BXL2 (BETA-XYLOSIDASE 2); hydrolase, hydrolyzing O-glycosyl compounds	0,938	1,573	0,739	1,083
260915_at	AT1G02660	lipase class 3 family protein	2,443	2,682	2,065	2,397
261385_at	AT1G05450	protease inhibitor/seed storage/lipid transfer protein (LTP)-related	1,111	2,028	1,720	1,620
261410_at	AT1G07610	MT1C (metallothionein 1C)	2,317	2,428	3,944	2,896
264782_at	AT1G08810	MYB60 (myb domain protein 60); DNA binding / transcription factor	1,253	0,936	1,279	1,156
264652_at	AT1G08920	sugar transporter, putative	2,391	2,572	2,485	2,483
264261_at	AT1G09240	nicotianamine synthase, putative	1,828	1,651	2,140	1,873
264505_at	AT1G09380	integral membrane family protein / nodulin MtN21-related	2,699	2,750	2,562	2,670
264506_at	AT1G09560	GLP5 (GERMIN-LIKE PROTEIN 5); manganese ion binding / metal ion binding / nutrient reservoir	1,323	1,386	1,462	1,390
262525_at	AT1G10060	ATBCAT-1; branched-chain-amino-acid transaminase/ catalytic	1,532	1,039	0,858	1,143
262454_at	AT1G11190	BFN1 (BIFUNCTIONAL NUCLEASE I); nucleic acid binding	5,098	5,608	5,168	5,291
255928_at	AT1G12640	membrane bound O-acyl transferase (MBOAT) family protein	1,676	1,763	1,199	1,546
262826_at	AT1G13080	CYP71B2 (CYTOCHROME P450 71B2); oxygen binding	1,200	1,513	1,257	1,323
262603_at	AT1G15380	lactoylglutathione lyase family protein / glyoxalase I family protein	1,048	0,986	1,291	1,109
262482_at	AT1G17020	SRG1 (SENESCENCE-RELATED GENE 1); oxidoreductase,	1,193	1,555	1,287	1,345
256014_at	AT1G19200	senescence-associated protein-related	1,539	1,896	2,004	1,813
255782_at	AT1G19850	MP (MONOPTEROS); transcription factor	1,285	1,343	0,644	1,090
261243_at	AT1G20180	similar to unknown protein [*Arabidopsis thaliana*]	4,122	4,073	4,019	4,071
264894_at	AT1G23040	hydroxyproline-rich glycoprotein family protein	0,759	1,144	1,571	1,158
263010_at	AT1G23330	similar to unknown protein [*Arabidopsis thaliana*]	1,646	1,405	1,224	1,425
263689_at	AT1G26820	RNS3 (RIBONUCLEASE 3); endoribonuclease	4,465	4,767	4,670	4,634

111

Affymetrix ID	AGI Identifier	Description	1st replicate (Est/Mock) log2 FCh	2nd (Est/Mock) log2 FCh	3rd (Est/Mock) log2 FCh	Average (log2 FCh) (Est/Mock)
263688_at	AT1G26920	similar to unknown protein [Arabidopsis thaliana]	1,128	1,352	1,796	1,425
261441_at	AT1G28470*	ANAC010 (Arabidopsis NAC domain containing protein 10); transcription factor	2,223	1,497	1,471	1,730
260887_at	AT1G29160	Dof-type zinc finger domain-containing protein	1,436	0,994	1,415	1,282
260943_at	AT1G45145	ATTRX5 (thioredoxin H-type 5); thiol-disulfide exchange intermediate	2,125	2,013	2,910	2,349
245803_at	AT1G47128	cysteine proteinase (RD21A) / thiol protease	1,092	1,580	1,335	1,336
262244_at	AT1G48260	CIPK17 (CIPK17); kinase	2,713	2,499	2,152	2,454
260753_at	AT1G49230	zinc finger (C3HC4-type RING finger) family protein	1,122	1,041	1,128	1,097
261366_at	AT1G53100	acetylglucosaminyltransferase	1,531	1,673	1,663	1,622
259653_at	AT1G55240	similar to unknown protein [Arabidopsis thaliana]	2,094	1,721	1,687	1,834
259661_at	AT1G55265	similar to unknown protein [Arabidopsis thaliana]	1,844	1,840	2,453	2,046
264532_at	AT1G55740	ATSIP1 (ARABIDOPSIS THALIANA SEED IMBIBITION 1); hydrolase, hydrolyzing O-glycosyl compounds	1,878	2,070	1,210	1,719
264562_at	AT1G55760	BTB/POZ domain-containing protein	2,020	1,396	1,317	1,578
246395_at	AT1G58170	disease resistance-responsive protein-related / dirigent protein-related	1,621	1,569	1,723	1,638
262640_at	AT1G62760	invertase/pectin methylesterase inhibitor family protein	4,090	4,734	4,349	4,391
260109_at	AT1G63260	TET10 (TETRASPANIN10)	1,767	1,805	1,395	1,656
264680_at	AT1G65510	similar to unknown protein [Arabidopsis thaliana]	0,932	0,731	2,019	1,227
260135_at	AT1G66400	calmodulin-related protein, putative	1,658	1,021	2,117	1,599
260012_at	AT1G67865	similar to unknown protein [Arabidopsis thaliana]	0,554	0,413	2,061	1,010
260261_at	AT1G68450	VQ motif-containing protein	1,768	1,598	1,325	1,563
260208_s_at	AT1G70670	[AT1G70670, caleosin-related family protein];[AT1G70680, caleosin-related family protein]	1,450	1,643	1,677	1,590
259915_at	AT1G72790	hydroxyproline-rich glycoprotein family protein	1,737	1,459	1,058	1,418
262356_at	AT1G73000	similar to Bet v I allergen family protein [Arabidopsis thaliana]	3,349	2,980	2,248	2,859
245736_at	AT1G73330	ATDR4 (Arabidopsis thaliana drought-repressed 4)	0,969	1,261	0,994	1,075
260048_at	AT1G73750	similar to unknown protein [Arabidopsis thaliana]	2,420	2,764	2,664	2,616
260335_at	AT1G74000	SS3 (STRICTOSIDINE SYNTHASE 3)	2,521	2,658	1,610	2,263
260386_at	AT1G74010	strictosidine synthase family protein	3,160	2,963	2,224	2,782
260391_at	AT1G74020	SS2 (STRICTOSIDINE SYNTHASE 2); strictosidine synthase	2,098	2,111	2,017	2,075

Affymetrix ID	AGI Identifier	Description	1st replicate (Est/Mock) log2 FCh	2nd (Est/Mock) log2 FCh	3rd (Est/Mock) log2 FCh	Average (Est/Mock) (log2 FCh)
264144_at	AT1G79320	latex abundant protein, putative (AMC5) / caspase family protein	1,747	2,175	1,414	1,779
262940_at	AT1G79520	cation efflux family protein	1,715	1,709	1,919	1,781
260276_at	AT1G80450	VQ motif-containing protein	1,366	1,131	1,078	1,191
263595_at	AT2G01890	PAP8 (PURPLE ACID PHOSPHATASE PRECURSOR); acid phosphatase/ protein serine/threonine phosphatase	1,546	1,430	1,994	1,657
266118_at	AT2G02130	LCR68/PDF2.3 (Low-molecular-weight cysteine-rich 68); protease inhibitor	0,534	0,423	2,127	1,028
266743_at	AT2G02990	RNS1 (RIBONUCLEASE 1); endoribonuclease	1,845	1,730	1,221	1,599
265511_at	AT2G05540	glycine-rich protein	0,903	1,255	2,403	1,520
266021_at	AT2G05910	similar to unknown protein [Arabidopsis thaliana]	2,821	3,173	2,816	2,936
263282_at	AT2G14095	similar to Peptidase A11B, Ty1 A and B [Medicago truncatula] (GB:ABE93074.1)	4,111	4,471	3,704	4,095
265539_at	AT2G15830	similar to unknown protein [Arabidopsis thaliana]	1,783	1,916	2,964	2,221
266532_at	AT2G16890	UDP-glucoronosyl/UDP-glucosyl transferase family protein	1,048	1,315	0,722	1,029
264590_at	AT2G17710	similar to Os04g0560700 [Oryza sativa (japonica cultivar-group)] (GB:NP_001053549.1)	1,776	1,646	1,640	1,687
267263_at	AT2G23110	similar to unknown protein [Arabidopsis thaliana]	1,760	1,673	1,450	1,628
266566_at	AT2G24040	hydrophobic protein, putative / low temperature and salt responsive protein, putative	1,232	0,875	2,412	1,506
265913_at	AT2G25625	similar to Os05g0575000 [Oryza sativa (japonica cultivar-group)] (GB:NP_001056395.1)	1,287	1,430	1,869	1,529
266849_at	AT2G25940	ALPHA-VPE (ALPHA-VACUOLAR PROCESSING ENZYME); cysteine-type endopeptidase	2,461	2,782	1,882	2,375
267617_at	AT2G26670	HY1 (HEME OXYGENASE 1)	1,424	1,610	1,391	1,475
265573_at	AT2G28200*	nucleic acid binding / transcription factor/ zinc ion binding	0,812	1,061	1,169	1,014
266808_at	AT2G29995	unknown protein	1,245	0,823	1,789	1,285
263475_s_at	AT2G31945	similar to unknown protein [Arabidopsis thaliana]	1,653	2,175	2,862	2,230
265680_at	AT2G32150	haloacid dehalogenase-like hydrolase family protein	1,932	2,076	1,902	1,970
267115_s_at	AT2G32540	[AT2G32540, ATCSLB04 (Cellulose synthase-like B4); transferase/	1,727	2,238	1,898	1,954
267548_at	AT2G32660	disease resistance family protein / LRR family protein	1,930	1,776	2,243	1,983
267546_at	AT2G32680	disease resistance family protein	2,168	1,358	1,780	1,769
255794_at	AT2G33480*	ANAC041 (Arabidopsis NAC domain containing protein 41); transcription factor	1,005	0,935	1,224	1,055
267411_at	AT2G34930	disease resistance family protein	1,383	1,538	0,518	1,146

Affymetrix ID	AGI Identifier	Description	1st replicate (Est/Mock) log2 FCh	2nd (Est/Mock) log2 FCh	3rd (Est/Mock) log2 FCh	Average (Est/Mock) (log2 FCh)
267036_at	AT2G38465	unknown protein	0,864	0,834	1,880	1,193
267038_at	AT2G38480	integral membrane protein, putative	1,060	1,084	0,929	1,024
267358_at	AT2G39890	ProT1 (PROLINE TRANSPORTER 1); amino acid permease	1,181	1,108	0,783	1,024
263382_at	AT2G40230	transferase family protein	1,278	1,213	0,639	1,043
266078_at	AT2G40670*	ARR16 (response regulator 16); transcription regulator/ two-component response regulator	1,695	1,276	2,353	1,775
265266_at	AT2G42890	AML2; RNA binding	1,864	1,845	1,649	1,786
267226_at	AT2G44010	similar to unknown protein [Arabidopsis thaliana]	0,926	1,237	1,451	1,204
267343_at	AT2G44255	[AT2G44260, similar to unknown protein [Arabidopsis thaliana]	3,577	3,307	2,959	3,281
266756_at	AT2G46950	CYP709B2 (cytochrome P450, family 709, subfamily B, polypeptide 2); oxygen binding	2,580	1,954	1,966	2,167
266486_at	AT2G47950	similar to unknown protein [Arabidopsis thaliana]	2,104	1,640	1,846	1,863
258947_at	AT3G01830	calmodulin-related protein, putative	1,873	0,883	1,971	1,575
259221_s_at	AT3G03530	[AT3G03530, NPC4 (NONSPECIFIC PHOSPHOLIPASE C4); hydrolase, acting on ester bonds]; [AT3G03540, phosphoesterase family protein]	2,420	2,258	1,996	2,225
259308_at	AT3G05180	GDSL-motif lipase/hydrolase family protein	1,284	1,094	1,124	1,167
259133_at	AT3G05400	sugar transporter, putative	1,311	1,369	1,554	1,412
257580_at	AT3G06210	binding	1,275	1,211	0,956	1,147
258880_at	AT3G06420	ATG8H (AUTOPHAGY 8H); microtubule binding	1,016	0,992	1,597	1,201
258919_at	AT3G10525	similar to unknown protein [Arabidopsis thaliana]	0,818	1,233	1,629	1,227
258960_at	AT3G10590*	myb family transcription factor	1,321	1,588	0,816	1,242
256789_at	AT3G13672	seven in absentia (SINA1) family protein	4,209	4,372	4,433	4,338
258374_at	AT3G14360	lipase class 3 family protein	0,997	0,771	1,360	1,043
256548_at	AT3G14770	nodulin MtN3 family protein	2,148	2,203	1,472	1,941
258251_at	AT3G15810	similar to unknown protein [Arabidopsis thaliana]	1,320	1,053	1,079	1,151
259328_at	AT3G16440	ATMLP-300B (MYROSINASE-BINDING PROTEIN-LIKE PROTEIN-300B)	2,959	3,094	2,494	2,849
257965_at	AT3G19900	similar to hypothetical protein [Oryza sativa (japonica cultivar-group)] (GB:BAD22944.1)	1,419	1,040	1,093	1,184
258183_at	AT3G21550	similar to unknown protein [Arabidopsis thaliana]	3,181	3,123	3,197	3,167
257942_at	AT3G21830	ASK8 (ARABIDOPSIS SKP1-LIKE 8); ubiquitin-protein ligase	5,040	5,069	3,941	4,683
257943_at	AT3G21840	ASK7 (ARABIDOPSIS SKP1-LIKE 7); ubiquitin-protein ligase	5,750	5,682	4,804	5,412

Affymetrix ID	AGI Identifier	Description	1st replicate (Est/Mock) log2 FCh	2nd (Est/Mock) log2 FCh	3rd (Est/Mock) log2 FCh	Average (log2 FCh) (Est/Mock)
257944_at	AT3G21850	ASK9 (*ARABIDOPSIS* SKP1-LIKE 9); ubiquitin-protein ligase	6,285	6,499	5,645	6,143
257945_at	AT3G21860	ASK10 (*ARABIDOPSIS* SKP1-LIKE 10); ubiquitin-protein ligase	2,557	2,605	2,510	2,557
258105_at	AT3G23605	UBX domain-containing protein	0,855	0,812	1,373	1,013
256861_at	AT3G23920	BMY7/TR-BAMY (beta-amylase 7); beta-amylase	1,561	1,944	1,622	1,709
257824_at	AT3G25290	auxin-responsive family protein	1,490	1,757	1,449	1,565
258078_at	AT3G25870	similar to unknown protein [*Arabidopsis* thaliana]	1,383	1,270	1,125	1,259
258085_at	AT3G26100	regulator of chromosome condensation (RCC1) family protein	1,416	1,401	1,255	1,357
257774_at	AT3G29250	oxidoreductase	1,046	0,604	1,441	1,030
252606_at	AT3G45010	SCPL48 (serine carboxypeptidase-like 48); serine carboxypeptidase	3,822	3,849	3,397	3,689
252320_at	AT3G48580	xyloglucan:xyloglucosyl transferase, putative / xyloglucan endotransglycosylase, putative / endo-xyloglucan transferase, putative	3,145	2,678	2,806	2,876
252303_at	AT3G49210	similar to unknown protein [*Arabidopsis* thaliana]	1,357	1,084	0,772	1,071
252097_at	AT3G51090	similar to unknown protein [*Arabidopsis* thaliana]	1,491	0,718	0,912	1,040
252076_at	AT3G51660	macrophage migration inhibitory factor family protein / MIF family protein	0,816	1,029	2,034	1,293
252004_at	AT3G52780	ATPAP20/PAP20; acid phosphatase/ protein serine/threonine phosphatase	3,370	3,778	4,084	3,744
251739_at	AT3G56170	CAN (CA-2+ DEPENDENT NUCLEASE); nuclease	1,308	1,346	0,874	1,176
251436_at	AT3G59900	(ARGOS); unknown protein	0,941	1,328	1,111	1,127
251336_at	AT3G61190	BAP1 (BON ASSOCIATION PROTEIN 1)	1,525	1,438	1,675	1,546
251293_at	AT3G61930	unknown protein	2,974	2,875	2,489	2,779
251273_at	AT3G61960	protein kinase family protein	1,583	1,302	1,064	1,316
251191_at	AT3G62590	lipase class 3 family protein	1,407	1,003	1,647	1,352
255609_s_at	AT4G01180	[AT4G01180, XH/XS domain-containing protein];[AT5G59390, XH/XS domain-containing protein]	1,918	1,200	1,671	1,596
255345_at	AT4G04460	aspartyl protease family protein	4,777	5,473	4,681	4,977
255340_at	AT4G04490	protein kinase family protein	1,814	1,591	1,410	1,605
254956_at	AT4G10850	nodulin MtN3 family protein	2,086	2,460	1,313	1,953
254823_at	AT4G12580	unknown protein	2,559	2,749	3,284	2,864
254764_at	AT4G13250	short-chain dehydrogenase/reductase (SDR) family protein	1,642	1,896	1,439	1,659
245436_at	AT4G16620	integral membrane family protein / nodulin MtN21-related	1,800	1,654	1,532	1,662

Affymetrix ID	AGI Identifier	Description	1st replicate (Est/Mock) log2 FCh	2nd (Est/Mock) log2 FCh	3rd (Est/Mock) log2 FCh	Average (log2 FCh) (Est/Mock)
254629_at	AT4G18425	similar to unknown protein [Arabidopsis thaliana]	4,918	5,124	4,910	4,984
254648_at	AT4G18550	lipase class 3 family protein	1,881	1,709	1,534	1,708
254608_at	AT4G18910	NIP1;2/NLM2 (NOD26-like intrinsic protein 1;2); water channel	1,320	1,460	0,809	1,196
254597_at	AT4G18980	similar to unknown protein [Arabidopsis thaliana]	2,343	2,038	1,695	2,025
254543_at	AT4G19810	glycosyl hydrolase family 18 protein	4,103	4,115	3,702	3,973
254346_at	AT4G21980	APG8A (autophagy 8A)	1,070	1,045	1,565	1,227
254299_at	AT4G22920	similar to unknown protein [Arabidopsis thaliana]	2,401	2,767	2,319	2,496
254101_at	AT4G25000	AMY1 (ALPHA-AMYLASE-LIKE); alpha-amylase	1,322	1,396	1,753	1,490
254020_at	AT4G25700	BETA-OHASE 1 (BETA-HYDROXYLASE 1); beta-carotene hydroxylase	1,478	1,556	1,314	1,449
253963_at	AT4G26470	calcium ion binding	1,380	1,223	0,518	1,040
253915_at	AT4G27280	calcium-binding EF hand family protein	1,270	1,080	1,802	1,384
253676_at	AT4G29570	cytidine deaminase, putative / cytidine aminohydrolase, putative	1,209	1,455	1,459	1,374
253582_at	AT4G30670	unknown protein	2,349	2,727	3,342	2,806
253289_at	AT4G34320	similar to unknown protein [Arabidopsis thaliana]	3,131	3,177	2,649	2,986
253228_at	AT4G34630	similar to unknown protein [Arabidopsis thaliana]	1,039	1,009	1,039	1,029
252908_at	AT4G39670	similar to ACD11 (ACCELERATED CELL DEATH 11) [Arabidopsis thaliana]	1,086	0,974	0,978	1,013
251084_at	AT5G01520	zinc finger (C3HC4-type RING finger) family protein	0,653	1,198	1,361	1,070
251060_at	AT5G01820	ATSR1 (SERINE/THREONINE PROTEIN KINASE 1); kinase	1,451	1,659	1,329	1,480
251019_at	AT5G02420	similar to unknown protein [Arabidopsis thaliana]	1,378	1,022	1,602	1,334
245697_at	AT5G04200	latex-abundant protein, putative (AMC9) / caspase family protein	3,403	3,523	2,576	3,168
245705_at	AT5G04390	zinc finger (C2H2 type) family protein	2,663	2,303	1,986	2,317
250639_at	AT5G07560	GRP20 (Glycine rich protein 20); nutrient reservoir	2,106	2,573	1,620	2,100
250535_at	AT5G08480	VQ motif-containing protein	2,455	2,153	1,936	2,181
245982_at	AT5G13170	nodulin MtN3 family protein (SAG29)	4,031	4,708	4,908	4,549
245987_at	AT5G13180*	VNI2/ANAC083 (Arabidopsis NAC domain containing protein 83); transcription factor	2,294	2,071	1,991	2,119
250213_at	AT5G13820	TBP1 (TELOMERIC DNA BINDING PROTEIN 1); DNA binding	1,180	0,821	1,150	1,050
250208_at	AT5G14000	ANAC084 (Arabidopsis NAC domain containing protein 84); transcription factor	1,493	1,646	2,075	1,738

Affymetrix ID	AGI Identifier	Description	1st replicate (Est/Mock) log2 FCh	2nd (Est/Mock) log2 FCh	3rd (Est/Mock) log2 FCh	Average (Est/Mock) (log2 FCh)
250177_at	AT5G14420	copine-related	1,751	1,421	1,354	1,509
246481_s_at	AT5G15960	[AT5G15960, KIN1];[AT5G15970, KIN2 (COLD-RESPONSIVE 6.6)]	1,417	0,971	2,543	1,644
250100_at	AT5G16570	GLN1;4 (Glutamine synthetase 1;4); glutamate-ammonia ligase	1,344	1,009	1,305	1,219
246429_at	AT5G17450	heavy-metal-associated domain-containing protein / copper chaperone (CCH)-related	1,054	0,741	1,513	1,103
249999_at	AT5G18640	lipase class 3 family protein	1,623	1,652	1,256	1,510
249794_at	AT5G23530	similar to ATGID1C/GID1C (GA INSENSITIVE DWARF1C) [Arabidopsis thaliana]	1,946	1,406	1,442	1,598
249797_at	AT5G23750	remorin family protein	1,260	1,507	1,185	1,318
249750_at	AT5G24570	unknown protein	0,570	0,497	1,995	1,021
246912_at	AT5G25820	exostosin family protein	1,588	1,268	0,884	1,247
246799_at	AT5G26940	exonuclease family protein	2,452	2,193	1,926	2,190
249518_at	AT5G38610	invertase/pectin methylesterase inhibitor family protein	1,295	1,288	0,992	1,192
249527_at	AT5G38710	proline oxidase, putative / osmotic stress-responsive proline dehydrogenase, putative	1,560	1,498	1,224	1,427
249454_at	AT5G39520	similar to unknown protein [Arabidopsis thaliana]	3,909	4,386	4,319	4,205
249377_at	AT5G40690	similar to unknown protein [Arabidopsis thaliana]	3,338	3,727	3,297	3,454
249195_s_at	AT5G42500	[AT5G42500, disease resistance-responsive family protein]	1,288	1,524	1,853	1,555
249178_at	AT5G42890	sterol carrier protein 2 (SCP-2) family protein	1,470	1,571	0,991	1,344
249187_at	AT5G43060	cysteine proteinase, putative / thiol protease, putative	0,631	0,707	1,751	1,030
248959_at	AT5G45630	similar to unknown protein [Arabidopsis thaliana]	1,458	1,541	1,259	1,419
248565_at	AT5G49710	similar to unknown protein [Arabidopsis thaliana]	1,459	1,558	0,998	1,338
248545_at	AT5G50260	cysteine proteinase, putative	1,224	0,918	1,088	1,077
248440_at	AT5G51260	acid phosphatase, putative	2,007	2,558	3,121	2,562
248168_at	AT5G54570	glycosyl hydrolase family 1 protein	1,038	1,137	1,051	1,075
248115_at	AT5G54870	similar to unknown protein [Arabidopsis thaliana]	2,358	1,542	1,646	1,849
248118_at	AT5G55050	GDSL-motif lipase/hydrolase family protein	1,239	1,258	0,818	1,105
247965_at	AT5G56540	AGP14 (ARABINOGALACTAN PROTEIN 14)	1,572	1,398	0,465	1,145
247933_at	AT5G56980	similar to unknown protein [Arabidopsis thaliana]	3,972	4,086	4,306	4,121
247699_at	AT5G59840	Ras-related GTP-binding family protein	2,574	2,194	1,598	2,122

Affymetrix ID	AGI Identifier	Description	1st replicate (Est/Mock) log2 FCh	2nd (Est/Mock) log2 FCh	3rd (Est/Mock) log2 FCh	Average (log2 FCh) (Est/Mock)
247657_at	AT5G59845	gibberellin-regulated family protein	1,572	1,477	1,294	1,448
247543_at	AT5G61600	ethylene-responsive element-binding family protein	2,971	1,951	3,106	2,676
247399_at	AT5G62960	similar to unknown protein [Arabidopsis thaliana]	0,881	0,962	1,159	1,001
247312_at	AT5G63970	copine-related	0,816	0,958	1,230	1,001
247246_at	AT5G64620	C/VIF2 (CELL WALL / VACUOLAR INHIBITOR OF FRUCTOSIDASE 2); pectinesterase inhibitor	1,901	2,016	1,589	1,835
246998_at	AT5G67370	similar to unknown protein [Arabidopsis thaliana]	1,062	0,669	1,592	1,108
245050_at	ATCG00070	PSII K protein	1,701	1,585	1,527	1,604
245024_at	ATCG00120	Encodes the ATPase alpha subunit, which is a subunit of ATP synthase and part of the CF1 portion	1,777	0,526	0,963	1,088
245026_at	ATCG00140	ATPase III subunit	2,060	2,373	1,186	1,873
245009_at	ATCG00380	Chloroplast encoded ribosomal protein S4	0,528	0,384	2,316	1,076
245017_at	ATCG00510	Encodes subunit I of photosystem I.	0,239	0,207	3,083	1,176
244965_at	ATCG00590	hypothetical protein	1,029	0,436	2,206	1,224
245193_at	AT1G67810	Fe-S metabolism associated domain-containing protein	0,382	0,620	2,634	1,212
264836_at	AT1G03610	similar to unknown protein [Arabidopsis thaliana]	-1,401	-1,227	-0,725	-1,118
263231_at	AT1G05680	UDP-glucoronosyl/UDP-glucosyl transferase family protein	-1,942	-2,011	-2,299	-2,084
264467_at	AT1G10140	similar to unknown protein [Arabidopsis thaliana]	-1,446	-1,210	-0,435	-1,030
259365_at	AT1G13300	myb family transcription factor	-1,661	-1,273	-1,107	-1,347
255895_at	AT1G18020	[AT1G18020, 12-oxophytodienoate reductase; putative]	-1,154	-1,946	-0,895	-1,332
262505_at	AT1G21680	similar to unknown protein [Arabidopsis thaliana]	-1,084	-1,826	-1,112	-1,341
245821_at	AT1G26270	phosphatidylinositol 3- and 4-kinase family protein	-0,759	-1,163	-1,084	-1,002
256159_at	AT1G30135	similar to unknown protein [Arabidopsis thaliana]	-1,197	-1,814	-0,057	-1,023
261567_at	AT1G33055	unknown protein	-1,610	-1,804	0,327	-1,029
260126_at	AT1G36370	SHM7 (serine hydroxymethyltransferase 7); glycine hydroxymethyltransferase	-1,111	-1,021	-1,107	-1,080
262072_at	AT1G59590	ZCF37	-1,402	-1,236	-0,912	-1,183
264246_at	AT1G60140	ATTPS10 (Arabidopsis thaliana trehalose phosphatase/synthase 10); transferase, transferring glycosyl groups	-1,077	-1,536	-0,912	-1,175
261545_at	AT1G63530	similar to hydroxyproline-rich glycoprotein family protein [Arabidopsis thaliana]	-1,059	-1,398	-0,881	-1,113
262884_at	AT1G64720	CP5	-0,980	-1,741	-0,509	-1,076

Affymetrix ID	AGI Identifier	Description	1st replicate (Est/Mock) log2 FCh	2nd (Est/Mock) log2 FCh	3rd (Est/Mock) log2 FCh	(Est/Mock) Average (log2 FCh)
245193_at	AT1G67810	Fe-S metabolism associated domain-containing protein	-1,269	-1,691	-0,942	-1,300
264339_at	AT1G70290	ATTPS8 (Arabidopsis thaliana trehalose phosphatase/synthase 8); transferase, transferring glycosyl groups	-1,638	-1,689	-0,976	-1,434
260205_at	AT1G70700	similar to unknown protein [Arabidopsis thaliana]	-1,124	-1,483	-0,707	-1,105
256337_at	AT1G72070	[AT1G72070, DNAJ heat shock N-terminal domain-containing protein];[AT1G72060, serine-type endopeptidase inhibitor]	-1,469	-2,031	-0,059	-1,186
259879_at	AT1G76650	calcium-binding EF hand family protein	-1,492	-1,374	-0,611	-1,159
264953_at	AT1G77120	ADH1 (ALCOHOL DEHYDROGENASE 1); alcohol dehydrogenase	-1,118	-1,130	-1,267	-1,172
260287_at	AT1G80440	kelch repeat-containing F-box family protein	-1,191	-1,093	-0,892	-1,059
264042_at	AT2G03760	ST (steroid sulfotransferase); sulfotransferase	-1,211	-1,256	-1,225	-1,231
263403_at	AT2G04040	ATDTX1; antiporter/ multidrug efflux pump/ multidrug transporter/ transporter	-1,448	-1,340	-1,808	-1,532
263402_at	AT2G04050	MATE efflux family protein	-1,003	-0,946	-1,423	-1,124
265536_at	AT2G15880	leucine-rich repeat family protein / extensin family protein	-1,351	-1,725	-0,238	-1,105
265478_at	AT2G15890	MEE14 (maternal effect embryo arrest 14)	-1,917	-1,998	-0,828	-1,581
263096_at	AT2G16060	AHB1 (ARABIDOPSIS HEMOGLOBIN 1)	-1,301	-1,346	-0,413	-1,020
263061_at	AT2G18190	AAA-type ATPase family protein	-0,849	-1,045	-1,151	-1,015
266072_at	AT2G18700	ATTPS11 (Arabidopsis thaliana trehalose phosphatase/synthase 11); transferase, transferring glycosyl groups	-1,274	-1,174	-0,654	-1,034
265428_at	AT2G20720	pentatricopeptide (PPR) repeat-containing protein	-0,913	-1,297	-1,180	-1,130
257365_x_at	AT2G26020	PDF1.2b (plant defensin 1.2b)	-1,587	-2,190	0,776	-1,000
263443_at	AT2G28630	beta-ketoacyl-CoA synthase family protein	-0,966	-0,892	-1,360	-1,072
266265_at	AT2G29340	short-chain dehydrogenase/reductase (SDR) family protein	-1,213	-1,889	-0,331	-1,144
265200_s_at	AT2G36800	[AT2G36800, DOGT1 (DON-GLUCOSYLTRANSFERASE); UDP-glucosyltransferase/ transferase, transferring glycosyl groups]	-1,782	-1,751	-1,628	-1,720
258856_at	AT3G02040	SRG3 (SENESCENCE-RELATED GENE 3); glycerophosphodiester phosphodiesterase	-2,139	-1,166	-0,413	-1,240
258487_at	AT3G02550	LOB domain protein 41 / lateral organ boundaries domain protein 41 (LBD41)	-1,291	-1,454	-1,162	-1,303
259017_at	AT3G07310	similar to unknown protein [Arabidopsis thaliana]	-1,272	-1,661	-1,135	-1,356
258930_at	AT3G10040	transcription factor	-1,595	-1,601	-1,781	-1,659
256252_at	AT3G11340	UDP-glucoronosyl/UDP-glucosyl transferase family protein	-0,987	-1,001	-1,822	-1,270
258402_at	AT3G15450	similar to unknown protein [Arabidopsis thaliana]	-2,184	-1,887	-0,057	-1,376

Affymetrix ID	AGI Identifier	Description	1st replicate (Est/Mock) log2 FCh	2nd (Est/Mock) log2 FCh	3rd (Est/Mock) log2 FCh	(Est/Mock) Average (log2 FCh)
257621_at	AT3G20410	CPK9 (CALMODULIN-DOMAIN PROTEIN KINASE 9); calcium- and calmodulin-dependent protein kinase/ kinase	-0,867	-1,054	-1,282	-1,068
257153_at	AT3G27220	kelch repeat-containing protein	-1,048	-1,396	-1,383	-1,276
256589_at	AT3G28740	cytochrome P450 family protein	-1,485	-1,053	-1,366	-1,301
252482_at	AT3G46670	UDP-glucoronosyl/UDP-glucosyl transferase family protein	-1,149	-0,568	-1,324	-1,014
252250_at	AT3G49790	similar to ATPP2-A10 (Phloem protein 2-A10) [Arabidopsis thaliana]	-1,559	-1,569	-0,575	-1,234
245264_at	AT4G17245	zinc finger (C3HC4-type RING finger) family protein	-1,201	-2,273	0,209	-1,088
254318_at	AT4G22530	embryo-abundant protein-related	-0,844	-1,018	-1,154	-1,005
253874_at	AT4G27450	similar to unknown protein [Arabidopsis thaliana]	-1,240	-1,463	-0,606	-1,103
253416_s_at	AT4G33070	pyruvate decarboxylase, putative	-2,095	-2,184	-2,591	-2,290
253161_at	AT4G35770	SEN1 (DARK INDUCIBLE 1)	-2,798	-2,527	-0,506	-1,943
253046_at	AT4G37370	CYP81D8 (cytochrome P450, family 81, subfamily D, polypeptide 8); oxygen binding	-1,290	-1,252	-1,927	-1,490
250464_at	AT5G10040	similar to unknown protein [Arabidopsis thaliana]	-2,646	-1,817	-0,432	-1,631
250152_at	AT5G15120	similar to unknown protein [Arabidopsis thaliana]	-1,739	-1,929	-1,235	-1,635
249923_at	AT5G19120	pepsin A	-1,890	-1,784	-0,974	-1,549
246071_at	AT5G20150	SPX (SYG1/Pho81/XPR1) domain-containing protein	-2,526	-1,506	-0,651	-1,561
249862_at	AT5G22920	zinc finger (C3HC4-type RING finger) family protein	-1,900	-1,586	-0,374	-1,287
249742_at	AT5G24490	30S ribosomal protein, putative	-1,417	-1,358	-0,649	-1,141
246854_at	AT5G26200	mitochondrial substrate carrier family protein	-2,048	-1,433	-1,289	-1,590
249606_at	AT5G37260	myb family transcription factor	-1,236	-2,052	-0,885	-1,391
249494_at	AT5G39050	transferase family protein	-1,139	-1,398	-1,251	-1,263
249384_at	AT5G39890	similar to unknown protein [Arabidopsis thaliana]	-1,556	-1,825	-1,314	-1,565
249188_at	AT5G42830	transferase family protein	-1,219	-0,963	-1,235	-1,139
249125_at	AT5G43450	2-oxoglutarate-dependent dioxygenase, putative	-1,112	-1,034	-0,990	-1,045
249052_at	AT5G44420	PDF1.2 (Low-molecular-weight cysteine-rich 77)	-2,287	-2,564	1,057	-1,265
248719_at	AT5G47910	RBOHD (RESPIRATORY BURST OXIDASE PROTEIN D)	-0,952	-1,083	-1,251	-1,096
248622_at	AT5G49360	BXL1 (BETA-XYLOSIDASE 1); hydrolase, hydrolyzing O-glycosyl compounds	-2,459	-2,025	-1,078	-1,854

120

Affymetrix ID	AGI Identifier	Description	1st replicate (Est/Mock) log2 FCh	2nd (Est/Mock) log2 FCh	3rd (Est/Mock) log2 FCh	Average (log2 FCh) (Est/Mock)
248040_at	AT5G55970	zinc finger (C3HC4-type RING finger) family protein	-1,077	-1,332	-0,693	-1,034
247949_at	AT5G57220	CYP81F2 (cytochrome P450, family 81, subfamily F, polypeptide 2); oxygen binding	-1,531	-1,476	-1,616	-1,541
247924_at	AT5G57655	xylose isomerase family protein	-0,972	-1,663	-0,515	-1,050
247524_at	AT5G61440	thioredoxin family protein	-1,496	-2,079	-0,131	-1,235
247431_at	AT5G62520	SRO5 (SIMILAR TO RCD ONE 5); NAD+ ADP-ribosyltransferase	-1,870	-2,073	-1,297	-1,747
247297_at	AT5G64100	peroxidase, putative	-1,340	-0,417	-1,550	-1,102
247024_at	AT5G66985	unknown protein	-2,208	-2,107	0,054	-1,420
247026_at	AT5G67080	MAPKKK19 (Mitogen-activated protein kinase kinase kinase 19); kinase	-1,542	-0,628	-1,237	-1,136

Annex 5

Expression of 643 up-regulated and 188 down-regulated genes (two-fold cut-off) upon transient overexpression of ORE1 in mesophyll cell protoplast (ATH1 Affymetrix Array). Data are means of two replicates. Bold letters indicate the selected putative ORE1 targets. (*) Transcription factors.

AGI Identifier	Description	Affymetrix ID	Log2 Fch
AT5G39610*	**ORE1/ANAC092/ATNAC2/ATNAC6 (*Arabidopsis* NAC domain containing protein 92)**	**249467_at**	**3,646**
AT2G26480	UDP-glucoronosyl/UDP-glucosyl transferase family protein	245056_at	3,808
AT1G01240	similar to unknown protein [*Arabidopsis* thaliana]	261026_at	2,299
AT1G02000	GAE2 (UDP-D-GLUCURONATE 4-EPIMERASE 2); catalytic	261624_at	1,438
AT1G02470*	similar to unknown protein [*Arabidopsis* thaliana]	260933_at	1,736
AT1G02640	BXL2 (BETA-XYLOSIDASE 2); hydrolase, hydrolyzing O-glycosyl compounds	260914_at	1,272
AT1G02660	lipase class 3 family protein	260915_at	3,677
AT1G02670	DNA repair protein, putative	260909_at	1,108
AT1G02860	SPX (SYG1/Pho81/XPR1) domain-containing protein / zinc finger (C3HC4-type RING finger) protein-related	262114_at	1,954
AT1G03610	similar to unknown protein [*Arabidopsis* thaliana]	264836_at	1,796
AT1G03660	similar to ankyrin repeat family protein [*Arabidopsis* thaliana]	264832_at	1,467
AT1G03990	alcohol oxidase-related	265099_at	2,593
AT1G04090	similar to unknown protein [*Arabidopsis* thaliana]	264320_at	2,487
AT1G04160	XIB (Myosin-like protein XIB)	264324_at	1,826
AT1G05100	MAPKKK18 (Mitogen-activated protein kinase kinase kinase 18); kinase	265216_at	1,681
AT1G05120	SNF2 domain-containing protein / helicase domain-containing protein / RING finger domain-containing protein	265191_at	1,465
AT1G05450	protease inhibitor/seed storage/lipid transfer protein (LTP)-related	261385_at	3,894
AT1G05790	lipase class 3 family protein	261312_at	1,022
AT1G06520	ATGPAT1/GPAT1 (GLYCEROL-3-PHOSPHATE ACYLTRANSFERASE 1); 1-acylglycerol-3-phosphate O-acyltransferase/ acyltransferase	262630_at	1,730
AT1G07590	pentatricopeptide (PPR) repeat-containing protein	261088_at	2,051
AT1G07610	MT1C (metallothionein 1C)	261410_at	1,853
AT1G08320	bZIP family transcription factor	261815_at	1,126
AT1G08340	rac GTPase activating protein, putative	261809_at	1,388
AT1G08920	sugar transporter, putative	264652_at	3,170

122

AGI Identifier	Description	Affymetrix ID	Log2 Fch
AT1G09240	nicotianamine synthase, putative	264261_at	3,989
AT1G09380	integral membrane family protein / nodulin MtN21-related	264505_at	7,756
AT1G09390	GDSL-motif lipase/hydrolase family protein	264501_at	1,438
AT1G09560	GLP5 (GERMIN-LIKE PROTEIN 5); manganese ion binding / metal ion binding / nutrient reservoir	264506_at	1,024
AT1G11090	hydrolase, alpha/beta fold family protein	260474_at	1,426
AT1G11170	similar to unknown protein [*Arabidopsis* thaliana], similar to putative lysine ketoglutarate reductase trans-splicing related 1 [Oryza sativa (japonica cultivar-group)]	262478_at	4,418
AT1G11190	**BFN1 (BIFUNCTIONAL NUCLEASE I); nucleic acid binding**	**262454_at**	**10,026**
AT1G12320	similar to unknown protein [*Arabidopsis* thaliana]	259520_at	1,220
AT1G12430	PAK (PHOSPHATIDIC ACID KINASE); microtubule motor	259513_at	1,285
AT1G12450	similar to unknown protein [*Arabidopsis* thaliana] (TAIR:AT4G22850.1);	259530_at	3,257
AT1G12640	membrane bound O-acyl transferase (MBOAT) family protein	255928_at	1,544
AT1G13080	CYP71B2 (CYTOCHROME P450 71B2); oxygen binding	262826_at	4,332
AT1G13110	CYP71B7 (cytochrome P450, family 71, subfamily B, polypeptide 7); oxygen binding	262793_at	1,423
AT1G13130	glycosyl hydrolase family 5 protein / cellulase family protein	262795_at	3,840
AT1G13470	similar to unknown protein [*Arabidopsis* thaliana]	259385_at	1,346
AT1G14260	zinc finger (C3HC4-type RING finger) family protein	261481_at	2,982
AT1G14530	(TOM THREE HOMOLOG); virion binding	261482_at	1,776
AT1G14780	similar to unknown protein [*Arabidopsis* thaliana] (TAIR:AT4G24290.2); similar to Membrane attack complex component/perforin/complement C9	262887_at	2,337
AT1G15380	lactoylglutathione lyase family protein / glyoxalase I family protein	262603_at	2,579
AT1G15740	leucine-rich repeat family protein	259500_at	1,414
AT1G16130	WAKL2 (WALL ASSOCIATED KINASE-LIKE 2); kinase	257478_at	1,283
AT1G16310	cation efflux family protein	262751_at	1,114
AT1G16680	DNAJ heat shock N-terminal domain-containing protein / S-locus protein, putative	246322_at	1,379
AT1G17020	SRG1 (SENESCENCE-RELATED GENE 1); oxidoreductase	262482_at	1,134
AT1G17310	MADS-box protein (AGL100)	260845_at	6,996
AT1G17580	MYA1 (*ARABIDOPSIS* MYOSIN); motor/ protein binding	260711_at	1,361
AT1G18470	zinc finger (C3HC4-type RING finger) family protein	261677_at	1,372
AT1G18730	similar to Os02g0744000 [Oryza sativa (japonica cultivar-group)] (GB:NP_001048099.1)	261422_at	3,262

123

AGI Identifier	Affymetrix ID	Log2 Fch	Description
AT1G18880	259478_at	1,640	germin-like protein, putative
AT1G19700	261139_at	1,163	BEL10 (BEL1-LIKE HOMEODOMAIN 10); DNA binding / transcription factor
AT1G19970	261220_at	2,579	ER lumen protein retaining receptor family protein
AT1G20180	261243_at	7,349	similar to unknown protein [Arabidopsis thaliana] ; similar to Protein of unknown function DUF677 [Medicago truncatula]
AT1G21140	261448_at	2,906	nodulin, putative
AT1G21370	260899_at	1,236	similar to H0315A08.13 [Oryza sativa (indica cultivar-group)] (GB:CAH67583.1)
AT1G21440	260902_at	3,050	mutase family protein
AT1G21780	262495_at	1,477	BTB/POZ domain-containing protein
AT1G21790	262496_at	2,535	similar to Os01g0869600 [Oryza sativa (japonica cultivar-group)]
AT1G22570	261937_at	1,173	proton-dependent oligopeptide transport (POT) family protein
AT1G22990	264729_at	1,381	heavy-metal-associated domain-containing protein / copper chaperone (CCH)-related
AT1G23060	264902_at	2,554	similar to unknown protein [Arabidopsis thaliana] (TAIR:AT1G70950.1); similar to Targeting for Xklp2 [Medicago truncatula] (GB:ABE84619.1)
AT1G23330	263010_at	2,321	similar to unknown protein [Arabidopsis thaliana]
AT1G23560	265186_at	3,064	similar to unknown protein [Arabidopsis thaliana]
AT1G23610	265165_at	1,443	similar to unknown protein [Arabidopsis thaliana]
AT1G23630	265177_at	4,438	similar to unknown protein [Arabidopsis thaliana] (TAIR:AT1G23660.1)
AT1G24430	265014_at	8,147	transferase family protein
AT1G24440	265023_at	1,051	protein binding / zinc ion binding
AT1G26230	245876_at	1,956	chaperonin, putative
AT1G26390	261020_at	1,146	FAD-binding domain-containing protein
AT1G26560	261016_at	5,356	glycosyl hydrolase family 1 protein
AT1G26730	261261_at	2,505	EXS family protein / ERD1/XPR1/SYG1 family protein
AT1G26820	**263689_at**	**10,553**	**RNS3 (RIBONUCLEASE 3); endoribonuclease**
AT1G26920	263688_at	2,519	similar to unknown protein [Arabidopsis thaliana] (TAIR:AT1G69760.1); similar to hypothetical protein [Ricinus communis] (GB:CAH56540.1)
AT1G27980	259598_at	1,075	pyridoxal-dependent decarboxylase family protein
AT1G28260	245659_at	2,380	binding
AT1G28470*	261441_at	4,021	ANAC010 (Arabidopsis NAC domain containing protein 10); transcription factor
AT1G28660	262733_s_at	4,391	[AT1G28660, lipase, putative];[AT1G28670, ARAB-1 (Arabidopsis lipase); carboxylic ester hydrolase]
AT1G29160	260887_at	5,902	Dof-type zinc finger domain-containing protein

AGI Identifier	Description	Affymetrix ID	Log2 Fch
AT1G30900	vacuolar sorting receptor, putative	265161_at	2,041
AT1G31290	PAZ domain-containing protein / piwi domain-containing protein	262549_at	5,018
AT1G32080	membrane protein, putative	255719_at	1,239
AT1G32090	early-responsive to dehydration protein-related / ERD protein-related	245789_at	1,304
AT1G32200	ATS1 (ACYLTRANSFERASE 1)	245790_at	3,334
AT1G34340	esterase/lipase/thioesterase family protein	262561_at	2,588
AT1G34750	protein phosphatase 2C, putative / PP2C, putative	262408_at	1,712
AT1G35666		262670_s_at	3,757
AT1G36640	similar to unknown protein [*Arabidopsis* thaliana]	256499_at	1,654
AT1G45145	ATTRX5 (thioredoxin H-type 5); thiol-disulfide exchange intermediate	260943_at	1,415
AT1G45180	zinc finger (C3HC4-type RING finger) family protein	260939_at	1,133
AT1G46768	RAP2.1 (related to AP2 1); DNA binding / transcription factor	245807_at	2,355
AT1G48260	CIPK17 (CIPK17); kinase	262244_at	4,437
AT1G48560	similar to PWWP domain-containing protein [*Arabidopsis* thaliana]	261300_at	1,035
AT1G48750	[AT1G48750, protease inhibitor/seed storage/lipid transfer protein (LTP) family protein]	256145_at	1,132
AT1G49740	phospholipase C	261609_at	1,234
AT1G50420	SCL3 (SCARECROW-LIKE 3); transcription factor	261866_at	1,113
AT1G50630	extracellular ligand-gated ion channel	261863_at	1,396
AT1G51830	ATP binding / kinase/ protein serine/threonine kinase	246375_at	1,313
AT1G52540	protein kinase, putative	262158_at	1,000
AT1G52720	similar to unknown protein [*Arabidopsis* thaliana]	262159_at	1,582
AT1G52910	similar to unknown protein [*Arabidopsis* thaliana]	260151_at	1,147
AT1G53100	acetylglucosaminyltransferase	261366_at	5,614
AT1G53500	MUM4 (MUCILAGE-MODIFIED 4); catalytic	260985_at	1,053
AT1G53580	ETHE1/GLX2-3 (GLYOXALASE 2-3); hydroxyacylglutathione hydrolase	260986_at	1,041
AT1G53730	leucine-rich repeat transmembrane protein kinase, putative	259958_at	2,061
AT1G54130	RSH3 (RELA/SPOT HOMOLOG 3); catalytic	263159_at	1,083
AT1G54290	eukaryotic translation initiation factor SUI1, putative	262959_at	1,211
AT1G54410	dehydrin family protein	262958_at	2,170

125

AGI Identifier	Description	Affymetrix ID	Log2 Fch
AT1G54740	similar to unknown protein [*Arabidopsis* thaliana]	264238_at	1,212
AT1G55120	ATFRUCT5 (BETA-FRUCTOFURANOSIDASE 5); hydrolase, hydrolyzing O-glycosyl compounds / levanase	256150_at	1,148
AT1G55240	similar to unknown protein [*Arabidopsis* thaliana]	259653_at	3,302
AT1G55265	similar to unknown protein [*Arabidopsis* thaliana]	259661_at	2,137
AT1G55690	SEC14 cytosolic factor family protein / phosphoglyceride transfer family protein	264535_at	1,239
AT1G55740	ATSIP1 (*ARABIDOPSIS* THALIANA SEED IMBIBITION 1); hydrolase, hydrolyzing O-glycosyl compounds	264532_at	6,484
AT1G55760	BTB/POZ domain-containing protein	264562_at	2,810
AT1G55960	similar to unknown protein [*Arabidopsis* thaliana]	260603_at	1,366
AT1G60960	IRT3 (Iron regulated transporter 3); cation transporter/ metal ion transporter	259723_at	2,021
AT1G62040	ATG8C (AUTOPHAGY 8C); microtubule binding	264285_at	1,145
AT1G62620	[AT1G62620, flavin-containing monooxygenase family protein / FMO family protein]	265108_s_at	2,347
AT1G62660	beta-fructosidase (BFRUCT3) / beta-fructofuranosidase / invertase, vacuolar	265118_at	2,456
AT1G62750	ATSCO1/ATSCO1/CPEF-G (SNOWY COTYLEDON1); translation elongation factor/ translation factor, nucleic acid binding	262645_at	1,347
AT1G62760	invertase/pectin methylesterase inhibitor family protein	262640_at	5,534
AT1G63260	TET10 (TETRASPANIN10)	260109_at	5,108
AT1G63640	kinesin motor protein-related	261557_at	1,106
AT1G63690	protease-associated (PA) domain-containing protein	260271_at	1,404
AT1G64380	AP2 domain-containing transcription factor, putative	259793_at	3,425
AT1G64930	CYP89A7 (cytochrome P450, family 87, subfamily A, polypeptide 7); oxygen binding	262865_at	2,807
AT1G65500	similar to unknown protein [*Arabidopsis* thaliana]	264635_at	2,038
AT1G65510	similar to unknown protein [*Arabidopsis* thaliana]	264680_at	1,424
AT1G65670	CYP702A1 (CYTOCHROME P450, FAMILY 702, SUBFAMILY A, POLYPEPTIDE 1); oxygen binding	264634_at	1,250
AT1G66400	calmodulin-related protein, putative	260135_at	1,804
AT1G67000	kinase	255879_at	1,701
AT1G67410	exostosin family protein	265000_at	1,331
AT1G67420	peptidase	264225_at	1,716
AT1G67960	similar to hypothetical protein [Oryza sativa (japonica cultivar-group)]	259993_at	1,254
AT1G68110	epsin N-terminal homology (ENTH) domain-containing protein / clathrin assembly protein-related	260011_at	1,015
AT1G68450	VQ motif-containing protein	260261_at	1,202

AGI Identifier	Description	Affymetrix ID	Log2 Fch
AT1G68760	ATNUDT1 (*Arabidopsis* thaliana Nudix hydrolase homolog 1); dihydroneopterin triphosphate pyrophosphohydrolase/ hydrolase	260033_at	2,651
AT1G68765	IDA (INFLORESCENCE DEFICIENT IN ABSCISSION)	260040_at	1,781
AT1G69030	similar to BSD domain-containing protein [*Arabidopsis* thaliana]	259642_at	2,267
AT1G69050	unknown protein	259370_at	1,311
AT1G69490	NAP (NAC-LIKE, ACTIVATED BY AP3/PI); transcription factor	256300_at	1,198
AT1G69680	similar to mog1 protein [Xenopus laevis] (GB:CAC35704.1)	260397_at	1,198
AT1G70330	ENT1,AT (EQUILIBRATIVE NUCLEOTIDE TRANSPORTER 1); nucleoside transporter	264316_at	1,395
AT1G70370	BURP domain-containing protein / polygalacturonase, putative	264315_at	2,910
AT1G70670	[AT1G70670, caleosin-related family protein]	260208_s_at	8,411
AT1G70690	kinase-related	260179_at	1,747
AT1G71530	protein kinase family protein	259947_at	1,235
AT1G71940	similar to unknown protein [*Arabidopsis* thaliana]	260174_at	1,023
AT1G72700	haloacid dehalogenase-like hydrolase family protein	259910_at	1,129
AT1G72790	hydroxyproline-rich glycoprotein family protein	259915_at	5,559
AT1G72990	glycosyl hydrolase family 35 protein	262351_at	2,493
AT1G73000	similar to Bet v I allergen family protein [*Arabidopsis* thaliana] (TAIR:AT2G26040.1)	262356_at	7,860
AT1G73220	sugar transporter family protein	260097_at	2,376
AT1G73655	immunophilin / FKBP-type peptidyl-prolyl cis-trans isomerase family protein	260044_at	1,771
AT1G73680	pathogen-responsive alpha-dioxygenase, putative	260060_at	1,150
AT1G73750	similar to unknown protein [*Arabidopsis* thaliana]	260048_at	2,928
AT1G74000	SS3 (STRICTOSIDINE SYNTHASE 3)	260335_at	2,714
AT1G74010	strictosidine synthase family protein	260386_at	1,303
AT1G74210	glycerophosphoryl diester phosphodiesterase family protein	260254_at	2,442
AT1G74440	similar to unknown protein [*Arabidopsis* thaliana]	260211_at	1,103
AT1G75210	5' nucleotidase family protein	256504_at	1,128
AT1G75450	CKX5 (CYTOKININ OXIDASE 5); cytokinin dehydrogenase	261109_at	2,013
AT1G76040	CPK29 (calcium-dependent protein kinase 29); calcium- and calmodulin-dependent protein kinase/ kinase	262671_at	4,313
AT1G76240	similar to unknown protein [*Arabidopsis* thaliana]	261772_at	1,437
AT1G77000	ATSKP2;2 (*ARABIDOPSIS* HOMOLOG OF HOMOLOG OF HUMAN SKP2 2); ubiquitin-protein ligase	264957_at	2,093

127

AGI Identifier	Description	Affymetrix ID	Log2 Fch
AT1G77150	[AT1G77150, similar to pentatricopeptide (PPR) repeat-containing protein [Arabidopsis thaliana] (TAIR:AT1G77170.1	264475_s_at	2,196
AT1G77890	similar to unknown protein [Arabidopsis thaliana]	262183_at	1,859
AT1G78050	phosphoglycerate/bisphosphoglycerate mutase family protein	262180_at	3,518
AT1G78290	serine/threonine protein kinase, putative	260774_at	1,169
AT1G78320	ATGSTU23 (Arabidopsis thaliana Glutathione S-transferase (class tau) 23); glutathione transferase	260805_at	1,116
AT1G78340	ATGSTU22 (Arabidopsis thaliana Glutathione S-transferase (class tau) 22); glutathione transferase	260803_at	2,643
AT1G78850	[AT1G78850, curculin-like (mannose-binding) lectin family protein];[AT1G78860, curculin-like (mannose-binding) lectin family protein]	264299_s_at	2,165
AT1G79320	latex abundant protein, putative (AMC5) / caspase family protein	264144_at	5,672
AT1G79330	AMC6/ATMCP2B (TYPE-II METACASPASES); caspase/ cysteine-type endopeptidase	264143_at	2,474
AT1G79380	copine-related	262919_at	1,214
AT1G79520	cation efflux family protein	262940_at	2,787
AT1G79900	ATMBAC2/BAC2 (Arabidopsis mitochondrial basic amino acid carrier 2); L-ornithine transporter/ binding / carnitine:acyl carnitine antiporter	260163_at	1,204
AT1G79910	similar to unknown protein [Arabidopsis thaliana]	260158_at	1,348
AT1G80450	VQ motif-containing protein	260276_at	1,642
AT1G80900	magnesium transporter CorA-like family protein (MGT1) (MRS2)	261894_at	3,046
AT1G80940	similar to predicted protein [Populus alba x Populus tremula] (GB:AAR14272.1); contains domain MAPKK-RELATED SERINE/THREONINE PROTEIN KINASES (PTHR22986)	261900_at	1,979
AT2G01460	MAPKK-RELATED SERINE/THREONINE PROTEIN KINASES (PTHR22986)	266349_at	2,524
AT2G01880	ATPAP7/PAP7 (purple acid phosphatase 7; acid phosphatase/ protein serine/threonine phosphatase	263594_at	1,351
AT2G01890	PAP8 (PURPLE ACID PHOSPHATASE PRECURSOR); acid phosphatase/ protein serine/threonine phosphatase	263595_at	1,527
AT2G02300	ATPP2-B5 (Phloem protein 2-B5)	266179_at	3,171
AT2G02310	ATPP2-B6 (Phloem protein 2-B6)	266232_at	2,793
AT2G03360	similar to serine carboxypeptidase [Arabidopsis thaliana]	265711_at	1,282
AT2G03760	ST (steroid sulfotransferase); sulfotransferase	264042_at	1,801
AT2G03850	late embryogenesis abundant domain-containing protein / LEA domain-containing protein	263363_at	1,673
AT2G05910	similar to unknown protein [Arabidopsis thaliana]	266021_at	2,801
AT2G14095	similar to Peptidase A11B, Ty1 A and B [Medicago truncatula] (GB:ABE93074.1)	263282_at	8,565
AT2G14110	similar to HAD-superfamily phosphatase subfamily IIIC; TonB box, N-terminal [Medicago truncatula]	263277_at	1,117
AT2G14560	similar to unknown protein [Arabidopsis thaliana]	265837_at	3,216
AT2G14620	xyloglucan:xyloglucosyl transferase, putative / xyloglucan endotransglycosylase, putative / endo-xyloglucan transferase, putative	266376_at	3,067

AGI Identifier	Description	Affymetrix ID	Log2 Fch
AT2G15120	[AT2G15220, secretory protein, putative]	265920_s_at	2,358
AT2G15230	ATLIP1 (*ARABIDOPSIS* THALIANA LIPASE 1); galactolipase/ hydrolase/ phospholipase/ triacylglycerol lipase	263359_at	3,162
AT2G15320	leucine-rich repeat family protein	263330_at	1,098
AT2G15830	similar to unknown protein [*Arabidopsis* thaliana] (TAIR:AT4G33960.1)	265539_at	4,469
AT2G16530	[AT2G16530, 3-oxo-5-alpha-steroid 4-dehydrogenase family protein / steroid 5-alpha-reductase family protein]	263240_s_at	2,110
AT2G16660	nodulin family protein	265414_at	2,802
AT2G16990	tetracycline transporter	263574_at	4,143
AT2G17265	HSK (HOMOSERINE KINASE); homoserine kinase	264855_at	1,332
AT2G17710	similar to Os04g0560700 [Oryza sativa (japonica cultivar-group)] (GB:NP_0010535 49.1)	264590_at	3,024
AT2G18490	zinc finger (C2H2 type) family protein	265921_at	2,059
AT2G19560	proteasome protein-related	265934_at	1,012
AT2G19570	CDA1 (CYTIDINE DEAMINASE 1)	265943_at	2,351
AT2G20030	zinc finger (C3HC4-type RING finger) family protein	265582_at	4,005
AT2G20290	XIG (Myosin-like protein XIG); motor/ protein binding	265309_at	3,526
AT2G21380	kinesin motor protein-related	263762_at	1,020
AT2G22560	kinase interacting protein-related	264053_at	1,626
AT2G22830	squalene monooxygenase, putative / squalene epoxidase, putative	266831_at	1,401
AT2G23110	similar to unknown protein [*Arabidopsis* thaliana]	267263_at	2,363
AT2G23380	CLF (CURLY LEAF); transcription factor	267129_at	1,390
AT2G23800	GGPS2 (GERANYLGERANYL PYROPHOSPHATE SYNTHASE 2); farnesyltranstransferase	267295_at	5,521
AT2G23960	defense-related protein, putative	266561_at	1,572
AT2G24040	hydrophobic protein, putative / low temperature and salt responsive protein, putative	266566_at	1,727
AT2G24762	similar to GDU1 (GLUTAMINE DUMPER 1) [*Arabidopsis* thaliana] (TAIR:AT4G31730.1)	263318_at	4,818
AT2G25460	similar to unknown protein [*Arabidopsis* thaliana]	265618_at	1,031
AT2G25680	sulfate transporter	265897_at	1,103
AT2G25940	ALPHA-VPE (ALPHA-VACUOLAR PROCESSING ENZYME); cysteine-type endopeptidase	266849_at	6,853
AT2G26340	similar to expressed protein [Oryza sativa (japonica cultivar-group)] (GB:ABF94264.1)	267379_at	1,189
AT2G26670	HY1 (HEME OXYGENASE 1)	267617_at	2,289
AT2G27080	harpin-induced protein-related / HIN1-related / harpin-responsive protein-related	266316_at	1,045

AGI Identifier	Description	Affymetrix ID	Log2 Fch
AT2G27920	SCPL51; serine carboxypeptidase	264071_at	1,797
AT2G28200*	nucleic acid binding / transcription factor/ zinc ion binding	265573_at	1,716
AT2G28470	BGAL8 (beta-galactosidase 8); beta-galactosidase	264078_at	2,770
AT2G29410	MTPB1; efflux permease/ zinc ion transporter	266273_at	2,952
AT2G29980	FAD3 (FATTY ACID DESATURASE 3); omega-3 fatty acid desaturase	266865_at	6,357
AT2G29995	unknown protein	266808_at	1,332
AT2G30460	similar to transporter-related [Arabidopsis thaliana]	267520_at	1,013
AT2G30580	zinc finger (C3HC4-type RING finger) family protein	267467_at	2,644
AT2G31130	similar to hypothetical protein MtrDRAFT_AC135231g7v1 [Medicago truncatula] (GB:ABE82891.1)	266480_at	1,417
AT2G31300	[AT2G31300, ARPC1b (actin-related protein C1b); nucleotide binding]	267194_s_at	1,060
AT2G31730	ethylene-responsive protein, putative	263467_at	1,018
AT2G31945	similar to unknown protein [Arabidopsis thaliana]	263475_at	1,469
AT2G31980	cysteine proteinase inhibitor-related	265672_at	1,607
AT2G31990	exostosin family protein	265728_at	2,349
AT2G32510	MAPKKK17 (Mitogen-activated protein kinase kinase kinase 17); kinase	267058_at	4,996
AT2G32540	[AT2G32540, ATCSLB04 (Cellulose synthase-like B4); transferase/ transferase, transferring glycosyl groups	267115_s_at	3,691
AT2G32610	ATCSLB01 (Cellulose synthase-like B1); transferase/ transferase, transferring glycosyl groups	267119_at	5,399
AT2G32660	disease resistance family protein / LRR family protein	267548_at	2,026
AT2G32670	ATVAMP725 (Arabidopsis thaliana vesicle-associated membrane protein 725)	267547_at	1,480
AT2G32930	ZFN2 (ZINC FINGER PROTEIN 2); nucleic acid binding	267604_at	1,116
AT2G33360	similar to unknown protein [Arabidopsis thaliana]	255832_at	2,042
AT2G33480*	ANAC041 (Arabidopsis thaliana NAC domain containing protein 41); transcription factor	255794_at	4,447
AT2G33830	dormancy/auxin associated family protein	267461_at	2,317
AT2G34340	similar to unknown protein [Arabidopsis thaliana]	267003_at	2,203
AT2G34790	EDA28/MEE23 (embryo sac development arrest 28, maternal effect embryo arrest 23); electron carrier	267414_at	5,194
AT2G35020	UTP--glucose-1-phosphate uridylyltransferase family protein	267432_at	1,214
AT2G35700	AP2 domain-containing transcription factor, putative	265842_at	1,812
AT2G36590	ProT3 (PROLINE TRANSPORTER 3); amino acid permease	263918_at	1,345
AT2G36650	similar to CHUP1 (CHLOROPLAST UNUSUAL POSITIONING 1) [Arabidopsis thaliana]	265204_at	1,324

AGI Identifier	Description	Affymetrix ID	Log2 Fch
AT2G37585	glycosyltransferase family 14 protein / core-2/I-branching enzyme family protein	267170_at	1,477
AT2G38400	AGT3 (ALANINE:GLYOXYLATE AMINOTRANSFERASE 3); alanine-glyoxylate transaminase	267035_at	1,841
AT2G38465	unknown protein	267036_at	1,624
AT2G38480	integral membrane protein, putative	267038_at	2,826
AT2G38490	CIPK22 (CBL-INTERACTING PROTEIN KINASE 22); kinase	267032_at	1,018
AT2G38580	similar to unknown protein [Arabidopsis thaliana]	266405_at	1,528
AT2G38700	MVD1 (mevalonate diphosphate decarboxylase 1)	266414_at	1,300
AT2G38710	AMMECR1 family	266416_at	1,388
AT2G38760	ANNAT3 (ANNEXIN 3, ANNEXIN ARABIDOPSIS 3); calcium ion binding / calcium-dependent phospholipid binding	266419_at	3,764
AT2G39080	similar to unnamed protein product [Ostreococcus tauri] (GB:CAL54696.1); similar to Os01g0367100	266192_at	1,311
AT2G39080	similar to unnamed protein product [Ostreococcus tauri] (GB:CAL54696.1);	266193_at	1,400
AT2G39710	aspartyl protease family protein	267592_at	1,173
AT2G39890	ProT1 (PROLINE TRANSPORTER 1); amino acid permease	267358_at	3,763
AT2G40110	yippee family protein	265720_at	3,006
AT2G40230	transferase family protein	263382_at	3,993
AT2G40670*	ARR16 (response regulator 16); transcription regulator/ two-component response regulator	266078_at	4,867
AT2G41140	CRK1 (CDPK-RELATED KINASE 1); calcium ion binding / calcium-dependent protein serine/threonine phosphatase/ kinase	267082_at	2,199
AT2G41540	GPDHC1; NAD binding / glycerol-3-phosphate dehydrogenase (NAD+)	245112_at	1,719
AT2G41850	endo-polygalacturonase, putative	260492_at	5,298
AT2G42890	AML2; RNA binding	265266_at	1,980
AT2G42900	similar to Os05g0582000 [Oryza sativa (japonica cultivar-group)] (GB:NP_001056435.1)	265265_at	5,146
AT2G43230	serine/threonine protein kinase, putative	266453_at	2,770
AT2G43580	chitinase, putative	260561_at	1,038
AT2G44010	similar to unknown protein [Arabidopsis thaliana] similar to conserved hypothetical protein [Medicago truncatula]	267226_at	1,358
AT2G44255	[AT2G44260, similar to unknown protein [Arabidopsis thaliana]	267343_at	7,525
AT2G44370	DC1 domain-containing protein	267384_at	1,607
AT2G45580	CYP76C3 (cytochrome P450, family 76, subfamily C, polypeptide 3); oxygen binding	267560_at	1,827
AT2G45630	oxidoreductase family protein	267514_at	1,156
AT2G45950	[AT2G45950, ASK20 (ARABIDOPSIS SKP1-LIKE 20); ubiquitin-protein ligase];[AT3G61415, ASK21 (ARABIDOPSIS SKP1-LIKE 21); ubiquitin-protein ligase]	266922_s_at	1,784

AGI Identifier	Description	Affymetrix ID	Log2 Fch
AT2G46030	UBC6 (UBIQUITIN-CONJUGATING ENZYME 6); ubiquitin-protein ligase	266604_at	1,712
AT2G46225	ABI1L1 (ABI-1-LIKE 1)	266591_at	4,559
AT2G46710	rac GTPase activating protein, putative	266324_at	1,765
AT2G46950	CYP709B2 (cytochrome P450, family 709, subfamily B, polypeptide 2); oxygen binding	266756_at	5,065
AT2G47200	unknown protein	260582_at	4,188
AT2G47910	CRR6 (CHLORORESPIRATORY REDUCTION 6)	266483_at	1,042
AT2G47950	similar to unknown protein [Arabidopsis thaliana] (TAIR:AT3G62990.1)	266486_at	1,803
AT2G48040	similar to Os01g0388500 [Oryza sativa (japonica cultivar-group)] (GB:NP_001043105.1)	265763_at	1,209
AT3G01080	WRKY58 (WRKY DNA-binding protein 58); transcription factor	259320_at	2,372
AT3G01470	ATHB-1 (Homeobox-leucine zipper protein HAT5); transcription factor	259165_at	1,036
AT3G02140	TMAC2 (TWO OR MORE ABRES-CONTAINING GENE 2)	259076_at	1,281
AT3G02290	zinc finger (C3HC4-type RING finger) family protein	259073_at	1,408
AT3G02480	ABA-responsive protein-related	258498_at	1,134
AT3G03530	[AT3G03530, NPC4 (NONSPECIFIC PHOSPHOLIPASE C4); hydrolase, acting on ester bonds]	259221_s_at	5,720
AT3G03610	phagocytosis and cell motility protein ELMO1-related	259198_at	1,089
AT3G03720	CAT4 (CATIONIC AMINO ACID TRANSPORTER 4); cationic amino acid transporter	259337_at	1,282
AT3G03910	glutamate dehydrogenase, putative	259346_at	2,798
AT3G05180	GDSL-motif lipase/hydrolase family protein	259308_at	4,258
AT3G05510	phospholipid/glycerol acyltransferase family protein	259113_at	1,215
AT3G05640	protein phosphatase 2C, putative / PP2C, putative	258901_at	2,472
AT3G06210	binding	257580_at	6,042
AT3G06580	GAL1 (GALACTOSE KINASE 1); ATP binding / galactokinase	258517_at	1,279
AT3G06850	DIN3/LTA1 (DARK INDUCIBLE 3); alpha-ketoacid dehydrogenase	258527_at	1,145
AT3G07320	glycosyl hydrolase family 17 protein	259014_at	4,453
AT3G07510	similar to unknown protein [Arabidopsis thaliana]	259023_at	2,246
AT3G07690	glycerol-3-phosphate dehydrogenase (NAD+)	259255_at	1,400
AT3G08860	alanine--glyoxylate aminotransferase, putative / beta-alanine-pyruvate aminotransferase, putative / AGT, putative	258983_at	2,225
AT3G08910	DNAJ heat shock protein, putative	258986_at	1,228
AT3G10590*	myb family transcription factor	258960_at	6,094

132

AGI Identifier	Description	Affymetrix ID	Log2 Fch
AT3G10740	ASD1 (ALPHA-L-ARABINOFURANOSIDASE); hydrolase, acting on glycosyl bonds	258774_at	4,399
AT3G10780	emp24/gp25L/p24 family protein	258760_at	1,189
AT3G10940	protein phosphatase-related	256441_at	1,955
AT3G12120	FAD2 (FATTY ACID DESATURASE 2); delta12-fatty acid dehydrogenase	256277_at	1,128
AT3G12700	aspartyl protease family protein	257697_at	1,323
AT3G12830	auxin-responsive family protein	257690_at	1,710
AT3G12920	protein binding / zinc ion binding	257858_at	2,196
AT3G13420	similar to unknown protein [*Arabidopsis thaliana*]	256957_at	1,754
AT3G13672	**seven in absentia (SINA) family protein**	**256789_at**	**4,002**
AT3G13700	[AT3G13700, RNA-binding protein, putative];[AT3G13710, prenylated rab acceptor (PRA1) family protein]	256771_at	1,163
AT3G14360	lipase class 3 family protein	258374_at	4,362
AT3G14770	nodulin MtN3 family protein	256548_at	1,601
AT3G14790	RHM3 (RHAMNOSE BIOSYNTHESIS 3); catalytic	256575_at	1,035
AT3G15350	glycosyltransferase family 14 protein / core-2/I-branching enzyme family protein	257056_at	1,954
AT3G15830	[AT3G15830, phosphatidic acid phosphatase-related / PAP2-related];[AT3G15820, phosphatidic acid phosphatase-related / PAP2-related]	258249_s_at	2,344
AT3G15850	FAD5 (FATTY ACID DESATURASE 5); oxidoreductase	258250_at	1,180
AT3G15900	similar to Os02g0804400 [Oryza sativa (japonica cultivar-group)] (GB:NP_001048433.1)	257800_at	1,574
AT3G16440	ATMLP-300B (MYROSINASE-BINDING PROTEIN-LIKE PROTEIN-300B)	259328_at	5,012
AT3G16500	PAP1 (PHYTOCHROME-ASSOCIATED PROTEIN 1); transcription factor	257232_at	1,438
AT3G16857	ARR1 (*ARABIDOPSIS* RESPONSE REGULATOR 1); transcription factor/ two-component response regulator	256790_at	1,315
AT3G16990	TENA/THI-4 family protein	257888_at	1,646
AT3G17520	late embryogenesis abundant domain-containing protein / LEA domain-containing protein	258347_at	1,523
AT3G18295	similar to unknown protein [*Arabidopsis thaliana*]	257728_at	1,061
AT3G19390	cysteine proteinase, putative / thiol protease, putative	258005_at	1,347
AT3G19580	AZF2 (*ARABIDOPSIS* ZINC-FINGER PROTEIN 2); nucleic acid binding / transcription factor/ zinc ion binding	257022_at	1,499
AT3G19720	ARC5 (ACCUMULATION AND REPLICATION OF CHLOROPLAST 5); GTP binding / GTPase	257044_at	2,075
AT3G19900	similar to hypothetical protein [Oryza sativa (japonica cultivar-group)] (GB:BAD22944.1)	257965_at	1,356
AT3G21550	similar to unknown protein [*Arabidopsis thaliana*]	258183_at	8,137
AT3G21830	ASK8 (*ARABIDOPSIS* SKP1-LIKE 8); ubiquitin-protein ligase	257942_at	7,987

AGI Identifier	Description	Affymetrix ID	Log2 Fch
AT3G21840	ASK7 (*ARABIDOPSIS* SKP1-LIKE 7); ubiquitin-protein ligase	257943_at	7,877
AT3G21850	ASK9 (*ARABIDOPSIS* SKP1-LIKE 9); ubiquitin-protein ligase	257944_at	9,888
AT3G21860	ASK10 (*ARABIDOPSIS* SKP1-LIKE 10); ubiquitin-protein ligase	257945_at	2,641
AT3G21890	zinc finger (B-box type) family protein	257262_at	1,906
AT3G22120	CWLP (CELL WALL-PLASMA MEMBRANE LINKER PROTEIN); lipid binding	256825_at	5,806
AT3G23030	IAA2 (indoleacetic acid-induced protein 2); transcription factor	257766_at	2,111
AT3G23050	IAA7 (AUXIN RESISTANT 2); transcription factor	257769_at	3,056
AT3G23430	PHO1 (PHOSPHATE 1)	258293_at	2,277
AT3G23605	UBX domain-containing protein	258105_at	1,631
AT3G24460	TMS membrane family protein / tumour differentially expressed (TDE) family protein	256619_at	2,086
AT3G25290	auxin-responsive family protein	257824_at	1,388
AT3G25870	similar to unknown protein [*Arabidopsis thaliana*]	258078_at	3,384
AT3G25950	similar to DNA-binding storekeeper protein-related [*Arabidopsis thaliana*]	257541_at	3,269
AT3G26100	regulator of chromosome condensation (RCC1) family protein	258085_at	1,742
AT3G26580	binding	257611_at	1,112
AT3G27210	similar to unknown protein [*Arabidopsis thaliana*]	257154_at	1,182
AT3G27580	ATPK7 (*Arabidopsis thaliana* serine/threonine-protein kinase 7); kinase	258029_at	1,413
AT3G28690	protein kinase, putative	257016_at	2,151
AT3G29250	oxidoreductase	257774_at	1,453
AT3G42950	glycoside hydrolase family 28 protein / polygalacturonase (pectinase) family protein	252781_at	1,735
AT3G43210	TES (TETRASPORE); microtubule motor	252736_at	1,266
AT3G45010	SCPL48 (serine carboxypeptidase-like 48); serine carboxypeptidase	252606_at	4,292
AT3G45090	2-phosphoglycerate kinase-related	252608_at	1,567
AT3G46900	COPT2 (Copper transporter 2); copper ion transporter	252502_at	1,552
AT3G48580	xyloglucan:xyloglucosyl transferase, putative / xyloglucan endotransglycosylase, putative / endo-xyloglucan transferase, putative	252320_at	2,594
AT3G49130	RNA binding	252289_at	1,126
AT3G49360	glucosamine/galactosamine-6-phosphate isomerase family protein	252282_at	1,303
AT3G49590	similar to unknown protein [*Arabidopsis thaliana*]	252264_at	1,784
AT3G49940	LOB domain protein 38 / lateral organ boundaries domain protein 38 (LBD38)	252220_at	4,547

AGI Identifier	Description	Affymetrix ID	Log2 Fch
AT3G51090	similar to unknown protein [*Arabidopsis* thaliana]	252097_at	1,839
AT3G51250	senescence/dehydration-associated protein-related	252099_at	1,378
AT3G51330	aspartyl protease family protein	252098_at	1,104
AT3G51960	bZIP family transcription factor	252083_at	1,354
AT3G51970	long-chain-alcohol O-fatty-acyltransferase family protein / wax synthase family protein	252084_at	2,529
AT3G52770	similar to Os02g0530500 [Oryza sativa (japonica cultivar-group)] (GB:NP_001047020.1)	252003_at	1,655
AT3G52780	ATPAP20/PAP20; acid phosphatase/ protein serine/threonine phosphatase	252004_at	6,503
AT3G52820	ATPAP22/PAP22 (purple acid phosphatase 22); acid phosphatase/ protein serine/threonine phosphatase	252006_at	6,481
AT3G52920	similar to unknown protein [*Arabidopsis* thaliana]	252023_at	2,509
AT3G53030	SRPK4 (SER/ARG-RICH PROTEIN KINASE 4); kinase/ protein kinase	252026_at	1,651
AT3G53620	inorganic pyrophosphatase, putative (soluble) / pyrophosphate phospho-hydrolase, putative / PPase, putative	251961_at	1,354
AT3G53990	universal stress protein (USP) family protein	251927_at	1,215
AT3G54690	sugar isomerase (SIS) domain-containing protein / CBS domain-containing protein	251855_at	2,274
AT3G54700	[AT3G54700, phosphate transporter, putative];[AT2G38940, ATPT2 (PHOSPHATE TRANSPORTER 2); carbohydrate transporter/ phosphate transporter/ sugar porter]	266184_s_at	2,035
AT3G56170	transporter/ phosphate transporter/ sugar porter]	251739_at	1,135
AT3G56760	calcium-dependent protein kinase, putative / CDPK, putative	246345_at	2,232
AT3G57810	OTU-like cysteine protease family protein	251558_at	1,475
AT3G58450	universal stress protein (USP) family protein	251580_at	2,745
AT3G59290	(EPSIN3); binding	251468_at	1,062
AT3G59695	[AT3G59690, IQD13 (IQ-domain 13); calmodulin binding]	251478_at	1,089
AT3G59900	(ARGOS); unknown protein	251436_at	2,680
AT3G60510	enoyl-CoA hydratase/isomerase family protein	251421_at	1,017
AT3G61160	shaggy-related protein kinase beta / ASK-beta (ASK2)	251358_at	1,752
AT3G61310	DNA-binding family protein	251365_at	1,000
AT3G61460	BRH1 (BRASSINOSTEROID-RESPONSIVE RING-H2); protein binding / zinc ion binding	251321_at	1,218
AT3G61590	F-box family protein	251326_at	1,686
AT3G61930	unknown protein	251293_at	2,724
AT3G61960	protein kinase family protein	251273_at	1,996
AT3G62650	binding	251189_at	1,699

AGI Identifier	Description	Affymetrix ID	Log2 Fch
AT3G62660	GATL7 (Galacturonosyltransferase-like 7); transferase, transferring glycosyl groups / transferase, transferring hexosyl groups	251225_at	1,219
AT3G62730	similar to unknown protein [*Arabidopsis thaliana*]	251188_at	2,540
AT3G63000	NPL4 family protein	251153_at	1,339
AT4G00150	scarecrow-like transcription factor 6 (SCL6)	255698_at	5,021
AT4G00700	C2 domain-containing protein	255630_at	1,196
AT4G00760	APRR8 (PSEUDO-RESPONSE REGULATOR 8); transcription regulator	255639_at	1,542
AT4G01120	GBF2 (G-BOX BINDING FACTOR 2); DNA binding / transcription factor	255625_at	1,112
AT4G01130	acetylesterase, putative	255607_at	4,130
AT4G01180	[AT4G01180, XH/XS domain-containing protein];[AT5G59390, XH/XS domain-containing protein]	255609_s_at	3,075
AT4G01430	nodulin MtN21 family protein	255575_at	2,918
AT4G01770	[AT4G01770, RGXT1 (RHAMNOGALACTURONAN XYLOSYLTRANSFERASE 1); UDP-xylosyltransferase]	255564_s_at	1,002
AT4G01920	DC1 domain-containing protein	255547_at	1,003
AT4G03510	RMA1 (Ring finger protein with Membrane Anchor 1); protein binding / ubiquitin-protein ligase/ zinc ion binding	255381_at	1,542
AT4G04460	aspartyl protease family protein	255345_at	10,076
AT4G04490	protein kinase family protein	255340_at	1,509
AT4G09100	zinc finger (C3HC4-type RING finger) family protein	255074_at	1,071
AT4G10850	nodulin MtN3 family protein	254956_at	5,210
AT4G10955	[AT4G10955, lipase class 3 family protein];[AT4G10960, UGE5 (UDP-D-glucose/UDP-D-galactose 4-epimerase 5)	254952_at	1,970
AT4G11100	similar to unknown protein [*Arabidopsis thaliana*]	254911_at	1,607
AT4G11980	ATNUDT14 (*Arabidopsis* thaliana Nudix hydrolase homolog 14); hydrolase	254863_at	1,424
AT4G12080	DNA-binding family protein	254853_at	1,013
AT4G12430	trehalose-6-phosphate phosphatase, putative	254806_at	2,197
AT4G12910	SCPL20 (serine carboxypeptidase-like 20); serine carboxypeptidase	254791_at	3,469
AT4G13250	short-chain dehydrogenase/reductase (SDR) family protein	254764_at	1,576
AT4G14340	CKI1 (CASEIN KINASE I); casein kinase I/ kinase	245294_at	2,298
AT4G14950	similar to unknown protein [*Arabidopsis thaliana*]	245273_at	1,634
AT4G15350	CYP705A2 (cytochrome P450, family 705, subfamily A, polypeptide 2); oxygen binding	245551_at	3,055
AT4G15920	nodulin MtN3 family protein	245524_at	1,263
AT4G16620	integral membrane family protein / nodulin MtN21-related	245436_at	4,052

AGI Identifier	Description	Affymetrix ID	Log2 Fch
AT4G16750	DRE-binding transcription factor, putative	245445_at	2,484
AT4G17483	palmitoyl protein thioesterase family protein	245423_at	2,582
AT4G17670	senescence-associated protein-related	245401_at	1,460
AT4G17790	similar to unknown protein [*Arabidopsis* thaliana]	245361_at	1,201
AT4G18080	similar to unknown protein [*Arabidopsis* thaliana]	254712_at	1,993
AT4G18220	[AT4G18220, purine permease family protein] (*Arabidopsis* thaliana purine permease 10); purine transporter]	254657_s_at	1,417
AT4G18340	glycosyl hydrolase family 17 protein	254665_at	1,669
AT4G18350	NCED2 (NINE-CIS-EPOXYCAROTENOID DIOXYGENASE 2)	254668_at	2,776
AT4G18425	similar to unknown protein [*Arabidopsis* thaliana]	254629_at	10,013
AT4G18430	AtRABA1e (*Arabidopsis* Rab GTPase homolog A1e); GTP binding	254673_at	2,403
AT4G18550	lipase class 3 family protein	254648_at	2,585
AT4G18910	NIP1;2/NLM2 (NOD26-like intrinsic protein 1;2); water channel	254608_at	1,306
AT4G18980	similar to unknown protein [*Arabidopsis* thaliana]	254597_at	1,984
AT4G19120	ERD3 (EARLY-RESPONSIVE TO DEHYDRATION 3)	254563_at	1,603
AT4G19420	pectinacetylesterase family protein	254573_at	3,220
AT4G19810	glycosyl hydrolase family 18 protein	254543_at	2,712
AT4G20140	leucine-rich repeat transmembrane protein kinase, putative	254506_at	1,147
AT4G20880	ethylene-responsive nuclear protein / ethylene-regulated nuclear protein (ERT2)	254434_at	1,629
AT4G22640	similar to unknown protein [Arabidopsis thaliana] (TAIR:AT4G22666.1); contains domain Bifunctional inhibitor/lipid-transfer protein/seed storage 2S albumin (SSF47699)	254324_at	3,524
AT4G22753	SMO1-3 (STEROL 4-ALPHA METHYL OXIDASE); catalytic	254333_at	3,880
AT4G22780	ACR7 (ACT Domain Repeat 7)	254300_at	1,411
AT4G22850	similar to unknown protein [*Arabidopsis* thaliana]	254272_at	1,393
AT4G22920	similar to unknown protein [Arabidopsis thaliana] (TAIR:AT4G11910.1); similar to senescence-inducible chloroplast stay-green protein 1 [Lycopersicon esculentum] (GB:AAY98500.1)	254299_at	1,638
AT4G23920	UGE2 (UDP-D-glucose/UDP-D-galactose 4-epimerase 2); UDP-glucose 4-epimerase/ protein dimerization	254188_at	1,191
AT4G25000	AMY1 (ALPHA-AMYLASE-LIKE); alpha-amylase	254101_at	1,105
AT4G25835	AAA-type ATPase family protein	254027_at	1,199
AT4G26470	calcium ion binding	253963_at	1,548
AT4G26490	[AT4G26490, similar to unknown protein [*Arabidopsis* thaliana]	253965_at	3,412

137

AGI Identifier	Description	Affymetrix ID	Log2 Fch
AT4G26700	ATFIM1 (*Arabidopsis* thaliana fimbrin 1); actin binding	253956_at	1,203
AT4G27480	glycosyltransferase family 14 protein / core-2/I-branching enzyme family protein	253866_at	1,047
AT4G27780	ACBP2 (ACYL-COA BINDING PROTEIN ACBP 2)	253840_at	1,181
AT4G28150	similar to unknown protein [*Arabidopsis* thaliana]	253813_at	1,543
AT4G28270	zinc finger (C3HC4-type RING finger) family protein	253806_at	4,506
AT4G28550	RabGAP/TBC domain-containing protein	253768_at	1,205
AT4G29100	ethylene-responsive family protein	253746_at	1,740
AT4G29230	ANAC075 (*Arabidopsis* NAC domain containing protein 75); transcription factor	253710_at	1,338
AT4G30270	MERI5B (MERISTEM-5); hydrolase, acting on glycosyl bonds	253666_at	1,258
AT4G30440	GAE1 (UDP-D-GLUCURONATE 4-EPIMERASE 1); UDP-glucuronate 4-epimerase/ catalytic	253631_at	1,043
AT4G30470	cinnamoyl-CoA reductase-related	253638_at	2,312
AT4G30550	glutamine amidotransferase class-I domain-containing protein	253639_at	2,213
AT4G30670	unknown protein	253582_at	2,093
AT4G30790	similar to protein transport protein-related [*Arabidopsis* thaliana] similar to Ubiquitin [Medicago truncatula]	253588_at	1,153
AT4G30810	SCPL29 (serine carboxypeptidase-like 29); serine carboxypeptidase	253600_at	1,496
AT4G30920	[AT4G30920, cytosol aminopeptidase family protein];[AT4G30910, cytosol aminopeptidase family protein]	253602_s_at	1,210
AT4G30993	similar to unknown protein [Oryza sativa (japonica cultivar-group)] (GB:BAD72545.1); contains domain no description (G3D.3.60.21.10)	253548_at	1,454
AT4G32250	protein kinase family protein	253473_at	1,260
AT4G32440	agenet domain-containing protein	253431_at	1,015
AT4G32450	pentatricopeptide (PPR) repeat-containing protein	253432_at	2,351
AT4G32840	phosphofructokinase family protein	253404_at	1,065
AT4G32870	similar to unknown protein [*Arabidopsis* thaliana]	253401_at	1,019
AT4G33090	APM1 (Aberrant peroxisome morphology 1)	253360_at	1,528
AT4G34215	hydrolase	253275_at	1,329
AT4G34320	similar to unknown protein [*Arabidopsis* thaliana]	253289_at	6,761
AT4G34630	similar to unknown protein [*Arabidopsis* thaliana]	253228_at	1,421
AT4G34950	nodulin family protein	253215_at	3,487
AT4G36710	scarecrow transcription factor family protein	246230_at	1,628
AT4G36920	AP2 (APETALA 2); transcription factor	246217_at	1,666

AGI Identifier	Description	Affymetrix ID	Log2 Fch
AT4G37050	PLA V/PLP4 (Patatin-like protein 4); nutrient reservoir	246241_at	2,918
AT4G37330	CYP81D4 (cytochrome P450, family 81, subfamily D, polypeptide 4); oxygen binding	253096_at	1,927
AT4G37430	[AT4G37430, CYP91A2 (CYTOCHROME P450 MONOOXYGENASE 91A2); oxygen binding]	253101_at	2,681
AT4G38060	similar to unknown protein [Arabidopsis thaliana]	253022_at	1,588
AT4G38930	ubiquitin fusion degradation UFD1 family protein	252931_at	1,357
AT4G39000	glycosyl hydrolase family 9 protein	252920_at	4,166
AT4G39090	RD19 (RESPONSIVE TO DEHYDRATION 19); cysteine-type peptidase	252927_at	1,014
AT4G39710	immunophilin, putative / FKBP-type peptidyl-prolyl cis-trans isomerase, putative	252853_at	1,187
AT5G01030	similar to unknown protein [Arabidopsis thaliana], contains domain Transcriptional factor tubby, C-terminal domain (SSF54518)	251123_at	1,727
AT5G01220	SQD2 (SULFOQUINOVOSYLDIACYLGLYCEROL 2); UDP-sulfoquinovose:DAG sulfoquinovosyltransferase/ transferase, transferring glycosyl groups	251143_at	1,704
AT5G01520	zinc finger (C3HC4-type RING finger) family protein	251084_at	2,608
AT5G01820	ATSR1 (SERINE/THREONINE PROTEIN KINASE 1); kinase	251060_at	1,496
AT5G02420	similar to unknown protein [Arabidopsis thaliana]	251019_at	2,608
AT5G02570	histone H2B, putative	250997_at	1,041
AT5G02580	similar to unknown protein [Arabidopsis thaliana]	251012_at	1,285
AT5G03510	zinc finger (C2H2 type) family protein	250949_at	4,168
AT5G03550	similar to unknown protein [Arabidopsis thaliana] (TAIR:AT3G58300.1)	250951_at	1,274
AT5G04200	latex-abundant protein, putative (AMC9) / caspase family protein	245697_at	8,219
AT5G04390	zinc finger (C2H2 type) family protein	245705_at	3,590
AT5G05230	similar to unknown protein [Arabidopsis thaliana]	250822_at	1,468
AT5G06760	late embryogenesis abundant group 1 domain-containing protein / LEA group 1 domain-containing protein	250648_at	1,637
AT5G07530	GRP17 (Glycine rich protein 17)	250637_at	3,051
AT5G07560	GRP20 (Glycine rich protein 20); nutrient reservoir	250639_at	3,329
AT5G08430	SWIB complex BAF60b domain-containing protein / plus-3 domain-containing protein / GYF domain-containing protein	246058_at	1,122
AT5G08480	VQ motif-containing protein	250535_at	6,222
AT5G08560	transducin family protein / WD-40 repeat family protein	250539_at	1,207
AT5G09870	CESA5 (CELLULASE SYNTHASE 5); transferase, transferring glycosyl groups	250505_at	1,093
AT5G10650	zinc finger (C3HC4-type RING finger) family protein	246012_at	1,735
AT5G10870	ATCM2 (CHORISMATE MUTASE 2); chorismate mutase	250407_at	1,318

AGI Identifier	Description	Affymetrix ID	Log2 Fch
AT5G11070	similar to unknown protein [*Arabidopsis* thaliana]	245906_at	2,170
AT5G11450	oxygen-evolving complex-related	250371_at	1,083
AT5G11920	ATCWINV6 (6-&1-FRUCTAN EXOHYDROLASE); hydrolase, hydrolyzing O-glycosyl compounds / inulinase/ levanase	250302_at	1,146
AT5G11950	Identical to Lysine decarboxylase-like protein At5g11950 [*Arabidopsis* Thaliana]	250346_at	1,211
AT5G13170	**nodulin MtN3 family protein (SAG29)**	**245982_at**	**9,151**
AT5G13180*	**VNI2/ANAC083 (*Arabidopsis* NAC domain containing protein 83); transcription factor**	**245987_at**	**1,035**
AT5G14420	copine-related	250177_at	1,800
AT5G14960	DEL2/E2FD/E2L1 (DP-E2F-LIKE 2); DNA binding / transcription factor	246568_at	1,780
AT5G15700	DNA-directed RNA polymerase (RPOT2)	246514_at	1,510
AT5G15860	ATPCME (PRENYLCYSTEINE METHYLESTERASE); prenylcysteine methylesterase	246524_at	1,673
AT5G15960	[AT5G15960, KIN1];[AT5G15970, KIN2 (COLD-RESPONSIVE 6.6)]	246481_s_at	2,650
AT5G16235	[AT5G16230, acyl-(acyl-carrier-protein) desaturase, putative / stearoyl-ACP desaturase, putative]	246498_at	6,967
AT5G16570	GLN1;4 (Glutamine synthetase 1;4); glutamate-ammonia ligase	250100_at	3,370
AT5G16800	GCN5-related N-acetyltransferase (GNAT) family protein	246448_at	1,318
AT5G16840	RNA recognition motif (RRM)-containing protein	246452_at	1,380
AT5G17170	rubredoxin family protein	250073_at	1,026
AT5G18120	ATAPRL7 (APR-LIKE 7)	250030_at	1,635
AT5G18130	similar to unknown protein [*Arabidopsis* thaliana]	250028_at	1,197
AT5G18350	disease resistance protein (TIR-NBS-LRR class), putative	250037_at	1,289
AT5G18470	curculin-like (mannose-binding) lectin family protein	249983_at	3,964
AT5G18640	lipase class 3 family protein	249999_at	3,260
AT5G18650	zinc finger (C3HC4-type RING finger) family protein	250000_at	1,546
AT5G19870	similar to unknown protein [*Arabidopsis* thaliana] (TAIR:AT1G55230.1)pl	246138_at	3,561
AT5G20280	ATSPS1F (sucrose phosphate synthase 1F); sucrose-phosphate synthase/ transferase, transferring glycosyl groups	246076_at	1,493
AT5G20700	senescence-associated protein-related	245993_at	5,090
AT5G20940	glycosyl hydrolase family 3 protein	246183_at	1,396
AT5G22460	esterase/lipase/thioesterase family protein	249917_at	1,686
AT5G23390	similar to unknown protein [*Arabidopsis* thaliana]	249825_at	1,257
AT5G23530	similar to ATGID1C/GID1C (GA INSENSITIVE DWARF1C) [*Arabidopsis* thaliana] (TAIR:AT5G27320.1); similar to Esterase/lipase/thioesterase [Medicago truncatula]	249794_at	3,692

140

AGI Identifier	Description	Affymetrix ID	Log2 Fch
AT5G23750	Esterase/lipase/thioesterase [Medicago truncatula]	249797_at	5,288
AT5G23920	similar to unknown protein [Arabidopsis thaliana]	249810_at	1,964
AT5G24030	C4-dicarboxylate transporter/malic acid transport family protein	249765_at	1,421
AT5G24570	unknown protein	249750_at	1,358
AT5G24655	similar to unknown protein [Arabidopsis thaliana]	249721_at	1,208
AT5G24860	FPF1 (FLOWERING PROMOTING FACTOR 1)	246967_at	4,090
AT5G24870	zinc finger (C3HC4-type RING finger) family protein	246968_at	2,117
AT5G25820	exostosin family protein	246912_at	1,163
AT5G25920	similar to unknown protein [Arabidopsis thaliana] (TAIR:AT3G29750.1)	246857_at	1,646
AT5G26940	exonuclease family protein	246799_at	4,003
AT5G27450	MK/MVK; mevalonate kinase	246778_at	2,401
AT5G27710	similar to At5g27710 [Medicago truncatula] (GB:ABE92866.1)	246737_at	2,948
AT5G28050	cytidine/deoxycytidylate deaminase family protein	246702_at	1,181
AT5G37180	SUS5; UDP-glycosyltransferase/ sucrose synthase	249633_at	2,355
AT5G37580	binding / protein binding	249628_at	2,676
AT5G37600	ATGSR1 (Arabidopsis thaliana glutamine synthase clone R1); glutamate-ammonia ligase	249581_at	1,419
AT5G37680	ATARLA1A (ADP-ribosylation factor-like A1A); GTP binding	249579_at	2,552
AT5G38070	zinc finger (C3HC4-type RING finger) family protein	249569_at	5,594
AT5G38400	unknown protein	249564_at	3,896
AT5G38610	invertase/pectin methylesterase inhibitor family protein	249518_at	5,666
AT5G39520	similar to unknown protein [Arabidopsis thaliana]	249454_at	3,047
AT5G39730	avirulence-responsive protein-related / avirulence induced gene (AIG) protein-related	249441_at	1,132
AT5G40210	nodulin MtN21 family protein	249406_at	4,011
AT5G40470	similar to F-box family protein (FBL4) [Arabidopsis thaliana] (TAIR:AT4G15475.1); similar to Leucine Rich Repeat family protein	249359_at	1,282
AT5G40510	similar to unknown protein [Arabidopsis thaliana];similar to Clostridium pasteurianum ferredoxin homolog [Solanum tuberosum]	249358_at	2,404
AT5G40610	glycerol-3-phosphate dehydrogenase (NAD+) / GPDH	249366_at	3,934
AT5G40640	similar to unknown protein [Arabidopsis thaliana], similar to Steroid nuclear receptor, ligand-binding [Medicago truncatula]	249368_at	2,334
AT5G40645	nitrate-responsive NOI protein, putative	249376_at	1,115
AT5G42200	zinc finger (C3HC4-type RING finger) family protein	249234_at	1,401

AGI Identifier	Description	Affymetrix ID	Log2 Fch
AT5G42500	[AT5G42500, disease resistance-responsive family protein];[AT5G42510, disease resistance-responsive family protein]	249195_s_at	4,559
AT5G43060	cysteine proteinase, putative / thiol protease, putative	249187_at	3,561
AT5G43410	ethylene-responsive factor, putative	249154_at	3,899
AT5G43620	[AT5G43620, S-locus protein-related];[AT1G66500, zinc finger (C2H2-type) family protein]	256356_s_at	1,030
AT5G43900	MYA2 (*ARABIDOPSIS* MYOSIN)	249095_at	1,936
AT5G43920	transducin family protein / WD-40 repeat family protein	249066_at	1,352
AT5G44060	similar to unknown protein [*Arabidopsis* thaliana]	249072_at	1,429
AT5G45630	similar to unknown protein [*Arabidopsis* thaliana]	248959_at	3,461
AT5G45810	CIPK19 (CIPK19); kinase	248909_at	3,200
AT5G47060	senescence-associated protein-related	248820_at	1,408
AT5G47635	similar to unknown protein [*Arabidopsis* thaliana]	248761_at	4,478
AT5G47740	similar to protein kinase family protein / U-box domain-containing protein [*Arabidopsis* thaliana]	248770_at	1,609
AT5G48230	ACAT2/EMB1276 (ACETOACETYL-COA THIOLASE 2, EMBRYO DEFECTIVE 1276); acetyl-CoA C-acetyltransferase	248690_at	1,077
AT5G48430	similar to extracellular dermal glycoprotein, putative / EDGP, putative [*Arabidopsis* thaliana] (TAIR:AT1G03220.1); similar to putative xylanase inhibitor [Oryza sativa (japonica cultivar-group)]	248703_at	1,761
AT5G48480	Identical to Protein At5g48480 [*Arabidopsis* Thaliana]	248710_at	1,838
AT5G49280	hydroxyproline-rich glycoprotein family protein	248592_at	1,012
AT5G49710	similar to unknown protein [*Arabidopsis* thaliana]	248565_at	2,827
AT5G49900	similar to unknown protein [*Arabidopsis* thaliana]	248581_at	1,564
AT5G50170	C2 domain-containing protein / GRAM domain-containing protein	248553_at	1,909
AT5G50260	cysteine proteinase, putative	248545_at	5,133
AT5G50450	zinc finger (MYND type) family protein	248502_at	1,901
AT5G50660	[AT5G50660, similar to unknown protein [*Arabidopsis* thaliana] (TAIR:AT5G50560.1)	248518_at	4,910
AT5G51180	similar to unknown protein [*Arabidopsis* thaliana]	248451_at	1,552
AT5G51260	acid phosphatase, putative	248440_at	1,634
AT5G51390	unknown protein	248432_at	1,242
AT5G52120	ATPP2-A14 (Phloem protein 2-A14)	248395_at	1,341
AT5G53550	YSL3 (YELLOW STRIPE LIKE 3); oligopeptide transporter	248276_at	2,047
AT5G53820	similar to unknown protein [*Arabidopsis* thaliana],similar to pollen coat protein [Brassica oleracea]	248227_at	5,474
AT5G53830	VQ motif-containing protein	248230_at	1,818

AGI Identifier	Description	Affymetrix ID	Log2 Fch
AT5G53920	ribosomal protein L11 methyltransferase-related	248239_at	1,638
AT5G54130	calcium ion binding	248190_at	1,575
AT5G54130	calcium ion binding	248191_at	2,239
AT5G54510	DFL1 (DWARF IN LIGHT 1); indole-3-acetic acid amido synthetase	248163_at	1,033
AT5G54570	glycosyl hydrolase family 1 protein	248168_at	5,360
AT5G54730	AtATG18f (Arabidopsis thaliana homolog of yeast autophagy 18 (ATG18) f)	248124_at	1,028
AT5G54870	similar to unknown protein [Arabidopsis thaliana]	248115_at	1,389
AT5G55050	GDSL-motif lipase/hydrolase family protein	248118_at	1,451
AT5G55400	fimbrin-like protein, putative	248082_at	1,972
AT5G56340	zinc finger (C3HC4-type RING finger) family protein	248014_at	1,308
AT5G56540	AGP14 (ARABINOGALACTAN PROTEIN 14)	247965_at	8,420
AT5G56790	protein kinase family protein	247985_at	4,359
AT5G56980	similar to unknown protein [Arabidopsis thaliana] (TAIR:AT4G26130.1); similar to cDNA-5-encoded protein (GB:AAA50235.1)	247933_at	1,993
AT5G57000	similar to unknown protein [Arabidopsis thaliana]	247934_at	1,680
AT5G57240	oxysterol-binding family protein	247951_at	1,197
AT5G57960	GTP-binding family protein	247891_at	1,511
AT5G58120	disease resistance protein (TIR-NBS-LRR class), putative	247848_at	1,724
AT5G59290	UXS3 (UDP-GLUCURONIC ACID DECARBOXYLASE); catalytic	247720_at	1,758
AT5G59340	WOX2 (WUSCHEL-related homeobox 2); transcription factor	247714_at	2,652
AT5G59350	similar to unknown protein [Arabidopsis thaliana]	247716_at	2,450
AT5G59400	similar to unknown protein [Arabidopsis thaliana] (TAIR:AT4G11960.1); contains domain DNA ligase/mRNA capping enzyme, catalytic domain (SSF56091)	247734_at	1,121
AT5G59490	haloacid dehalogenase-like hydrolase family protein	247727_at	2,326
AT5G59840	Ras-related GTP-binding family protein	247699_at	1,005
AT5G61340	similar to unknown protein [Arabidopsis thaliana]	247522_at	4,033
AT5G61640	PMSR1 (PEPTIDEMETHIONINE SULFOXIDE REDUCTASE 1); protein-methionine-S-oxide reductase	247514_at	1,778
AT5G62480	ATGSTU9 (GLUTATHIONE S-TRANSFERASE TAU 9); glutathione transferase	247435_at	3,146
AT5G63060	transporter	247415_at	2,356
AT5G63600	flavonol synthase, putative	247333_at	2,544
AT5G63990	3'(2'),5'-bisphosphate nucleotidase, putative / inositol polyphosphate 1-phosphatase, putative	247318_at	1,297

AGI Identifier	Affymetrix ID	Description	Log2 Fch
AT5G64080	247268_at	protease inhibitor/seed storage/lipid transfer protein (LTP) family protein	1,392
AT5G64190	247324_at	similar to unknown protein [Arabidopsis thaliana]	5,470
AT5G64572	247266_at	[AT5G64570, XYL4 (beta-xylosidase 4); hydrolase, hydrolyzing O-glycosyl compounds]	1,604
AT5G64620	247246_at	C/VIF2 (CELL WALL / VACUOLAR INHIBITOR OF FRUCTOSIDASE 2); pectinesterase inhibitor	1,016
AT5G65440	247183_at	similar to unknown protein [Arabidopsis thaliana]	1,480
AT5G65640	247151_at	BHLH093 (BETA HLH PROTEIN 93); DNA binding / transcription factor	2,171
AT5G65870	247109_at	ATPSK5 (PHYTOSULFOKINE 5 PRECURSOR); growth factor	1,866
AT5G66390	247091_at	peroxidase 72 (PER72) (P72) (PRXR8)	6,847
AT5G66550	247102_at	Maf family protein	1,543
AT5G66930	247045_at	similar to Os12g0446700 [Oryza sativa (japonica cultivar-group)] (GB:NP_001066715.1)	1,348
AT5G67280	247034_at	CYCD3;2 (CYCLIN D3;2); cyclin-dependent protein kinase	1,527
AT5G67360	246990_at	ARA12; subtilase	2,788
AT5G67370	246998_at	similar to unknown protein [Arabidopsis thaliana]	2,093
Genes down-regulated			
AT1G01480	259439_at	ACS2 (1-Amino-cyclopropane-1-carboxylate synthase 2)	-1,577
AT1G02390	259418_at	ATGPAT2/GPAT2 (GLYCEROL-3-PHOSPHATE ACYLTRANSFERASE 2); acyltransferase	-1,326
AT1G03360	264357_at	ATRRP4; exonuclease	-1,388
AT1G05680	263231_at	UDP-glucoronosyl/UDP-glucosyl transferase family protein	-1,171
AT1G08230	261785_at	similar to amino acid transporter family protein [Arabidopsis thaliana] (japonica cultivar-group)] (GB:NP_001056462.1); similar to Amino acid/polyamine transporter II [Medicago truncatula] (GB:ABE8	-1,540
AT1G09970	264663_at	leucine-rich repeat transmembrane protein kinase, putative	-1,159
AT1G10990	260472_at	unknown protein	-1,548
AT1G11330	262507_at	S-locus lectin protein kinase family protein	-1,516
AT1G12200	261023_at	flavin-containing monooxygenase family protein / FMO family protein	-1,852
AT1G13930	262609_at	similar to nodulin-related [Arabidopsis thaliana]	-1,251
AT1G14040	262649_at	similar to EXS family protein / ERD1/XPR1/SYG1 family protein [Arabidopsis thaliana] (TAIR:AT2G03260.1); similar to EXS family protein / ERD1/XPR1/SYG1 family protein [Arabidopsis thaliana]	-1,019
AT1G15040	260741_at	glutamine amidotransferase-related	-1,620
AT1G18020	255895_at	[AT1G18020, 12-oxophytodienoate reductase, putative];[AT1G17990, 12-oxophytodienoate reductase, putative]	-1,134
AT1G18570	255753_at	MYB51 (myb domain protein 51); DNA binding / transcription factor	-1,897

AGI Identifier	Description	Affymetrix ID	Log2 Fch
AT1G18590	sulfotransferase family protein	255773_at	-1,124
AT1G19610	LCR78/PDF1.4 (Low-molecular-weight cysteine-rich 78)	261135_at	-1,414
AT1G19670	ATCLH1 (CORONATINE-INDUCED PROTEIN 1)	255786_at	-1,532
AT1G21130	O-methyltransferase, putative	261453_at	-1,826
AT1G21590	protein kinase family protein	260924_at	-1,627
AT1G21830	similar to unknown protein [Arabidopsis thaliana]	262488_at	-1,090
AT1G21920	MORN (Membrane Occupation and Recognition Nexus) repeat-containing protein /phosphatidylinositol-4-phosphate 5-kinase-related	260855_at	-1,469
AT1G22890	similar to unknown protein [Arabidopsis thaliana] (TAIR:AT5G44568.1); contains domain FAMILY NOT NAMED (PTHR12953); contains domain SUBFAMILY NOT NAMED (PTHR12953:SF10)	264774_at	-1,783
AT1G23830	similar to unknown protein [Arabidopsis thaliana] (TAIR:AT1G23840.1)	265132_at	-1,451
AT1G24825	[AT1G25170, similar to unknown protein [Arabidopsis thaliana]	245638_s_at	-1,051
AT1G26440	ATUPS5 (ARABIDOPSIS THALIANA UREIDE PERMEASE 5)	261013_at	-1,102
AT1G26460	pentatricopeptide (PPR) repeat-containing protein	261014_at	-1,061
AT1G28680	transferase family protein	262744_at	-1,388
AT1G30380	PSAK (PHOTOSYSTEM I SUBUNIT K)	256309_at	-1,093
AT1G32690	similar to unknown protein [Arabidopsis thaliana]	261700_at	-1,263
AT1G33960	AIG1 (AVRRPT2-INDUCED GENE 1); GTP binding	260116_at	-1,309
AT1G34200	oxidoreductase family protein	262515_at	-1,029
AT1G35210	similar to unknown protein [Arabidopsis thaliana] (TAIR:AT1G72240.1); similar to Avr9/Cf-9 rapidly elicited protein 75 [Nicotiana tabacum] (GB:AAG43558.1)	245755_at	-1,058
AT1G43160	RAP2.6 (related to AP2 6); DNA binding / transcription factor	264415_at	-1,092
AT1G48430	dihydroxyacetone kinase family protein	261294_at	-1,109
AT1G51270	structural molecule	265136_at	-1,173
AT1G51700	ADOF1 (Arabidopsis dof zinc finger protein 1); DNA binding / transcription factor	256185_at	-1,218
AT1G53560	similar to unknown protein [Arabidopsis thaliana]	260983_at	-1,009
AT1G59990	DEAD/DEAH box helicase, putative (RH22)	263679_at	-1,004
AT1G60000	29 kDa ribonucleoprotein, chloroplast, putative / RNA-binding protein cp29, putative	263736_at	-1,004
AT1G62570	flavin-containing monooxygenase family protein / FMO family protein	265119_at	-1,267
AT1G65240	aspartyl protease family protein	263108_at	-1,084
AT1G66480	PMI2 (plastid movement impaired 2)	257583_at	-1,346

AGI Identifier	Description	Affymetrix ID	Log2 Fch
AT1G66690	[AT1G66690, S-adenosyl-L-methionine:carboxyl methyltransferase family protein]	256376_s_at	-1,392
AT1G67740	PSBY (photosystem II BY)	245195_at	-1,088
AT1G67810	Fe-S metabolism associated domain-containing protein	245193_at	-1,108
AT1G67980	CCoAMT (caffeoyl-CoA 3-O-methyltransferase); caffeoyl-CoA O-methyltransferase	260015_at	-1,265
AT1G69890	similar to unknown protein [Arabidopsis thaliana] (TAIR:AT1G27100.1); similar to Cytosolic fatty-acid binding; Actin-crosslinking proteins [Medicago truncatula] (GB:ABE82702.1); contains InterPro domain Protein of unknown function DUF569; (InterPro:IPR007	260411_at	-1,272
AT1G69920	ATGSTU12 (*Arabidopsis* thaliana Glutathione S-transferase (class tau) 12); glutathione transferase	260406_at	-2,000
AT1G69930	ATGSTU11 (*Arabidopsis* thaliana Glutathione S-transferase (class tau) 11); glutathione transferase	260405_at	-1,198
AT1G71830	SERK1 (SOMATIC EMBRYOGENESIS RECEPTOR-LIKE KINASE 1); kinase	261521_at	-1,045
AT1G72910	[AT1G72910, disease resistance protein;TIR (TOLL/INTERLEUKIN-1 RECEPTOR-LIKE); transmembrane receptor]	262374_s_at	-1,142
AT1G72920	disease resistance protein (TIR-NBS class), putative	262382_at	-2,171
AT1G72940	disease resistance protein (TIR-NBS class), putative	262383_at	-1,397
AT1G73080	PEPR1 (PEP1 RECEPTOR 1); ATP binding / kinase/ protein binding / protein serine/threonine kinase	262360_at	-1,061
AT1G73500	ATMKK9 (*Arabidopsis* thaliana MAP kinase kinase 9); kinase	245731_at	-1,039
AT1G74080	MYB122 (myb domain protein 122); DNA binding / transcription factor	260394_at	-1,195
AT1G74090	sulfotransferase family protein	260385_at	-1,046
AT1G74470	geranylgeranyl reductase	260236_at	-1,094
AT1G78820	[AT1G78820, curculin-like (mannose-binding) lectin family protein / PAN domain-containing protein];[AT1G78830, curculin-like (mannose-binding) lectin family protein]	264279_s_at	-1,094
AT1G80560	3-isopropylmalate dehydrogenase, chloroplast, putative	260285_at	-1,103
AT1G80820	CCR2 (CINNAMOYL COA REDUCTASE)	261899_at	-1,053
AT2G04040	ATDTX1; antiporter/ multidrug efflux pump/ multidrug transporter/ transporter	263403_at	-1,762
AT2G15890	MEE14 (maternal effect embryo arrest 14)	265478_at	-1,410
AT2G17480	MLO8 (MILDEW RESISTANCE LOCUS O 8); calmodulin binding	264852_at	-1,016
AT2G18050	HIS1-3 (HISTONE H1-3); DNA binding	265817_at	-1,395
AT2G22300	ethylene-responsive calmodulin-binding protein, putative (SR1)	263457_at	-1,251
AT2G22330	CYP79B3 (cytochrome P450, family 79, subfamily B, polypeptide 3); oxygen binding	264052_at	-1,772
AT2G23270	similar to unknown protein [*Arabidopsis thaliana*]	245082_at	-1,635
AT2G23420	nicotinate phosphoribosyltransferase family protein / NAPRTase family protein	267132_at	-1,195

AGI Identifier	Description	Affymetrix ID	Log2 Fch
AT2G27390	proline-rich family protein	265643_at	-1,351
AT2G29340	short-chain dehydrogenase/reductase (SDR) family protein	266265_at	-1,560
AT2G30600	BTB/POZ domain-containing protein	267523_at	-1,261
AT2G30770	CYP71A13 (cytochrome P450, family 71, subfamily A, polypeptide 13); oxygen binding	267567_at	-1,157
AT2G31750	UGT74D1 (UDP-glucosyl transferase 74D1); transferring glycosyl groups / transferase, transferring hexosyl groups	263473_at	-1,047
AT2G32030	GCN5-related N-acetyltransferase (GNAT) family protein	265725_at	-1,251
AT2G35660	[AT2G35660, CTF2A; monooxygenase];[AT2G29720, CTF2B; monooxygenase]	266615_s_at	-1,064
AT2G39210	nodulin family protein	266993_at	-1,041
AT2G39980	transferase family protein	267337_at	-1,645
AT2G41880	GK-1 (GUANYLATE KINASE 1); guanylate kinase	267537_at	-1,004
AT2G46220	similar to unknown protein [Arabidopsis thaliana]	266583_at	-1,053
AT2G46450	ATCNGC12 (cyclic nucleotide gated channel 12); cyclic nucleotide binding / ion channel	263777_at	-1,408
AT2G48010	RKF3 (RECEPTOR-LIKE KINASE IN IN FLOWERS 3); kinase	265772_at	-1,660
AT3G04210	disease resistance protein (TIR-NBS class), putative	258537_at	-1,013
AT3G04220	disease resistance protein (TIR-NBS-LRR class), putative	258577_at	-1,100
AT3G04550	similar to unknown protein [Arabidopsis thaliana]	258800_at	-1,196
AT3G05200	ATL6 (Arabidopsis T?xicos en Levadura 6); protein binding / zinc ion binding	259312_at	-1,135
AT3G06510	SFR2 (SENSITIVE TO FREEZING 2); hydrolase, hydrolyzing O-glycosyl compounds	258512_at	-1,126
AT3G08760	ATSIK; kinase	258683_at	-1,322
AT3G10930	unknown protein	256442_at	-1,027
AT3G12080	EMB2738 (EMBRYO DEFECTIVE 2738); GTP binding	256274_at	-1,156
AT3G14840	leucine-rich repeat family protein / protein kinase family protein	256547_at	-1,265
AT3G14850	similar to unknown protein [Arabidopsis thaliana] (TAIR:AT1G29050.1)	256600_at	-1,287
AT3G16720	ATL2 (Arabidopsis T?xicos en Levadura 2); protein binding / zinc ion binding	258436_at	-1,121
AT3G20660	carbohydrate transporter/ sugar porter	256697_at	-1,213
AT3G20860	protein kinase family protein	257978_at	-1,233
AT3G21140	FMN binding	256972_at	-1,049
AT3G21230	4CL5 (4-COUMARATE:COA LIGASE 5); 4-coumarate-CoA ligase	258037_at	-1,264
AT3G21240	4CL2 (4-coumarate:CoA ligase 2); 4-coumarate-CoA ligase	258047_at	-1,130

AGI Identifier	Affymetrix ID	Log2 Fch	Description
AT3G21780	257950_at	-1,475	UGT71B6 (UDP-glucosyl transferase 71B6); UDP-glycosyltransferase/ Transferring glycosyl groups
AT3G23550	258100_at	-1,438	MATE efflux family protein
AT3G26280	257635_at	-1,342	CYP71B4 (cytochrome P450, family 71, subfamily B, polypeptide 4); oxygen binding
AT3G26570	257311_at	-1,059	PHT2;1 (phosphate transporter 2;1)
AT3G26830	258277_at	-1,289	PAD3 (PHYTOALEXIN DEFICIENT 3); oxygen binding
AT3G28180	257071_at	-1,492	ATCSLC04 (Cellulose synthase-like C4); transferase, transferring glycosyl groups
AT3G44260	252679_at	-1,775	CCR4-NOT transcription complex protein, putative
AT3G46110	252533_at	-2,057	signal transducer
AT3G46600	252483_at	-1,048	scarecrow transcription factor family protein
AT3G47800	252387_at	-1,389	aldose 1-epimerase family protein
AT3G48640	252345_at	-1,371	similar to unknown protein [Arabidopsis thaliana] (TAIR:AT5G66670.2)
AT3G49620	252265_at	-1,019	DIN11 (DARK INDUCIBLE 11); oxidoreductase
AT3G51895	246310_at	-1,159	SULTR3;1 (SULFATE TRANSPORTER 1); sulfate transporter
AT3G52150	252032_at	-1,319	RNA recognition motif (RRM)-containing protein
AT3G53160	251971_at	-1,059	UGT73C7 (UDP-glucosyl transferase 73C7); UDP-glycosyltransferase/ transferase, transferring glycosyl groups
AT3G55010	251830_at	-1,048	phosphoribosylformylglycinamidine cyclo-ligase, chloroplast / phosphoribosyl-aminoimidazole synthetase / AIR synthase (PUR5)
AT3G57760	251603_at	-1,237	protein kinase family protein
AT3G59080	251507_at	-1,027	aspartyl protease family protein
AT3G59940	251443_at	-1,326	kelch repeat-containing F-box family protein
AT3G60120	251456_at	-2,317	glycosyl hydrolase family 1 protein
AT3G61430	251324_at	-1,026	PIP1A (plasma membrane intrinsic protein 1;1); water channel
AT3G61890	251272_at	-1,064	ATHB-12 (ARABIDOPSIS THALIANA HOMEOBOX PROTEIN 1); transcription factor
AT3G62150	251248_at	-1,240	PGP21 (P-GLYCOPROTEIN 21); ATPase, coupled to transmembrane movement of substances
AT4G00430	255674_at	-1,072	TMP-C (plasma membrane intrinsic protein 1,4); water channel
AT4G02410	255502_at	-1,147	lectin protein kinase family protein
AT4G08770	255110_at	-1,429	peroxidase, putative
AT4G08980	255066_at	-1,168	F-box family protein (FBW2)
AT4G11280	254926_at	-1,381	ACS6 (1-AMINOCYCLOPROPANE-1-CARBOXYLIC ACID (ACC) SYNTHASE 6)
AT4G13660	254726_at	-1,149	pinoresinol-lariciresinol reductase, putative

| AGI Identifier	Description	Affymetrix ID	Log2 Fch
AT4G15120	VQ motif-containing protein	245363_at	-1,249
AT4G16860	RPP4 (RECOGNITION OF PERONOSPORA PARASITICA 4)	245448_at	-1,130
AT4G17490	ATERF6 (ETHYLENE RESPONSIVE ELEMENT BINDING FACTOR 6); DNA binding / transcription factor	245250_at	-1,249
AT4G18010	IP5PII (INOSITOL POLYPHOSPHATE 5-PHOSPHATASE II); inositol-polyphosphate 5-phosphatase	254707_at	-1,087
AT4G18360	(S)-2-hydroxy-acid oxidase, peroxisomal, putative / glycolate oxidase, putative / short chain alpha-hydroxy acid oxidase, putative	254630_at	-1,096
AT4G19160	binding	254561_at	-1,424
AT4G21390	B120; protein kinase/ sugar binding	254408_at	-1,414
AT4G22710	[AT4G22710, CYP706A2 (cytochrome P450, family 706, subfamily A, polypeptide 2); oxygen binding	254331_s_at	-1,752
AT4G24110	similar to Hypothetical protein [Oryza sativa (japonica cultivar-group)] (GB:AAO17020.1)	254200_at	-1,194
AT4G24120	YSL1 (YELLOW STRIPE LIKE 1); oligopeptide transporter	254174_at	-1,203
AT4G24570	mitochondrial substrate carrier family protein	254120_at	-1,510
AT4G24930	thylakoid lumenal 17.9 kDa protein, chloroplast	254137_at	-1,046
AT4G26120	ankyrin repeat family protein / BTB/POZ domain-containing protein	254014_at	-1,098
AT4G28040	nodulin MtN21 family protein	253829_at	-1,292
AT4G28085	unknown protein	253827_at	-1,014
AT4G31500	CYP83B1 (CYTOCHROME P450 MONOOXYGENASE 83B1); oxygen binding	253534_at	-1,163
AT4G32340	binding	253421_at	-1,078
AT4G35110	similar to unknown protein [Arabidopsis thaliana] (TAIR:AT2G16900.1); similar to pEARLI 4 gene product (GB:AAC37472.1); contains InterPro domain Arabidopsis phospholipase-like; (InterPro:IPR007942)	253173_at	-1,079
AT4G35770	SEN1 (DARK INDUCIBLE 1)	253161_at	-2,309
AT4G38810	calcium-binding EF hand family protein	252915_at	-1,311
AT4G39230	isoflavone reductase, putative	252939_at	-1,209
AT5G01215	[AT5G01210, transferase family protein]	251144_at	-1,305
AT5G01670	aldose reductase, putative	251100_at	-1,288
AT5G01880	zinc finger (C3HC4-type RING finger) family protein	251066_at	-1,263
AT5G06530	ABC transporter family protein	250690_at	-1,433
AT5G06870	PGIP2 (POLYGALACTURONASE INHIBITING PROTEIN 2); protein binding	250669_at	-1,098
AT5G09470	mitochondrial substrate carrier family protein	245882_at	-1,225
AT5G10390	histone H3	250434_at	-1,017
AT5G12170	similar to unknown protein [Arabidopsis thaliana]	250306_at	-1,043
AT5G14180	lipase family protein	250199_at	-1,217
AT5G15190	unknown protein	250158_at	-1,092
AT5G17760	AAA-type ATPase family protein	250062_at	-1,029

AGI Identifier	Description	Affymetrix ID	Log2 Fch
AT5G18170	GDH1 (GLUTAMATE DEHYDROGENASE 1); oxidoreductase	250032_at	-1,002
AT5G18290	SIP1;2 (SMALL AND BASIC INTRINSIC PROTEIN1B)	250025_at	-1,203
AT5G18500	protein kinase family protein	249985_at	-1,027
AT5G19140	auxin/aluminum-responsive protein, putative	249922_at	-1,146
AT5G22860	serine carboxypeptidase S28 family protein	249860_at	-1,708
AT5G25170	similar to unknown protein [Arabidopsis thaliana]	246931_at	-1,297
AT5G38870	transferase family protein	249505_at	-1,459
AT5G39090	transferase family protein	249489_at	-1,463
AT5G41610	[AT5G41610, ATCHX18 (cation/hydrogen exchanger 18); monovalent cation:proton antiporter]	249255_at	-1,109
AT5G42060	similar to unknown protein [Arabidopsis thaliana] (TAIR:AT1G64490.1)	249253_at	-1,118
AT5G42250	alcohol dehydrogenase, putative	249242_at	-1,278
AT5G44580	similar to unknown protein [Arabidopsis thaliana]	249010_at	-1,291
AT5G47220	ATERF-2/ATERF2/ERF2 (ETHYLENE RESPONSE FACTOR 2); DNA binding / transcription factor/ transcriptional activator	248794_at	-1,317
AT5G47230	ERF5 (ETHYLENE RESPONSIVE ELEMENT BINDING FACTOR 5); DNA binding / transcription factor/ transcriptional activator	248799_at	-1,185
AT5G49230	HRB1 (HYPERSENSITIVE TO RED AND BLUE)	248595_at	-1,037
AT5G52380	zinc knuckle (CCHC-type) family protein	248357_at	-1,229
AT5G55120	similar to VTC2 (VITAMIN C DEFECTIVE 2) [Arabidopsis thaliana] (TAIR:AT4G26850.1)	248091_at	-1,071
AT5G57220	CYP81F2 (cytochrome P450, family 81, subfamily F, polypeptide 2); oxygen binding	247949_at	-1,253
AT5G57655	xylose isomerase family protein	247924_at	-1,172
AT5G59530	2-oxoglutarate-dependent dioxygenase, putative	247729_at	-1,333
AT5G59700	protein kinase, putative	247686_at	-1,149
AT5G61380	TOC1 (TIMING OF CAB1 1); transcription regulator	247525_at	-1,110
AT5G62730	proton-dependent oligopeptide transport (POT) family protein	247447_at	-1,100
AT5G64890	PROPEP2 (Elicitor peptide 2 precursor)	247205_at	-1,498
AT5G64905	PROPEP3 (Elicitor peptide 3 precursor)	247215_at	-1,286
AT5G65240	leucine-rich repeat family protein / protein kinase family protein	247197_at	-1,150
AT5G65600	legume lectin family protein / protein kinase family protein	247145_at	-1,002
AT5G66530	aldose 1-epimerase family protein	247101_at	-1,169
AT5G67080	MAPKKK19 (Mitogen-activated protein kinase kinase kinase 19); kinase	247026_at	-1,049

Annex 6

Subcellular localization of ORE1-GFP fusion protein in *Arabidopsis*

Upper panel: *ORE1* cDNA was amplified using a combination of primer forward and reverse (123-124 respectively) (**Annex 1**) and then cloned into the Gateway pENTR-D-TOPO entry vector. The entry vector construct was recombined into Gateway destination vector *pK7FWG2.0* (Karimi *et al.* 2002) using the LR reaction mix II (Invitrogen) to obtain the final reporter vector *ORE1-GFP*. The recombination reactions were done according with the manufacturer's instructions (Invitrogen).

Bottom panel: The p35S-driven ORE1-GFP fusion protein was expressed in wild type (Col-0) after *Agrobacterium*-mediated transformation as described in **section 2.4.4** and viewed under fluorescence light using a confocal laser scanning microscopy (LSCM) SP5, Leica with software LAS AF (Leica). (**I**) is shown in bright field (**II**) shows the red auto-fluorescence of chlorophyll, (**III**) the GFP-signal, and (**IV**) the merged signals. (**A**) The image shows and overview of epidermal cells, guard cells and stomata from a leaf of 15-day-old *Arabidopsis* seedling. Seedlings were grown in MS media as described in **section 2.4.2.** (**B**) Close-up of a pair of guard cells forming the stoma. ORE1-GFP protein is expressed in nucleus. Chloroplasts are visible in guard cells fluorescing red.
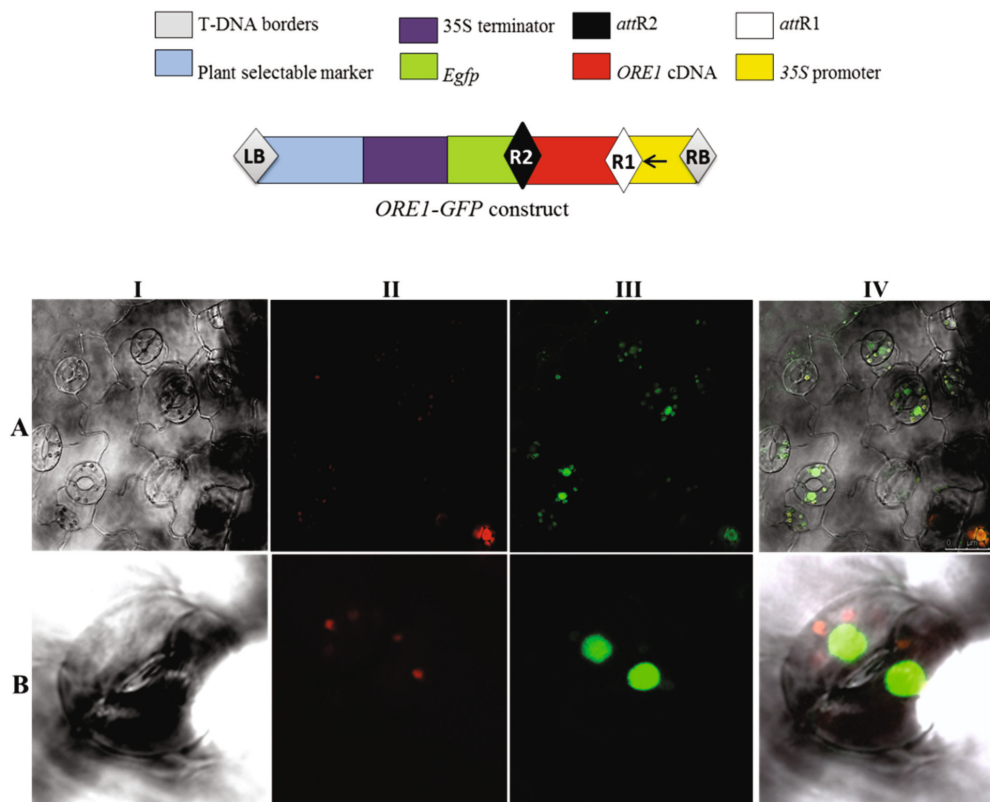
References

Abreu, M.E. and Munné-Bosch, S. (2008) Salicylic acid may be involved in the regulation of drought-induced leaf senescence in perennials: A case study in field-grown *Salvia officinalis* L. plants. *Environmental and Experimental Botany*, **64,** 105-112.

Adam, Z. (1996) Protein stability and degradation in chloroplasts. *Plant molecular biology*, **32,** 773-783.

Adam, Z., Adamska, I., Nakabayashi, K., Ostersetzer, O., Haussuhl, K., Manuell, A., Zheng, B., Vallon, O., Rodermel, S.R. and Shinozaki, K. (2001) Chloroplast and mitochondrial proteases in *Arabidopsis*. A proposed nomenclature. *Plant Physiology,* **125,** 1912-1918.

Adam, Z. and Clarke, A.K. (2002) Cutting edge of chloroplast proteolysis. *Trends in Plant Science*, 7, 451-456.

Aeong Oh, S., Park, J.H., In Lee, G., Hee Paek, K., Ki Park, S. and Gil Nam, H. (1997) Identification of three genetic loci controlling leaf senescence in *Arabidopsis thaliana*. *The Plant Journal*, 12, 527-535.

Aida, M., Ishida, T., Fukaki, H., Fujisawa, H. and Tasaka, M. (1997) Genes involved in organ separation in *Arabidopsis*: an analysis of the cup-shaped cotyledon mutant. *The Plant Cell Online*, **9,** 841-857.

Al-Daoud, F. and Cameron, R.K. (2011) ANAC055 and ANAC092 contribute non-redundantly in an EIN2-dependent manner to Age-Related Resistance in *Arabidopsis*. *Physiological and Molecular Plant Pathology*, **76,** 212-222.

Alonso, J.M., Hirayama, T., Roman, G., Nourizadeh, S. and Ecker, J.R. (1999) EIN2, a bifunctional transducer of ethylene and stress responses in *Arabidopsis*. *Science*, **284,** 2148.

Altschul, S.F., Madden, T.L., Schäfer, A.A., Zhang, J., Zhang, Z., Miller, W. and Lipman, D.J. (1997) Gapped BLAST and PSI-BLAST: a new generation of protein database search programs. *Nucleic Acids Research*, **25,** 3389-3402.

An, Y.Q.C. and Meagher, R.B. (2010) Strong expression and conserved regulation of ACT2 in *Arabidopsis thaliana* and *Physcomitrella patens*. *Plant Molecular Biology Reporter,* **28,** 481-490.

Arabidopsis, G.I. (2000) Analysis of the genome sequence of the flowering plant *Arabidopsis thaliana*. Nature, **408,** 796.

Bailey, T.L., Boden, M., Buske, F.A., Frith, M., Grant, C.E., Clementi, L., Ren, J., Li, W.W. and Noble, W.S. (2009) MEME SUITE: tools for motif discovery and searching. *Nucleic Acids Research*, **37**, W202-W208.

Baker, N.R. (1992) Crop photosynthesis: spatial and temporal determinants: Elsevier Science & Technology.

Baker, S.S., Wilhelm, K.S. and Thomashow, M.F. (1994) The 5`-region of *Arabidopsis thaliana cor15a* has *cis*-acting elements that confer cold-, drought-and ABA-regulated gene expression. *Plant molecular biology*, **24**, 701-713.

Balazadeh, S., Kwasniewski, M., Caldana, C., Mehrnia, M., Zanor, M.I., Xue, G.P. and Mueller-Roeber, B. (2011) ORS1, an H2O2-responsive NAC transcription factor, controls senescence in *Arabidopsis thaliana. Molecular plant,* **4,** 346.

Balazadeh, S., Parlitz, S., Mueller Roeber, B. and Meyer, R.C. (2008a) Natural developmental variations in leaf and plant senescence in *Arabidopsis thaliana. Plant Biology,* **10,** 136-147.

Balazadeh, S., Riaño-Pachón, D.M. and Mueller-Roeber, B. (2008b) Transcription factors regulating leaf senescence in *Arabidopsis thaliana. Plant Biology,* **10,** 63-75.

Balazadeh, S., Siddiqui, H., Allu, A.D., Matallana-Ramirez, L.P., Caldana, C., Mehrnia, M., Zanor, M.I., Köhler, B. and Mueller-Roeber, B. (2010a) A gene regulatory network controlled by the NAC transcription factor ANAC092/AtNAC2/ORE1 during salt-promoted senescence. *The Plant Journal*, **62**, 250-264.

Balazadeh, S., Wu, A. and Mueller-Roeber, B. (2010b) Salt-triggered expression of the ANAC092-dependent senescence regulon in *Arabidopsis thaliana. Plant signaling & behavior*, **5,** 733.

Bariola, P.A., Howard, C.J., Taylor, C.B., Verburg, M.T., Jaglan, V.D. and Green, P.J. (1994) The *Arabidopsis* ribonuclease gene RNS1 is tightly controlled in response to phosphate limitation. *The Plant Journal*, **6,** 673-685.

Barton, R. (1966) Fine structure of mesophyll cells in senescing leaves of *Phaseolus. Planta,* **71,** 314-325.

Bechtold, N. and Pelletier, G. (1998) In Planta *Agrobacterium*-Mediated-Transformation of Adult *Arabidopsis thaliana* Plants by Vacuum Infiltration. *Arabidopsis protocols*, **82,** 259.

Benedetti, C.E. and Arruda, P. (2002) Altering the Expression of the Chlorophyllase GeneATHCOR1 in Transgenic *Arabidopsis* Caused Changes in the Chlorophyll-to-Chlorophyllide Ratio. *Plant Physiology*, **128,** 1255-1263.

Bishop, G.J. and Koncz, C. (2002) Brassinosteroids and plant steroid hormone signaling. *The Plant Cell Online,* **14,** S97-S110.

Biswal, B. (1995) Carotenoid catabolism during leaf senescence and its control by light. *Journal of Photochemistry and Photobiology B: Biology*, **30,** 3-13.

Biswal, U.C. and Biswal, B. (1984) Photocontrol of leaf senescence. *Photochemistry and photobiology*, **39,** 875-879.

Biswal, U.C., Biswal, B. and Raval, M.K. (2003) *Chloroplast biogenesis: from proplastid to gerontoplast:* Springer Netherlands. ISBN: 1402016026.

Blank, A. and McKeon, T.A. (1989) Single-strand-preferring nuclease activity in wheat leaves is increased in senescence and is negatively photoregulated. *Proceedings of the National Academy of Sciences*, **86,** 3169.

Blank, A. and McKeon, T.A. (1991) Expression of three RNase activities during natural and dark-induced senescence of wheat leaves. *Plant Physiology*, **97,** 1409.

Bleecker, A.B. (1998) The evolutionary basis of leaf senescence: Method to the madness? *Current Opinion in Plant Biology*, **1,** 73-78.

Bolle, C., Sopory, S., Lübberstedt, T., Herrmann, R.G. and Oelmüler, R. (1994) Segments encoding 5´untranslated leaders of genes for thylakoid proteins contain cis-elements essential for transcription. *The Plant Journal,* **6,** 513-523.

Bradford, M.M. (1976) A rapid and sensitive method for the quantitation of microgram quantities of protein utilizing the principle of protein-dye binding. *Analytical biochemistry,* **72,** 248-254.

Breeze, E., Harrison, E., McHattie, S., Hughes, L., Hickman, R., Hill, C., Kiddle, S., Kim, Y., Penfold, C.A. and Jenkins, D. (2011) High-Resolution Temporal Profiling of Transcripts during *Arabidopsis* Leaf Senescence Reveals a Distinct Chronology of Processes and Regulation. *The Plant Cell Online*, **23,** 873.

Buchanan-Wollaston, V. (1994) Isolation of cDNA Clones for Genes That Are Expressed during Leaf Senescence in *Brassica napus* (Identification of a Gene Encoding a Senescence-Specific Metallothionein-Like Protein). *Plant Physiology*, **105,** 839-846.

Buchanan-Wollaston, V. (1997) The molecular biology of leaf senescence. *Journal of Experimental Botany*, **48,** 181.

Buchanan-Wollaston, V., Earl, S., Harrison, E., Mathas, E., Navabpour, S., Page, T. and Pink, D. (2003) The molecular analysis of leaf senescences - a genomics approach. *Plant Biotechnology Journal*, **1,** 3-22.

Buchanan-Wollaston, V., Page, T., Harrison, E., Breeze, E., Lim, P.O., Nam, H.G., Lin, J.F., Wu, S.H., Swidzinski, J. and Ishizaki, K. (2005) Comparative transcriptome analysis reveals significant differences in gene expression and signalling pathways between developmental and dark/starvation-induced senescence in *Arabidopsis. The Plant Journal*, **42,** 567-585.

Caldana, C., Scheible, W.R., Mueller-Roeber, B. and Ruzicic, S. (2007) A quantitative RT-PCR platform for high-throughput expression profiling of 2500 rice transcription factors. *Plant Methods*, **3,** 7.

Carbonell-Bejerano, P., Urbez, C., Carbonell, J., Granell, A. and Perez-Amador, M.A. (2010) A fertilization-independent developmental program triggers partial fruit development and senescence processes in pistils of *Arabidopsis. Plant Physiology*, **154,** 163-172.

Cheng, S.H., Willmann, M.R., Chen, H.C. and Sheen, J. (2002) Calcium signaling through protein kinases. The *Arabidopsis* calcium-dependent protein kinase gene family. *Plant Physiology*, **129,** 469-485.

Chiba, A., Ishida, H., Nishizawa, N.K., Makino, A. and Mae, T. (2003) Exclusion of ribulose-1, 5-bisphosphate carboxylase/oxygenase from chloroplasts by specific bodies in naturally senescing leaves of wheat. *Plant and Cell Physiology*, **44,** 914.

Christiansen, M., Holm, P. and Gregersen, P. (2011) Characterization of barley (*Hordeum vulgare L.*) NAC transcription factors suggests conserved functions compared to both monocots and dicots. *BMC Research Notes*, **4.**

Clough, S.J. and Bent, A.F. (1998) Floral dip: a simplified method for *Agrobacterium*-mediated transformation of *Arabidopsis thaliana. The Plant Journal*, **16,** 735-743.

Clouse, S.D. (1997) Molecular genetic analysis of brassinosteroid action. *Physiologia Plantarum*, **100,** 702-709.

Clouse, S.D., Langford, M. and McMorris, T.C. (1996) A brassinosteroid-insensitive mutant in *Arabidopsis thaliana* exhibits multiple defects in growth and development. *Plant Physiology*, **111,** 671-678.

Collinge, D.B., Jensen, M.K., Lyngkjaer, M.F. and Rung, J. (2008) How can we exploit functional genomics approaches for understanding the nature of plant defences? Barley as a case study. *Sustainable disease management in a European context*, 257-266.

Creelman, R.A. and Mullet, J.E. (1997) Biosynthesis and action of jasmonates in plants. *Annual Review of Plant Biology*, **48,** 355-381.

Cullis, P.R., Fenske, D.B. and Hope, M.J. (1996) Biochemistry of Lipids, Lipoproteins and Membranes. *by DE Vance & J. Vance*, **20,** 1-41.

Daraselia, N.D., Tarchevskaya, S. and Narita, J.O. (1996) The promoter for tomato 3-hydroxy-3-methylglutaryl coenzyme A reductase gene 2 has unusual regulatory elements that direct high-level expression. *Plant Physiology*, **112,** 727-733.

Davuluri, R., Sun, H., Palaniswamy, S., Matthews, N., Molina, C., Kurtz, M. and Grotewold, E. (2003) AGRIS: *Arabidopsis* gene regulatory information server, an information resource of *Arabidopsis cis*-regulatory elements and transcription factors. *BMC Bioinformatics*, **4,** 25.

de Zélicourt, A., Diet, A., Marion, J., Laffont, C., Ariel, F., Moison, M., Zahaf, O., Crespi, M., Gruber, V. and Frugier, F. (2011) Dual involvement of a Medicago truncatula NAC transcription factor in root abiotic stress response and symbiotic nodule senescence. *The Plant Journal*.

Duval, M., Hsieh, T.F., Kim, S.Y. and Thomas, T.L. (2002) Molecular characterization of AtNAM: a member of the *Arabidopsis* NAC domain superfamily. *Plant molecular biology*, **50,** 237-248.

Eckardt, N.A. (2009) A new chlorophyll degradation pathway. *The Plant Cell Online*, **21,** 700-700.

Ellis, R.J. (1979) The most abundant protein in the world. *Trends in Biochemical Sciences*, **4,** 241-244.

Ernst, H.A., Olsen, A.N., Skriver, K., Larsen, S. and Leggio, L.L. (2004) Structure of the conserved domain of ANAC, a member of the NAC family of transcription factors. *EMBO reports*, **5,** 297-303.

Evans, I.M., Rus, A.M., Belanger, E.M., Kimoto, M. and Brusslan, J.A. (2009) Dismantling of *Arabidopsis thaliana* mesophyll cell chloroplasts during natural leaf senescence. *Plant Biology*, **12,** 1-12.

Facciotti, M.T., Reiss, D.J., Pan, M., Kaur, A., Vuthoori, M., Bonneau, R., Shannon, P., Srivastava, A., Donohoe, S.M. and Hood, L.E. (2007) General transcription factor specified global gene regulation in *archaea. Proceedings of the National Academy of Sciences*, **104**, 4630.

Fait, A., Nesi, A.N., Angelovici, R., Lehmann, M., Pham, P.A., Song, L., Haslam, R.P., Napier, J.A., Galili, G. and Fernie, A.R. (2011) Targeted Enhancement of Glutamate-to- γ- Aminobutyrate Conversion in *Arabidopsis* Seeds Affects Carbon-Nitrogen Balance and Storage Reserves in a Development-Dependent Manner. *Plant Physiology,* **157,** 1026-1042.

Farage-Barhom, S., Burd, S., Sonego, L., Mett, A., Belausov, E., Gidoni, D. and Lers, A. (2011) Localization of the *Arabidopsis* Senescence-and Cell Death-Associated BFN1 Nuclease: From the ER to Fragmented Nuclei. *Molecular plant*.

Farage-Barhom, S., Burd, S., Sonego, L., Perl-Treves, R. and Lers, A. (2008) Expression analysis of the BFN1 nuclease gene promoter during senescence, abscission, and programmed cell death-related processes. *Journal of Experimental Botany*, **59,** 3247.

Feilner, T., Hultschig, C., Lee, J., Meyer, S., Immink, R.G.H., Koenig, A., Possling, A., Seitz, H., Beveridge, A. and Scheel, D. (2005) High throughput identification of potential *Arabidopsis* mitogen-activated protein kinases substrates. *Molecular & Cellular Proteomics*, **4,** 1558-1568.

Feller, U., Anders, I. and Demirevska, K. (2008a) Degradation of Rubisco and other chloroplast proteins under abiotic stress. *General and Applied Plant Physiology*, **34,** 5-8.

Feller, U., Anders, I. and Mae, T. (2008b) Rubiscolytics: fate of Rubisco after its enzymatic function in a cell is terminated. *Journal of Experimental Botany*, **59,** 1615.

Ferguson, C.H.R. and Simon, E.W. (1973) Membrane Lipids in Senescing Green Tissues2. *Journal of Experimental Botany*, **24,** 307-316.

Ferrándiz, C., Pelaz, S. and Yanofsky, M.F. (1999) Control of carpel and fruit development in *Arabidopsis. Annual Review of Biochemistry*, **68,** 321-354.

Fong, F. and Heath, R.L. (1977) Age dependent changes in phospholipids and galactolipids in primary bean leaves (*Phaseolus vulgaris*). *Phytochemistry*, **16,** 215-217.

Forde, B.G. and Lea, P.J. (2007) Glutamate in plants: metabolism, regulation, and signalling. *Journal of Experimental Botany,* **58,** 2339-2358.

Freeman, B.A., Platt-Aloia, K., Mudd, J.B. and Thomson, W.W. (1978) Ultrastructural and lipid changes associated with the aging of citrus leaves. *Protoplasma*, **94,** 221-233.

Fridlender, M., Lev-Yadun, S., Baburek, I., Angelis, K. and Levy, A.A. (1996) Cell divisions in cotyledons after germination: localization, time course and utilization for a mutagenesis assay. *Planta,* **199,** 307-313.

Furihata, T., Maruyama, K., Fujita, Y., Umezawa, T., Yoshida, R., Shinozaki, K. and Yamaguchi-Shinozaki, K. (2006) Abscisic acid-dependent multisite phosphorylation regulates the activity of a transcription activator AREB1. *Proceedings of the National Academy of Sciences of the United States of America*, **103,** 1988-1993.

Gan, S. (2003) Mitotic and postmitotic senescence in plants. Science of Aging Knowledge Environment, **2003,** 7.

Gan, S. (2010) The hormonal regulation of senescence. *Plant Hormones*, 597-617.

Gan, S. and Amasino, R.M. (1995) Inhibition of leaf senescence by autoregulated production of cytokinin. *Science*, **270,** 1986.

Gan, S. and Amasino, R.M. (1996) Cytokinins in plant senescence: from spray and pray to clone and play. *Bioessays*, **18,** 557-565.

Gan, S. and Amasino, R.M. (1997) Making Sense of Senescence (Molecular Genetic Regulation and Manipulation of Leaf Senescence). *Plant Physiology*, **113,** 313.

Gaspar, T., Franck, T., Bisbis, B., Kevers, C., Jouve, L., Hausman, J.F. and Dommes, J. (2002) Concepts in plant stress physiology. Application to plant tissue cultures. *Plant Growth Regulation*, **37,** 263-285.

Gasteiger, E., Gattiker, A., Hoogland, C., Ivanyi, I., Appel, R.D. and Bairoch, A. (2003) ExPASy: the proteomics server for in-depth protein knowledge and analysis. *Nucleic Acids Research*, **31,** 3784-3788.

Geng, J. and Klionsky, D.J. (2008) The Atg8 and Atg12 ubiquitin-like conjugation systems in macroautophagy. *EMBO reports*, **9,** 859-864.

Gentleman, R.C., Carey, V.J., Bates, D.M., Bolstad, B., Dettling, M., Dudoit, S., Ellis, B., Gautier, L., Ge, Y. and Gentry, J. (2004) Bioconductor: open software development for computational biology and bioinformatics. *Genome Biology*, **5,** R80.

Gepstein, S., Sabehi, G., Carp, M.J., Hajouj, T., Nesher, M.F.O., Yariv, I., Dor, C. and Bassani, M. (2003) Large-scale identification of leaf senescence-associated genes. *The Plant Journal*, **36,** 629-642.

Gerhardt, B. (1992) Fatty acid degradation in plants. *Progress in lipid research*, **31,** 417.

Godbold, D.L. (1998) Stress concepts and forest trees. *Chemosphere*, **36,** 859-864.

Golldack-Brockhausen, D., Luking, I. and Yang, O. (2011) Plant tolerance to drought and salinity: stress regulating transcription factors and their functional significance in the cellular transcriptional network. *Plant Cell Reports*, **30,** 1383-1391.

Goodstein, D.M., Shu, S., Howson, R., Neupane, R., Hayes, R.D., Fazo, J., Mitros, T., Dirks, W., Hellsten, U. and Putnam, N. (2012) Phytozome: a comparative platform for green plant genomics. *Nucleic Acids Research*, **40,** D1178-D1186.

Gottesman, S. (1996) Proteases and their targets in *Escheriquia coli. Annual Review of Genetics*, **30,** 465-506.

Graham, I.A. (2008) Seed storage oil mobilization. *Annu. Rev. Plant Biol.*, **59,** 115-142.

Grbic and Bleecker, A.B. (1995) Ethylene regulates the timing of leaf senescence in *Arabidopsis. The Plant Journal*, **8,** 595-602.

Greve, K., La Cour, T., Jensen, M.K., Poulsen, F.M. and Skriver, K. (2003) Interactions between plant RING-H2 and plant-specific NAC (NAM/ATAF1/2/CUC2) proteins: RING-H2 molecular specificity and cellular localization. *Biochemical Journal*, 371, 97.

Grudkowska, M. and Zagdanska, B. (2004) Multifunctional role of plant cysteine proteinases. *Acta Biochimica Polonica-English Edition-*, 609-624.

Guo, A., He, K., Liu, D., Bai, S., Gu, X., Wei, L. and Luo, J. (2005) DATF: a database of *Arabidopsis* transcription factors. *Bioinformatics*, **21,** 2568-2569.

Guo, Y., Cai, Z. and Gan, S. (2004) Transcriptome of *Arabidopsis* leaf senescence. *Plant, Cell & Environment*, **27,** 521-549.

Guo, Y. and Gan, S. (2006) AtNAP, a NAC family transcription factor, has an important role in leaf senescence. *The Plant Journal*, **46,** 601-612.

Guo, Y. and Gan, S.S. (2012) Convergence and divergence in gene expression profiles induced by leaf senescence and 27 senescence-promoting hormonal, pathological and environmental stress treatments. *Plant, Cell & Environment*, **35,** 644-655.

Hao, Y.J., Song, Q.X., Chen, H.W., Zou, H.F., Wei, W., Kang, X.S., Ma, B., Zhang, W.K., Zhang, J.S. and Chen, S.Y. (2010) Plant NAC-type transcription factor proteins contain a NARD domain for repression of transcriptional activation. *Planta,* **232,** 1033-1043.

Harms, K., Atzorn, R., Brash, A., Kuhn, H., Wasternack, C., Willmitzer, L. and Pena-Cortes, H. (1995) Expression of a flax allene oxide synthase cDNA leads to increased endogenous jasmonic acid (JA) levels in transgenic potato plants but not to a corresponding activation of JA-responding genes. *The Plant Cell Online*, **7,** 1645-1654.

Harwood, J.L., Jones, A.V.H.M. and Thomas, H. (1982) Leaf senescence in a non-yellowing mutant of *Festuca pratensis. Planta*, **156,** 152-157.

He, X.J., Mu, R.L., Cao, W.H., Zhang, Z.G., Zhang, J.S. and Chen, S.Y. (2005) AtNAC2, a transcription factor downstream of ethylene and auxin signaling pathways, is involved in salt stress response and lateral root development. *The Plant Journal*, **44,** 903-916.

He, Y., Fukushige, H., Hildebrand, D.F. and Gan, S. (2002) Evidence supporting a role of jasmonic acid in *Arabidopsis* leaf senescence. *Plant Physiology*, **128,** 876-884.

He, Y. and Gan, S. (2002) A gene encoding an acyl hydrolase is involved in leaf senescence in *Arabidopsis. The Plant Cell Online*, **14,** 805-815.

He, Y., Tang, W., Swain, J.D., Green, A.L., Jack, T.P. and Gan, S. (2001) Networking senescence-regulating pathways by using *Arabidopsis* enhancer trap lines. *Plant Physiology*, **126,** 707-716.

Hegedus, D., Yu, M., Baldwin, D., Gruber, M., Sharpe, A., Parkin, I., Whitwill, S. and Lydiate, D. (2003) Molecular characterization of Brassicanapus NAC domain transcriptional activators induced in response to biotic and abiotic stress. *Plant molecular biology*, **53,** 383-397.

Hill, J. (1980) The remobilization of nutrients from leaves. *Journal of Plant Nutrition*, 2, 407-444.

Himelblau, E. and Amasino, R.M. (2001) Nutrients mobilized from leaves of *Arabidopsis thaliana* during leaf senescence. *Journal of Plant Physiology*, **158,** 1317-1323.

Hinder, B., Schellenberg, M., Rodoni, S., Ginsburg, S., Vogt, E., Martinoia, E., Matile, P. and Hörtensteiner, S. (1996) How plants dispose of chlorophyll catabolites. *Journal of Biological Chemistry*, **271,** 27233.

Hörtensteiner, S. and Feller, U. (2002) Nitrogen metabolism and remobilization during senescence. *Journal of Experimental Botany*, **53,** 927-937.

Hörtensteiner, S. (2006) Chlorophyll degradation during senescence. *Annu. Rev. Plant Biol.*, **57,** 55-77.

Howard, T., Lin, H., Mike, Y. and Helen, O. (2009) Evolution of plant senescence. *BMC Evolutionary Biology*, **9.**

Hruz, T., Laule, O., Szabo, G., Wessendorp, F., Bleuler, S., Oertle, L., Widmayer, P., Gruissem, W. and Zimmermann, P. (2008) Genevestigator V3: a reference expression database for the meta-analysis of transcriptomes. *Adv Bioinformatics*, **420747.**

Hurkman, W.J. (1979) Ultrastructural changes of chloroplasts in attached and detached, aging primary wheat leaves. *American Journal of Botany*, 64-70.

Iida, K., Fukami-Kobayashi, K., Toyoda, A., Sakaki, Y., Kobayashi, M., Seki, M. and Shinozaki, K. (2009) Analysis of multiple occurrences of alternative splicing events in *Arabidopsis thaliana* using novel sequenced full-length cDNAs. *DNA research*, **16,** 155.

Ito, J. and Fukuda, H. (2002) ZEN1 is a key enzyme in the degradation of nuclear DNA during programmed cell death of tracheary elements. *The Plant Cell Online*, **14,** 3201-3211.

Jacob-Wilk, D., Holland, D., Goldschmidt, E.E., Riov, J. and Eyal, Y. (1999) Chlorophyll breakdown by chlorophyllase: isolation and functional expression of the Chlase1 gene from ethylene treated Citrus fruit and its regulation during development. *The Plant Journal*, **20,** 653-661.

Jefferson, R.A., Kavanagh, T.A. and Bevan, M.W. (1987) GUS fusions: beta-glucuronidase as a sensitive and versatile gene fusion marker in higher plants. *The EMBO Journal*, **6,** 3901.

Jiang, Y. and Deyholos, M.K. (2009) Functional characterization of *Arabidopsis* NaCl-inducible WRKY25 and WRKY33 transcription factors in abiotic stresses. *Plant molecular biology*, **69,** 91-105.

Jiang, Z., Liu, X., Peng, Z., Wan, Y., Ji, Y., He, W., Wan, W., Luo, J. and Guo, H. (2011) AHD2. 0: an update version of *Arabidopsis* Hormone Database for plant systematic studies. *Nucleic Acids Research*, **39,** D1123.

Jing, H.C., Anderson, L., Sturre, M.J.G., Hille, J. and Dijkwel, P.P. (2007) *Arabidopsis* CPR5 is a senescence-regulatory gene with pleiotropic functions as predicted by the evolutionary theory of senescence. *Journal of Experimental Botany*, **58,** 3885.

Kang, S.M., Matsui, H. and Titus, J.S. (1982) Characteristics and activity changes of proteolytic enzymes in apple leaves during autumnal senescence. *Plant Physiology*, **70,** 1367.

Kappers, I.F., Jordi, W., Tsesmetzis, N., Maas, F.M. and Van der Plas, L.H.W. (1998) GA 4 Does Not Require Conversion into GA1 to Delay Senescence of *Alstroemeria* hybrida Leaves. *Journal of Plant Growth Regulation*, **17,** 89-93.

Karimi, M., Inz, D. and Depicker, A. (2002) GATEWAY (TM) vectors for *Agrobacterium*-mediated plant transformation. *Trends in Plant Science*, **7,** 193-195.

Kaufmann, K., Muino, J.M., Jauregui, R., Airoldi, C.A., Smaczniak, C., Krajewski, P. and Angenent, G.C. (2009) Target genes of the MADS transcription factor SEPALLATA3:

integration of developmental and hormonal pathways in the *Arabidopsis* flower. *PLoS biology*, **7,** e1000090.

Kim, J.H., Woo, H.R., Kim, J., Lim, P.O., Lee, I.C., Choi, S.H., Hwang, D. and Nam, H.G. (2009) Trifurcate feed-forward regulation of age-dependent cell death involving miR164 in *Arabidopsis. Science*, **323,** 1053.

Kim, J.I., Murphy, A.S., Baek, D., Lee, S.W., Yun, D.J., Bressan, R.A. and Narasimhan, M.L. (2011) YUCCA6 over-expression demonstrates auxin function in delaying leaf senescence in *Arabidopsis thaliana. Journal of Experimental Botany*, **62,** 3981-3992.

Kim, S.G. and Park, C.M. (2008) Gibberellic acid-mediated salt signaling in seed germination. *Plant signaling & behavior*, **3,** 877.

Kim, S.Y., Kim, S.G., Kim, Y.S., Seo, P.J., Bae, M., Yoon, H.K. and Park, C.M. (2007) Exploring membrane-associated NAC transcription factors in *Arabidopsis*: implications for membrane biology in genome regulation. *Nucleic Acids Research*, **35,** 203-213.

Kirkwood, T.B.L. and Austad, S.N. (2000) Why do we age? *NATURE-LONDON-*, 233-238.

Kirkwood, T.B.L. and Cremer, T. (1982) Cytogerontology since 1881: a reappraisal of August Weismann and a review of modern progress. *Human Genetics*, **60,** 101-121.

Kleber-Janke, T. and Krupinska, K. (1997) Isolation of cDNA clones for genes showing enhanced expression in barley leaves during dark-induced senescence as well as during senescence under field conditions. *Planta*, **203,** 332-340.

Klionsky, D.J. and Ohsumi, Y. (1999) Vacuolar import of proteins and organelles from the cytoplasm. *Annual Review of Cell and Developmental Biology*, **15,** 1-32.

Knight, H., Trewavas, A.J. and Knight, M.R. (1997) Calcium signalling in *Arabidopsis thaliana* responding to drought and salinity. *The Plant Journal*, **12,** 1067-1078.

Koiwai, A., Matsuzaki, T., Suzuki, F. and Kawashima, N. (1981) Changes in total and polar lipids and their fatty acid composition in tobacco leaves during growth and senescence. *Plant and Cell Physiology*, **22,** 1059.

Kräutler, B. and Hörtensteiner, S. (2006) Chlorophyll catabolites and the biochemistry of chlorophyll breakdown. *Chlorophylls and Bacteriochlorophylls*, 237-260.

Krebs, E.G. (1993) Protein phosphorylation and cellular regulation I (Nobel lecture). *Angewandte Chemie International Edition in English*, **32,** 1122-1129.

Laemmli, U.K. (1970) Cleavage of structural proteins during the assembly of the head of bacteriophage T4. *Nature*, **227,** 680-685.

Lang, D., Weiche, B., Timmerhaus, G., Richardt, S., Riaño-Pachón, D.M., Corréa, L.G.G., Reski, R., Mueller-Roeber, B. and Rensing, S.A. (2010) Genome-wide phylogenetic comparative analysis of plant transcriptional regulation: a timeline of loss, gain, expansion, and correlation with complexity. *Genome Biology and Evolution*, **2,** 488-503.

Latchman, D.S. (2008) *Eukaryotic transcription factors:* Academic press.

Lee, B.H. and Zhu, J.K. (2010) Phenotypic analysis of *Arabidopsis* mutants: germination rate under salt/hormone-induced stress. *Cold Spring Harb Protoc*, **2010.**

Lers, A., Lomaniec, E., Burd, S. and Khalchitski, A. (2001) The characterization of LeNUC1, a nuclease associated with leaf senescence of tomato. *Physiologia Plantarum,* **112,** 176-182.

Lescot, M., Déhais, P., Thijs, G., Marchal, K., Moreau, Y., Van de Peer, Y., Rouzé, P. and Rombauts, S. (2002) PlantCARE, a database of plant cis-acting regulatory elements and a portal to tools for in silico analysis of promoter sequences. *Nucleic Acids Research*, **30,** 325-327.

Li, Y., Rosso, M.G., Strizhov, N., Viehoever, P. and Weisshaar, B. (2003) GABI-Kat SimpleSearch: a flanking sequence tag (FST) database for the identification of T-DNA insertion mutants in *Arabidopsis thaliana. Bioinformatics*, **19,** 1441.

Licausi, F., Weits, D.A., Pant, B.D., Scheible, W.R., Geigenberger, P. and Van Dongen, J.T. (2011) Hypoxia responsive gene expression is mediated by various subsets of transcription factors and miRNAs that are determined by the actual oxygen availability. *New Phytologist*, **190,** 442-456.

Lim, P.O., Kim, H.J. and Gil Nam, H. (2007) Leaf senescence. *Annu. Rev. Plant Biol.*, **58,** 115-136.

Lim, P.O., Woo, H.R. and Nam, H.G. (2003) Molecular genetics of leaf senescence in *Arabidopsis. Trends in Plant Science*, **8,** 272-278.

Lin, J.F. and Wu, S.H. (2004) Molecular events in senescing *Arabidopsis* leaves. *The Plant Journal*, **39,** 612-628.

Liu, J., Wu, Y.H., Yang, J.J., Liu, Y.D. and Shen, F.F. (2008) Protein degradation and nitrogen remobilization during leaf senescence. *Journal of Plant Biology*, **51,** 11-19.

López-Molina, L., Mongrand, S. and Chua, N.H. (2001) A postgermination developmental arrest checkpoint is mediated by abscisic acid and requires the ABI5 transcription factor in Arabidopsis. *Proceedings of the National Academy of Sciences*, **98,** 4782.

Lu, P.L., Chen, N.Z., An, R., Su, Z., Qi, B.S., Ren, F., Chen, J. and Wang, X.C. (2007) A novel drought-inducible gene, ATAF1, encodes a NAC family protein that negatively regulates the expression of stress-responsive genes in *Arabidopsis. Plant molecular biology*, **63,** 289-305.

Luscombe, N.M. and Thornton, J.M. (2002) Protein-DNA interactions: amino acid conservation and the effects of mutations on binding specificity. *Journal of Molecular Biology*, **320,** 991-1010.

Mandre, M. (2002) Stress concepts and plants. *Metsanduslikud uurimused*.

Marcotte Jr, W.R., Russell, S.H. and Quatrano, R.S. (1989) Abscisic acid-responsive sequences from the Em gene of wheat. *The Plant Cell Online*, **1,** 969-976.

Martínez, D.E., Costa, M.L., Gomez, F.M., Otegui, M.S. and Guiamet, J.J. (2008) "Senescence-associated vacuoles" are involved in the degradation of chloroplast proteins in tobacco leaves. *The Plant Journal*, **56,** 196-206.

Masferrer, A., Arro, M., Manzano, D., Schaller, H., Fernández-Busquets, X., Moncalean, P., Fernández, B., Cunillera, N., Boronat, A. and Ferrer, A. (2002) Overexpression of *Arabidopsis thaliana* farnesyl diphosphate synthase (FPS1S) in transgenic *Arabidopsis*

induces a cell death/senescences-like response and reduced cytokinin levels. *The Plant Journal*, **30,** 123-132.

Matile, P., Hörtensteiner, S. and Thomas, H. (1999) Chlorophyll degradation. *Annual Review of Plant Biology*, **50,** 67-95.

Mattoo, A.K. and Aharoni, N. (1988) Ethylene and plant senescence. Chapter 8. In: Senescence and Aging of Plants (L. Nooden and A.C. Leopold, eds.), pp. 241-280. Academic Press, NY.

Mauch-Mani, B. and Flors, V. (2009) The ATAF1 transcription factor: at the convergence point of ABA-dependent plant defense against biotic and abiotic stresses. *Cell Research*, **19,** 1322-1323.

McCabe, M.S., Garratt, L.C., Schepers, F., Jordi, W.J.R.M., Stoopen, G.M., Davelaar, E., van Rhijn, J.H.A., Power, J.B. and Davey, M.R. (2001) Effects of PSAG12-IPT gene expression on development and senescence in transgenic lettuce. *Plant Physiology*, **127,** 505-516.

McKersie, B.D. and Thompson, J.E. (1978) Phase behavior of chloroplast and microsomal membranes during leaf senescence. *Plant Physiology*, **61,** 639.

Mei, H.S. and Thimann, K.V. (1984) The relation between nitrogen deficiency and leaf senescence. *Physiologia Plantarum*, **62,** 157-161.

Meshi, T. and Iwabuchi, M. (1995) Plant transcription factors. *Plant and Cell Physiology*, **36,** 1405.

Minamikawa, T., Toyooka, K., Okamoto, T., Hara-Nishimura, I. and Nishimura, M. (2001) Degradation of ribulose-bisphosphate carboxylase by vacuolar enzymes of senescing French bean leaves: immunocytochemical and ultrastructural observations. *Protoplasma*, **218,** 144-153.

Miyoshi, K., Kagaya, Y., Ogawa, Y., Nagato, Y. and Hattori, T. (2002) Temporal and spatial expression pattern of the OSVP1 and OSEM genes during seed development in rice. *Plant and Cell Physiology*, **43,** 307.

Morita, K. (1980) Release of nitrogen from chloroplasts during leaf senescence in rice (*Oryza sativa L.*). *Annals of Botany*, **46,** 297.

Morris, K., Mackerness, S.A.H., Page, T., John, C.F., Murphy, A.M., Carr, J.P. and Buchanan-Wollaston, V. (2000) Salicylic acid has a role in regulating gene expression during leaf senescence. *The Plant Journal*, **23,** 677-685.

Mundy, J., Yamaguchi-Shinozaki, K. and Chua, N.H. (1990) Nuclear proteins bind conserved elements in the abscisic acid-responsive promoter of a *rice rab* gene. *Proceedings of the National Academy of Sciences*, **87,** 1406.

Murashige, T. and Skoog, F. (1962) A revised medium for rapid growth and bio assays with tobacco tissue cultures. *Physiologia Plantarum*, **15,** 473-497.

Nakashima, K., Takasaki, H., Mizoi, J., Shinozaki, K. and Yamaguchi-Shinozaki, K. (2011) NAC Transcription Factors in Plant Abiotic Stress Responses. *Biochimica et Biophysica Acta (BBA)-Gene Regulatory Mechanisms*, **1819,** 97-103.

Nakashima, K., Tran, L.S.P., Van Nguyen, D., Fujita, M., Maruyama, K., Todaka, D., Ito, Y., Hayashi, N., Shinozaki, K. and Yamaguchi-Shinozaki, K. (2007) Functional

analysis of a NAC-type transcription factor OsNAC6 involved in abiotic and biotic stress-responsive gene expression in rice. *The Plant Journal*, **51,** 617-630.

Nam, H.G. (1997) The molecular genetic analysis of leaf senescence. *Current Opinion in Biotechnology*, **8,** 200-207.

Nelson, C.J. (1988) Genetic associations between photosynthetic characteristics and yield: review of the evidence. *Plant Physiology and Biochemistry*, **26,** 543-554.

Nishimura, M., Takeuchi, Y., De Bellis, L. and Hara-Nishimura, I. (1993) Leaf peroxisomes are directly transformed to glyoxysomes during senescence of pumpkin cotyledons. *Protoplasma*, **175,** 131-137.

Noodén, L.D. and Guiamet, J.J. (1996) Genetic control of senescence and aging in plants. *Handbook of the Biology of Aging*, 94-118.

Noodén, L.D. and Leopold, A.C. (1988) *Senescence and aging in plants:* Academic Press. 526 pp.

Olsen, A.N., Ernst, H.A., Leggio, L.L. and Skriver, K. (2005a) DNA-binding specificity and molecular functions of NAC transcription factors. *Plant Science*, **169,** 785-797.

Olsen, A.N., Ernst, H.A., Leggio, L.L. and Skriver, K. (2005b) NAC transcription factors: structurally distinct, functionally diverse. *Trends in Plant Science*, **10,** 79-87.

Ooka, H., Satoh, K., Doi, K., Nagata, T., Otomo, Y., Murakami, K., Matsubara, K., Osato, N., Kawai, J. and Carninci, P. (2003) Comprehensive analysis of NAC family genes in *Oryza sativa* and *Arabidopsis thaliana. DNA research*, **10,** 239-247.

Orcutt, D.M. and Hale, M.G. (2000) The physiology of plants under stress: soil and biotic factors: John Wiley & Sons Inc.

Otegui, M.S., Noh, Y.-S., Martínez, D.E., Vila Petroff, M.G., Andrew Staehelin, L., Amasino, R.M. and Guiamet, J.J. (2005) Senescence-associated vacuoles with intense proteolytic activity develop in leaves of *Arabidopsis* and soybean. *The Plant Journal*, **41,** 831-844.

Ougham, H., Hörtensteiner, S., Armstead, I., Donnison, I., King, I., Thomas, H. and Mur, L. (2008) The control of chlorophyll catabolism and the status of yellowing as a biomarker of leaf senescence. *Plant Biology*, **10,** 4-14.

Pablo, C.B., Cristina, U., Antonio, G., Juan, C. and Miguel, P.A. (2011) Ethylene is involved in pistil fate by modulating the onset of ovule senescence and the GA-mediated fruit set in *Arabidopsis. BMC Plant Biology*, **11.**

Paliyath, G. and Droillard, M.J. (1992) The mechanisms of membrane deterioration and disassembly during senescence. *Plant Physiology and Biochemistry*, **30,** 789-812.

Panavas, T. (1999) Programmed cell death in daylily (*Hemerocallis* hybrid) petals: biochemical and molecular aspects: University of Massachusetts at Amherst.

Park, H.C., Kim, M.L., Kim, H.S., Park, J.H., Jung, M.S., Shen, M., Kang, C.H., Kim, M.C. and Lee, S.Y. (2010) Specificity of DNA sequences recognized by the zinc-finger homeodomain protein, GmZF-HD1 in soybean. *Phytochemistry*, **71,** 1832-1838.

Park, J.H., Oh, S.A., Kim, Y.H., Woo, H.R. and Nam, H.G. (1998) Differential expression of senescence-associated mRNAs during leaf senescence induced by different senescence-inducing factors in *Arabidopsis. Plant molecular biology*, **37,** 445-454.

Parlitz, S., Kunze, R., Mueller-Roeber, B. and Balazadeh, S. (2011) Regulation of photosynthesis and transcription factor expression by leaf shading and re-illumination in *Arabidopsis thaliana* leaves. *Journal of Plant Physiology*, **168,** 1311-1319.

Parthier, B. (1988) Gerontoplasts- the yellow end in the ontogenesis of chloroplasts. *Endocytobiosis Cell Res*, **5,** 163-190.

Patterson, S.E. and Bleecker, A.B. (2004) Ethylene-dependent and-independent processes associated with floral organ abscission in *Arabidopsis. Plant Physiology*, **134,** 194-203.

Penfield, S., Li, Y., Gilday, A.D., Graham, S. and Graham, I.A. (2006) *Arabidopsis ABA INSENSITIVE4* regulates lipid mobilization in the embryo and reveals repression of seed germination by the endosperm. *The Plant Cell Online*, **18,** 1887-1899.

Pérez-Amador, M.A., Abler, M.L., De Rocher, E.J., Thompson, D.M., van Hoof, A., LeBrasseur, N.D., Lers, A. and Green, P.J. (2000) Identification of BFN1, a bifunctional nuclease induced during leaf and stem senescence in *Arabidopsis. Plant Physiology*, **122,** 169-180.

Pérez-Rodríguez, P., Riaño-Pachón, D.M., Corréa, L.G.G., Rensing, S.A., Kersten, B. and Mueller-Roeber, B. (2010) PlnTFDB: updated content and new features of the plant transcription factor database. *Nucleic Acids Research*, **38,** D822-D827.

Pesquet, E., Korolev, A.V., Calder, G. and Lloyd, C.W. (2010) The microtubule-associated protein AtMAP70-5 regulates secondary wall patterning in *Arabidopsis* wood cells. *Current Biology*, **20,** 744-749.

Pontier, D., Gan, S., Amasino, R.M., Roby, D. and Lam, E. (1999) Markers for hypersensitive response and senescence show distinct patterns of expression. *Plant molecular biology*, **39,** 1243-1255.

Popescu, S.C., Popescu, G.V., Bachan, S., Zhang, Z., Gerstein, M, Snyder, M. and Dinesh-Kumar, S.P. (2009) MAPK target networks in *Arabidopsis thaliana* revealed using functional protein microarrays. *Genes & Development*, **23,** 80-92.

Quirino, B.F., Noh, Y.S., Himelblau, E. and Amasino, R.M. (2000) Molecular aspects of leaf senescence. *Trends in Plant Science*, **5,** 278-282.

Ranwala, A.P. and Miller, W.B. (2000) Preventive mechanisms of gibberellin4+7 and light on low-temperature-induced leaf senescence in Lilium cv. Stargazer. *Postharvest biology and technology*, **19,** 85-92.

Redman, J.C., Haas, B.J., Tanimoto, G. and Town, C.D. (2004) Development and evaluation of an *Arabidopsis* whole genome Affymetrix probe array. *The Plant Journal*, **38,** 545-561.

Rice, P., Longden, I. and Bleasby, A. (2000) EMBOSS: the European molecular biology open software suite. *Trends in Genetics*, **16,** 276-277.

Richmond, A.E. and Lang, A. (1957) Effect of kinetin on protein content and survival of detached Xanthium leaves. *Science*, **125,** 650.

Riechmann, J.L., Heard, J., Martin, G. and Reuber, L. (2000) *Arabidopsis* transcription factors: genome-wide comparative analysis among eukaryotes. *Science*, **290,** 2105.

Roberts, I.N., Murray, P.F., Caputo, C.P., Passeron, S. and Barneix, A.J. (2003) Purification and characterization of a subtilisin-like serine protease induced during the senescence of wheat leaves. *Physiologia Plantarum*, **118,** 483-490.

Roca, M. and Mínguez-Mosquera, M.I. (2003) Involvement of chlorophyllase in chlorophyll metabolism in olive varieties with high and low chlorophyll content. *Physiologia Plantarum*, **117,** 459-466.

Rodoni, S., Muhlecker, W., Anderl, M., Krautler, B., Moser, D., Thomas, H., Matile, P. and Hortensteiner, S. (1997) Chlorophyll breakdown in senescent chloroplasts (cleavage of pheophorbide a in two enzymic steps). *Plant Physiology*, **115,** 669-676.

Rushton, P.J., Torres, J.T., Parniske, M., Wernert, P., Hahlbrock, K. and Somssich, I.E. (1996) Interaction of elicitor-induced DNA-binding proteins with elicitor response elements in the promoters of parsley PR1 genes. *The EMBO Journal*, **15,** 5690.

Sakamoto, W. (2006) Protein degradation machineries in plastids. *Annu. Rev. Plant Biol.*, **57,** 599-621.

Sambrook, J. and Russell, D.W. (2001) *Molecular cloning: a laboratory manual:* CSHL press.

Schenk, N., Schelbert, S., Kanwischer, M., Goldschmidt, E.E., Dörmann, P. and Hörtensteiner, S. (2007) The chlorophyllases AtCLH1 and AtCLH2 are not essential for senescence-related chlorophyll breakdown in *Arabidopsis thaliana*. *FEBS letters*, **581,** 5517-5525.

Schmid, K.M. and Ohlrogge, J.B. (2002) Lipid metabolism in plants. *New Comprehensive Biochemistry*, **36,** 93-126.

Seki, M., Narusaka, M., Ishida, J., Nanjo, T., Fujita, M., Oono, Y., Kamiya, A., Nakajima, M., Enju, A. and Sakurai, T. (2002) Monitoring the expression profiles of 7000 *Arabidopsis* genes under drought, cold and high-salinity stresses using a full-length cDNA microarray. *The Plant Journal*, **31,** 279-292.

Seo, P.J., Kim, S.G. and Park, C.M. (2008) Membrane-bound transcription factors in plants. *Trends in Plant Science*, **13,** 550-556.

Sheen, J. (2002) A transient expression assay using *Arabidopsis* mesophyll protoplasts.

Shioi, Y., Tomita, N., Tsuchiya, T. and Takamiya, K.I. (1996) Conversion of chlorophyllide to pheophorbide by Mg-dechelating substance in extracts of *Chenopodium album*. *Plant Physiology and Biochemistry*, **34,** 41-47.

Skirycz, A., Reichelt, M., Burow, M., Birkemeyer, C., Rolcik, J., Kopka, J., Zanor, M.I., Gershenzon, J., Strnad, M. and Szopa, J. (2006) DOF transcription factor *AtDof1. 1* (*OBP2*) is part of a regulatory network controlling glucosinolate biosynthesis in *Arabidopsis*. *The Plant Journal*, **47,** 10-24.

Skriver, K., Jensen, M.K., Kjaersgaard, T., Nielsen, M.M., Galberg, P., Petersen, K. and O'Shea, C. (2010) The *Arabidopsis thaliana* NAC transcription factor family: structure-function relationships and determinants of ANAC019 stress signaling. *Biochemical Journal*, **426,** 183-196.

Smalle, J. and Vierstra, R.D. (2004) The ubiquitin 26S proteasome proteolytic pathway. *Annu. Rev. Plant Biol.*, **55,** 555-590.

Smart, C.M. (1994) Tansley Review No. 64. Gene Expression During Leaf Senescence. *New Phytologist*, 419-448.

Smyth, D.R., Bowman, J.L. and Meyerowitz, E.M. (1990) Early flower development in *Arabidopsis. The Plant Cell Online*, **2,** 755-767.

Souer, E., van Houwelingen, A., Kloos, D., Mol, J. and Koes, R. (1996) The No Apical Meristem Gene of Petunia Is Required for Pattern Formation in Embryos and Flowers and Is Expressed at Meristem and Primordia Boundaries. *Cell*, **85,** 159-170.

Stitt, M. and Fernie, A.R. (2003) From measurements of metabolites to metabolomics: an ´on the fly' perspective illustrated by recent studies of carbon-nitrogen interactions. *Current Opinion in Biotechnology*, **14,** 136-144.

Sundqvist, C. and Dahlin, C. (1997) With chlorophyll pigments from prolamellar bodies to light-harvesting complexes. *Physiologia Plantarum*, **100,** 748-759.

Suzuki, J.Y., Bollivar, D.W. and Bauer, C.E. (1997) Genetic analysis of chlorophyll biosynthesis. *Annual Review of Genetics*, **31,** 61-89.

Tanaka, A. and Tanaka, R. (2006) Chlorophyll metabolism. *Current Opinion in Plant Biology*, **9,** 248-255.

Taylor, C.B., Bariola, P.A., Delcardayre, S.B., Raines, R.T. and Green, P.J. (1993) RNS2: a senescence-associated RNase of *Arabidopsis* that diverged from the S-RNases before speciation. *Proceedings of the National Academy of Sciences*, **90,** 5118.

Thatcher, L.F., Carrie, C., Andersson, C.R., Sivasithamparam, K., Whelan, J. and Singh, K.B. (2007) Differential gene expression and subcellular targeting of Arabidopsis glutathione S-transferase F8 is achieved through alternative transcription start sites. *Journal of Biological Chemistry,* **282,** 28915-28928.

Thomas, H. (1997) Chlorophyll: a symptom and a regulator of plastid development. *New Phytologist*, **136,** 163-181.

Thomas, H. (2002) Ageing in plants. *Mechanisms of ageing and development*, **123,** 747-753.

Thomas, H., Ougham, H.J., Wagstaff, C. and Stead, A.D. (2003) Defining senescence and death. *Journal of Experimental Botany*, **54,** 1127-1132.

Thompson, J.E., Froese, C.D., Madey, E., Smith, M.D. and YuWen, H. (1998) Lipid metabolism during plant senescence. *Progress in lipid research*, **37,** 119-141.

Thompson, J.E., Mayak, S., Shinitzky, M. and Halevy, A.H. (1982) Acceleration of membrane senescence in cut carnation flowers by treatment with ethylene. *Plant Physiology*, **69,** 859-863.

Tommasini, R., Vogt, E., Fromenteau, M., Hörtensteiner, S., Matile, P., Amrhein, N. and Martinoia, E. (1998) An ABC-transporter of *Arabidopsis thaliana* has both glutathione-conjugate and chlorophyll catabolite transport activity. *The Plant Journal*, **13,** 773-780.

Tompa, P. (2005) The interplay between structure and function in intrinsically unstructured proteins. *FEBS letters*, **579,** 3346-3354.

Tran, L.S., Nishiyama, R., Yamaguchi-Shinozaki, K. and Shinozaki, K. (2010) Potential utilization of NAC transcription factors to enhance abiotic stress tolerance in plants by biotechnological approach. *GM crops*, **1,** 32.

Tran, L.S.P., Nakashima, K., Sakuma, Y., Simpson, S.D., Fujita, Y., Maruyama, K., Fujita, M., Seki, M., Shinozaki, K. and Yamaguchi-Shinozaki, K. (2004) Isolation and functional analysis of *Arabidopsis* stress-inducible NAC transcription factors that bind to a drought-responsive cis-element in the early responsive to dehydration stress 1 promoter. *The Plant Cell Online*, **16,** 2481-2498.

Tsuchiya, T., Ohta, H., Okawa, K., Iwamatsu, A., Shimada, H., Masuda, T. and Takamiya, K. (1999) Cloning of chlorophyllase, the key enzyme in chlorophyll degradation: finding of a lipase motif and the induction by methyl jasmonate. *Proceedings of the National Academy of Sciences*, **96,** 15362.

Usadel, B., Nagel, A., Steinhauser, D., Gibon, Y., Bläsing, O., Redestig, H., Sreenivasulu, N., Krall, L., Hannah, M. and Poree, F. (2006) PageMan: an interactive ontology tool to generate, display, and annotate overview graphs for profiling experiments. *BMC bioinformatics*, 7, 535.

V., G. (2003) SAG2 and SAG12 protein expression in senescing *Arabidopsis* plants. *Physiologia Plantarum*, **119,** 263-269.

Van Der Graaff, E., Schwacke, R., Schneider, A., Desimone, M., Flügge, U.I. and Kunze, R. (2006) Transcription analysis of *Arabidopsis* membrane transporters and hormone pathways during developmental and induced leaf senescence. *Plant Physiology*, **141,** 776-792.

Vierstra, R.D. (1996) Proteolysis in plants: mechanisms and functions. *Plant molecular biology*, **32,** 275-302.

Wagstaff, C., Yang, T.J.W., Stead, A.D., Buchanan-Wollaston, V. and Roberts, J.A. (2009) A molecular and structural characterization of senescing *Arabidopsis* siliques and comparison of transcriptional profiles with senescing petals and leaves. *The Plant Journal*, **57,** 690-705.

Wang, X., Basnayake, B.M.V.S., Zhang, H., Li, G., Li, W., Virk, N., Mengiste, T. and Song, F. (2009) The *Arabidopsis* ATAF1, a NAC transcription factor, is a negative regulator of defense responses against necrotrophic fungal and bacterial pathogens. *Molecular Plant-Microbe Interactions*, **22,** 1227-1238.

Wanner, L., Keller, F. and Matile, P.H. (1991) Metabolism of radiolabelled galactolipids in senescent barley leaves. *Plant Science*, **78,** 199-206.

Warnes, G.R., Bolker, B. and Lumley, T. (2009) gplots: Various R programming tools for plotting data. *R package version*, **2.**

Weaver, L.M. and Amasino, R.M. (2001) Senescence is induced in individually darkened *Arabidopsis* leaves, but inhibited in whole darkened plants. *Plant Physiology*, **127,** 876-886.

Whitmarsh, A.J. and Davis, R.J. (2000) Regulation of transcription factor function by phosphorylation. *Cellular and Molecular Life Sciences*, **57,** 1172-1183.

Williams, G.C. (1957) Pleiotropy, natural selection, and the evolution of senescence. *Evolution*, **11,** 398-411.

Winter, D., Vinegar, B., Nahal, H., Ammar, R., Wilson, G.V. and Provart, N.J. (2007) An "Electronic fluorescent pictograph" browser for exploring and analyzing large-scale biological data sets. *PloS one*, **2,** e718.

Witte, C.P., Noel, L., Gielbert, J., Parker, J. and Romeis, T. (2004) Rapid one-step protein purification from plant material using the eight-amino acid StrepII epitope. *Plant molecular biology*, **55,** 135-147.

Wittenbach, V.A., Lin, W. and Hebert, R.R. (1982) Vacuolar localization of proteases and degradation of chloroplasts in mesophyll protoplasts from senescing primary wheat leaves. *Plant Physiology*, **69,** 98.

Woo, H.R., Kim, J.H., Nam, H.G. and Lim, P.O. (2004) The delayed leaf senescence mutants of *Arabidopsis*, ore1, ore3, and ore9 are tolerant to oxidative stress. *Plant and Cell Physiology*, **45,** 923.

Wu, A., Allu, A.D., Garapati, P., Siddiqui, H., Dortay, H., Zanor, M.I., Asensi-Fabado, M.A., Munné-Bosch, S., Antonio, C. and Tohge, T. (2012) JUNGBRUNNEN1, a Reactive Oxygen Species-Responsive NAC Transcription Factor, Regulates Longevity in *Arabidopsis. The Plant Cell Online*.

Wu, Y., Deng, Z., Lai, J., Zhang, Y., Yang, C., Yin, B., Zhao, Q., Zhang, L. and Li, Y. (2009) Dual function of *Arabidopsis* ATAF1 in abiotic and biotic stress responses. *Cell Research*, **19,** 1279-1290.

Wu, Z. and Irizarry, R.A. (2004) Preprocessing of oligonucleotide array data. *Nature biotechnology*, 22, 656-658.

Xie, Q., Frugis, G., Colgan, D. and Chua, N.H. (2000) *Arabidopsis* NAC1 transduces auxin signal downstream of TIR1 to promote lateral root development. *Genes & Development*, **14,** 3024.

Xu, W., Yu, Y., Zhou, Q., Ding, J., Dai, L., Xie, X., Xu, Y., Zhang, C. and Wang, Y. (2011) Expression pattern, genomic structure, and promoter analysis of the gene encoding stilbene synthase from Chinese wild *Vitis pseudoreticulata. Journal of Experimental Botany,* **62,** 2745-2761.

Xu, Y. and Hanson, M.R. (2000) Programmed cell death during pollination-induced petal senescence in Petunia. *Plant Physiology,* **122,** 1323-1334.

Xue, G.P. (2005) A CELD-fusion method for rapid determination of the DNA-binding sequence specificity of novel plant DNA-binding proteins. *The Plant Journal*, **41,** 638-649.

Xue, T., Wang, D., Zhang, S., Ehlting, J., Ni, F., Jakab, S., Zheng, C. and Zhong, Y. (2008) Genome-wide and expression analysis of protein phosphatase 2C in rice and *Arabidopsis. BMC Genomics*, **9,** 550.

Yamaguchi-Shinozaki, K., Koizumi, M., Urao, S. and Shinozaki, K. (1992) Molecular Cloning and Characterization of 9 cDNAs for Genes That Are Responsive to Desiccation in *Arabidopsis thaliana*: Sequence Analysis of One cDNA Clone That Encodes a Putative Transmembrane Channel Protein. *Plant and Cell Physiology*, **33,** 217.

Yamaguchi-Shinozaki, K. and Shinozaki, K. (1994) A novel *cis*-acting element in an *Arabidopsis* gene is involved in responsiveness to drought, low-temperature, or high-salt stress. *The Plant Cell Online*, **6,** 251-264.

Yamaguchi, M., Ohtani, M., Mitsuda, N., Kubo, M., Ohme-Takagi, M., Fukuda, H. and Demura, T. (2010) VND-INTERACTING2, a NAC domain transcription factor, negatively regulates xylem vessel formation in *Arabidopsis. The Plant Cell Online*, **22,** 1249-1263.

Yamasaki, K., Kigawa, T., Inoue, M., Watanabe, S., Tateno, M., Seki, M., Shinozaki, K. and Yokoyama, S. (2008) Structures and evolutionary origins of plant-specific transcription factor DNA-binding domains. *Plant Physiology and Biochemistry*, **46,** 394-401.

Yamauchi, N., Iida, S., Minamide, T. and Iwata, T. (1986) Polar lipids content and their fatty acid composition with reference to yellowing of stored spinach leaves. *Journal of the Japanese Society for Horticultural Science*, **55.**

Yang, S.D., Seo, P.J., Yoon, H.K. and Park, C.M. (2011) The *Arabidopsis* NAC Transcription Factor VNI2 Integrates Abscisic Acid Signals into Leaf Senescence via the COR/RD Genes. *The Plant Cell Online*, **23,** 2155-2168.

Yang, Z. and Ohlrogge, J.B. (2009) Turnover of fatty acids during natural senescence of *Arabidopsis*, Brachypodium, and switchgrass and in *Arabidopsis*-oxidation mutants. *Plant Physiology*, **150,** 1981-1989.

Yoshida, S. (2003) Molecular regulation of leaf senescence. *Current Opinion in Plant Biology,* **6,** 79-84.

Zhong, R., Lee, C. and Ye, Z.H. (2010) Global analysis of direct targets of secondary wall NAC master switches in *Arabidopsis. Molecular plant*, **3,** 1087.

Zhou, J., Lee, C., Zhong, R. and Ye, Z.H. (2009) MYB58 and MYB63 are transcriptional activators of the lignin biosynthetic pathway during secondary cell wall formation in *Arabidopsis. The Plant Cell Online*, **21,** 248-266.

Zhu, J.K. (2002) Salt and drought stress signal transduction in plants. *Annual Review of Plant Biology*, **53,** 247.

Zhu, Y.X. and Davies, P.J. (1997) The control of apical bud growth and senescence by auxin and gibberellin in genetic lines of peas. *Plant Physiology*, **113,** 631.

Zuo, J., Niu, Q.W. and Chua, N.H. (2000) An estrogen receptor-based transactivator XVE mediates highly inducible gene expression in transgenic plants. *The Plant Journal*, **24,** 265-273.

Allgemeinverständliche Zusammenfassung

Der Alterungsprozess lebender Organismen wird seit vielen Jahren wissenschaftlich untersucht. In Pflanzen wird der Alterungsprozess Seneszenz genannt. Er ist für das Überleben der Pflanze von großer Bedeutung. Dennoch ist unser Wissen über die molekularen Mechanismen der Blattseneszenz, dessen komplexe Steuerung und die Wechselwirkungen mit Umweltsignale noch sehr limitiert. Ein wichtiges Steuerungselement besteht in der Aktivierung bestimmter Transkriptionsfaktoren (TFs) die während der Seneszenz unterschiedlich exprimiert werden. Aus der Literatur ist bekannt, dass Mitglieder der NAC TF Familie (*NAM/ATAF/CUC*) an der Regulation der Seneszenz bei Pflanzen beteiligt sind. ORE1 (ANAC092/AtNAC2), ein NAC TF mit erhöhter Genexpression während der Seneszenz, wurde erstmals in Mutanten mit verzögerte Seneszenz beschrieben, die molekularen Mechanismen, wie ORE1 die Seneszenz kontrolliert und die Stoffwechselwege reguliert, sind aber noch weitgehend unbekannt.

Die Arbeiten im Rahmen dieser Dissertation wurden durchgeführt, um einen tieferen Einblick in die Regulationsmechanismen von ORE1 auf natürliche, dunkel induzierte sowie Salzstress-induzierte Seneszenz zu erhalten. Ergebnisse von Untersuchungen an zwei unterschiedlichen Pflanzenspezies (*Arabidopsis thalinana* und *Nicotiana tabacum*) deuten auf ein ähnliches Expressionsmuster von ORE1 während der natürlichen als auch der Salz-induzierten Seneszenz hin. In der Promotorregion von ORE1 wurde ein für natürliche Seneszenz charakteristisches Muster identifiziert. In vivo Analysen ergaben darüber hinaus. Hinweise auf zwei weitere ORE1 Regulatoren. Debei handelt es sich umeinen weiteren NAC TF (*ATAF1*) und (ii) CKOR, einer Calcium-abhängige Protein-Kinase (CDPK).In weiteren Studien wurden sechs Gene identifiziert, die durch ORE1 reguliert werden. In den Promotoren dieser Gene wurden entsprechende Bindestellen für ORE1 lokalisiert. Die ORE1-Bindung an die Promotoren wurde daraufhin sowohl in vitro als auch in vivo verifiziert. Zwei dieser Gene, die *BIFUNCTIONAL Nuclease 1* (*BFN1*) und *VND-Interacting2* (*VNI2*), wurden zudem auf molekularer und physiologischer Ebene untersucht.

170

Lilian Paola Matallana-Ramírez

Contact information matallana@mpimp-golm.mpg.de – lilianmatallana@gmail.com

Personal information Nationality   Colombian
Place of Birth   Bogotá D.C
Date of Birth   31.03.1980

Research interests Plant physiology, *in vitro* culture and micropropagation of tropical fruits crops, transcriptional regulation.

Education **University of Potsdam,** Potsdam, Germany
Department of Molecular Biology
Ph.D Student (2008-2012)
* Dissertation Topic: Unraveling the ORE1 Regulon in *Arabidopsis thaliana:* Molecular and Functional Characterization of Up- and Down-stream Components
* Supervisors: Prof. Dr. Bernd Mueller-Roeber and Dr. Salma Balazadeh

Universidad Nacional de Colombia, Bogotá D.C., Colombia
Department of Biology
Biologist, July 2006 (Equivalent to the German
"Diplome Biologie")
* Dissertation Topic: Standardization of *in vitro* protocol in *Tropaeolum majus* (*Tropaeolaceae*) for development its morphogenic potential
* Supervisors: Prof. Dr. Margarita Perea-Dallos
* Grade: (5.0/5.0 maximum grade)

Honors and Awards DAAD complete fellowship for Ph.D. project (2008-2012). Potsdam University and Max Planck Institute for Plant Molecular Physiology. Potsdam-Germany.
Mariano Ospina-Perez Prize 2010. Special Mention: Contribution to the sustainable development of Colombia for the work and publication: Biotechnology applied to tropical fruit crops improvement. Bogotá-Colombia.

Publications

Luisa Ballesteros, Ivan Perez, Tania Galindo, Julian Ortiz, Victor Vera, **Lilian Matallana**, Jenny Jimenez, Alicia Caro, Karina Avendaño, Sonia León, Miguel Rodríguez, Rubén Arroyo, Yisela Figueroa, Diana Corredor, Paola Espinosa, Gersain Medina, Maria Marcela Camacho Navarro (2003) Genre differences on visual perception of color range and depth of field. Acta Biológica Colombiana 8(2): 3-8.

Matallana L, Kleinwaechter M, Selmar D. (2006) Sulfur is limiting the glucosinolate accumulation in nasturtium *in vitro* plants (*Tropaeolum majus* L.). Journal of Applied Botany 80:1-5.

Margarita Perea Dallos, **Lilian Paola Matallana R.**, Andrea Tirado Perea (2010) Biotechnology applied to tropical fruit crops improvement. Agricultural Book. Biology Department. Science Faculty. National University of Colombia. ISBN: 9789587195361. p. 581.

Balazadeh S, Siddiqui H, Allu AD, **Matallana-Ramirez LP**, Caldana C, Mehrnia M, Zanor MI, Köhler B and Mueller-Roeber B. (2010) A gene regulatory network controlled by the NAC transcription factor ANAC092/AtNAC2/ORE1 during salt-promoted senescence. *The Plant Journal*. 62: 250-264.

Matallana-Ramirez LP, Rauf M, Dortay, H, Sorego L, Lers A, Xue GP, Dröge-Laser W, Balazadeh S and Mueller-Roeber B. (Manuscript on preparation). Expression of *BIFUNCTIONAL NUCLEASE1* (*BFN1*) gene during senescence in *Arabidopsis* is regulated by the NAC transcription factor ANAC092/AtNAC2/ORE1.

Erklärung

Hiermit erkläre ich, dass ich die vorliegende Arbeit selbständig und unter Verwendung keiner anderen als den von mir angegeben Quellen und Hilfsmitteln verfasst habe.

Ferner erkläre ich, dass ich bisher weder an de Universität Potsdam noch anderweitig versucht habe, eine Dissertation einzureichen oder mich einer Doktorprüfung zu unterziehen.

Lilian Paola Matallana-Ramírez   Potsdam, 11.04. 2012